People's Democratic Republic of Algeria
Ministry of Higher Education and Scientific Research
Ferhat ABBAS University Sétif 1

Faculty of Sciences
Department of Computer Science

Energy Optimization in the Energy Internet

Ph.D. Thesis

Submitted by
Assala Nacef

In partial fulfillment of the requirements for the degree of

Doctor of Philosophy in Computer Science
(Networking and Distributed Systems)

Committee of Examiners

Prof. Fouzi SEMCHEDDINE	President	Ferhat ABBAS University Sétif-1
Prof. Abdelmalek BOUDRIES	Examiner	University of Béjaïa
prof. Farouq ZITOUNI	Examiner	University of Ouargla
Dr. Sarra CHERBAL	Examiner	Ferhat ABBAS University Sétif-1
Prof. Djamila MECHTA	Supervisor	Ferhat ABBAS University Sétif-1
Dr. Lemia LOUAIL	Co-Supervisor	Université de Lorraine

Defense Year: 2026

Abstract

Energy has always been a fundamental pillar of human civilization and economic prosperity. In the modern era, global electricity demand is surging, driven by widespread economic development and the rapid growth of energy-intensive technologies like Artificial Intelligence. To manage this escalating demand sustainably, greater focus has been placed on integrating Renewable Energy Sources (RES)—such as solar, wind, and hydropower—to alleviate pressure on finite, polluting fossil fuels. Consequently, research into effectively harnessing RES has become critically important, with significant efforts directed toward managing their inherent intermittency and volatility to ensure grid stability and reliability. Electricity networks are therefore undergoing a transformation from centralized, fossil-fuel-based grids to decentralized, sustainable infrastructures. Smart Grids (SG) and the Energy Internet (EI) have emerged to enable two-way communication, distributed generation, and peer-to-peer (P2P) energy trading. Yet existing P2P trading frameworks often overlook the network's physical constraints, leading to inefficiencies, congestion, and unreliable energy transfers. This thesis aims to bridge the gap between energy routing and P2P energy trading by developing a system that integrates both the economic and physical dimensions of energy exchange. The objectives are to optimally match prosumers, maximize producer profits, minimize consumer costs, and ensure efficient, reliable, and collision-free energy transfers. To achieve these objectives, several models and algorithms are proposed. First, the trading problem is formulated as a fractional knapsack problem and solved using a greedy algorithm combined with Dijkstra's shortest-path algorithm. Second, simulated annealing is applied to producer subset determination, demonstrating superior convergence and ability to escape local optima compared to other heuristic optimization approaches proposed in the literature. Third, power loss is incorporated into path optimization through a modified greedy search algorithm that outperforms traditional shortest-path methods. Fourth, a quantum genetic algorithm is employed to pair prosumers, accounting for both costs and physical losses, thereby significantly reducing computation time while improving efficiency. A dynamic scheduling mechanism is then introduced to mitigate congestion, prevent collisions, and enhance fairness and reliability. Finally, an adaptive multi-commodity flow (MCF) framework with Mirror Descent learning is developed to simultaneously address all three routing challenges in a unified optimization approach validated on a real-world dataset of 300 Australian households over 2,648 trading hours. The proposed framework demonstrates significant improvements in cost-effectiveness, transmission efficiency, and system reliability. Results show up to 39.34% cost reduction depending on infrastructure capacity, transmission losses maintained below 1.2%, 55.9% grid independence, and sub-millisecond optimization enabling real-time market operation. The adaptive approach eliminates manual parameter tuning through online learning, automatically identifying binding constraints and adjusting routing priorities across diverse operating conditions. By unifying economic and physical aspects of energy transfers at scale, this thesis contributes a novel foundation for sustainable, decentralized, and intelligent energy markets.

Keywords: Energy Internet, Smart Grid, Energy Routing, Peer-to-Peer Energy Trading, efficient path, Producer Subset, Scheduling.

Résumé

L'énergie a toujours été un pilier fondamental de la civilisation humaine et de la prospérité économique. À l'ère moderne, la demande mondiale en électricité augmente rapidement, stimulée par le développement économique généralisé et la croissance rapide des technologies à forte consommation énergétique comme l'Intelligence Artificielle. Pour gérer cette demande croissante de manière durable, une attention croissante a été portée à l'intégration des Sources d'Énergie Renouvelable (SER)—telles que le solaire, l'éolien et l'hydroélectricité—afin de réduire la pression sur les combustibles fossiles finis et polluants. Par conséquent, la recherche sur l'exploitation efficace des SER est devenue d'une importance critique, avec des efforts significatifs visant à gérer leur intermittence et leur volatilité inhérentes pour assurer la stabilité et la fiabilité du réseau. Les réseaux électriques subissent donc une transformation, passant de réseaux centralisés basés sur les combustibles fossiles vers des infrastructures décentralisées et durables. Les Réseaux Intelligents (Smart Grids - SG) et l'Internet de l'Énergie (Energy Internet - EI) ont émergé pour permettre une communication bidirectionnelle, la production distribuée et le commerce d'énergie pair-à-pair (P2P). Cependant, les cadres de commerce P2P existants négligent souvent les contraintes physiques du réseau, entraînant des inefficacités, de la congestion et des transferts d'énergie peu fiables. Cette thèse vise à combler le fossé entre le routage énergétique et le commerce d'énergie P2P en développant un système qui intègre les dimensions économiques et physiques de l'échange d'énergie. Les objectifs sont d'optimiser l'appariement des prosommateurs, de maximiser les profits des producteurs, de minimiser les coûts pour les consommateurs, et d'assurer des transferts d'énergie efficaces, fiables et sans collision. Pour atteindre ces objectifs, plusieurs modèles et algorithmes sont proposés. Premièrement, le problème commercial est formulé comme un modèle de sac à dos fractionnaire et résolu à l'aide d'un algorithme glouton combiné à la sélection de chemin basée sur Dijkstra. Deuxièmement, le recuit simulé est appliqué à la détermination du sous-ensemble de producteurs, démontrant une convergence supérieure et une capacité à échapper aux optima locaux par rapport aux autres approches d'optimisation heuristique proposées dans la littérature. Troisièmement, la perte de puissance est intégrée dans l'optimisation du chemin via un algorithme de recherche gloutonne modifié qui surpasse les méthodes traditionnelles de plus court chemin. Quatrièmement, un algorithme génétique quantique est employé pour apparier les prosommateurs en tenant compte à la fois du coût et des pertes physiques, réduisant considérablement le temps de calcul tout en améliorant l'efficacité. Un mécanisme d'ordonnancement dynamique est ensuite introduit pour atténuer la congestion, prévenir les collisions et améliorer l'équité et la fiabilité. Enfin, un cadre de flux multi-commodités (MCF) adaptatif avec apprentissage par descente miroir est développé pour traiter simultanément les trois défis de routage dans une approche d'optimisation unifiée validée sur un ensemble de données réel de 300 ménages australiens sur 2 648 heures de transaction. Le cadre proposé démontre des améliorations significatives en termes de rentabilité, d'efficacité de transmission et de fiabilité du système. Les résultats montrent une réduction des coûts de 33 à 83% selon la capacité de l'infrastructure, des pertes de transmission maintenues en dessous de 1,2%, une indépendance du réseau de 55,9% et une optimisation sub-milliseconde permettant un fonctionnement du marché en temps réel. L'approche adaptative élimine le réglage manuel des paramètres grâce à l'apprentissage en ligne, identifiant automatiquement les contraintes contraignantes et ajustant les priorités de routage dans diverses conditions d'exploitation. En unifiant les aspects économiques et physiques des transferts d'énergie à grande échelle, cette thèse apporte une base novatrice pour des marchés énergétiques durables, décentralisés et intelligents.

Mots-clés : Internet de l'Énergie, Réseau Intelligent, Routage Énergétique, Commerce d'Énergie Pair-à-Pair, Chemin Efficace, Sous-ensemble de Producteurs, Ordonnancement.

الملخص

لطالما كانت الطاقة ركيزة أساسية للحضارة الإنسانية والازدهار الاقتصادي. في العصر الحديث، يشهد الطلب العالمي على الكهرباء ارتفاعاً متسارعاً، مدفوعاً بالتنمية الاقتصادية الواسعة والنمو السريع للتقنيات كثيفة الاستهلاك للطاقة مثل الذكاء الاصطناعي. لإدارة هذا الطلب المتصاعد بشكل مستدام، تم التركيز المتزايد على دمج مصادر الطاقة المتجددة—مثل الطاقة الشمسية وطاقة الرياح والطاقة الكهرومائية—للتخفيف من الضغط على الوقود الأحفوري المحدود والملوث. وبالتالي، أصبح البحث في الاستغلال الفعال لمصادر الطاقة المتجددة ذا أهمية بالغة، مع توجيه جهود كبيرة نحو إدارة تقطعها وتقلبها المتأصل لضمان استقرار الشبكة وموثوقيتها.

تخضع شبكات الكهرباء بالتالي لتحول من شبكات مركزية قائمة على الوقود الأحفوري نحو بنى تحتية لامركزية ومستدامة. ظهرت الشبكات الذكية وإنترنت الطاقة لتمكين الاتصال ثنائي الاتجاه، والتوليد الموزع، وتداول الطاقة من نظير إلى نظير. ومع ذلك، غالباً ما تتجاهل أطر التداول من نظير إلى نظير الحالية القيود المادية للشبكة، مما يؤدي إلى عدم الكفاءة والازدحام ونقل الطاقة غير الموثوق.

تهدف هذه الأطروحة إلى سد الفجوة بين توجيه الطاقة وتداول الطاقة من نظير إلى نظير من خلال تطوير نظام يدمج كلاً من الأبعاد الاقتصادية والمادية لتبادل الطاقة. الأهداف هي مطابقة المستهلكين المنتجين على النحو الأمثل، وتعظيم أرباح المنتجين، وتقليل تكاليف المستهلكين، وضمان نقل طاقة فعال وموثوق وخالٍ من التصادمات.

لتحقيق هذه الأهداف، تم اقتراح عدة نماذج وخوارزميات. أولاً، تمت صياغة مشكلة التداول كنموذج حقيبة ظهر كسرية وحلها باستخدام خوارزمية جشعة مقترنة باختيار المسار القائم على خوارزمية دايكسترا. ثانياً، تم تطبيق التلدين المحاكى على تحديد المجموعة الفرعية من المنتجين، مما يوضح تقارباً متفوقاً وقدرة على الهروب من الحلول المحلية المثلى مقارنة بأساليب التحسين الاستدلالية الأخرى المقترحة في الأدبيات. ثالثاً، تم دمج فقدان الطاقة في تحسين المسار من خلال خوارزمية بحث جشعة معدلة تتفوق على طرق أقصر مسار التقليدية. رابعاً، تم استخدام خوارزمية جينية كمومية لمطابقة المستهلكين المنتجين مع الأخذ في الاعتبار كل من التكلفة والخسائر المادية، مما يقلل بشكل كبير من وقت الحساب مع تحسين الكفاءة. تم بعد ذلك تقديم آلية جدولة ديناميكية للتخفيف من الازدحام ومنع التصادمات وتعزيز العدالة والموثوقية. أخيراً، تم تطوير إطار تدفق متعدد السلع تكيفي مع التعلم بالنزول المرآة لمعالجة تحديات التوجيه الثلاثة في وقت واحد ضمن نهج تحسين موحد تم التحقق من صحته على مجموعة بيانات واقعية من 300 أسرة أسترالية على مدى 2648 ساعة تداول.

يُظهر الإطار المقترح تحسينات كبيرة في الفعالية من حيث التكلفة وكفاءة النقل وموثوقية النظام. تُظهر النتائج خفضاً في التكلفة بنسبة 33-83% حسب سعة البنية التحتية، وخسائر نقل محافظ عليها أقل من 2%.1، واستقلالية عن الشبكة بنسبة 55%.9، وتحسين دون الميلي ثانية يتيح تشغيل السوق في الوقت الفعلي. يلغي النهج التكيفي الضبط اليدوي للمعاملات من خلال التعلم عبر الإنترنت، مع تحديد القيود الملزمة تلقائياً وتعديل أولويات التوجيه عبر ظروف التشغيل المتنوعة. من خلال توحيد الجوانب الاقتصادية والمادية لنقل الطاقة على نطاق واسع، تساهم هذه الأطروحة بأساس جديد لأسواق الطاقة المستدامة واللامركزية والذكية.

الكلمات المفتاحية: إنترنت الطاقة، الشبكة الذكية، توجيه الطاقة، تداول الطاقة من نظير إلى نظير، المسار الفعال، المجموعة الفرعية من المنتجين، الجدولة.

Dedication

This thesis would not have been possible without the support, guidance, and encouragement of many individuals.

First and foremost, I would like to express my deepest gratitude to my supervisor, Professor Djamila Mechta, and my co-supervisors, Professor Lemia Louail and Professor Saad Harous, for their invaluable guidance, unwavering support, and patience throughout my doctoral journey. Their insightful feedback and constructive criticism have been instrumental in shaping this research and my development as a researcher.

I would like to extend my gratitude to the members of my thesis committee: Professor Abdelmalek Boudries, Professor Farouq Zitouni, and Dr. Sarra Cherbal, as well as to the president of the jury, Professor Fouzi Semcheddine, for their time and expertise in evaluating this work.

Special thanks to my friends, with whom I shared the same academic journey, for the countless discussions, collaborations, and moments of laughter that made this experience memorable.

I am profoundly grateful to my family for their unconditional love and support. To my parents, thank you for always believing in me and encouraging me to pursue my dreams. To my siblings—Imen, Ilhem, Meriem, Khadidja, and Amine—with whom I shared all my struggles and stress, and who always managed to be there for me and support me through every challenge. To my mother, who handled all of my ups and downs with grace and strength.

Finally, I dedicate this work to my father, whose dreams for me reached beyond the horizon of his own life. He planted the seeds of ambition in my heart and taught me that excellence is not a destination but a continuous journey. Though he cannot witness this moment with earthly eyes, I feel his presence in every accomplishment, his pride in every milestone. His memory has been the gentle hand guiding me through darkness, the unwavering faith sustaining me through doubt.

Above all, I am humbled by the grace of Allah, who blessed this journey with faith when my spirit faltered, perseverance when the path grew steep, and light when shadows loomed. This achievement is but a reflection of His infinite mercy and the strength He bestows upon those who seek His guidance.

Contents

Abstract i

Résumé ii

Acknowledgment iv

Table of contents vii

List of figures ix

List of tables xi

List of algorithms xii

Nomenclature xiii

General Introduction 1

I Background 4

1 Foundations of Smart Grids and the Energy Internet 5

1.1 Introduction . . . 5
1.2 Evolution and core principles of smart grids and the Energy Internet . . . 6
1.3 Background and history . . . 6
1.4 From smart grids to Energy Internet . . . 8
1.5 Energy internet naming . . . 8
1.6 EI physical components . . . 9
1.6.1 Renewable energy resources . . . 9
1.6.2 Storage devices . . . 9
1.6.3 Electric vehicles . . . 9
1.6.4 The energy router . . . 10
1.6.5 The energy hub . . . 10
1.6.6 Smart meter . . . 12
1.6.7 Microgrid . . . 13
1.6.8 UAV Networks . . . 13
1.7 EI software components . . . 14
1.7.1 Blockchain technology . . . 14
1.7.2 Energy management software . . . 14
1.7.3 Cybersecurity software . . . 14
1.7.4 Artificial intelligence and machine learning . . . 14
1.7.5 Digital twinning . . . 15
1.7.6 Peer-to-peer energy trading . . . 15
1.7.7 Plug and play interface . . . 16

1.8 Working principle of EI . . . 16
1.9 Energy internet challenges . . . 17
1.10 Conclusion . . . 18

2 Classification of Energy Routing Strategies in Energy Internet and Smart Grids 19
2.1 Introduction . . . 19
2.1.1 Energy routing algorithm . . . 19
2.1.2 Load forecasting . . . 22
2.1.3 Demand response (DR) . . . 24
2.2 Optimization algorithms used in energy routing . . . 25
2.2.1 Mathematical optimization framework . . . 25
2.2.2 Autonomous routing algorithm . . . 31
2.2.3 Heuristic and Bio-inspired metaheuristic optimization algorithms . . . 32
2.2.4 Topology-based solutions . . . 33
2.3 Conclusion . . . 38

II Contributions 41

3 FKD-RA: Efficient Energy Routing Protocol in SG and EI Networks Using Fractional Knapsack and Dijkstra Algorithm 42
3.1 Introduction . . . 42
3.2 Problematic . . . 43
3.2.1 Fractional knapsack . . . 43
3.2.2 Network model . . . 43
3.2.3 Control center management . . . 43
3.2.4 Addressing the optimal producer's subset problem . . . 43
3.2.5 Finding the shortest path . . . 45
3.3 Simulation and performance analysis . . . 45
3.3.1 Use case 1: Optimal path . . . 45
3.3.2 Use case 2: Multiple sources and multiple energy demands . . . 46
3.3.3 Use case 3: Multiple sources and mono-source . . . 46
3.3.4 A comparative analysis with the firefly algorithm . . . 47
3.4 Conclusion . . . 48

4 SA-RA: Simulated Annealing for Producer Subset Determination in Smart Grids 49
4.1 Methodology of Analysis . . . 50
4.1.1 Energy System Architecture . . . 50
4.1.2 Simulated Annealing . . . 50
4.1.3 Initial solution . . . 51
4.1.4 Initializing Parameter . . . 51
4.1.5 Energy Function . . . 51
4.1.6 Perturbation . . . 52
4.2 Simulation Results And Analyses . . . 54
4.3 Conclusion . . . 56

5 GQA-RA: A Quantum Genetic-based Routing Protocol for Real-Time Peer-to-Peer Energy Transactions 57
5.1 Introduction . . . 57
5.2 Energy Internet: Paramount Component and Topology . . . 58
5.2.1 Network Model . . . 58
5.2.2 Energy router . . . 59
5.3 Energy routing protocol . . . 60
5.3.1 Minimum path loss algorithm . . . 60

5.3.2 Producer subset determination using quantum genetic algorithm . . . 64
5.3.3 Dynamic Scheduling for Smart Grid Networks . . . 68
5.4 Simulation and performance analysis . . . 69
5.4.1 Network topologies and simulation parameters . . . 69
5.4.2 Evaluation metrics . . . 70
5.4.3 6-Node network . . . 70
5.4.4 30-Node network . . . 74
5.4.5 Greedy search comparison analyses . . . 77
5.5 Complexity and scalability analysis . . . 78
5.6 Discussion . . . 80
5.7 Conclusion . . . 81

6 Adaptive MCF: Adaptive Multi-Objective Optimization for P2P Energy Trading: A Multi-Commodity Flow Approach with Mirror Descent Learning 82
6.1 Introduction . . . 82
6.2 Network model and system architecture . . . 83
6.2.1 Dataset and preprocessing . . . 83
6.2.2 Household aggregation into energy routers . . . 84
6.2.3 Router-level power aggregation . . . 85
6.2.4 Physical network topology . . . 85
6.2.5 Electrical parameters and line modeling . . . 86
6.2.6 Economic framework . . . 87
6.2.7 Utility grid modeling . . . 89
6.3 Methodology . . . 89
6.3.1 MCF formulation . . . 89
6.3.2 Mirror descent for adaptive weight learning . . . 90
6.3.3 Mirror Descent for Weight Adaptation . . . 91
6.4 Results and performance analysis . . . 92
6.4.1 Energy flow analysis . . . 95
6.4.2 Economic performance analysis . . . 97
6.4.3 Fairness analysis . . . 99
6.4.4 Adaptive weight learning dynamics . . . 102
6.4.5 Computational complexity and runtime analysis . . . 103
6.5 Discussion . . . 105
6.6 Conclusion . . . 105

7 Comparative Analysis and Discussion 108
7.1 Energy flow analysis . . . 108
7.2 Cost analysis . . . 110
7.3 Fairness analysis . . . 111
7.4 Computational analysis . . . 113
7.4.1 Theoretical complexity . . . 113
7.4.2 Measured execution times . . . 115
7.5 Discussion . . . 116
7.6 Conclusion . . . 116

General Conclusion 118

List of Publications 120

Bibliography 121

List of Figures

1.1 Example of an energy internetmodel . . . 8
1.2 Example of an ER model . . . 11
1.3 Example of an energy hub model . . . 12
1.4 A simple breakdown of a Micro-grid structure . . . 13
1.5 Layered architecture of the EI network . . . 16
1.6 The 10 countries with the most research in energy routing, Load forecasting, and demand response . . . 17

2.1 The 10 countries with the most research in energy routing . . . 20
2.2 Yearly progression of research in efficient path, matching subscribers, and scheduling . . . 20
2.3 Steps of power lost in transmission and conversion . . . 22
2.4 Classification of demand-response methods . . . 25
2.5 Energy routing steps . . . 27
2.6 Energy routing based on graph theory . . . 30

3.1 11-Nodes network topology . . . 46

4.1 Microgrid topology . . . 50
4.2 SA for optimal producer subset determination . . . 53
4.3 The seventeen-node network topology . . . 55
4.4 The thirty-node network topology . . . 55

5.1 Energy internet architecture. . . . 58
5.2 Energy router Architecture. . . . 60
5.3 Steps of the Modified Greedy Search Algorithm. . . . 63
5.4 GRA-RA Flowchart. . . . 68
5.5 QGA-RA running Workflow for one consumer . . . 69
5.6 6-Node Network Topology. . . . 70
5.7 30 Nodes Network Topology. . . . 74
5.8 Power Loss Comparison in the 6-Node Network. . . . 77
5.9 Power Loss Comparison in the 30-Node Network. . . . 77
5.10 Cost Comparison in the 6-Node Network. . . . 77
5.11 Cost Comparison in the 30-Node Network. . . . 77

6.1 Geographic network topologies. **Left:** MST (11 edges, 180.5 km). **Right:** Dense topology (22 edges, 413.9 km) with MST backbone (green) and k-NN shortcuts (gray). . . . 86
6.2 Schematic comparison of network topologies showing logical connectivity structure. . . . 87
6.3 Flowchart of adaptive MCF-based P2P energy trading system. . . . 93
6.4 Energy performance of MCF Static and MCF Adaptive across scenarios S1–S4 over 2,648 trading hours. . . . 96
6.5 Average hourly cost ($/h) by SDR regime and network scenario across all algorithmic configurations over 2,648 trading hours. . . . 100

6.6 Average Jain fairness index per scenario for MCF Adaptive and MCF Static, computed over 2,648 trading hours. 101
6.7 MCF Adaptive weight evolution across scenarios. 107

7.1 P2P trading volume (a) and cost reduction relative to the grid-only baseline (b) for all four algorithms across the four experimental scenarios. 109
7.2 Average Jain fairness index for all four algorithms across the four experimental scenarios, computed over a rolling 168-hour window. 112
7.3 Mean execution time per trading hour (ms, log scale) for all four algorithms across the four experimental scenarios. 114
7.4 Overview of energy routing problems and proposed solutions. 119

List of Tables

1.1 Comparison between SG and EI. . . . 9

2.1 Comparison of different DR methods. . . . 26
2.2 Comparison of Energy Routing Strategies 34
2.4 Comparison of Different Protocols 37
2.3 Comparison of different optimization methods. . . . 39

3.1 Information details of the network distribution 46
3.2 The relationship between the demand and the cost for every consumer 47
3.3 Simulation results of the Firefly algorithm 47

4.1 Energy Router Characteristics for 17-Node Network 54
4.2 Power Line Characteristics for a 17-Node Network 54
4.3 17-Node Energy Profile 55
4.4 Comparative Results of SA-ERP and IACO-ERP 56
4.5 30-Node Energy Profile 56
4.6 Comparative Results for 30-Node Network 56

5.1 Lookup Table of Rotation Angle 67
5.2 Parameters of Energy Routers (6 MGs) 70
5.3 Power lines parameters (6 MGs) 71
5.4 Energy profile for 6-MGs Network 71
5.5 Transmission times, consumer demand, and energy values for different cases 71
5.6 Transmission paths and power loss for different cases 72
5.7 Energy profile for 30-MGs Network 74
5.8 Transmission times, consumer demand, and energy values for different cases 75
5.9 Transmission paths and power loss for different cases 75
5.10 Test Parameters for 6-Node and 30-Node Topologies 78
5.11 Test results for 6-Node Topology with a demand of 30kW 78
5.14 Test results for 30-Node Topology with a demand of 10kW 78
5.12 Test results for 6-Node Topology with a demand of 50kW 79
5.13 Test results for 30-Node Topology with a demand of 30kW 79
5.15 Comparison of Routing Algorithms 79
5.16 Comparison of MLR Protocol and QGA-RA Protocol 79

6.1 Electrical Network Parameters 87
6.2 Experimental scenario specifications 94
6.3 Energy Flow Summary Across All Scenarios 95
6.4 Average Energy Flow by SDR Regime 96
6.5 Cost and Revenue Summary Across All Scenarios (2,648 Trading Hours). . . . 97
6.6 Average Hourly Cost ($/h) by SDR Regime. . . . 99
6.7 Trading Fairness Across All Scenarios (2,648 Trading Hours). . . . 100
6.8 Average Fairness by SDR Regime 102

6.9 MCF Adaptive weight convergence summary across experimental scenarios. 102
6.10 Theoretical time complexity of each algorithmic component. 104
6.11 Average per-hour runtime (ms) across all scenarios. 104

7.1 Energy Flow Summary Across All Scenarios (2,648 Trading Hours). 109
7.2 Average Energy Flow (kWh/h) by SDR Regime. 110
7.3 Cost and Revenue Summary Across All Scenarios (2,648 Trading Hours). 111
7.4 Average Hourly Cost ($/h) by SDR Regime. 112
7.5 Trading Fairness Across All Scenarios (2,648 Trading Hours). Bold values indicate the highest fairness per scenario. 113
7.6 Average Jain Fairness Index by SDR Regime. 114
7.7 Execution Time per Trading Hour (ms) Across All Scenarios (2,648 Hours). Bold values indicate the fastest algorithm per scenario. SA-RA 95th-percentile values are reported in place of the maximum due to extreme outliers caused by DFS path explosion on dense topologies. 115

List of Algorithms

1 Control Center main algorithm 44
2 Greedy function 45
3 Powerloss_Assessment 52
4 Optimal Path Calculation in an Energy Network. 62
5 Capacity-Aware Allocation. 64
6 Process Producers (MeasureQbits) 66
7 K-Means Clustering for Energy Router Construction 84
8 Dense Network Construction (MST + k-NN) 86
9 Adaptive Multi-Commodity Flow with Mirror Descent 92

Nomenclature

ABCO	Artificial Bee Colony Optimization
AC	Alternating Current
ACO	Ant Colony Optimization
ADR	Automated Demand Response
AI	Artificial Intelligence
AIS	Artificial Immune System
ANN	Artificial Neural Network
AOA	Arithmetic Optimization Algorithm
AVOA	Arithmetic Valued Optimization Algorithm
BCO	Bee Colony Optimization
BDR	Behavioral Demand Response
BFO	Bacterial Foraging Optimization
BiGRU	Bidirectional Gated Recurrent Unit
CAES	Compressed Air Energy Storage
CC	Control Center
CHIO	Coronavirus Herd Immunity Optimization
CNN	Convolutional Neural Network
CPP	Critical Peak Pricing
DC	Direct Current
DCRB	Densely Connected Residual Blocks
DER	Distributed Energy Resources
DFBB	Depth-First Branch-and-Bound
DFS	Depth-First Search
DFSD	Depth-First Search with Dijkstra
DMS	Distributed Management System
DO	Data Object
DPSO	Dynamic Particle Swarm Optimization
DR	Demand Response
DRER	Distributed Renewable Energy Resources
DRSD	Distributed Renewable Storage Device
DSM	Demand-Side Management
E-DFBB	Extended Depth-First Branch-and-Bound
EH	Energy Hub
EI	Energy Internet
EMS	Energy Management System
ER	Energy Router
ESD	Energy Storage Device
ESS	Energy Storage System
EV	Electric Vehicle
FIFO	First-In-First-Out
FKD-RA	Fractional Knapsack-Dijkstra Routing Algorithm

FREEDM	Future Renewable Electric Energy Delivery and Management
GA	Genetic Algorithm
GOA	Grasshopper Optimization Algorithm
GOER	Global Optimal Energy Routing Protocol
GPS	Global Positioning System
GRU	Gated Recurrent Unit
IAROA	Improved Artificial Rabbits Optimization Algorithm
IBDR	Incentive-Based Demand Response
IEA	International Energy Agency
IEC 61850	International Electrotechnical Commission Standard 61850
IEMS	Integrated Energy Management System
IoE	Internet of Energy
IoT	Internet of Things
ISCA	Improved Sine Cosine Algorithm
KKT	Karush-Kuhn-Tucker
kNN	k-Nearest Neighbors
LHS	Latin Hypercube Sampling
LN	Logical Node
LOER	Local Optimal Energy Routing Protocol
LSTM	Long Short-Term Memory
LTLF	Long-Term Load Forecasting
LV	Low Voltage
MAMES	Multi-Area Multi-Energy System
MCF	Multi-Commodity Flow
MER	Multi-Energy Router
MG	Microgrid
MGCC	Microgrid Central Controller
MGCE	Microgrid Controllable Element
MGO	Microgrid Operator
ML	Machine Learning
MLCP	Minimum Loss Cost Path
MLP	Multi-Layer Perceptron
MLR	Minimum Loss Routing
MLRM	Multiple Linear Regression Model
MPC	Multiport Converter
MPR	Multi-path Power Routing
MQTT	Message Queuing Telemetry Transport
MSML	Multi Source Multi Load
MST	Minimum Spanning Tree
MTLF	Medium-Term Load Forecasting
MU	Measurement Unit
MV	Medium Voltage
NARX	Nonlinear Autoregressive with Exogenous Inputs
NSO	Network System Operator
OFV	Objective Function Value

OMPR	Optimal-Walk Multi-path Power Routing
OPEN	Online Purchase Electricity Now
OSPF	Open Shortest Path First
P2P	Peer-to-Peer
P2PET	Peer-to-Peer Energy Trading
PBDR	Price-Based Demand Response
PCX	Parent-Centric Crossover
PFD	Power Flow Conflict
PLC	Power Line Communication
PSO	Particle Swarm Optimization
PV	Photovoltaic
QGA	Quantum Genetic Algorithm
QGA-RA	Quantum Genetic Algorithm Routing Algorithm
RCGA	Real-Coded Genetic Algorithm
RES	Renewable Energy Sources
RF	Random Forest
RL	Reinforcement Learning
RTP	Real-Time Pricing
SA	Simulated Annealing
SAMES	Single-Area Multi-Energy System
SDR	Supply-Demand Ratio
SG	Smart Grid
SIEM	Security Information and Event Management
SM	Smart Meter
SST	Solid-State Transformer
STLF	Short-Term Load Forecasting
SVM	Support Vector Machine
SVR	Support Vector Regression
TCN	Temporal Convolutional Network
TDMA	Time-Division Multiple Access
ToUP	Time-of-Use Pricing
UAV	Unmanned Aerial Vehicle
U-NSGA-III	Unified Non-dominated Sorting Genetic Algorithm III
V2G	Vehicle-to-Grid
VER	Virtual Multi-Energy Router
VPP	Virtual Power Plant

Electrical Parameters

C_{ij}	kW	Capacity of edge (i, j)
E	kWh	Energy
E_{loss}	kWh	Energy loss
I	A	Current
$I_{\max}$	A	Maximum allowable current (406 A)
P	kW	Active power
PF		Power factor (0.95)
P_{line}	kW	Line power capacity
P_{loss}	kW	Power loss
$P_{\max}$	kW	Maximum power capacity
R	Ω/km	Resistance per unit length
R_{LV}	Ω/km	LV cable resistance (0.32 Ω/km)
R_{MV}	Ω/km	MV cable resistance (0.10 Ω/km)
V	V	Voltage
V_{LV}	V	Low voltage (415 V in this work)
V_{MV}	V	Medium voltage (11 kV in this work)

Energy Trading and Economic Parameters

C_{grid}	$	Cost of grid transactions
C_{P2P}	$	Cost of P2P transactions
C_{total}	$	Total system cost
E_{grid}	kWh	Total energy from/to grid
$E_{\text{grid}}^{\text{buy}}$	kWh	Energy purchased from grid
$E_{\text{grid}}^{\text{sell}}$	kWh	Energy sold to grid
E_{P2P}	kWh	Total energy traded via P2P
p_{buy}	$/kWh	P2P buy price
p_{sell}	$/kWh	P2P sell price
SDR		Supply-Demand Ratio (total supply / total demand)
λ_b	$/kWh	Grid electricity buy price
λ_c	$/kWh	Compensation parameter for P2P pricing
λ_s	$/kWh	Grid electricity sell price

Constants and System Parameters

`CONGEST_THRESH`	0.8	Congestion threshold (80% utilization)
`FAIRNESS_WINDOW`	168 hours	Rolling window for fairness calculation (1 week)
`GRID_BUY`	0.30 $/kWh	Grid electricity purchase price
`GRID_SELL`	0.06 $/kWh	Grid electricity sell-back price
`LV_RANGE`	0.5 km	Length of LV segment at each end of transmission line
`P_LINE_MAX`	221.79 kW	Baseline line capacity
`R_LV_PER_KM`	0.32 Ω/km	LV cable resistance per kilometer
`R_MV_PER_KM`	0.10 Ω/km	MV cable resistance per kilometer
`SCALE`	10	Integer scaling factor for MCF solver

General Introduction

Background and Motivation

Reducing our reliance on the traditional power grid has become one of the most sought-after goals in today's world. The global community faces a dual challenge: a looming energy crisis driven by the depletion of fossil fuels and the escalating severity of global warming [1]. Furthermore, energy demand has surged dramatically, particularly following the emergence of energy-intensive technologies such as artificial intelligence. Under these combined pressures, renewable energy has emerged as a critical solution for both planetary sustainability and economic stability [2].

However, the transition to RES introduces unprecedented technical challenges. Unlike predictable centralized power plants, solar and wind generation exhibit inherent intermittency, fluctuating with weather conditions independently of demand. This causes frequency instability, voltage fluctuations, reverse power flow, and grid congestion [3].

This paradigm shift necessitates intelligent, adaptive, and resilient energy management systems [4]. These systems must balance supply and demand in real time under uncertainty, coordinate DERs across heterogeneous network topologies, manage bidirectional power flows while respecting physical grid constraints, and optimize both economic efficiency and system reliability. Two complementary frameworks have emerged to address these requirements: SG and the EI.

An SG is an advanced electrical network that integrates digital communication and control technologies to enable bidirectional flows of both power and information between utilities and end users. The EI extends this concept by enabling decentralized P2P energy trading among prosumers through internet-inspired routing and coordination mechanisms [5]. In both paradigms, the system can be viewed as a network of interconnected users, where each user represents a microgrid (MG) composed of loads, DERs, and energy storage devices (ESDs) [6]. Within these systems, users are commonly classified into two categories:

- **Consumers:** Users without DERs who cannot generate energy and therefore rely entirely on the grid to meet their demand [7].
- **Prosumers:** Users who own DERs and can generate energy. Due to the variability of renewable sources, a prosumer can alternate between being an energy producer and an energy consumer [8].

For both SG and EI, two critical technical challenges must be addressed for practical deployment: energy routing and peer-to-peer energy trading (P2PET) [9]. P2PET is a decentralized market mechanism in which prosumers and consumers exchange electricity directly based on agreed prices and quantities. It aims to optimally match sellers and buyers in a way that maximizes sellers' rewards and reduces buyers' costs. This process is referred to by several names in the literature, such as producer subset determination and prosumer matching [10], [11]. Energy routing, in contrast, focuses on selecting efficient and feasible paths for delivering electricity from sources to loads in a power network. It handles congestion by taking network topology constraints into consideration.

While both P2PET and energy routing are essential for decentralized energy systems, prior research has treated them as independent problems, where routing algorithms ignore economic incentives, while trading mechanisms neglect physical network constraints [11]. This fragmentation yields suboptimal outcomes: economically efficient trades may violate transmission limits, and loss-minimizing routes may result in unfair cost distribution.

Research Questions

In this thesis we aim to bridge this gap by answering and providing solutions to the following questions:

- R1: What are the EI and SG, and what is the difference between these concepts?
- R2: What are energy routing and peer-to-peer energy trading, and how do they correlate?
- R3: What is the relation between demand response and load forecasting with energy routing and P2PET?
- R4: What are the challenges that face energy routing and P2PET in both SG and EI, and how can we classify its proposed solutions?
- R5: How can we solve the efficient path problem?
- R6: How can we solve the producer subset determination problem?
- R7: How can we handle congestion and avoid energy transmission collisions?
- R8: Can we integrate fairness into our routing algorithms?

Contributions

The main contributions of this thesis are as follows:

1. In Chapter 1, we address R1, R2, and R3 by defining the terminology and establishing the theoretical foundation.
2. In Chapter 2, we address research question R4 by presenting a comprehensive and structured review of energy routing optimization strategies in SGs and the EI, including demand response and load forecasting, and highlighting their interdependencies and limitations.
3. In Chapter 3, we address research questions R5 and R6 by formulating the energy routing and P2PET problems as a fractional knapsack problem. We solve the producer subset determination using a greedy algorithm, while we solve the efficient path problem using Dijkstra's algorithm.
4. In Chapter 4, we address research questions R5 and R6, similarly to Chapter 3, by proposing a simulated annealing-based optimization approach for producer subset determination and a brute-force method for path selection. Compared to our previous contribution, we incorporate network constraints and introduce a power loss metric, thereby improving scalability and solution quality.
5. In Chapter 5, we extend our previous contributions by addressing research questions R5, R6, and R7. We propose a novel real-time routing framework based on a quantum genetic algorithm coupled with a modified greedy path selection strategy (R5 and R6), and we introduce a dynamic scheduling algorithm that handles congestion while explicitly accounting for transmission losses and economic cost (R7).
6. In Chapter 6, we address research questions R5, R6, R7, and R8 by developing an adaptive multi-commodity flow (MCF) framework with Mirror Descent online learning that simultaneously optimizes prosumer-consumer matching, loss-minimal path selection, and congestion avoidance without manual parameter tuning. We introduce Jain's fairness index to quantify and ensure equitable resource allocation across all participants. We validate the framework on a real-world dataset of 300 households spanning 2,648 trading hours. We demonstrate that the integration of explicit fairness optimization into energy routing protocols achieves equitable participation with minimal cost trade-offs (0.07% cost increase for 2.2% fairness improvement).

7. We conduct extensive simulation-based evaluation on multiple network topologies, validating the efficiency, scalability, and robustness of our proposed solutions under both normal and stress conditions.

Thesis Structure

This thesis comprises two main parts: background and contributions. The background part provides an overview of SGs and the EI and a classification of existing optimization strategies. The contributions part presents our proposed algorithmic frameworks addressing efficient path determination, producer subset selection, congestion management, and fairness optimization in decentralized energy systems. More specifically, this thesis is structured as follows:

- **General Introduction** presents the background and motivation, formulates the research questions, summarizes the main contributions, and outlines the structure of this thesis.

Part I: Background

- **Chapter 1: Foundation of Smart Grids and the Energy Internet** presents the background and historical evolution of SGs and the EI. It highlights the key differences between SGs and the EI, reviews the various terminologies used to describe the EI in the literature, and describes the physical and software components of the EI. The chapter also explains its operational principles and outlines the main challenges associated with its deployment.
- **Chapter 2: Classification of Energy Routing Strategies in Energy Internet and Smart Grids** provides a comprehensive state-of-the-art review of energy routing in SGs and the EI. It presents a structured classification of existing algorithms addressing energy routing, demand response, and load forecasting, and discusses their advantages and limitations.

Part II: Contributions

- **Chapter 3 (FKD-RA)** details the formulation, methodology, implementation, and performance evaluation of an energy routing protocol based on fractional knapsack and Dijkstra algorithms for optimal producer subset selection and path determination.
- **Chapter 4 (SA-RA)** presents an improved energy routing framework using simulated annealing for producer subset determination, demonstrating enhanced scalability and solution quality under network constraints.
- **Chapter 5 (QGA-RA)** introduces a real-time energy routing framework based on quantum genetic algorithms, combined with a modified greedy path selection strategy and a dynamic scheduling mechanism, to ensure efficient, reliable, and collision-free energy transmission.
- **Chapter 6 (Adaptive MCF)** presents an adaptive multi-commodity flow optimization framework with Mirror Descent online learning that unifies prosumer-consumer matching, loss-optimal path selection, congestion management, and fairness optimization. The framework is validated on real-world data from 300 Australian households over 2,648 trading hours, demonstrating scalability, adaptability, and production-readiness.
- **Chapter 7 (Comparison)** conducts a unified comparative evaluation of all four proposed algorithms (FKD-RA, SA-RA, QGA-RA, and Adaptive MCF) on the same real-world dataset of 300 households spanning 2,648 trading hours, across four network scenarios.
- **General Conclusion** summarizes the main contributions, discusses the limitations of the proposed approaches, and outlines potential future research directions toward more efficient, scalable, reliable, and equitable energy routing algorithms for next-generation peer-to-peer energy markets.

Part I

Background

Chapter 1

Foundations of Smart Grids and the Energy Internet

Contents

1.1 Introduction . . . 5
1.2 Evolution and core principles of smart grids and the Energy Internet . . . 6
1.3 Background and history . . . 6
1.4 From smart grids to Energy Internet . . . 8
1.5 Energy internet naming . . . 8
1.6 EI physical components . . . 9
1.6.1 Renewable energy resources . . . 9
1.6.2 Storage devices . . . 9
1.6.3 Electric vehicles . . . 9
1.6.4 The energy router . . . 10
1.6.5 The energy hub . . . 10
1.6.6 Smart meter . . . 12
1.6.7 Microgrid . . . 13
1.6.8 UAV Networks . . . 13
1.7 EI software components . . . 14
1.7.1 Blockchain technology . . . 14
1.7.2 Energy management software . . . 14
1.7.3 Cybersecurity software . . . 14
1.7.4 Artificial intelligence and machine learning . . . 14
1.7.5 Digital twinning . . . 15
1.7.6 Peer-to-peer energy trading . . . 15
1.7.7 Plug and play interface . . . 16
1.8 Working principle of EI . . . 16
1.9 Energy internet challenges . . . 17
1.10 Conclusion . . . 18

1.1 Introduction

Smart grids and the energy internet rely on energy routing as a fundamental enabling component. However, energy routing problems in SG and the EI cannot be effectively addressed without a clear understanding of the underlying system architecture and operational context. This chapter therefore,

serves as a background and orientation chapter, providing the essential concepts and terminology required for the remainder of the thesis.

The chapter reviews the historical evolution from traditional power grids to Smart Grids and subsequently to the EI. It describes the physical and software components that enable decentralized energy systems and explains how these components interact during energy generation, exchange, and delivery. By establishing this background, the chapter provides a common reference framework for the energy routing models and optimization techniques developed in the subsequent chapters.

1.2 Evolution and core principles of smart grids and the Energy Internet

Electricity is an essential component of modern life, supporting nearly all aspects of daily life, including lighting, heating, transportation, healthcare, manufacturing, and communication. It plays a critical role in economic growth and technological advancement [12]. Traditionally, electricity was supplied through centralized grids, where power is generated at large-scale plants—often fossil-fueled—and transmitted over long distances to end users. While effective in the past, this system suffers from one-way power flow, high transmission losses, lack of flexibility, and reliance on fossil fuels, which contribute to greenhouse gas emissions and environmental degradation [13, 14, 15].

In response to these structural and environmental challenges, RERs such as solar and wind power have emerged as sustainable alternatives. However, their intermittency and unpredictability pose significant operational challenges for conventional power systems [16]. To overcome these issues, the SG concept was introduced.

An SG integrates advanced sensing, communication, and control technologies to enable two-way communication and dynamic control of power flows. It is often composed of interconnected microgrids, each functioning as a localized and autonomous energy system. A typical microgrid includes renewable generation units, storage systems, electrical loads, and a local controller (such as an Energy Router in EI-oriented architectures). The ER plays a key role by coordinating local power distribution, managing storage, and enabling decentralized decision-making.

Building on the SG paradigm, the EI extends this vision by treating energy as a transferable commodity that can be dynamically exchanged among users. One of its core innovations is peer-to-peer (P2P) energy trading, which enables users to act as both producers and consumers (prosumers) and supports decentralized energy markets. Unlike conventional electricity trading, however, P2P energy trading requires robust energy transfer mechanisms to ensure power is exchanged efficiently and securely.

The process of directing and managing these energy flows is known as energy routing. Energy routing ensures that electricity is transferred along optimal paths to minimize transmission losses, avoid congestion, and prevent collisions in the network [17]. It introduces three major challenges:

- Producer subset selection: identifying the most cost-effective producers for each consumer.
- Path selection: finding routes with the least transmission losses.
- Scheduling: coordinating transmissions to avoid conflicts on shared links.

Together, SGs and the EI provide the foundations for a modern, flexible, and sustainable electricity system. By integrating renewable resources, enabling decentralized trading, and ensuring reliable routing, they aim to reduce dependence on fossil fuels, enhance efficiency, and contribute to a low-carbon energy future.

1.3 Background and history

In 2004, The Economist magazine published a report conceptualizing a "self-healing" grid with real-time sensors and "plug and play" software that integrates distributed generators and storage devices. This concept was given the term "Energy Internet" [18]. They aimed to propose an efficient, fail-proof

grid that handles natural disasters and accidents. They were influenced by the 2003 blackout, which forced 50 million Americans and Canadians into darkness because of a natural accident. The lack of a fail-proof and flexible mechanism led to the spread of the blackout. This accident inspired the integration of the internet into the grid and the spread of the EI.

Later in 2008, [19] presented some assumptions and requirements for building the energy infrastructure. They wanted to create an energy system capable of self-healing and self-configuring, aided by smart agents. Their idea was inspired by the usage of agents on the internet.
A self-healing system is flexible and can automatically solve new problems. They first assumed that using a virtual buffer would probably fix the network's lack of energy storage capacity. A virtual buffer will use dynamic scheduling, which can be carried out by intelligent agents that predict the client's consumption pattern.
The second assumption is price elasticity to manage the uncertainty of the predictions made by the system.
They also presented an architecture and highlighted the requirement for building an EI, such as smart metering, Multi-resolution agents, etc.

A 2011 research paper published by the NSF FREEDM Systems Center at North Carolina State University was the turning point for the energy system [20], as it laid the groundwork for the EI's actual implementation and architecture. The proposed FREEDM system takes its inspiration from the internet and defines three major functionalities necessary for building an EI.
The first one is a plug-and-play interface. This interface should include both a 400-volt direct current (DC) bus and a 120-volt alternating current (AC) bus, along with a standard communication interface that recognizes any device connected to the grid.
The second feature is an ER, also known as an "intelligent energy management device" (IEMD). Similar to the internet router, the ER manages information, communication, and energy flow. It monitors the status and data collection of all devices and provides control references to each device, etc. The envisioned IEM is formed by multiple solid-state transformers (SSTs). These SSTs are responsible for controlling the conversions from AC to DC, DC to AC, and voltage regulation.
The third feature is an open-standard-based operating system (DGI). It is a distributed operating system integrated into all ERs that controls and synchronizes all communications on all devices.
The FREEDM system also introduces an intelligent fault-tolerant device (IFM) that isolates potential faults and avoids their spread. However, the paper did not specify any security issues.

In 2010, research on EI and SGs made significant advances with the introduction of secure transactions, demand management, and other innovations. These developments propelled research on EI to new heights, marking a notable leap forward.
The paper proposed by [21] is one of the unique works of that period that dived deeper into the security aspect of EI. The paper also briefly explained the need for internet communication and demand-side management to create a real sustainable energy system.

In the same year, a new demand-side management system named Online Purchase Electricity Now (OPEN), was proposed by [22]. It enables the purchase of electricity online. The system comprises physical and logical components; the hardware components mainly consist of smart meters used to manage energy consumption. The software components consist of the following:

1. A database used to collect orders from customers and store data generated by the smart meter.
2. A data mining engine that predicts the consumer's future consumption.
3. A decision-making tool to determine the optimal generation and distribution scheme.

Works published in 2013 mainly focused on implementing EI and integrating new technologies, such as the work proposed by [23], which features a new implementation strategy for ERs. A novel framework, proposed by [24] and based on game-theoretic methodologies, is presented to enable flexible energy exchange, allowing customers to compete and maximize their profits in a self-regulating market.

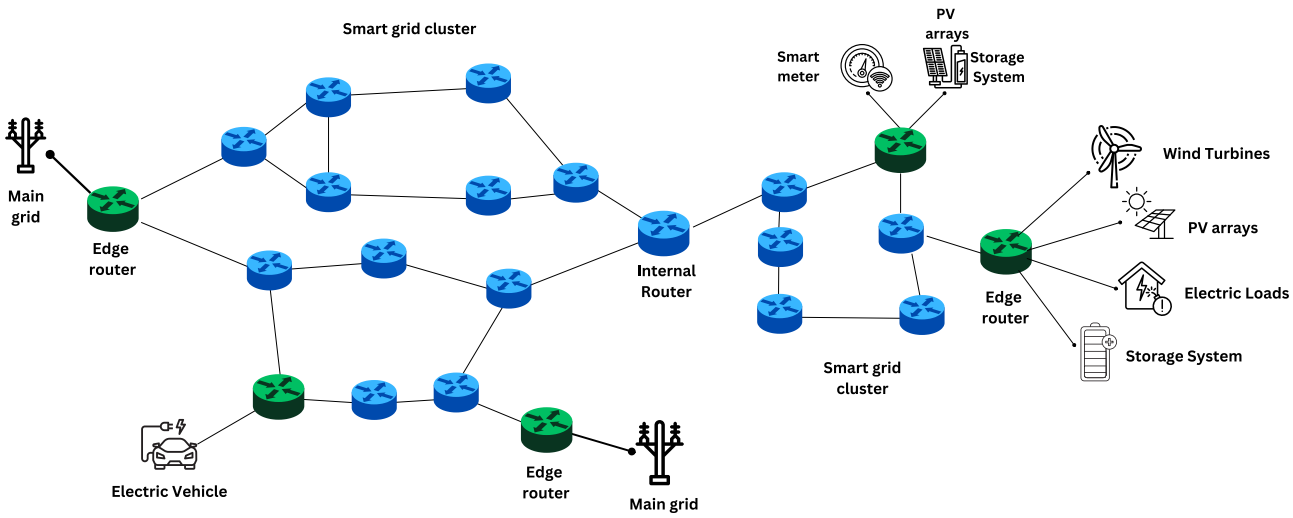

Figure 1.1: Example of an energy internetmodel

[25] proposed a multi-layer architecture of a virtual buffer controlled by intelligent agents. Its goal is to achieve reliable power transmission by reducing power loss and information flow in the system.

By 2015, China had taken the lead in research on EI due to the rapid development of its economy and industrialization. [26]; [27] are Some of the best-known publications of that period.

1.4 From smart grids to Energy Internet

[19] described the EI as "an implementation of the SG, where energy flows from suppliers to customers similar to data packets on the Internet". [28] followed a similar approach in introducing EI, naming EI an advanced form of SG, and highlighting the similarities between EI and the Internet in terms of the infrastructure. However, [29] and [30] presented differences between EI and SG, ranging from their structures to their coverage areas, the types of energy used, etc. The differences are detailed in Table 1.1, while Figure 1.4 represents the EI topology.

1.5 Energy internet naming

Since the emergence of EI, many countries have been interested in its concept. Thus, many researchers have proposed different models to solve EI-related problems. However, it leads to a different name for the conceptualization and modeling of EI. Energy internet is the term mostly used in the USA and China. It was proposed by the Economist magazine in 2004 [18] and modeled by the Future Renewable Electric Energy Delivery and Management (FREEDM) systems center at North Carolina State University [20].

Quantum grid is another name for EI, proposed by German researchers such as [31]. It is a packet-based power transmission concept similar to the internet, in which power is transmitted via energy packets. The quantum grid is a system comprising power nodes (consumers, prosumers, and routers). Each node has its IP address. The grid router acts similarly to the internet router, by choosing the closest and least expensive subscriber.

E-Energy is the second term proposed by the German "Expertise Center for Electrotechnical Standardization" organization in their paper [32]. It attempts to expand the SG and build a sustainable, distributed network with intelligent synchronization of power generation and consumption.
Moving from Europe to Asia, some Japanese studies such as the work made by [33] refer to EI as a digital grid. Although the names differ, the meaning is the same: an electricity network based on digital technology.

Table 1.1: Comparison between SG and EI.

Criteria	**Smart Grid**	**Energy Internet**
Definition	Modernized electricity network using advanced sensors, meters, and communication technologies for real-time monitoring and management of electricity generation, distribution, and consumption	Future vision of a decentralized and democratized energy system incorporating various forms of energy beyond electricity, based on internet principles
Main Focus	Electricity generation, distribution, and consumption	Different types of energy beyond electricity, including transportation and heating
Goal	Improve efficiency, reduce blackouts, and integrate RERs	Democratize and decentralize energy, promote renewable energy adoption, and enable peer-to-peer energy trading
Key Technologies	Efficient energy delivery and consumption, reduced risk of blackouts, and renewable energy integration	Decentralized and democratized energy system, peer-to-peer energy trading, and renewable energy adoption
Current State	Being implemented globally	Future vision in early stages of development
Main Players	Electric utilities, government agencies, technology companies	Renewable energy companies, startups, technology companies
Examples	U.S. SG Initiative, European SGs Platform	Brooklyn Microgrid, Power Ledger, LO3 Energy

1.6 EI physical components

This section presents the various physical components of EI:

1.6.1 Renewable energy resources

They refer to technologies such as solar panels, wind turbines, and hydroelectric plants that produce clean, renewable, distributed energy. They are small power generation units connected to the grid, typically located near load centers.

1.6.2 Storage devices

EI uses green, RERs to feed the energy system. It is a well-known fact that nuclear power is the only green power source that operates 24 hours a day, as stated by [34]. Solar panels and wind turbines only work at specific times and produce only a small amount of energy. As a result, an energy storage system (ESS) is required to ensure the energy system's availability and stability.

There are various types of energy storage systems, including battery storage systems, pumped hydro storage, compressed air energy storage (CAES), thermal energy storage, and flywheel energy storage.

ESS enables a more reliable, stable energy network by storing surplus energy for use when needed. It helps balance the grid and reduce the dependence on fossil fuels, leading to a more sustainable energy system.

1.6.3 Electric vehicles

Cars are a major contributor to air pollution, as they emit various pollutants into the atmosphere, including carbon monoxide, nitrogen oxides, and other pollutants. Most cars on the road today run on

gasoline or diesel fuel. Both are derived from fossil fuels. Following the International Energy Agency (IEA), the transportation sector accounted for around 60% of total global oil consumption in 2020. Thus, it is important to encourage alternative modes of transportation, such as electric vehicles (EVs), to reduce pollution caused by cars. EVs need a significant amount of energy that the traditional power system can not provide. Thus, the EI plays a vital role in enabling EVs' utilization by providing enough green energy to power the vehicle. EVs can also serve as storage units during emergencies or high-demand periods.

1.6.4 The energy router

The Internet inspired the emergence of EI. One of the critical components of the Internet is the data router, which enables the efficient distribution of data on a large scale across the entire globe. Although the ER concept was derived from the Internet router, they are very different. The ER is required to transmit both energy and data efficiently.
The first preliminary architectural design of ER was proposed by the FREEDM Center [23], where functional expectations, ER functions, and design requirements were detailed. The initial proposal split ER functionalities into two groups: The first group consists of the functions of routers at the edge of the grid, directly connected to the users (DRER, DESD, loads). These functions are:

1. User attachment: It means ER is responsible for configuring new users in the microgrid.
2. Status update: where users send a "status update" to the ER, which in turn updates the status of the users.
3. Service Termination: The ER informs the SSTs to stop energy output when it receives a "service termination" from the user.
4. User detachment: The router updates its user interface after detecting its disconnection.

The second group comprises routers' functions placed at the heart of the grid and directly connected to other ERs. These routers regulate the energy flow that enters and exits the microgrid and disconnect from the grid in case of a failure in the system. The suggested design is composed of three modules:

1. The power electronics module: It converts electricity from high voltages to low voltages suitable for use, using a series of sub-transformers connected in sequence.
2. The communication module is composed of two components.
   (a) The inter-communication component: used for communications inside the ER between the SST controller and each electrical port.
   (b) The intra-communication component: used for communications between different routers.
3. The intelligence module is intelligent software that uses information collected by the communication modules and the SST board to make optimal decisions regarding port activation, grid connections, etc.

In general, an ER is composed of input/output ports, an SST controller, a common DC/AC bus, a routing controller that contains a microprocessor and communication module, and a plug-and-play interface [35]. Figure 1.2 showcases an example of an ER model.

1.6.5 The energy hub

Humans use different energies in their daily life, such as electricity, heating, cooling, gas, etc. However, these energies are presented to the user separately, leading to energy loss and reducing the system's efficiency. The concept of EI demands the efficient integration and coupling of diverse renewable energy sources and RERs. The aim is to reduce power loss and maximize the system's output.
The idea is to use energy that might otherwise be lost in the system, such as the heat emitted during

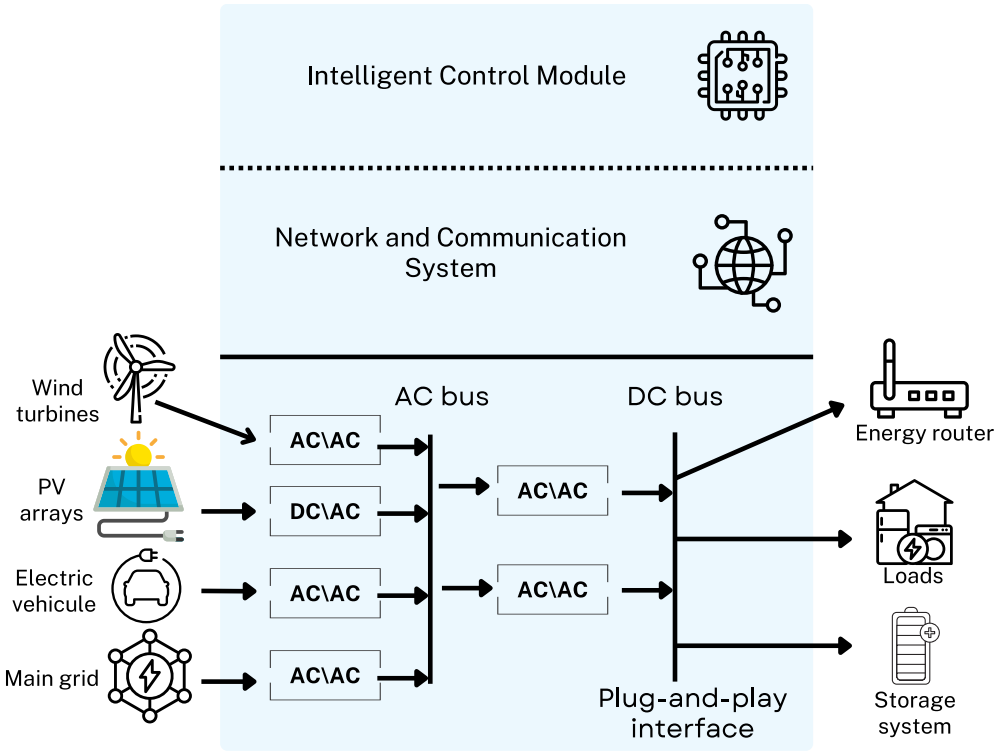

Figure 1.2: Example of an ER model

electricity production, which could be used in the heating system. To counter this issue, [36] proposed the first conceptualized implementation of a hybrid energy hub, that couples multiple energy carriers, such as electricity, gas, cooling, and heating, in an optimized and uniform manner [37].
The E-hub is a device that optimally combines various energy sources to meet the end user's demand [37]. It can be modeled as a combination of different converters, as stated by [38], namely fuel cells that use a chemical reaction to produce electricity, micro-turbines that use rotational energy to generate heat or electricity, and many more. The goal of an energy hub is to improve the efficiency, reliability, and sustainability of the energy system by managing distribution and energy storage, and reducing dependence on centralized power generation. An energy hub typically consists of the following components:

1. Input, also known as the energy source or supply: This may include RERs, such as solar panels and wind turbines, as well as conventional energy sources, such as natural gas.

2. Energy storage systems: This can include batteries, flywheels, and other forms of energy storage that can store excess energy generated by the energy sources and provide energy during periods of high demand.

3. Energy management system: The central control system that manages energy flow within the energy hub. It optimizes the use and storage of energy sources to meet energy demand and reduce energy waste.

4. Energy monitoring and control systems: These systems monitor and control the energy flow within the energy hub, providing real-time data on energy usage and enabling the energy management system to make optimal decisions.

5. Communication and control systems: This includes the hardware and software that enable communication and control between the different components of the energy hub and with the outside world.

6. Converters: The purpose of an E-hub is the interconnection of different energies into one system. To do that, the E-hub contains converters that transform the input energy into another form of output energy without reducing its quality. Examples include heat exchangers, inverters, fuel cells, and combustion engines.

The goal of an energy hub is to provide a more efficient, reliable, and sustainable energy system by integrating different energy sources and optimizing their usage. Thus, it is becoming increasingly important as the world moves towards a more decentralized, low-carbon energy system.

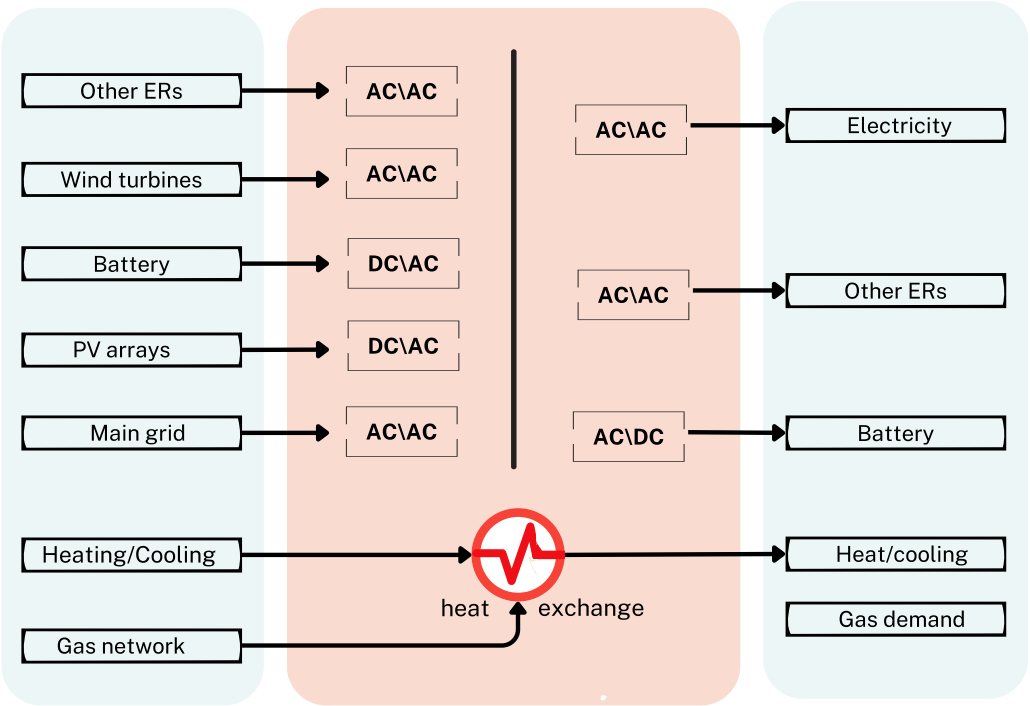

Figure 1.3: Example of an energy hub model

1.6.6 Smart meter

The smart meter is an electronic device that provides real-time measurement and recording of electricity, gas, or water consumption. It can communicate the measurements to the user via a secure communication network. The smart meter is a crucial component of the SG and EI technology [37]. It provides several benefits over traditional meters, including:

1. Accurate measurement: Smart meters provide more accurate energy consumption readings at regular intervals, reducing the need for manual meter readings and eliminating the need for estimated billing.

2. Real-time monitoring: With smart meters, consumers can monitor their energy consumption in real time and make optimal decisions about energy use and costs.

3. Improved energy efficiency: By providing consumers with detailed information about their energy consumption patterns, smart meters can encourage energy efficiency and help reduce energy waste.

4. Better outage management: In the event of a power outage, smart meters can help utility companies quickly identify and resolve the issue, reducing the duration and impact of outages.

5. Integration with SG technology: Smart meters can help ease the integration of RERs, energy storage systems, and other essential technologies into the energy network.

1.6.7 Microgrid

A microgrid is a small-scale, localized energy system that integrates DERs—such as solar panels, wind turbines, batteries, and controllable loads—to supply electricity to a specific area, like a neighborhood, campus, or industrial site. Unlike traditional power grids, microgrids can operate both while connected to the main grid and independently in "island mode" during outages or faults, enhancing energy reliability and resilience [39]. Microgrids require an intelligent management system to optimize their performance and manage the variability of renewable energy generation and demand. This functionality is often facilitated by an ER, which plays a central role in coordinating energy flow and control within and between microgrids. Figure 1.4 represents these components in the Microgrid topology.

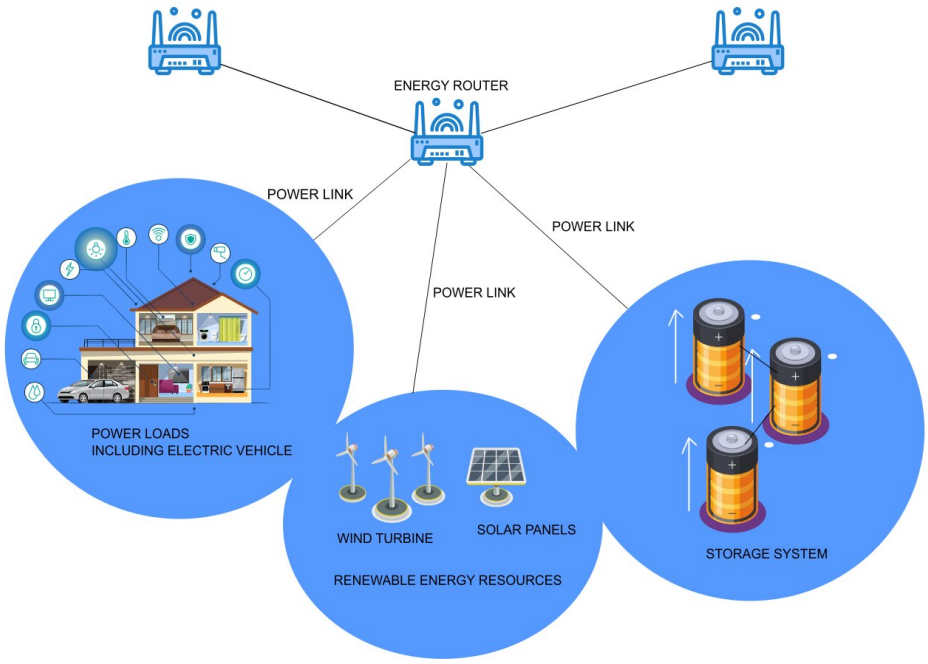

Figure 1.4: A simple breakdown of a Micro-grid structure

1.6.8 UAV Networks

Unmanned Aerial Vehicle (UAV) networks, also known as drone networks, consist of interconnected UAVs equipped with sensors, communication modules, global positioning systems (GPS), batteries, and an intelligent module [40]. UAVs can serve as mobile nodes for real-time monitoring, data collection, and communication within the energy system. Their mobility and autonomous operation make them particularly valuable in inaccessible or remote areas where traditional infrastructure may be limited. In the field of energy management, UAV networks contribute in several ways. First, they support infrastructure inspection and fault detection by surveying power lines, solar panels, and wind turbines [41], [42]. Second, UAVs enhance forecasting accuracy by collecting environmental data, such as solar irradiance and wind speed, which is critical for load and generation predictions [43]. Third, they assist in rapid response and recovery during outages by locating faults and enabling faster maintenance [44]. In addition, UAVs can act as communication relays to maintain grid connectivity in the event of system failures or disasters [45], [46].

1.7 EI software components

This section describes the major software components of EI:

1.7.1 Blockchain technology

Blockchain was first proposed in 2008 to secure Bitcoin transactions between accounts recorded by individuals. The blockchain has four essential elements as stated by [47]: smart contracts, decentralization, transparency, and traceability of transaction records, all of which are necessary features of the EI system.
The EI uses blockchain technologies to secure energy trading and enhance the efficiency and reliability of the grid in distributed energy transactions [48]. It can also be used for peer-to-peer energy trading, tracking renewable energy certificates, managing demand response programs, and ensuring energy data security. Each user can share the price of energy and consult the prices of other prosumers, thereby deciding which prosumer to buy from in a safe, decentralized manner.

1.7.2 Energy management software

EMS enables providers and customers to track, control, and optimize their energy use. It manages energy consumption while allowing users to make data-driven decisions to reduce energy waste, increase efficiency, and save money. It helps integrate diverse energy resources, such as solar and wind energy, by monitoring their availability and capacity in real time. The EMS schedules energy dispatch using optimization algorithms that account for predicted demand, time-of-use pricing, and renewable generation forecasts. This ensures that renewable energy is prioritized when available, storage is used strategically, and grid dependency is minimized.

It can also help businesses and consumers manage their energy usage across multiple locations, such as factories, offices, and homes.
One key benefit of the EMS is that it enables businesses and consumers to participate in demand response programs. These programs reduce energy consumption during periods of high demand, such as during a heat wave, by offering incentives to customers who reduce their energy usage.
The first EMS is the intelligent energy management software (IEMS) proposed by the FREEDM system center [37]. It optimally uses RERs and the storage system by adapting to the load demand curve. It minimizes circuit loss and regulates the voltage. Another example is the EMS proposed by [49]. It is a communication-focused system that integrates ThingSpeak, MQTT, and TCP/IP protocols into a smart energy platform. The system employs Mixed-Integer Linear Programming (MILP) for optimal scheduling and demonstrates how real-time data flow can be leveraged to enhance microgrid performance, scalability, and responsiveness.

1.7.3 Cybersecurity software

Cybersecurity software is critical in EI networks because it secures energy and monetary transaction in the grid. The complex structure of EI and its enormous coverage area make it more vulnerable to cyber-attacks. Therefore, building a reliable cybersecurity system is essential.
Cybersecurity software uses firewalls, intrusion detection and prevention systems, security information and event management (SIEM) systems, and identity and access management (IAM) systems to protect energy transactions and operational technology (OT) systems from malware, phishing attacks, denial of service (DoS) attacks, and other forms of cyber attacks.

1.7.4 Artificial intelligence and machine learning

Incorporating AI and ML into the energy sector will improve energy efficiency, reduce costs, and optimize energy use by analyzing vast amounts of data from sources such as SGs, weather sensors, and energy management systems. An example would be predicting energy demand, also known as

Load forecasting, using ML algorithms. ML algorithms can also be implemented in demand response programs to push consumers to shift their energy consumption to periods of low demand, reducing the need for expensive peak power and balancing the grid. AI and ML can analyze consumer behavior and make personalized recommendations for energy-saving actions, helping to identify and mitigate energy waste and inefficiencies, such as identifying and addressing energy leaks in buildings or detecting and repairing faulty equipment in industrial processes. By leveraging AI and ML insights, energy providers can achieve significant cost savings and improve sustainability.

1.7.5 Digital twinning

A digital twin is a virtual replica of a physical system. This concept was first introduced by Michael Grieves and John Vickers of NASA in a 2003 lecture on product lifecycle management [50]. This technology is widely recognized as one of the key enablers of Industry 4.0 [51]. Industry 4.0, also known as the Fourth Industrial Revolution, refers to the integration of digital technologies into manufacturing and industrial processes, transforming traditional factories into smart, interconnected, and data-driven systems. In the context of energy systems, digital twinning can be used to model the entire infrastructure or specific components such as an SG, microgrid, or ER, enabling real-time simulation, monitoring, and optimization [52].

Digital twinning is a groundbreaking innovation in the energy sector, offering transformative capabilities for monitoring, simulation, and optimization. The energy system is inherently complex and traditionally difficult to model with high realism due to its dynamic nature, interdependencies, and variability, especially when integrating RERs. However, digital twins overcome these limitations by creating virtual replicas of physical components such as microgrids, renewable sources, storage systems, and ERs. These replicas enable simulation of energy transfer processes without the risks associated with real-world testing, such as energy loss, system instability, or component failure. Digital twinning is also used at the SG level for power grid design, control center emulation, network security, and failure diagnosis [53].

1.7.6 Peer-to-peer energy trading

Electricity production techniques are rapidly developing, paving the way for consumers to become energy producers and actively participate in the energy market [54]. Prosumer is the new term proposed for the user who buys and sells energy. Peer-to-peer energy trading refers to electricity trading between prosumers and consumers. Prosumers can sell their surplus energy to the grid or to other consumers, or store it in DESDs for later use.
The traditional electricity market is unidirectional, with electricity traveling over long-distance transmission lines, leading to energy losses and delivery latency. However, P2P electricity trading involves bidirectional trading within a small geographical area, thereby minimizing energy loss and latency [54]. P2P has three types:

1. Complete P2P where users, also known as peers, trade with one another without the interference of a central coordinator,

2. Centralized P2P where peers trade with one another through a coordinator that controls and manages the transactions,

3. Hybrid P2P is a combination of complete and centralized P2P, where the chosen coordinator changes every transaction in the P2P system based on a multitude of parameters [55].

P2P energy trading is a particular application of the EI. It is important to note that although the EI strives to be a complete P2P network of transactions and energy trade, it is still far from achieving that goal.

1.7.7 Plug and play interface

A plug-and-play interface in an energy network is a user-friendly mechanism that allows the effortless integration of various energy devices and systems into the network. The plug-and-play interface is a logical function implemented within the ER's control firmware. It helps connect loads, RERs, and storage devices to the ER, forming a single, interconnected system without specialized technical knowledge or expertise, i.e., a microgrid. The plug-and-play interface simplifies the configuration and management of an MG, allowing users to easily attach and detach devices. It also improves network efficiency and facilitates the creation of microgrids.

Figure 1.5 presents the layered architecture of the EI network, synthesizing the physical and software components described above. Each layer incorporates specific components that collectively enable the functionality of the EI system.

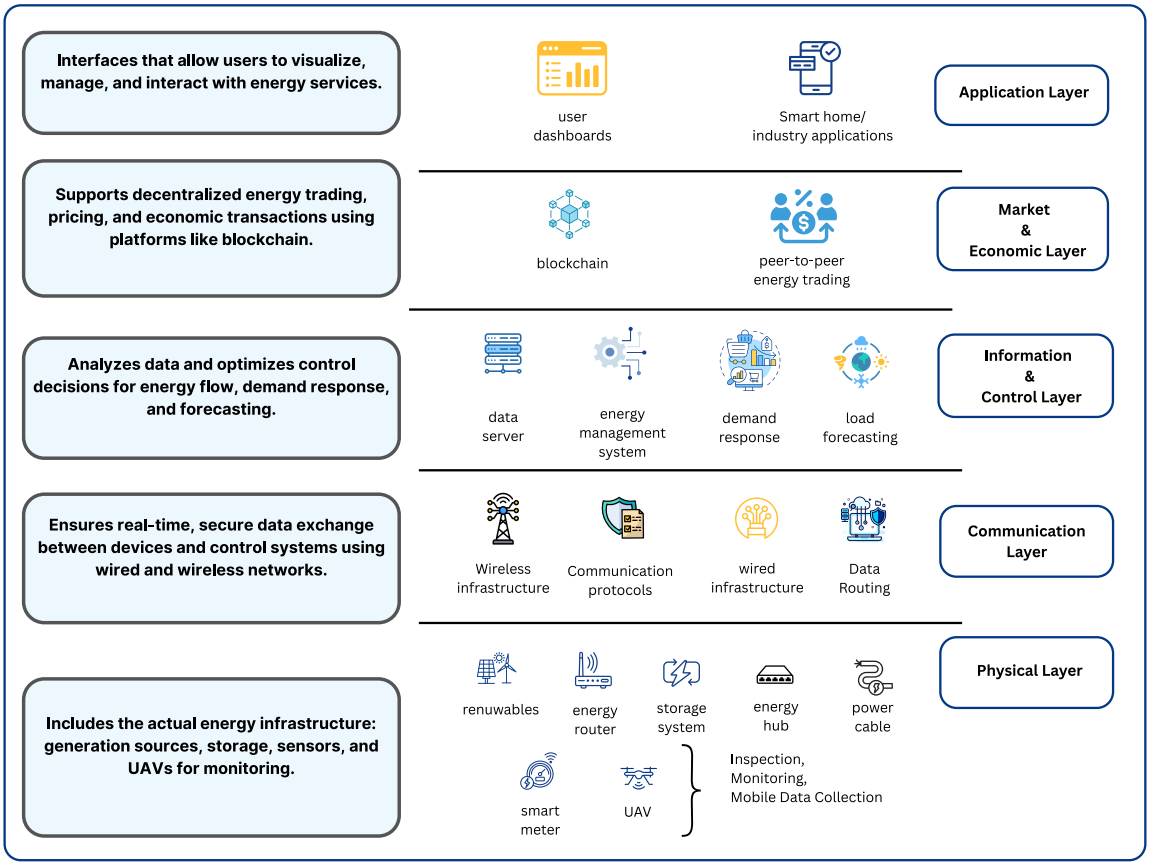

Figure 1.5: Layered architecture of the EI network

1.8 Working principle of EI

EI uses green energy produced by DERs to power the system. The energy produced travels through electric cables to the ER. The ER has two key components: SSTs and ICTs, which are managed and controlled by the IEMS.

After receiving energy from DERs, the ER makes optimal decisions based on information sent to it by the smart meter device and the storage system.
These decisions include providing a load with the energy required to power it, transforming the energy from AC to DC or from DC to AC via its SST module, and adjusting the voltage level based on the load's power parameters. The EMS also coordinates energy generation, storage, and consumption to ensure that the right amount of energy is delivered at the right time. This process is known as microgrid scheduling. An example of this is the hybrid approach proposed by [56], which combines day-ahead and

real-time optimization, solved using an improved Artificial Rabbits Optimization Algorithm (IAROA), to minimize operational costs based on current load demand, energy prices, and generation capacities. ERs communications with DERs and storage systems, and loads facilitate the following planning based on the FREEDM system proposed by [20]:

1. During the sunny periods of the day, the photovoltaic system asks the ER to start energy production, to which the ER responds based on load demand and current storage.

2. During sunset, solar panels stop generating electricity. The ER sends an activation message to the storage system.

3. At night, when demand decreases, the ER sends a message of activation to the wind turbines or uses DESDs to charge the electric vehicle.

To date, there is no standardized IEMS architecture. However, many studies have proposed custom IEMS frameworks using various approaches. These include traditional optimization techniques [57], metaheuristic algorithms such as Bacterial Foraging Optimization (BFO) [58] and the Artificial Immune System (AIS) [59], as well as more recent hybrid metaheuristics that combine Arithmetic Optimization Algorithm (AOA), Arithmetic Valued Optimization Algorithm (AVOA), and Grasshopper Optimization Algorithm (GOA), as demonstrated by [60]. In addition, artificial intelligence-based methods, such as the reinforcement learning strategy proposed by [61].

1.9 Energy internet challenges

Energy systems like SGs and the EI heavily rely on renewable energy, which is subject to variability and beyond direct human control. RERs are also complex and difficult to manage optimally. This makes the development of a reliable and sustainable energy system a very challenging task. The most well-known challenges include energy routing, demand response, and Load forecasting. Addressing these challenges requires extensive research and collaboration among experts across various domains to develop consensus-based solutions that address the unpredictability and volatility of DER. Figure 1.6 depicts the top ten countries with the most research in energy routing, Load forecasting, and demand response for EI and SGs.

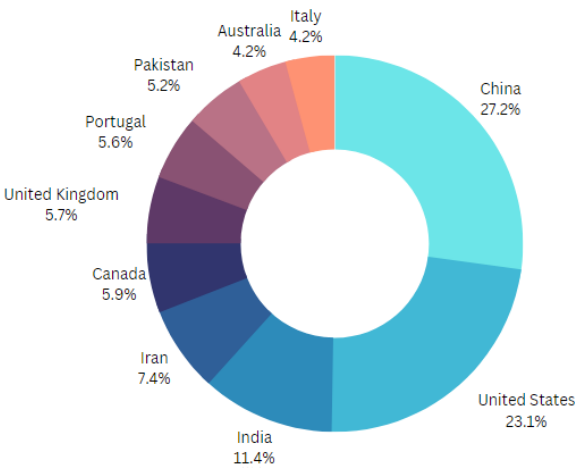

Figure 1.6: The 10 countries with the most research in energy routing, Load forecasting, and demand response

1.10 Conclusion

This chapter provides a comprehensive overview of the historical development of modern energy systems, tracing the transition from traditional power grids to SGs and, more recently, to the EI. The analysis highlighted how technological, infrastructural, and conceptual advances have progressively shaped the evolution of these paradigms. Having established the foundational architecture, components, and operational principles of SG and EI, the natural next step is to examine how energy is routed effectively within these complex systems. The following chapter therefore shifts the focus from the structural foundations to the algorithmic strategies used to address these routing challenges. It provides a comprehensive classification of optimization approaches and examines the complementary roles of load forecasting and demand response in enhancing routing efficiency and system reliability.

Chapter 2

Classification of Energy Routing Strategies in Energy Internet and Smart Grids

Contents

2.1 Introduction . . . 19
2.1.1 Energy routing algorithm . . . 19
2.1.2 Load forecasting . . . 22
2.1.3 Demand response (DR) . . . 24
2.2 Optimization algorithms used in energy routing . . . 25
2.2.1 Mathematical optimization framework . . . 25
2.2.2 Autonomous routing algorithm . . . 31
2.2.3 Heuristic and Bio-inspired metaheuristic optimization algorithms . . . 32
2.2.4 Topology-based solutions . . . 33
2.3 Conclusion . . . 38

2.1 Introduction

SG and EI have emerged as advanced paradigms enabling decentralized energy exchange, including P2P energy trading. While these systems offer significant opportunities for efficiency and sustainability, they also introduce new challenges, particularly in energy routing, load forecasting, and demand response.

This chapter provides a detailed classification of different optimization strategies applied in SG and EI, highlighting their advantages, limitations, and applicability. In addition, it examines key influencing concepts—such as load forecasting and demand response—that play a central role in improving the reliability, efficiency, and adaptability of decentralized energy systems.

2.1.1 Energy routing algorithm

Sending energy from a supplier to a consumer in an extensive network requires various conditions to be checked, such as the delivery speed, quality of energy delivered, minimal energy loss in transmission, etc. These conditions can be achieved using an efficient and reliable routing algorithm. The energy routing algorithm aims to determine the most cost-effective and efficient path for energy to flow from one user to another in the network. It considers energy demand and resources, storage capacity, transmission losses, and energy cost to determine the optimal route for energy transfer. Energy routing differs from traditional data routing because it is demand-based, which means the source and destination are unknown as stated by [17]. Figure 2.1 depicts the top ten countries with the most research in energy routing.

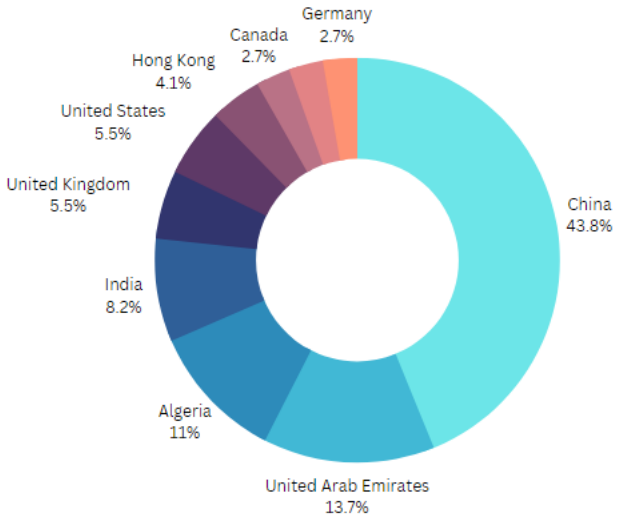

Figure 2.1: The 10 countries with the most research in energy routing

Energy routing algorithms are intended to address problems such as subscriber matching, efficient path determination, and transmission scheduling. Figure 2.2 describes the yearly progression of research made to solve these problems.

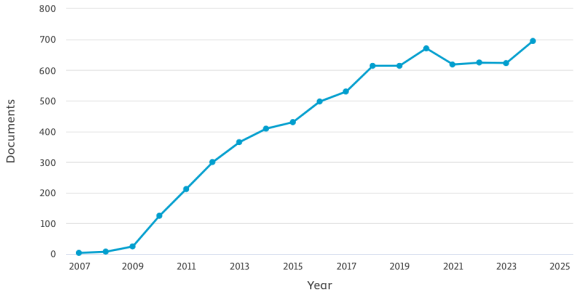

Figure 2.2: Yearly progression of research in efficient path, matching subscribers, and scheduling

Pair matching

Pair matching, Subscriber matching, or optimal producer's subset is a function performed by the ER or the control center (CC) that determines which supplier or group of suppliers can satisfy the load energy demand of a specific consumer in real-time, considering the energy price, distance, customer priority, power type, power loss, and energy amount. Many researcher, such as [62]; [63]; [64] have attempted to solve this problem.

Energy efficient path

Identifying the most cost-effective and efficient pathways for energy to flow from its source to its destination is vital to route energy efficiently in the EI. Finding the optimal path involves many constraints, such as power link impedance, network congestion, distance, energy transmission loss, and energy conversion loss.

To calculate the power loss of a given path, it's necessary to measure both the active and reactive power losses. Active power and reactive power are two fundamental concepts in electrical engineering. They define the flow of electrical energy in a system. Both are crucial in maintaining the stability and efficiency of an electrical network.

Active power, often called real power, is measured in watts (W) and represents the portion of electrical energy that performs useful work, such as illuminating a light bulb or driving an electric motor.

Reactive power, although it does not directly perform useful work, is essential for the operation of certain electrical equipment and transmission systems. It is exchanged between inductive and capacitive elements in the circuit, helps generate magnetic fields in motors and transformers, and plays a vital role in maintaining voltage stability across transmission lines. However, in much of the literature, reactive power losses are often neglected in P2P energy routing models, as it is typically assumed that reactive power compensation is handled by the utility grid or local compensation devices.

In such cases, the power loss along a given path is considered to be only the active power loss. The following steps outline the procedure for calculating active power loss along a transmission path.

For every power line of the given path, active power loss is calculated using Equation 2.1 [65]:

$$P_{\text{loss}} = R \cdot I^2 \tag{2.1}$$

Where R represents the resistance of the component, measured in ohms, and I represents the current flowing through the component, measured in amperes. According to Watt's Law:

$$P = V \cdot I \tag{2.2}$$

Thus:

$$I = P/V \tag{2.3}$$

where P is the power, and V represents the voltage across the component, measured in volts

By substituting the value of I from Equation 2.3 into Equation 2.1 , the power lost in transmission is calculated as follows:

$$P_{\text{loss}} = \frac{R}{V^2} \cdot P^2 \tag{2.4}$$

Equation 2.4 provides a simplified way to calculate the power loss associated with transmitting power between ERs. However, it is important to note that this equation assumes an idealized scenario where there is only the transmitted power (P_{tran}) and no existing power (P_e) on the line [62].

In more complicated situations where power (P_e) is already present on the line, Equation 2.5 is more fitting as stated by [66]:

$$p_{\text{loss}} = \frac{R}{V^2} \cdot ((P_{tran} + P_e)^2 - P_e^2) \tag{2.5}$$

Where p_{loss} is the active power lost in transmission, R is the resistance, V is the voltage, P_{tran} is the power being transmitted, and P_e is the existing power already flowing on the line.

In SGs, a transmission path typically consists of power lines and ERs. From the source to the destination, energy flows through a combination of these components. Power is lost at each ER due to conversion inefficiencies, and additional losses occur along the power lines due to resistive heating in the cables. In conclusion, the power loss due to conversion occurs at the ER level and is calculated as follows:

$$P_{\text{conv}_{(i)}} = (1 - \eta) \times E \tag{2.6}$$

Where $P_{c_{(i)}}$ is the power loss due to conversion, η is the efficiency of the conversion process (a value between 0 and 1), and E is the energy being transmitted.

The total active power loss along a given path is the sum of the active power losses (P_{loss}) in transmission through all power lines, and the power losses due to conversion at each ER along the path. This Total loss is calculated as shown by [66] using Equation 5.1:

$$Total p_{\text{loss}} = \sum_{i \in R} P_{\text{conv}_{(i)}} + \sum_{(i,j) \in R} P_{\text{loss}_{(i,j)}} \tag{2.7}$$

where R is the list of ERs, i represents an ER, $(i, j) \in R$ represents a power line between nodes i and j, $P_{\text{conv},i}$ is the power loss due to conversion at router i, and $P_{\text{loss},(i,j)}$ is the transmission power loss along

the power line between nodes i and j. The term $P_{\text{total\_loss}}$ denotes the total active power loss along the path.

The quickest route may not be the best, as it could cause greater power loss or insufficient link capacity to transport the energy [67].

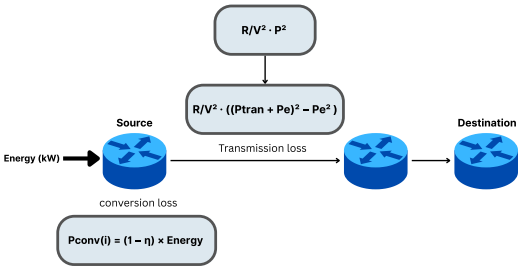

Figure 2.3: Steps of power lost in transmission and conversion

Transmission scheduling

As with the Internet, EI can suffer from overload and congestion. Congestion can occur due to an imbalance between energy stockpiles and energy demand, transmission infrastructure obstructions, voltage instability, unpredictable power generation, or bidirectional power flow. It can cause delays, degrade service quality, or lead to total system breakdowns. Thus, it is necessary to manage energy flow across the network to prevent this by scheduling transmission using techniques such as Time-division multiple access (TDMA) [37].

[68] presented an optimal communication scheduling scheme for smart meters based on a chain of wireless network channels with equal and increasing transmission rates. The work used the Shannon capacity formula to determine the transmission power model.

It is worth noting that energy dispatching can be single- or multi-source, i.e., the load energy demand can be satisfied by a single or multiple sources.

2.1.2 Load forecasting

Load forecasting is a method for predicting electricity consumption by users at a specific time in the future. Predicting energy demand lowers power generation costs and supports the development of an organized and reliable power system.

Future consumption patterns of customers is influenced by various dynamic factors, including weather conditions (such as temperature, humidity, solar irradiance, and wind speed, cloud cover, visibility), indoor environmental parameters (such as indoor temperature and humidity), the time of day, season of the year, day of the week (weekday vs. weekend), holidays, and behavioral patterns of consumers. To ensure accurate predictions, load forecasting models require realistic datasets that capture these variables comprehensively [69].

To prepare such data for forecasting, the key preprocessing steps involve: Data Collection, Data Cleaning which Handles missing values and sensor errors, Data Normalization, Feature Engineering, Data Segmentation which Divides data into training, validation, and testing sets, Resampling/Aggregation which Converts data into a consistent time resolution (e.g., 15-minute, hourly, daily) suitable for the forecast horizon, and finally, Correlation Analysis that Evaluate how each factor (e.g., temperature, time, day type) influences energy consumption to refine the model inputs. In recent years, several studies have moved beyond algorithm design to develop physical and software platforms that support accurate, scalable load forecasting in SGs. For instance, [70] proposed an edge computing framework that integrates a load forecasting model with task offloading strategies, thereby enhancing system responsiveness and computational efficiency. The authors in [71] developed a cloud-edge collaborative method in which a pool of pretrained forecasting models is deployed and incrementally updated on edge devices to provide adaptive, localized predictions. The study in [72] introduced a spatio-temporal graph convolutional model within a distributed edge-enabled system, using smart sockets as data nodes to

enable real-time forecasting. Similarly, [73] proposed FedForecast, a federated learning framework that allows edge devices to collaboratively learn a global forecasting model while preserving user privacy and data location. Complementing these efforts, [74] designed a scalable compute continuum architecture that spans edge-to-cloud infrastructure, comparing centralized and federated forecasting schemes to support flexibility, privacy, and performance in energy prediction tasks. Another study [75] introduced a low-cost embedded load-forecasting platform based on a Raspberry Pi. This system supports edge-level short-term forecasting using lightweight ML models (e.g., k-NN, SVR), demonstrating that accurate, private, and sustainable forecasting can be achieved without cloud infrastructure. The load forecast is divided into three main categories: short-term, medium-term, and long-term.

Short-term load forecasting (STLF)

refers to the prediction of electricity demand over short horizons, typically from one hour to several days ahead. Recent STLF studies leverage various intelligent approaches to enhance forecast accuracy. Several works focus on hybrid deep learning models, such as combining LSTM with transformer architectures [76], BiGRU with CNN [77], or GRU with TCN [78], while others integrate metaheuristic optimization, such as Beluga Whale Optimization, to fine-tune hybrid models [79]. Ensemble-based strategies are explored by [80, 81, 82], offering robust and adaptive performance under data drift. Graph-based deep learning is applied by [83] to capture spatial dependencies, whereas personalized federated learning is used by [84] to address privacy and data heterogeneity. Further privacy-preserving approaches are proposed by [85] using encryption and a decentralized architecture. Traditional machine learning methods, such as SVR, are employed by [86], while [87] tackles data scarcity using meta-learning for few-shot prediction.

Medium-term load forecasting (MTLF)

refers to the prediction of electricity demand over time horizons ranging from a week to a year in the future. It is essential for strategic planning tasks such as grid maintenance scheduling, seasonal energy procurement, and contract management. Recent MTLF studies apply a range of machine learning and deep learning methods to enhance forecast accuracy. Ensemble-based approaches are widely used to improve robustness and adaptability, as proposed by [82], which combines multiple models: neural networks, linear regression, support vector regression, random forests, and sparse regression. Hybrid models that integrate deep learning and optimization are explored by [88], where CNN and SVM are combined with Coronavirus Herd Immunity Optimization (CHIO) for feature selection and hyperparameter tuning. Classic machine learning models are used by [89] for district-level medium- and long-term forecasting, employing ANN-NAEMI, MLRM, and AdaBoost. Deep learning strategies are also applied by [90], which proposes a multiscale LSTM model trained on half-hourly, daily, and monthly time frames. Parameter-optimized SVR is introduced by [91] using a hierarchical state transition algorithm for tuning, while [92] evaluates machine learning (SVM, RF) and deep learning (LSTM, NARX) techniques for regional forecasting of electricity demand.

Long-term load forecasting (LTLF)

refers to the prediction of electricity demand over extended periods, typically ranging from one year to several decades in the future. It is critical for infrastructure planning, policy development, investment decisions, and grid expansion strategies. Unlike short- or medium-term forecasting, LTLF focuses less on operational detail and more on macro-level planning and resilience of power systems. Recent LTLF studies have increasingly adopted advanced deep learning and hybrid approaches to enhance forecasting accuracy under complex, long-range conditions. Ensemble-based deep learning is applied by [93], which integrates a feature extraction module, Densely Connected Residual Blocks (DCRB), LSTM layers, and ensemble thinking to forecast load trends across regional dispatch centers. Hierarchical attention mechanisms are introduced by [94] through the LTSNet model, which uses residual self-attention blocks to capture high-dimensional, long-term dependencies in time series data. Hybrid methods combining artificial neural networks with optimization strategies are proposed by [95], where ANN is coupled with

Firefly Optimization to assess long-term reliability indicators such as power losses and idle energy. A more traditional but effective ANN model is presented in [96], which uses smart meter data and climate correlation analysis to estimate long-term distribution-level demand.

2.1.3 Demand response (DR)

DR is used in EI to manage electricity consumption during periods of high demand or supply constraints. It motivates consumers to reduce energy consumption during peak periods, such as hot summer afternoons or cold winter evenings, by offering encouragement or financial rewards. DR is used to solve the imbalance between energy reserve and demand. This imbalance could push both sellers and customers to buy energy from the traditional grid, thereby increasing costs and potentially crippling the entire grid, as stated by [97]. DR can reduce peak demand and improve grid reliability, saving utility companies and consumers money and reducing greenhouse gas emissions.

Automated demand response (ADR)

ADR uses intelligent systems, such as smart meters, to adjust energy use based on diverse criteria, including energy prices and weather. Sensors in an ADR system monitor energy consumption, while automated controls use the data to manage energy use to meet users' energy needs. During peak times, for example, the ADR system automatically turns down air conditioning units or dims lights in commercial buildings to reduce electricity consumption, preventing blackouts, and relieving strain on the power grid.

Price-based demand response (PBDR)

PBDR encourages users to lower their consumption by manipulating energy prices based on demand. Users are charged more during high-demand periods, prompting them to reduce their energy consumption, thereby helping balance the grid and avoid blackouts. Price-based DR programs consist of four types:

1. Time-of-use pricing (TOUP): TOUP divides the day into periods based on the demand as explained by [98]. When electricity generation costs and demand are low (e.g., in the dead of night), the rate charged for electricity is drastically reduced. When both generation costs and demand are high (as on a hot summer afternoon), the electricity cost rate is significantly higher [99].

2. Real-time pricing (RTP): Electricity prices rise and fall throughout the day, with higher prices during peak demand. Electricity cost rates depend directly on changes in wholesale power prices [98].

3. Critical peak pricing (CPP): It works similarly to TOU. However, it increases the prices tremendously during selective peak periods throughout the year, where normal demand response techniques do not work. This program is used for a couple of hours yearly to improve power system reliability [98]. The time and duration of the CPP energy cost are prearranged.

4. Inclining block tariffs: the price of electricity is divided into several blocks based on a consumer's total consumption [98]. The first block of electricity is the most cost-effective. As the customer's electricity usage increases throughout the month, the electricity purchased will eventually be transitioned to Block 2, which is more expensive. This cycle is repeated indefinitely as the electricity consumption increases, and the cost moves to the next block [100].

Incentive-based demand response (IBDR)

IBDR is a system that incentivizes users to minimize electricity consumption during peak demand periods, such as national and international holidays and events that trigger spikes in energy consumption, by offering financial rewards. This system is designed to alleviate stress on the power grid during peak demand, helping prevent blackouts while promoting the stability and reliability of the power system. An excellent example of this is presented in the work by [101], which proposes a demand-side

management (DSM) strategy tailored for smart urban buildings. In this approach, electrical appliances are categorized as deferrable or non-deferrable, and an optimized appliance scheduling model is applied using a hybrid metaheuristic algorithm that combines the Improved Sine Cosine Algorithm (ISCA) and the Grasshopper Optimization Algorithm (GOA). This intelligent load management reduces peak loads and electricity costs without compromising user comfort. Incentive-based demand response programs require smart meters (SMs) to monitor electricity usage in real time, enabling users to identify peak hours and reward consumers who reduce their usage during those times.

Behavioral demand response (BDR)

In recent years, the novel behavioral demand response (BDR) model, has been the subject of growing attention. Contrary to other DR programs, BDR takes advantage of human psychology rather than economic indicators as a motivating force to encourage users to minimize their electricity consumption during times of peak demand as explained by [102]. Customers voluntarily reduce demand in response to a personalized home energy report the system sends periodically. Figure 2.4 presents the classification of the discussed demand-response methods.

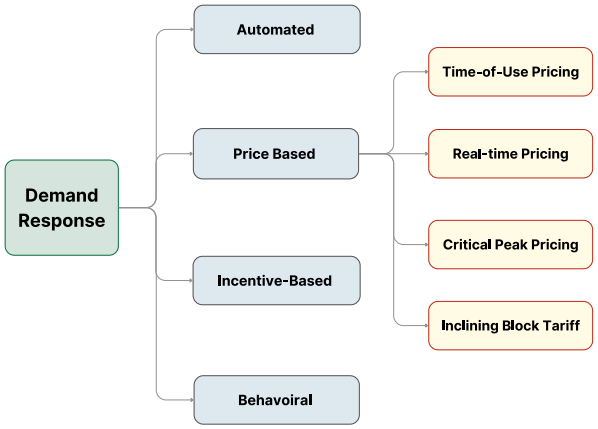

Figure 2.4: Classification of demand-response methods

2.2 Optimization algorithms used in energy routing

Numerous solutions have been proposed to address routing challenges within the EI framework. These solutions encompass a diverse range of methodologies, including graph theory, game theory, multi-agent systems, metaheuristics, stochastic approaches, and topology-based methods, among others. Each of these approaches offers distinct perspectives and methodologies to optimize energy routing, thereby improving the efficiency and reliability of EI.

2.2.1 Mathematical optimization framework

Graph theory-based routing algorithm

Graph theory-based optimization is used in discovering the shortest and most optimal route between two nodes, often time in data routing. It is also used for optimal path selection in EI and SG, given the similarities between EI and the Internet in terms of routing and infrastructure. EI network is modeled as an undirected weighted graph G={V, E, W} where nodes (V) represent users (microgrid, ERs, etc) and edges (E) describe the transmission lines between them. Every edge is assigned a weight (W) that represents distance, line transmission capacity, power loss, or cost. Algorithms often used in graph theory are Dijkstra's and Bellman-Ford's. Figure 2.5 presents the routing steps in EI and SG.

[103] proposes a graph-based routing algorithm for P2P energy trading in SG, addressing producer selection, path efficiency, and congestion. Using depth-first search, it evaluates all source-load paths,

Table 2.1: Comparison of different DR methods.

Method	**Advantages**	**Disadvantages**
Automated Demand Response	It enables effortless automation and integration with SG systems, responds swiftly and spontaneously to fluctuations in electricity demand, helps reduce peak demand, and improves grid stability.	It could require significant infrastructure and technology costs, as well as ongoing maintenance and monitoring to ensure adequate performance. A lack of consumer comprehension may lead to mistrust or rejection of the technology.
Price-Based Demand Response	It provides clear and immediate financial incentives for reducing energy consumption and is easier to automate and implement with the help of SG technologies. It helps satisfy peak energy demand and avoid the need for new power generation facilities.	It is not practical for low- or fixed-income customers; it is hard to understand and could lead to price volatility and unpredictability for consumers.
Incentive-Based Demand Response	Provides clear financial incentives to reduce energy consumption during periods of high demand. It can also target a specific group. It can be combined with other demand response methods to reduce energy consumption during peak periods, thereby easing strain on the electrical grid and mitigating the risk of power outages.	It can be expensive to implement. If not carefully designed and implemented, the system is susceptible to manipulation or deception, potentially leading to gaming or fraud.
Behavioral Demand Response	Cheaper implementation. Helps reduce energy consumption with no financial cost. Builds a culture of energy efficiency and conservation. More efficient in the long term.	Relies on the customer's willingness to reduce their energy use, which can be challenging.

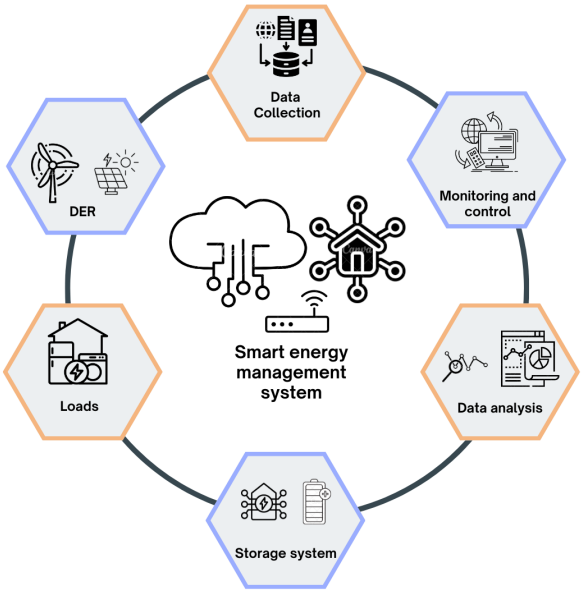

Figure 2.5: Energy routing steps

prioritizing minimum-loss routes (power loss is calculated using equation 5.1). Producer subsets favor single-source solutions for reliability unless capacity constraints force multi-source use. Congestion triggers dynamic rerouting via underutilized lines. The framework uniquely supports multi-source/multi-load (MSML) scenarios, enabling simultaneous transactions.

A novel two-stage graph-theory-based routing algorithm is proposed by [35]. The first stage is the routing policy of day-ahead P2P transactions. The ER predicts energy usage based on historical transaction data and uploads trading information to the communication center. The optimal route is determined using a minimum-cost routing algorithm based on OSPF and policy-based routing. Paths between two nodes are determined using a depth-first search algorithm (DFS). Because the algorithm is executed offline, it incurs little computational cost. The second stage is the routing policy for intraday power balance. Here, nodes requesting energy broadcast a query to the communication center, which determines the transmission path using the DFS algorithm. Congestion is avoided by minimizing the number of transmission paths and the power allocated to each route. Heavy load demand is managed by using the multi-source scenario.

[104] introduced an energy routing algorithm centered on power transactions, focusing specifically on the computational complexity of the mesh topology employed in the EI. It aims to find a minimum-energy-loss path (MLP) without congestion and to balance demand and supply for both small and heavy loads in the SG, while maximizing energy cost. To achieve these goals, the authors combines a matchmaking tradeoff mechanism (for buyer-seller pairing) with the Dijkstra algorithm to identify minimum-loss paths (MLPs). The algorithm then checks if the found MLPs can be transmitted within the capacity of the shared lines and the energy bought. The final solution is chosen based on the constraints of an MLP with no congestion.

The algorithm proposed by [105] uses the shortest path algorithm (Dijkstra algorithm) to select a minimum loss path. It models the network as a graph, where the node and edge weights represent the conversion loss of ERs and the transmission loss, respectively. To enhance the efficiency of cable layout among ERs within a cost-effective EI framework, a tailored Minimum Spanning Tree (MST) algorithm has been introduced. Moreover, a mesh topology derived from an adapted version of the Prim algorithm is employed to increase reliability and reduce construction expenses.

An algorithm for source selection based on the OSPF routing method is proposed by [65]. It constructs a weighted graph from the network, where nodes represent ERs and edges represent power

links. The weights assigned to nodes and edges represent power loss. Routing tables contain the total power capacity, power link capacity, and efficiency of all devices, routers, and power links. ERs communicate this information to all routers whenever the topology changes. An algorithm is proposed for multi-source selection under heavy load.

[106] proposed an information model for ERs based on the IEC 61850 standard to use in the communication and control of microgrids. The model includes logical nodes (LNs) and data objects (DOs) to represent various ER parameters, including voltage, frequency, power ratings, efficiency, and temperature. The ER communicates this data to the distribution system operator/microgrid central controller, which uses it to optimize generator dispatch and determine efficient power flow routes. The routing algorithm uses information about power line characteristics to calculate real-time current demand at each node. Using an objective function for power loss calculation, the algorithm computes the Objective Function Value (OFV). Once the algorithm has determined the least-cost path for each neighboring energy source, it selects the source with the minimum overall cost. This source serves as the starting point, or "foundation," for establishing the virtual circuit.

In the same context, [55] proposed a semi-decentralized routing algorithm aimed at achieving minimum-loss transmission. The algorithm functions by exploring all routes between the source and the destination. It then selects the path with the smallest power loss for energy transmission. The study focuses on a community-sized network.

The ER performs route calculations individually and directs energy when no overlapping paths are detected. In scenarios where overlaps occur, a centralized system is employed. The ER employs a depth-first search (DFS) algorithm to identify all feasible non-congested routes linking energy trading pairs.

[107] introduced a method for managing energy flow in the SG. This method aims to find the optimal way to deliver energy from suppliers to consumers, accounting for supply and demand levels and the limits of power lines. They present two main strategies: the Global Optimal Energy Routing Protocol (GOER) and the Local Optimal Energy Routing Protocol (LOER). The grid is represented as a graph with nodes for users and edges for power lines. Each line's cost depends on factors like distance and the amount of energy it carries. Users can get energy from multiple sources, and suppliers can send energy to multiple users.

The efficient path-loss problem is addressed by [108] for a topology of 9 nodes, each representing a microgrid system. It also aims to address the subscriber-matching problem and prevent congestion. The authors classify ERs into three categories based on their roles. The first category is the 'load ER', representing an ER with an energy demand. The second type is the 'source ER', which represents an ER with excess energy to sell. The last type is the 'route ER', which helps in energy transmission and contributes to balancing the energy system. Source ERs sell their excess energy at a specified price. The algorithm aims to identify the best source ERs for the load ER, meeting its demand while minimizing power loss during transmission and into consideration the price. To achieve this, the authors present a graph-theoretic routing strategy to address these problems while avoiding congestion. Congestion is mitigated by selecting the second-best solution, even if it elevates the total energy price and power loss for the 'load ER'.

The energy routing protocol proposed by [109] employs a semi-decentralized approach that combines decentralized and centralized phases to optimize energy transmission in EI. The network is modeled as a graph where each ER exchange collects information, establishing a basic understanding of the network in a decentralized manner. ERs act as agents by sharing crucial information, such as power lines and routing conditions, over a platform. Each ER uses Depth-First Search (DFS) to identify all possible paths between source-sink pairs, and then computes multi-path solutions (splitting power across paths) using nonlinear programming to minimize transmission loss, while considering line capacity constraints. If the CC detects collisions between two or more generated paths, it resolves them centrally. This involves finding the optimal paths while adhering to power-loss constraints and avoiding congestion and collisions for all pairs of source and sink.

In the same context, an innovative energy routing scheme proposed by [15] addresses the efficient path problem and the producer's subset problem in SGs. It formulates the producer's subset problem as a fractional knapsack problem and solves it using the greedy algorithm. The Dijkstra algorithm is used

to determine the optimal power transmission path. Simulations affirm the effectiveness of the proposed method in resolving these routing challenges within a small residential area network. [110] proposed an Optimal-Walk Multi-path Power Routing (OMPR) approach for P2P energy trading in EI. The optimal walk connectivity algorithm computes the shortest paths based on the number of hops between all nodes. The Multi-path Power Routing (MPR) algorithm solves the producer subset problem, prioritizing single-path solutions for speed. It also handles congestion by rerouting power during link disruptions. [111] introduces a novel energy routing strategy that minimizes carbon emissions and power losses in EI. It employs the DFS algorithm to identify all feasible energy supply paths between sources and loads within a graph-structured network. These paths are then evaluated using an improved Unified Non-dominated Sorting Genetic Algorithm III (U-NSGA-III), which optimizes the dual objectives of carbon reduction and loss minimization. The enhanced U-NSGA-III incorporates Riesz's energy to generate uniformly distributed reference points along the Pareto front, ensuring balanced exploration of trade-off solutions, and employs Parent-Centric Crossover (PCX) to diversify offspring generation using multiple parents, thereby escaping local optima. [112] proposes a Minimum Loss Cost Path (MLCP) routing strategy for the EI, addressing the loss costs of DERs. EI is modeled as an undirected weighted graph, where node weights represent DER conversion losses and edge weights reflect transmission losses, both quantified by marginal generation costs. This paper aims to identify paths that minimize total loss costs by combining transmission losses and the marginal costs of DERs. The decentralized MLCP algorithm evaluates feasible paths within a predefined hop limit and selects the optimal route. During congestion, power is redistributed across multiple paths to avoid line overloads while maintaining minimal loss costs.

[113] introduces two innovative strategies for P2P energy trading: ST1 (Supply-Demand Matching) and ST2 (Distance-Based Matching). ST1 dynamically pairs households with surplus energy (producers) to those with high demand (consumers). It uses a normalization matrix to calculate hourly coefficients based on real-time supply and demand data, prioritizing economically efficient matches where surplus and deficit align. This strategy maximizes local energy utilization but may limit trades during periods of low supply-demand overlap. ST2 optimizes grid efficiency by prioritizing trades between physically proximate households. The network is modeled as a radial tree (common in residential grids), where proximity is determined by hop count—the number of connections between nodes. Households closer in the network hierarchy (e.g., parent-child or shared branches) receive lower trading coefficients, reducing transmission losses and encouraging localized energy exchange. Unlike ST1, ST2's coefficients are static, derived once from the network topology.

[114] proposed a Minimum Loss Routing (MLR) algorithm that selects energy-efficient paths using a modified Dijkstra algorithm incorporating capacity constraints. In this approach, consumers and producers are matched based on a real-time bidding mechanism. The transaction sponsor (either a consumer or a producer) initiates the bidding process, and counterparties respond based on price and availability. When the consumer is the transaction sponsor, producers are sorted in ascending order of their bidding prices, ensuring selection of the most economical suppliers. Congestion in the MLR algorithm is handled by transmitting power in packets across multiple paths, using real-time capacity updates. In [115], the energy network is modeled as a tripartite graph to simultaneously represent buyers, sellers, and transmission paths (bridge nodes). Exhaustively exploring all possible routes up to a specified hop count, without relying on traditional shortest-path algorithms, the authors develop an Extended Depth-First Branch-and-Bound (E-DFBB) algorithm to prune paths with low utility. This approach ensures that each buyer considers only efficient and feasible paths when selecting energy routes.

[116] proposes an energy routing protocol based on graph theory. The microgrid network is modeled as a graph using an adjacency matrix to represent sparse P2P connectivity among nodes. All multi-hop paths between producers and consumers are identified by computing successive powers of the adjacency matrix. This deterministic graph-theoretical approach enables exhaustive exploration of all possible routes up to a specified hop count, without relying on traditional shortest-path algorithms such as Dijkstra. [117] proposes a secure, semi-decentralized energy routing algorithm for the Internet of Energy (IoE) that minimizes power loss while ensuring cybersecurity. The method uses graph-based path discovery via depth-first search and selects the optimal route based on a power-loss minimization

model that accounts for node and line losses. ERs locally compute losses using real-time efficiency, resistance, and voltage data shared via a central IoE database. Security is integrated through encrypted communication and malware filtering.

virtual circuit-based algorithms: There are two main types of data transmission technologies: energy packet transmission and virtual circuit transmission.
Energy packet transmission, also known as packet switching, involves sending individual energy packets along different paths from the source to the destination.
On the other hand, virtual circuit transmission establishes a dedicated communication path, or circuit, between the sender and receiver before data transmission. It has a significant drawback: it typically results in lower data link utilization than energy packet transmission. In energy transportation, once a load is connected, energy transmission typically continues until the load is disconnected. Thus, virtual circuit transmission is more suitable for EI and is used by [65], [35], and [112].

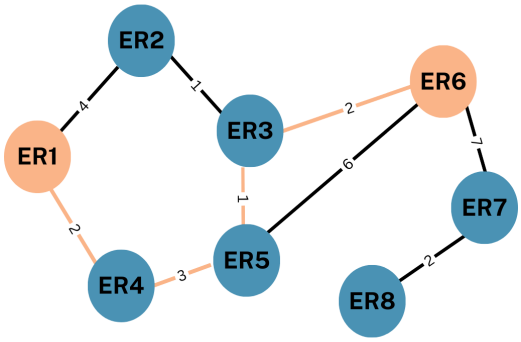

Figure 2.6: Energy routing based on graph theory

Game theory-based routing algorithm

Game theory is a decision-making framework that uses mathematical analysis to explore the consequences of decisions made by two or more people in a game where their outcomes are linked. It serves as a structure for assessing the consequences of strategic interactions and forecasting the actions of individuals or teams. Each individual in game theory is known as a "player". All players have a selection of strategies available. The purpose of game theory is to calculate the result of a game based on decisions made by each of the players.
In the context of the EI, game theory is used to analyze energy trading markets by modeling the strategic behavior of energy producers and consumers regarding pricing, resource availability, and demand fluctuations. This enables the design of mechanisms that reward energy producers to offer competitive prices while incentivizing consumers to optimize their energy usage patterns. Game theory can examine interactions between various energy producers and consumers and develop mechanisms that promote efficient and sustainable resource use.

[118] introduces a game theory-based model for managing monetary energy transactions among prosumers in an SG, where each player independently decides to sell, buy, or store energy based on their current demand level and blackout threshold. Transactions are governed by consensus and follow a FIFO (First-In-First-Out) monetary system, with incentives favoring P2P trading over reliance on the main grid. The model is designed to promote cooperation, preserve energy reserves, and optimize monetary outcomes. Simulations with 500 prosumers over 100 rounds show that this approach significantly improves financial returns compared to always-sell and always-buy strategies.

[119] presented a pricing strategy for power exchange based on game theory energy routing. The CC implements this strategy in an SG model featuring N player nodes and L power links to determine the most suitable buyer/seller and the optimal power transmission route. Each supplier or buyer node

communicates to the CC how much electricity they want to sell or buy and at what cost. The CC matches suppliers and buyers based on their prices and determines the transaction price (p) at the point of matching. The work presents a simulation of a set of strategies with presumably good results.

[115] proposes a multi-leader multi-follower Stackelberg game model where sellers act as leaders, setting electricity prices, while buyers act as followers who respond to these prices by selecting trading partners and corresponding transmission paths to maximize their utility. Each buyer's utility function accounts for the valuation of received energy, the electricity cost (as determined by the sellers), and transmission costs, including line losses, ER inefficiencies, and congestion-based pricing. To determine their optimal strategy, buyers apply Lagrange multipliers and Karush-Kuhn-Tucker (KKT) conditions. To handle congestion in a fair and decentralized manner, the authors introduce a loss-compensation market in which a Network System Operator (NSO) dynamically adjusts line prices based on line utilization. Higher prices on congested lines discourage overuse and help redistribute network traffic efficiently.

[120] proposes a comprehensive framework for optimizing P2P energy trading, addressing the challenges of decentralized market clearing and cooperative energy routing. In the first stage, the authors formulate a global social welfare maximization problem and solve it in a decentralized manner using dual decomposition. The framework accounts for key constraints such as line capacities and congestion, and introduces a penalty for bidirectional power flow conflicts (PFD). In the second stage, the framework introduces a Nash bargaining model to cooperatively resolve PFD conflicts among prosumers sharing transmission lines. This ensures that energy can be routed through multiple paths while maintaining network feasibility and fairness. The model guarantees that all participants benefit more from cooperation than from acting independently, and it provides a cost-sharing mechanism for transmission expenses.

2.2.2 Autonomous routing algorithm

Multi-agent systems (MAS) have been widely employed in EI to address the complex challenges of decentralized energy management. In the EI, multi-agent systems are sets of intelligent agents that cooperate to achieve a specific aim, such as improving energy efficiency or reducing energy costs, through communication among themselves and with the environment. They are used in energy trading, energy management, grid management, and renewable energy integration.

[16] proposed a multi-agent system to manage RERs using the Internet of Things (IoT). The MG can operate in two modes: grid-connected and island mode. In the event of a grid failure, the SG operates in island mode, which reduces its performance. Thus, a secondary control system is introduced to ensure that the voltage and frequency remain at their ideal values while achieving peak power sharing during island mode. The model comprises renewable energy resources, static and dynamic loads, and diesel generators. Every RES is linked and managed by an autonomous agent that can access the internet to control the MG remotely. The MG is represented as a graph of multiple agents, each regulated by the second controller.

The CC is a virtual data management and analysis platform that monitors power usage and cost through a cloud server. The cloud server updates its information regularly based on data from measurement units (MUs). The paper uses the ThingSpeak cloud IoT platform and MATLAB software to simulate communications inside the SG. IoT communication uses the MQTT (Message Queuing Telemetry Transport) protocol, which runs over TCP/IP for message delivery.

The energy routing protocol proposed by [109] employs a semi-decentralized approach that combines decentralized and centralized phases to optimize energy transmission in the EI. The first phase consists of finding optimal routes for energy transfer in a decentralized manner using graph theory. The second phase resolves path overlaps in a centralized manner by forming a coalition of affected source-sink pairs. Using cooperative game theory, the coalition centrally replans paths to minimize total transmission loss, distributing the resulting savings equitably among coalition members using the Shapley value.

[99] proposed a multi-agent system to solve the global optimization problem presented by the components' lack of knowledge of each other. It also uses the energy storage system to manage unpredictable renewable energy production and to support demand response for both power and

heat, balancing energy output and reducing computational costs. The approach chose the time-of-use price-based demand response model for its simple execution. To effectively combine MAS, DR, and ESS, the work constructs a three-layer MAS model composed of distributed management system (DMS) agents, microgrid central controller (MGCC) agents, and MG controllable element (MGCE) agents. The first layer of the system (DMS agent) communicates with other MGs and oversees the second layer (MGCC), which balances power supply and demand and optimizes MG operations. The third layer, represented by MGCE, oversees the operation of the MG's components and receives signals from the MGCC agent. This model incorporates a refined PSO algorithm with an adaptive weight method and a chaotic search algorithm to find a near-optimal global solution while avoiding local optima. The adjustable weight is used to stabilize the overall search and reduce repetition, while the chaotic search algorithm detects stagnation in the iterative process and initiates a new search using its pseudo-code. The obtained results highlight the importance of DR management and ESS in optimizing the cost of the MG and the SG.

2.2.3 Heuristic and Bio-inspired metaheuristic optimization algorithms

A heuristic is a problem-solving technique that uses practical, experience-based strategies to find good enough solutions quickly, especially when finding an optimal solution is too slow or impossible. Bio-inspired meta-heuristic optimization algorithms are a class of optimization methods that draw inspiration from natural processes and phenomena to solve complex optimization problems. They are frequently used to solve complex energy routing problems in SGs, such as identifying minimum-loss paths, matching producers and consumers optimally, and avoiding congestion. A classification of the heuristic and bio-inspired meta-heuristic optimization algorithms used in energy routing is presented as follows:

Ant Colony Optimization (ACO) was applied in energy routing by [121] to determine optimal paths and producer-consumer pairs based on cost and energy loss using a graph-based energy network model. The authors enhanced their ACO path determination protocol in [62] by incorporating dynamic power-loss and capacity constraints into the path-selection process.

Inspired by the foraging behavior of honeybees, ABCO solves optimization problems by simulating bees searching for nectar. It has been used for energy routing by [122] to find the path with the minimum power loss. The protocol portrays consumers as the beehive and producers as flower patches, with producers providing the energy (nectar) needed by consumers. It uses two types of bees, i.e., scout bees and forager bees, which emulate the behavior of users within SGs. Scout bees explore the environment to locate new energy sources, while forager bees travel to these sources and gather nectar (energy). [123] proposed an enhanced version of their previous work [122] that uses the discrete form of BCO to find the path with the least power loss (MLP). The new algorithm finds the MLP based on the power lost in conversion and transmission. It combines the crossover and mutation strategies of the genetic algorithm during the BCOs employed and onlooker bee phases to explore more of the solution space. Congestion is avoided by removing power lines with capacities below the energy required for transmission. The algorithm then chooses paths that could handle the power flow. However, if there is no other path available the algorithm would divide the transmission into 2 separate paths.

A novel approach for centralized P2P energy trading, inspired by the foraging behavior of bees, is proposed by [64]. The goal is to find the best path with minimal congestion and power loss, and to select the best producers to meet consumer demand. The proposed method accommodated scenarios with single-source, multi-source, and multiple consumers. The approach used two types of bees: scouts and foragers. Scouts are dispatched to collect data and perform power-loss calculations for all potential paths. Meanwhile, foragers evaluate the quality of different solutions. The solutions are rated based on their transmission loss and energy prices, and the best solution is chosen to minimize congestion.

[124] proposed an enhanced energy routing method that uses particle swarm optimization (PSO) to solve the minimum power loss path problem in SGs. In this case, the network used is defined as a weighted graph, with nodes representing users (consumers and producers) and edges representing power links. The optimal path is chosen based on the power link's quality, the distance between the consumer and producer, transmission cost, and transmission latency.

The PSO algorithm is employed by [62] to determine the optimal subset of producers that can satisfy the consumer's demand. Additionally, it calculates the optimal amount of energy to purchase from each producer, accounting for energy losses and costs. [125] used the Discrete Particle Swarm Optimization (DPSO) algorithm to address the path selection problem. The authors opted for the discrete form of PSO due to the discontinuous nature of the problem. The DPSO algorithm accounts for power losses during conversion and transmission. Additionally, it effectively manages congestion by selecting the second-best route in case the optimal path is unavailable.

Firefly Optimization is a nature-inspired metaheuristic algorithm that mimics the interactions and movements of fireflies in their natural environment to solve complex optimization problems. It is employed by [63] to address the challenge of the producer subset within the context of the EI. This approach aims to group energy producers (subscribers) to satisfy consumer demand while adhering to specific constraints, such as cost, offered quantity, power loss, and distance. [126] proposed a routing protocol that solves the producer subset selection problem using firefly and the efficient path using the A* algorithm.

The genetic algorithm (GA) is an optimization method based on evolutionary theory, initially presented by [127]. GA is known for its fast convergence and versatility in handling a wide range of optimization problems. It was used by [128] to solve the path determination problem, while [129] used GA to solve the optimal producer subgroup determination in SG and EI. Both algorithms select the fittest solutions based on the roulette wheel method for crossover. [116] proposed a routing algorithm that identifies all possible paths between two peers. It then uses a Real-Coded Genetic Algorithm (RCGA) to optimally distribute the energy among them. The RCGA aims to minimize transmission cost and balance the load by avoiding congestion across routes. Simulated annealing (SA) is a heuristic optimization strategy proposed in 1983 to solve optimization problems with large solution spaces. It has been used in energy routing due to its fast convergence and ability to avoid local optima even in highly complex problems. SA was used to solve the path determination problem in SGs by [130].

[131] solves the producer subset problem using a differential evolution algorithm, while [111] solved the producer subset problem using an improved unified third version of the non-dominated sorting genetic algorithm (U-NSGA-III). The algorithm was employed to achieve Pareto optimality of carbon emission reduction and power loss minimization. Parent-Centric Crossover (PCX) was introduced to leverage multiple parents for better exploration and avoid suboptimal results.

[132] is inspired by the biological behavior of slime mould and is used to find the least-cost energy routing paths. It handles congestion and collisions by incorporating capacity constraints and dynamically evolving link conductivities and flows. The problem of determining an optimal subset of producers to meet demand is solved using a combination of the slime mould algorithm and the Hungarian matching algorithm (Kuhn-Munkres).

2.2.4 Topology-based solutions

An improved minimum spanning tree algorithm (MST) and an energy routing control scheme were proposed by [105]. The suggested topology design is graph-theoretic, with nodes representing ERs and edges representing power lines. The edge weights are the cable costs. The MST algorithm uses the physical locations of ERs to determine the most efficient cabling layout, thus reducing constructional costs. The constructed MST is then improved by adding two additional cables, further enhancing the system's reliability.

The energy routing method uses the Dijkstra algorithm to identify the optimal, non-congested path with minimum power loss. In the graph model used by Dijkstra to find the minimal-loss path (MLP), the weights of nodes and edges represent the conversion loss and transmission loss of the power cables, respectively. The algorithm identifies the MLP for each source-and-load pair based on their transmission time, using the MST topology design. Congestion is avoided by increasing the transmission capacity of the chosen path. Special consideration has been given to the real-time and asynchronous of power transmission.

An energy routing optimization strategy [133], based on long short-term memory, is designed to predict congestion and minimize power loss in SGs. It starts by establishing a graph model of the energy

transmission network. Then it uses long short-term memory (LSTM), a recurrent neural network, for real-time congestion prediction. The LSTM model is the preferred choice given that the ER data exhibit a long-term time-series structure, which the model handles best. The gates of the LSTM model regulate information flow. It also introduces the Comprehensive Weighted Loss, based on the Entropy Weight Method, to optimize the LSTM's evaluation process. After analyzing real-time ER data, it was determined that the comprehensive weighted loss could be calculated using the entropy-weighted method. Next, the Dijkstra algorithm was applied to identify the path with the lowest power loss. The scheme was then tested through simulation experiments, which confirmed its feasibility and effectiveness.

The scheduling problem in energy routing is addressed by [134] by managing the network's topology. The author starts by defining an ER design that operates at low voltage and manages multiple RERs, devices, and storage units simultaneously. The management is implemented using two topologies: star-shaped and series-shaped. It uses matrices, called ER control matrices, to coordinate access to all devices shared by multiple ERs in the network. An energy routing matrix describes the real-time operational status in six function modes: startup mode, operation mode, renewable energy joining mode, load joining mode, renewable energy dropping mode, and load dropping mode. Simulations return good results, proving the effectiveness of topology control in managing energy systems and achieving power balance in the local grid.

The study by [135] introduces an energy routing method for a multi-area multi-energy system (MAMES) to address the energy planning and management problem. MAMES is composed of N Single-Area Multi-Energy systems (SAMES). All SAMES consist of multiple microgrids connected through a virtual ER. The virtual multi-energy router (VER) is a centralized management system for all multi-energy routers (MERs). It ensures the coordination and control of multi-energy router resources. MER is the new ER architecture designed to accommodate multiple energy resources in the EI, including electricity, gas, and heat. Energy routing algorithms are of two types. The first one is the internal routing algorithm that manages routing in a MAMES network. The second is the external energy routing algorithm proposed to handle energy routing between MAMES networks. It is a centralized management applied by the EI's control center. Both have different constraints. Only the internal energy routing, which minimizes energy loss in transmission and conversion within and between MAMES using an energy matrix, is considered. The proposed algorithm selects the best path from a source to a consumer. It ensures connectivity between users, minimizes energy costs, and handles unpredictable scenarios. It builds an MST-based prim from the network's graph to reduce construction costs and find the best path. Latin hypercube sampling (LHS) (a statistical sampling method) and K-means (used for clustering) are both used to generate operational scenarios that explore the parameter space by sampling from its subset. It is designed to identify a candidate set of energy networks that offer optimal routes for energy flow across diverse networks, including electricity, heat, and gas. Simulations conducted using LTS and k-means demonstrate the effectiveness of the proposed algorithm. The paper [136] proposes an energy routing protocol using the Zbus impedance matrix to address energy transfer challenges in the EI. The protocol selects efficient paths based on Thevenin impedance distance as the weighting measure and considers power line capacity constraints. If a line's capacity is exceeded, energy is split into packets and routed across sub-routes based on their remaining capacities to manage congestion.

Table 2.2: Comparison of Energy Routing Strategies

Ref.	Advantages	Limitations	Contribution
[103]	Real-time adaptability, Multi-source routing under load	Scalability issues (>50 nodes), Ignores energy pricing	GT-based path selection + capacity constraints
[35]	Day-ahead OSPF planning, Multi-source load balancing	Security risks, Delay-sensitive communications	OSPF + DFS for P2P trading
[104]	Simple implementation, Real-time grid adaptation	Fixed pricing, Centralized SPOF	Dijkstra-based P2P routing

Continued on next page

Table 2.2 – continued from previous page

Ref.	Advantages	Limitations	Contribution
[105]	Cost-effective MST, Mesh redundancy	Sequential congestion management, Ignores terrain costs	MST-based topology design
[65]	Virtual circuit stability, Real-time loss optimization	High computational overhead	Dynamic loss-aware routing
[106]	IEC 61850 compliance, Voltage stability focus	No field validation, Infrastructure upgrade costs	OFV algorithm for power loss minimization
[55]	Real-time congestion adaptation	Single-path only, Ignores heavy loads	Dijkstra-based protocol with power constraints
[107]	Scalable (GOER/LOER)	Comms-dependent	Hierarchical routing protocols
[108]	Layer-wise congestion reduction	Unrealistic ER efficiency	Congestion-aware routing
[109]	26% loss reduction (multi-path), Shapley fairness	Exponential complexity, Delay-sensitive	DFS + game theory for loss minimization
[15]	Multi-procurement resilience, Low complexity	Uniform cable assumptions, No congestion handling	Dijkstra + knapsack cost optimization
[110]	Improved infrastructure use	Prioritizes speed over loss, Ignores power loss	Hop-count multi-path P2P trading
[111]	Enhanced U-NSGA-III performance	Static parameters, DFS scalability issues	Pareto-optimal carbon-loss tradeoffs
[112]	DER cost integration, Renewable prioritization	Static network assumptions, Predefined paths	Graph-based MLCP strategy
[113]	Privacy Preservation, Maximizes financial benefits by pairing surplus-deficit households, real-time responsiveness	Computational Complexity, Relies on accurate, real-time data	Decentralized P2P energy trading with dynamic matching
[114]	Real-time capacity awareness, Scalable matching mechanism	Assumes complete system knowledge, Sequential transaction processing	Capacity-constrained Dijkstra routing with packet-based transmission
[115]	Decentralized Optimization Framework, Congestion-Aware Pricing, Multi-Path Routing	High Computational Complexity, Requires Accurate Info	Tripartite graph + Stackelberg game for P2P trading
[120]	Resolves PFD Conflicts, Privacy Preservation	High Computational Complexity	Cooperative routing with Nash bargaining in energy LANs
[118]	Effective Use of Game Theory	Idealized Player Behavior, overlooking human decision-making biases, Scalability Concerns	A game-theoretic framework for optimizing energy trading decisions among prosumers in smart grids
[119]	Adaptive Pricing Strategies, Transportation Problem Integration	Scalability Concerns	Game theory + Hungarian algorithm for energy routing
[16]	Real-time monitoring and control, Scalable	High reliance on IoT infrastructure	Secondary control with MAS and IoT
[109]	Reduces loss and handles overlapping paths	High complexity, Coordination overhead	Decentralized route + Centralized resolution
[99]	Combines DR, ESS, and intelligent control, Enhanced convergence	Complex design, Heavy tuning dependency	MAS integrating DR and ESS with chaotic PSO

Continued on next page

Table 2.2 – continued from previous page

Ref.	Advantages	Limitations	Contribution
[121]	Adaptive learning	Complex, does not consider power loss and power line congestion, No Comparative Analysis	ACO-based protocol for efficient path selection
[62]	Handles power loss and congestion	Overly simplified congestion, High computation	ACO + PSO + congestion management
[122]	Incorporates dynamic grid behavior	High complexity, Poor scalability	Dynamic latency-aware routing
[137]	Handles overlapping paths, Dynamic topology	Computationally intensive, Needs full grid state	ACO for path selection, mono/multi source routing, and scheduling
[124]	Simple implementation	Ignores power loss and congestion, lacks comparative analyses	PSO for path selection in EI
[138]	Simple, Handles mono- and multi-source	No congestion, No power loss considered	FA for producer selection in EI
[126]	Fast and simple to implement, effective mono/multi source selection	Does not consider power loss and congestion	FA for subscriber matching + A* for path selection
[139]	Effective optimal path selection, fast conversion	Static Network Assumptions, complex with high Computational Overhead	GA for path selection in EI and SG
[129]	Effective mono/multi source selection, fast conversion	Complex with high Computational Overhead	GA for subscriber matching + dijkstra for path selection
[130]	Avoids local optima, Simple	Slow convergence	SA for path selection
[131]	Incorporates Prospect Theory (PT) to address consumers' irrational decision-making, incorporates dynamic pricing and solves the producer matching problem	Scalability Concerns due to Computational Overhead	Differential Evolution-based protocol for matching subscribers + Dynamic Pricing with Reinforcement Learning
[132]	Demonstrates scalability, addresses least-cost routing and maximum flow capacity, fast execution time	Ignores physical power flow dynamics	Slime mould for path selection and producer matching in SG
[133]	Incorporation of Real-Time Data, Accurate Congestion Prediction	Dependence on Historical Data Quality, Computational Overhead	LSTM for congestion prediction + Dijkstra for optimal path selection
[134]	Flexible Network Topologies (series-shaped and star-shaped), standardized interfaces for renewable energy devices	Implementation Complexity, Scalability Concerns	Low-voltage energy routing with renewable integration

Continued on next page

Table 2.2 – continued from previous page

Ref.	Advantages	Limitations	Contribution
[135]	Integrates diverse energy vectors (electricity, heat, gas), Minimizes network construction costs via Prim's algorithm	Unverified scalability, lacks comparison with Existing Methods	Prim + MST for the network topology, Latin Hypercube Sampling + k-means clustering to handle high-dimensional uncertainties, PSO to optimize equipment capacities
[136]	Real-time grid adaptation to line loading, dynamic congestion management scheme, scalable, more accurate calculation of power loss (dynamic adjustment of line resistance)	Compared their findings to Dijkstra, which is old and overused, matching subscribers are not considered	Zbus impedance matrix for path selection
[116]	Scalable Multi-hop Routing, Low Computational Overhead	Assumes Equal Link Capacities, Pricing mechanisms and economic incentives for energy trading are not integrated	GT + RCGA for path selection
[117]	Secure Communication, Semi-Decentralized Control	Central Database Dependency, Scalability Uncertain for Large Networks	DFS for path discovery + GT for path selection + Encryption & Malware Filtering

Table 2.4: Comparison of Different Protocols

Paper	Method		
	Subscriber's Matching	**Efficient Path**	**Scheduling / Congestion Management**
[35]		Graph Theory based OSPF and DFS	Graph Theory
[103]		Graph Theory	Graph Theory
[104]	Graph Theory	Graph Theory based Dijkstra	Topology based on Mesh
[105]		Graph Theory based Dijkstra	Topology based on Minimum spanning tree (MST) and Dijkstra
[65]	Graph Theory	Graph Theory based OSPF	
[106]	Graph Theory	Graph Theory	
[55]	Graph Theory	Graph Theory (brute force)	Graph Theory using Depth-first Search (DFS)
[107]	Graph Theory	Graph Theory	centralized control management
[108]	Graph Theory	Graph Theory	Graph Theory by selecting the second best solution
[109]		Graph Theory	Graph Theory
[15]	Greedy algorithm	Dijkstra	
[110]		Graph Theory	Graph Theory
[111]	Graph Theory+U-NSGA-III	Graph Theory + Source Matching	Graph Theory

Continued on next page

Paper	Subscriber's Matching	Efficient Path	Scheduling / Congestion Management
[112]	Graph Theory based Dijkstra		
[113]	Graph Theory	Graph Theory	
[114]	Graph Theory based Dijkstra	Graph Theory	Graph Theory
	Subscriber's matching	Efficient path	Scheduling and congestion management
[115]	Graph Theory based DFBB	Stackelberg Game Theory	Game and Graph Theory
[120]	Graph Theory	Nash bargaining Game Theory	Game Theory + Graph Theory
[116]	Graph Theory		
[117]	Graph Theory based DFS		
[119]		Game Theory	Game Theory
[118]	Game Theory	Consensus + FIFO	
[109]	Graph Theory	Cooperative Game Theory	Graph + Game Theory
[121]		ACO	
[122]		BCO	
[137]	BCO	BCO	BCO
[124]		PSO	
[62]	PSO	ACO	ACO
[138]	FFO		
[123]		ABCO	Chooses the second best solution
[125]		DPSO	Chooses the second best solution
[129]		GA	
[130]		SA	FIFO and Round Robin
[126]	Graph Theory A*	FA	
[139]	GA		FIFO
[116]		RCGA	
[131]		Differential Evolution	
[111]		U-NSGA-III	
[132]	Slime Mould	Slime Mould + Hungarian Algorithm	
[105]	Topology based on MST	Graph Theory based Dijkstra	Graph Theory based Dijkstra and Topology based on MST
[133]		Graph Theory based Dijkstra	Short-term long-term memory neural network
[134]			Topology based on star-shaped, series-shaped coordination
[135]		Topology based on MST-based Prim	Topology based

2.3 Conclusion

This chapter has provided a comprehensive classification of optimization strategies employed in SGs and the EI, examining mathematical frameworks, autonomous routing algorithms, bio-inspired metaheuristics, and topology-based solutions. The literature review reveals two critical research gaps. First, energy routing remains significantly underexplored compared to load forecasting and demand response. Second, and more fundamentally, existing approaches fail to bridge the economic layer (peer-to-peer trading and prosumer-consumer matching) with the physical layer (path selection and congestion management).

Table 2.3: Comparison of different optimization methods.

Method	**Advantages**	**Disadvantages**
Graph theory	• Simplifies complex networks for better visualization. • Adapts easily to topology changes, making it flexible in dynamic systems. • Offers various algorithms for optimization and routing problems. • Identifies efficient pathways for energy transmission.	• High computational cost for large graphs. • Limited to problems representable as graphs. • Lack of real-time dynamic representation. • Multiple ideal solutions can lead to ambiguity.
Game theory	• Analyzes strategic interactions in energy systems. • Optimizes resource allocation considering costs. • Enhances decentralized energy systems.	• Complex mathematics and calculations. • Relies on certain behavior assumptions. • Multiple solutions or lack of clear solution. • Computational challenges for complex games.
Autonomous algorithms	• Decentralized decision-making. • Adjusts routing based on changing conditions. • Enhances system resilience.	• Complexity of algorithm design. • Lack of global coordination. • Vulnerability to manipulation and cyber attacks.
heuristic optimization algorithms	• Addresses uncertainties in energy environments. • Produces robust solutions against fluctuations. • Considers risk factors for better decision-making.	• Requires substantial computational resources. • Depends on extensive and accurate data. • Complex modeling might lead to inaccuracies.
Topology-based optimization algorithms	• Efficient utilization of energy resources. • Minimization of energy losses in transmission. • Optimization of energy flow paths.	• Complex algorithm design and implementation. • Computational demands for large-scale networks. • Dependency on accurate network topology data.

Most P2P trading frameworks focus on market mechanisms while treating the network as constraint-free, leading to economically optimal trades that may be physically infeasible or inefficient when transmission losses, capacity limits, and collision avoidance are taken into account. While load forecasting and demand response address temporal prediction and behavioral aspects of energy management, they do not solve the core routing challenge: how to physically transfer energy through the network once supply and demand are determined. The routing algorithms developed in this thesis directly address these gaps by integrating prosumer-consumer matching with loss-aware path selection and congestion-aware scheduling. This ensures energy trades are both economically beneficial and physically realizable. The proposed solutions are designed to complement, rather than replace, forecasting and demand response systems, accepting their inputs and translating them into efficient, reliable, collision-free energy transfers. Despite promising developments, several gaps remain. Current optimization approaches often address routing, forecasting, or scheduling in isolation, rather than through integrated frameworks that jointly consider the economic and physical aspects of P2P energy trading. Moreover, computational complexity, data requirements, and the absence of standard benchmarks continue to limit scalability and real-world deployment.

Part II

Contributions

Chapter 3

FKD-RA: Efficient Energy Routing Protocol in SG and EI Networks Using Fractional Knapsack and Dijkstra Algorithm

Contents

3.1 Introduction . . . 42
3.2 Problematic . . . 43
3.2.1 Fractional knapsack . . . 43
3.2.2 Network model . . . 43
3.2.3 Control center management . . . 43
3.2.4 Addressing the optimal producer's subset problem . . . 43
3.2.5 Finding the shortest path . . . 45
3.3 Simulation and performance analysis . . . 45
3.3.1 Use case 1: Optimal path . . . 45
3.3.2 Use case 2: Multiple sources and multiple energy demands . . . 46
3.3.3 Use case 3: Multiple sources and mono-source . . . 46
3.3.4 A comparative analysis with the firefly algorithm . . . 47
3.4 Conclusion . . . 48

3.1 Introduction

Existing energy routing approaches in SG and EI environments often treat economic decision-making and physical power delivery as separate problems. Many peer-to-peer energy trading mechanisms focus on price negotiation and matching between producers and consumers while overlooking network constraints such as transmission losses and path efficiency. As a result, economically optimal trades may lead to inefficient or even infeasible physical energy transfers.

This chapter addresses this gap by formulating energy routing as a joint producer-selection and path-optimization problem. The proposed approach integrates economic and physical considerations by first determining an optimal subset of energy producers and then identifying efficient transmission paths to satisfy consumer demand. To achieve this, the producer selection problem is modeled as a Fractional Knapsack problem, enabling flexible allocation of energy from multiple producers based on cost and availability. Subsequently, Dijkstra's algorithm is employed to compute minimum-cost transmission paths, ensuring efficient and reliable energy delivery.

The resulting framework, referred to as FKD-RA, provides a computationally efficient routing solution suitable for real-time operation in decentralized energy systems. By combining greedy optimization with shortest-path routing, the proposed method achieves a balance between solution quality and computational complexity. Simulation results demonstrate that the proposed approach reduces energy delivery cost and transmission losses compared to baseline routing strategies, while maintaining scalability across different network sizes.

3.2 Problematic

We aim to balance supply and demand in the smart grid by proposing an energy routing protocol that solves the efficient path problem and finds the best set of sellers for the consumer to buy from. We formalized this problem as an optimization problem and proposed a greedy method to solve it. Specifically, we represented the problem as a fractional knapsack problem.

3.2.1 Fractional knapsack

The fractional knapsack problem is a classic optimization problem in computer science and mathematics. It involves selecting items from an assembly of objects, each with a weight and a value, to increase the total value while keeping the total weight below a given limit.

In the fractional knapsack problem, unlike the 0/1 knapsack problem, items can be divided (fractional) to maximize the value-to-weight ratio.

3.2.2 Network model

The network consists of a control center and users, some of whom are producers and others consumers at different times. Every user is a microgrid comprising an energy router, a smart meter, loads, a storage system, and renewables. The ER plays a crucial role in facilitating communication between the microgrid participants and the Control Center (CC). The ER conveys its energy needs or surplus to the CC, providing important information for energy management in the smart grid.

3.2.3 Control center management

The CC serves as the central decision-making entity and receives buy requests from consumers and sell requests from producers. These requests indicate the amount of energy consumers want to purchase, and the amount of excess energy producers are willing to sell. Upon receiving these requests, the CC applies the proposed greedy method to efficiently allocate the available energy resources. The primary objective is to optimize energy allocation within the smart grid. The CC selects the best producers for each consumer, taking into account cost, distance, and reliability. The FIFO approach handles consumer energy requests, giving priority to the first requester. However, exceptions occur when suitable producers are unavailable, prompting the CC to explore alternatives. The CC executes algorithm 2 after receiving a buy request from a consumer:

The algorithm takes consumer demand and a list of producers as input. The algorithm iterates through each producer, using Dijkstra's algorithm to find the shortest distance and calculate power loss.The 'Greedy' function is called to find the minimum cost and chosen producers based on the demand and producer list.

3.2.4 Addressing the optimal producer's subset problem

In the context of the smart grid, finding the best producers to buy from requires considering factors such as energy loss, distance, and cost. In the fractional knapsack problem, each producer can be viewed as an item with a given weight (pure energy) and value (the objective function). The goal is to select a subset of producers so that the total weight meets demand while minimizing the total cost. Our proposed greedy method involves iteratively selecting the producers with the highest ratio of value (objective function) to weight (energy) and assigning their pure energy to the demand until it is fulfilled

Algorithm 1 Control Center main algorithm

Input: *demand*: Consumer demand, *producers*: List of producers
Output: *min_cost*: Minimum cost, *chosenproducers*: Chosen producers
Initialize *demand* and *producers*
Create an empty set *chosenproducers*
for each consumer c in *consumers* **do**
    for each producer p in *producers* **do**
        find the shortest distance between p and c using the Dijkstra algorithm;
        memorize the best route between p and c
        calculates power loss using equation 3.1
        calculate pure energy using equation 3.2;
        calculate objective function using equation 3.3;
        Add *obj_fun* to *producer* list
        Add *pure_energy* to *producer* list
    end for
end for
min_cost = Greedy(*demand*,*producers*, *ChosenProducers*)
Print the updated list of producers with their attributes
Print *min_cost*
Print the chosen producers (*chosenproducers*)

or until no more producers are available. This approach uses a greedy strategy that always chooses the most efficient option at each step.

The power loss is obtained by multiplying the distance to the consumer by a factor, represented by σ, which represents the power loss in one meter of power cable. while pure energy is calculated by subtracting the power loss from the producer's energy. Mathematically, we can express these relationships as follows:

$$\text{Ploss} = distance \times \sigma \tag{3.1}$$

$$pure\_energy = \text{energy} - Ploss \tag{3.2}$$

On the other hand, the value is equivalent to the objective function, computed as the product of the producer's price and energy.

$$obj\_func = \text{price} \times \text{energy} \tag{3.3}$$

To evaluate the effectiveness of our solution, we assess various factors, including the cost of each path, the total cost of purchasing from a producer, and latency. The cost formula is:

$$\text{cost\_path} = \sum_{k=1}^{k-1} \text{cost\_k} \tag{3.4}$$

The cost-path formula represents the cost of purchasing energy from the chosen producers.

where k represents the chosen producers. The latency of a path $PATH$ is calculated as the sum of the product of the links and the transmission rate:

$$\text{Latency}(PATH_i) = \sum_{l=1}^{l-1} \text{links} \times \text{TransmissionRate} \tag{3.5}$$

where l represents the link of the path.

Algorithm 2 Greedy function

Input: *demand*: Consumer demand , *producers*: List of producers
Output: *min_ cost*: Minimum cost, *chosenproducers*: Chosen producers
Sort producers based on the ratio of objfun to pure_energy
for each producer p in producers **do**
    if p[pure_energy] $\leq$ demand **then**
        $demand = demand - p$[pure_energy]
        $cost = p$[price] $\times$ p[energy]
        Set the energy of the chosen producer to 0
        chosenproducers.add(p)
        p[pure_energy] $= 0$
    else if p[pure_energy] $>$ demand **then**
        Calculate the fractional part of the item based on demand and p[pure_energy]
        p[pure_energy] $= p$[pure_energy] $-$ (p[pure_energy] $-$ demand)
        $cost = p$[price] $\times$ (demand $+ p$[Ploss])
        p[pure_energy] $= p$[pure_energy] $-$ (demand $+ p$[Ploss])
        demand $= 0$
        chosenproducers.add(p)
    end if
end for

3.2.5 Finding the shortest path

The greedy algorithm efficiently stores the optimal routes between producers and consumers, reducing computational costs. It uses the Dijkstra algorithm to determine the shortest distances and identify the best energy transfer routes. Once the optimal subset of producers is selected, the algorithm shares the list of chosen producers along with their best routes to the consumer and their chosen producers.

We assume all cables are identical and have the same energy loss per meter.

3.3 Simulation and performance analysis

To demonstrate the effectiveness and efficiency of the proposed method, we conducted a simulation on a network comprising 11 users, including 7 producers and 4 consumers. The simulation was carried out with the following parameters: power loss rate $\alpha = 0.1$ and transmission rate (0.22 %). The simulations were performed in the Python programming language. We assume all cables have the same capacity and there is no initial power flow through them before executing the algorithm. Additionally, we assume that there is no congestion, eliminating the need for scheduling.
The simulation process is organized into rounds. For each consumer, the code selects a set of producers based on considerations of power loss and price.

Figure 4.3 illustrates an SG consisting of eleven nodes and a control center. Users in the grid are classified as producers (P) or consumers (C) based on their residual energy levels. Table 3.1 explains the network distribution in detail.

The results obtained from the simulation are highlighted in detail in Table 3.2.

3.3.1 Use case 1: Optimal path

1. Case 1:long distance between the consumer and producer
   We selected consumer 4 and producer 7. The Dijkstra algorithm yielded the following result: 7 $\rightarrow$ C2 $\rightarrow$ 5 $\rightarrow$ 4 $\rightarrow$ C4, with a power loss of 2.32 Kw/h.

2. Case 2: short distance between the consumer and producer We selected consumer 2 and producer 7, and the Dijkstra algorithm yielded the following result: 7$\rightarrow$C2 with a power loss of 0.4 Kw/h.

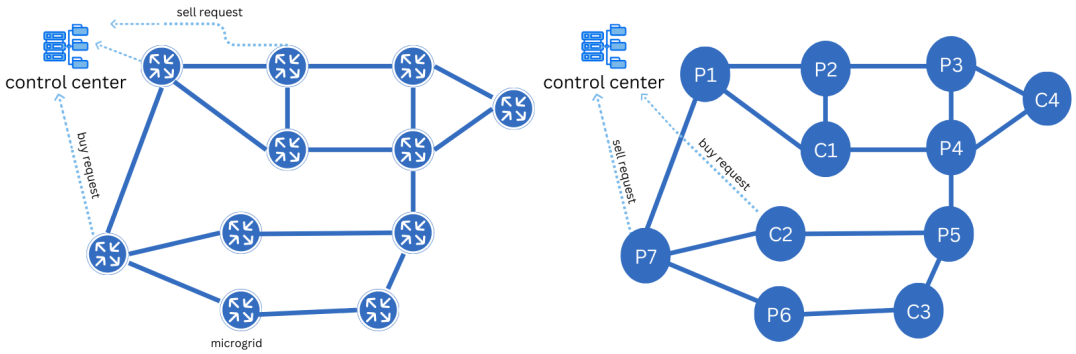

Figure 3.1: 11-Nodes network topology

Table 3.1: Information details of the network distribution

Node	Demand/Production (kW)	Price ($)	X	Y
Consumer1	−50	—	10	10
Consumer2	−20	—	6	5
Consumer3	−35	—	12	2
Consumer4	−10	—	20	8
Producer1	22	1	5	15
Producer2	200	2	10	15
Producer3	40	2	15	15
Producer4	40	1	15	10
Producer5	100	3	15	5
Producer6	10	2	6	2
Producer7	5	1	2	5

The results demonstrate a direct relationship between the distance separating the consumer and the producer and the power loss incurred. Specifically, as the distance increases, the power loss also increases. Conversely, a smaller distance between the consumer and the producer results in reduced power loss.

3.3.2 Use case 2: Multiple sources and multiple energy demands

This scenario involves multiple sources and load requests, with the total available power insufficient to meet the combined load requirements. By increasing consumer 1's demand to 200, the algorithm necessitates multiple sources to fulfill this demand. Specifically, the algorithm selects producers 4, 1, 7, and 2, with a cumulative cost of 339.9. Consequently, as consumer demand rises, the options for lower prices diminish, leading to higher costs to satisfy the increased demand.

3.3.3 Use case 3: Multiple sources and mono-source

Consumer 2's demand is set to 50 kW, and we calculate the cost of purchasing energy from individual sources and from multiple sources combined.

1. Producer 2 supplies 200 kW of energy at a rate of 2$ per kW. The cost to purchase 50 kW from Producer 2 is 100$. When the cost of the lost energy in the transmission is included, the total cost for Consumer 2, the furthest consumer, amounts to 98.05$.

2. Producer 5 offers 100 kW of energy at a rate of 3$ per kW. The cost to purchase 50 kW from Producer 5 amounts to 150$. After accounting for the cost of the lost energy in transmission, the total cost for Consumer 2, who is the furthest consumer, equals 148.97$.

Table 3.2: The relationship between the demand and the cost for every consumer

Consumer	Demand	Producer	Energy	Pure Energy	Price ($)	Quantity	Total Price ($)
C1	50	4 1	40 22	39.5 21.29	1 1	40 11.2	51.20
C2	20	7 1 2	5 10.79 200	4.6 9.34 198.05	1 1 2	5 10.79 7.99	31.78
C3	35	2	192.004	190.08	2	36.92	73.84
C4	10	2	155.08	153.72	2	11.36	22.72

3. By executing the algorithm for Consumer 2, we find that both Producer 4 and Producer 1 together can supply the required 50 kW at a total cost of 51.2$.

Both 98.05$ and 148.97$ are far more expensive than 51.2$ This highlights the advantage of using a multi-source approach over relying on a single source in this particular scenario.

The greedy function calculates and returns the optimal set of producers for each consumer, taking into account factors such as power loss, price, residual energy, and the consumer's energy demand constraints From table 3.2, it is evident that consumers who execute first achieve better outcomes, as they benefit from greater energy availability. On the other hand, consumers who arrive later tend to face higher prices.

3.3.4 A comparative analysis with the firefly algorithm

To evaluate the performance of the proposed protocol, we conducted a comparative analysis by applying the Firefly Algorithm proposed in paper [63] using identical network parameters (table 3.1) to those used in our proposed algorithm. We present here the results obtained from the simulation carried out under the following parameters, as shown in Table 3.3.

Table 3.3: Simulation results of the Firefly algorithm

Consumer	Chosen Producer	Quantity (kW)	Total Cost ($)
C1	4 1	40 10	51.20
C2	1 3	12 8	31.34
C3	3 5	32 8	91.84
C4	5	10	31.03

Upon observation, it is evident that the total cost for Consumer 1 and 2 aligns with our findings. However, a notable discrepancy arises for the remaining consumers, as the cost shows substantial growth compared to the outcomes obtained through the implementation of our proposed protocol. The Firefly algorithm shows a stronger preference for proximate producers, despite factors such as price and power loss. Which affects its overall performance as the network size and complexity increase.

3.4 Conclusion

The integration of distributed RERs into modern electricity networks has introduced new complexities in energy transmission and distribution. These challenges are further amplified in the context of peer-to-peer (P2P) energy trading, where ensuring efficient and reliable routing becomes essential.

This chapter addressed two fundamental challenges in energy routing: determining producer groups and routing energy efficiently. By formulating the problem as a fractional knapsack model and employing the greedy method in combination with Dijkstra's algorithm, the proposed approach demonstrated its ability to minimize consumer costs while maximizing producer profits. The simulation results confirmed the effectiveness and efficiency of this method in small-scale energy networks, showing that it can reduce transmission losses and improve overall allocation performance.

Nonetheless, scalability remains a limitation. While the greedy and Dijkstra-based approach performs well in smaller systems, its efficiency may decline as network size and complexity grow. This underlines the need for more advanced approaches capable of maintaining optimality in larger-scale networks.

Chapter 4

SA-RA: Simulated Annealing for Producer Subset Determination in Smart Grids

Contents

4.1 Methodology of Analysis 50
4.1.1 Energy System Architecture 50
4.1.2 Simulated Annealing 50
4.1.3 Initial solution 51
4.1.4 Initializing Parameter 51
4.1.5 Energy Function 51
4.1.6 Perturbation 52
4.2 Simulation Results And Analyses 54
4.3 Conclusion 56

Introduction

RERs offer an environmentally sustainable alternative to fossil fuels, yet their intermittent and unpredictable nature introduces significant challenges for ensuring a stable energy supply. Smart Grids have emerged to address these issues by integrating renewable generation with advanced communication and control technologies, enabling decentralized management of prosumers and DERs.

The energy routing framework introduced in Chapter 3 provided an efficient baseline solution by jointly addressing producer selection and path determination. To maintain low computational complexity, transmission efficiency was approximated using distance-based metrics, and power losses were implicitly modeled through simplified path costs. While this abstraction enabled fast routing decisions, it does not fully capture the physical behavior of electrical networks, particularly in realistic Smart Grid environments where losses depend on line characteristics, power flow, and equipment capacities.

To overcome these limitations, this chapter introduces a power-aware energy routing framework based on a realistic IEEE Smart Grid architecture. Transmission losses are explicitly calculated using physical cable parameters and energy router capacities, enabling accurate modeling of power dissipation and network constraints. The producer subset determination problem is reformulated accordingly and solved using an SA optimization approach, which is well-suited for exploring complex, non-linear solution spaces arising from detailed physical modeling.

By incorporating accurate power loss calculations and realistic infrastructure constraints, the proposed approach significantly improves routing fidelity while preserving scalability. Simulation results demonstrate that the SA-based framework achieves lower transmission losses and more reliable energy

delivery compared to the simplified distance-based model, particularly under constrained and large-scale network conditions.

This chapter details the IEEE-based system architecture, the power-loss formulation, and the Simulated Annealing procedure, followed by a comprehensive performance evaluation. The proposed framework bridges the gap between abstract routing models and physically grounded Smart Grid implementations, providing a critical step toward deployable energy routing solutions.

4.1 Methodology of Analysis

In a peer-to-peer energy network, such as smart grids, Producer Group Determination is a critical step for ensuring effective and efficient energy routing. This determination process involves solving a combinatorial problem that aims to allocate the most suitable producers to each consumer. This allocation is based on factors such as producers' listed prices and transmission losses, with the primary goal of minimizing both costs and power losses within the energy system. This paper aims to solve the Producer Group Determination using simulated annealing optimization.

4.1.1 Energy System Architecture

The architecture we developed is a network represented as a graph, where nodes represent microgrids and edges are weighted to reflect energy losses during conversion and transmission. A microgrid is a complex electric system capable of operating independently or in conjunction with the main power grid [140]. It typically consists of renewable energy resources (e.g., solar panels, wind turbines), storage systems, and loads interconnected using an energy router as shown in Figure 4.1. An energy router is a critical piece of equipment capable of managing energy and data transactions, communication between the microgrid and the main grid, as well as between different components within the microgrid [23].

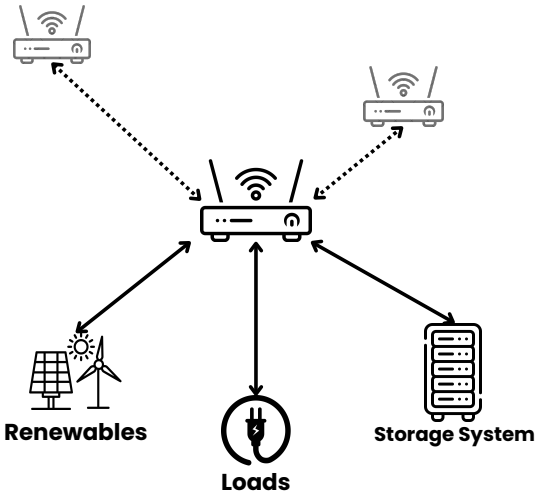

Figure 4.1: Microgrid topology

In this paper, the network is managed by a control center (CC) that oversees all data, energy, and monetary transactions. The CC is equipped with network topology data, including power-line parameters, user locations, and related data. It receives energy requests from both consumers and producers within the network and executes the routing algorithm based on the received information. The interconnection between the microgrids and the control center forms a smart grid network.

4.1.2 Simulated Annealing

Simulated annealing (SA) is a metaheuristic optimization method developed in 1983 by Kirkpatrick et al. to solve complex, combinatorial problems. The evolution of the SA search space is modeled after the annealing process in metallurgy, where heated metal is gradually cooled to allow atoms to move

into a more organized and structured final arrangement [141]. The steps of the proposed algorithm are as follows:

4.1.3 Initial solution

The algorithm starts by creating an initial solution, which consists of a group of energy producers and the amounts of energy they supply and offer to the consumer.

4.1.4 Initializing Parameter

The algorithm begins with an initial temperature set to 1000°C. This temperature gradually decreases following a cooling rate of 0.995, as described by Equation 4.1:

$$\text{temperature} = \text{cooling\_rate} \cdot \text{temperature} \tag{4.1}$$

4.1.5 Energy Function

The energy function of the Simulated Annealing (SA) algorithm is used to measure the effectiveness of a solution. In the context of optimal producer subset determination, the energy function is calculated based on both the total power loss and the total cost.

The total power loss, P_{loss}, is the sum of power losses occurring in both energy conversion and transmission for all transmission paths. In the scenario where a solution involves two producers, the total power loss comprises the sum of optimal paths from Producer 1 to the consumer and from Producer 2 to the consumer. The total power loss is represented as:

$$\text{Total\_Loss} = \sum_{i=1}^{n} Ploss(i_{\text{consumer}}) \tag{4.2}$$

Here, i represents each producer in the solution list. and n represents the number of producers in a solution.

The total cost, C_{total}, is calculated as the sum of costs associated with each producer's energy supply to the respective consumer, which can be represented similarly.

$$\text{Total\_cost} = \sum_{i=1}^{n} producer(i) * price(i) \tag{4.3}$$

Thus, the energy function is as follows:

$$\text{Energy} = (0.5 \cdot \text{total\_cost}) + (0.5 \cdot \text{total\_loss}) \tag{4.4}$$

We selected a weighting factor of 0.5 for both the cost and power-loss components to give equal weight to both.

To calculate power loss along a given path, we need to consider both the conversion losses in the energy router and the transmission losses through the power line. Although heating power cables causes only a relatively small power loss, it is still significant. In energy systems such as smart grids, even small losses are significant given limited energy production and the unpredictability of renewable sources. The transmission power is the sum of active and reactive power losses; in this paper, we chose to disregard reactive power loss due to its triviality. The active transmission loss is calculated using Equation:

$$P_{\text{ij}} = \frac{R_{\text{ij}}}{V_{\text{ij}}^2} \cdot \left((P + P_{\text{existing}})^2 - P_{existing}^2 \right) \tag{4.5}$$

Where R_{ij} represents the resistance of cable i-j in ohms, I_{ij} represents the current of power line i-j in amperes. P is the power transmitted along the power line, while $P_{existing}$ defines the already existing power in the link.

The conversion power loss depends on the router's efficiency, it is calculated using equation 4.6:

$$E_{\text{converted(KW)}} = E_{\text{in}} \times \text{Conversion Efficiency} \tag{4.6}$$

As a conclusion, the total power loss is computed using equation 4.7.

$$\text{TPloss} = \sum_{i=1}^{n} P_{\text{loss},i} + \sum_{j=1}^{m} P_{E_{\text{converted}},j} \tag{4.7}$$

where n and m represent the number of power links and the number of routers along the path, respectively.

Algorithm 3 Powerloss_Assessment

```
procedure POWERLOSS_ASSESSMENT(G, p, c)
    demand ← c["Demand"]
c: consumer, p: producer
    paths ← FINDALLROUTES(G, p, c)
    for p in paths do
        for i ← 0 to len(path) − 1 do
            R1, R2 ← path[i], path[i + 1]
            measure energy lost in conversion at R1 with eq:4.6
            Add conversion loss to power loss
            update the energy to send
            measure power lost from R1 to R2 using eq:4.5
            update energy_to_send_temp
            total_ploss ← total_ploss + power_loss
        end for
        eff ← graph.nodes[R1]['Efficiency']
        Compute the conversion loss at R1 using eq:4.6
        Add conversion loss to powerloss
        return the minimum loss path
    end for
    cost ← producer['UnitPrice'] · energy_to_send
    return cost, optimal_path_loss, optimal_path
end procedure
```

Let G represent the network graph, c the consumer, and p the producer. The algorithm utilizes the 'FINDAllROUTES' function to identify all possible routes from the producer to the consumer. For each route, it calculates power losses from both conversion and transmission, selecting the route with the lowest loss as the optimal path.

4.1.6 Perturbation

The perturbation function explores the solution space by making small adjustments to the current solution, enabling the algorithm to escape local optima—similar to the role of mutation in genetic algorithms. Typically, these slight adjustments lead to new potential solutions. However, in our work, the perturbation function takes a different approach: it introduces an entirely new solution rather than altering the existing one. This is due to the sensitivity and complexity of our problem, where preserving the integrity of the current solution is critical. This method not only expands the search space but also enhances flexibility, making it particularly well-suited for identifying the optimal producer subset. The flowchart in Figure 4.2 provides a visual representation of the SA protocol and its steps in determining the best subset of producers.

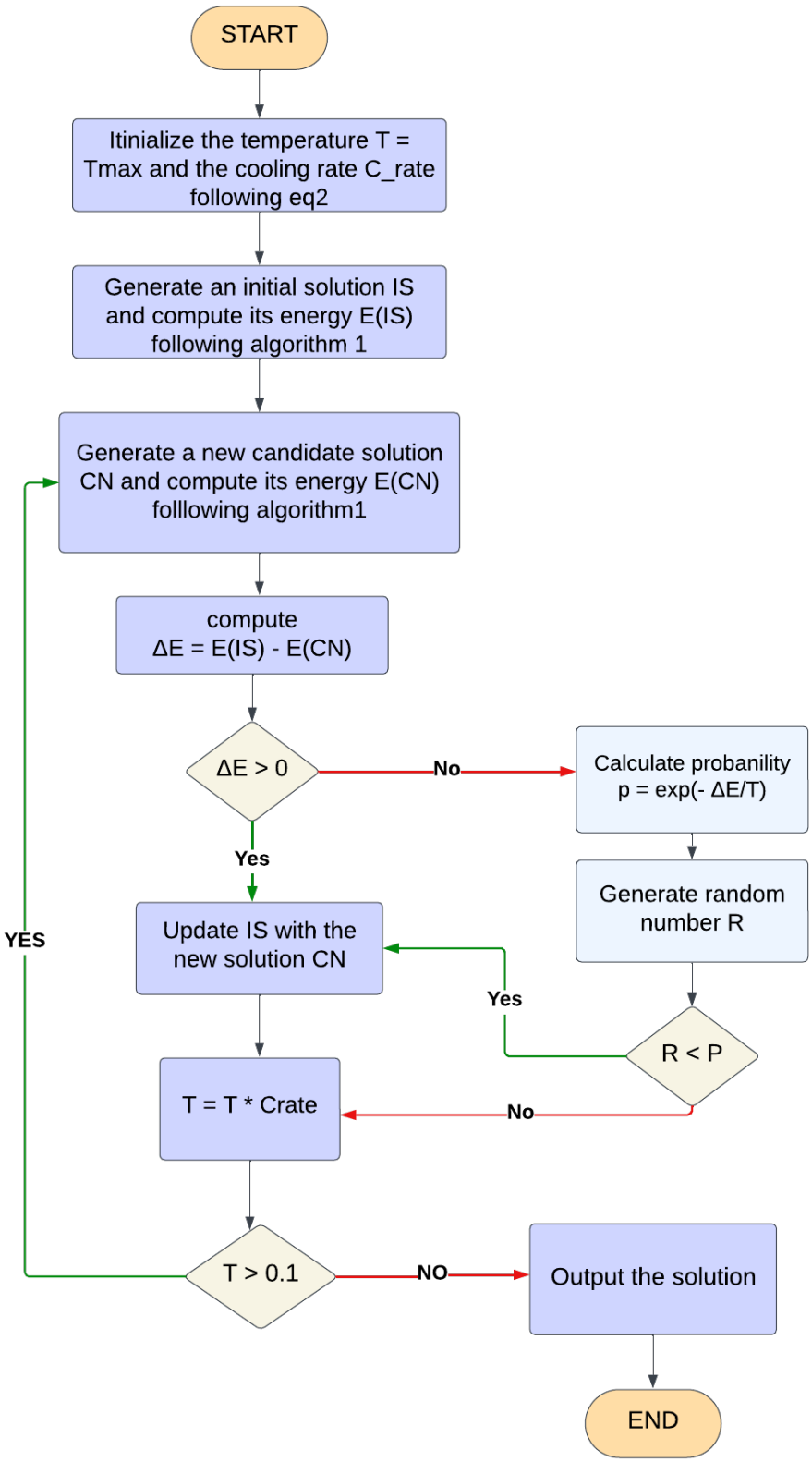

Figure 4.2: SA for optimal producer subset determination

4.2 Simulation Results And Analyses

In this section, we present the results of a simulation conducted in Python on networks of 17 and 30 nodes. The network consists of users, each a microgrid, interconnected by power lines. Figures 4.3 and 4.4 illustrate the network topology.We assume that the power lines have no pre-existing power.

case 1: seventeen nodes network

We compared our findings to the work published in paper [142]. We used the same router and power line parameters as shown in tables 4.1 and 4.2.

Table 4.1: Energy Router Characteristics for 17-Node Network

ER	Efficiency	Capacity	ER	Efficiency	Capacity
1	1.00	20	10	0.97	20
2	0.98	15	11	1.00	27
3	1.00	25	12	0.98	25
4	1.00	24	13	1.00	30
5	0.98	22	14	0.98	19
6	0.97	20	15	1.00	18
7	0.98	25	16	0.97	18
8	0.97	30	17	0.98	20
9	1.00	30			

Table 4.2: Power Line Characteristics for a 17-Node Network

Cable	Capacity	R_{ij}	V_{ij}	Cable	Capacity	R_{ij}	V_{ij}
L_{1-3}	30	0.60	400	L_{6-7}	40	0.24	400
L_{1-9}	45	0.45	400	L_{6-13}	30	0.21	400
L_{1-14}	40	0.21	400	L_{7-8}	10	0.21	400
L_{1-17}	30	0.24	400	L_{8-9}	32	0.65	400
L_{2-3}	20	0.64	400	L_{8-13}	40	0.19	400
L_{2-5}	20	0.51	400	L_{9-12}	32	0.45	400
L_{2-10}	30	0.19	400	L_{10-11}	30	0.24	400
L_{2-17}	30	0.19	400	L_{11-15}	32	0.60	400
L_{3-7}	45	0.94	400	L_{11-17}	40	0.24	400
L_{4-5}	24	0.19	400	L_{12-16}	40	0.21	400
L_{4-10}	30	0.64	400	L_{14-15}	30	0.45	400
L_{5-6}	7	0.45	400	L_{14-16}	35	0.19	400

Figure 4.3 depicts the seventeen-node network topology, where node D4 is the consumer, and nodes D9, D15, and D16 are the producers. .

The energy profiles of the consumers and producers in the network are illustrated in Table 4.3. This table displays the energy demand or overflow of each node, with values assigned accordingly. For example, -22 represents the demand of consumer D4, while 9, 12, and 15 represent the producers D9, D15, and D16, respectively, along with their proposed energy prices. Results are highlighted in Table 4.4.

Table 4.4 presents a comparison of the results achieved by SA-ERP and IACO-ERP with node D4.

Upon detailed analysis of the results, we observe a clear trend: SA-ERP outperforms IACO-ERP in delivering superior outcomes for consumer D4. This advantage is most evident in three key areas: total power loss, the energy metric that defines the fitness function for IACO-ERP, and overall cost.

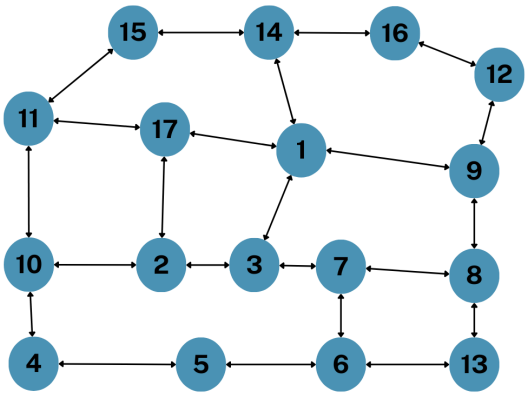

Figure 4.3: The seventeen-node network topology

Table 4.3: 17-Node Energy Profile

MG	D4	D9	D15	D16
Power (kW)	-22	9	12	15
Price (USD/kW)	–	0.068	0.056	0.043

case 2: thirty-node network

We conducted a simulation on a 30-node network and compared our findings with IACO-ERP. Figure 4.4 illustrates the network topology.

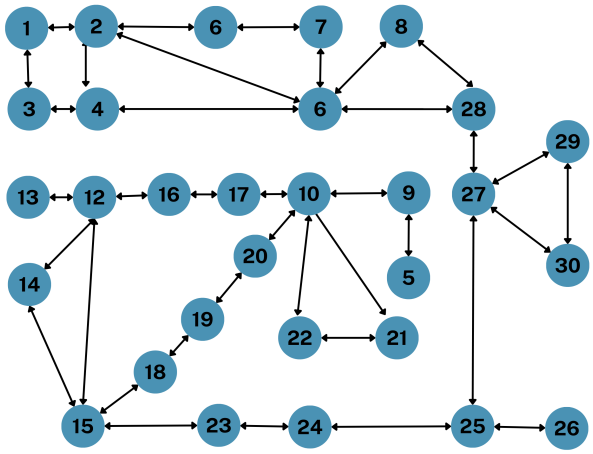

Figure 4.4: The thirty-node network topology

We used the same power line parameters and router efficiencies of the 30-node network presented in paper [62].

The energy profiles of the consumers and producers in the network are illustrated in Table 4.5.

Results are highlighted in Table 4.4.

The observed results highlight a trade-off between Ant Colony Optimization (ACO) and Simulated Annealing (SA). ACO provides better performance in terms of energy function but has higher power loss in some scenarios. This indicates that SA is more effective at exploring the solution space comprehensively and identifying an optimal producer subset. The difference stems from SA's stochastic exploration strategy, which allows it to escape local optima and evaluate a broader range of configurations compared to ACO's pheromone-guided, path-reinforcing mechanism.

Table 4.4: Comparative Results of SA-ERP and IACO-ERP

Protocol	Producer	Energy	Price	Optimal Path	Power Loss	Capacity	Energy Function	Cost
SA-ERP	15	12	0.056	15→11→10→4	0.363	18	1.06	1.037
	9	9	0.068	9→1→3→2→5→4	0.357	15		
	16	1	0.043	16→14→15→11→10→4	0.078	17		
IACO-ERP	15	12	0.056	15→11→10→4	0.360	18	1.20	1.14
	16	10	0.043	16→14→1→3→2→5→4	0.900	17		

Table 4.5: 30-Node Energy Profile

MG	D26	D24	D17	D30	D2	D3	D8
Power amount (Kw)	-6	-22	-5	7	12	7	17
Price(USD/Kw)	–	–	–	0.043	0.056	0.068	0.041

Table 4.6: Comparative Results for 30-Node Network

Consumer	Protocol	Producer	Price (USD/kW)	Path	Energy Function	Power Loss (kW)	Cost (USD)
26	IACO-ERP	30	0.043	30→27→25→26	0.42	0.30	0.54
	SA-ERP	8	0.041	8→28→27→25→26	0.35	0.46	0.246
24	IACO-ERP	2	0.056	2→4→12→15→23→24	1.59	2.09	1.09
		8	0.041	8→28→27→25→24			
	SA-ERP	3	0.068	3→4→12→15→23→24	1.50	1.92	0.97
		8	0.041	8→28→27→25→24			
17	IACO-ERP	8	0.041	8→6→10→17	0.49	0.55	0.43
	SA-ERP	3	0.068	3→4→12→16→17	0.341	0.342	0.34

4.3 Conclusion

Energy routing is a pivotal building block in creating a sustainable and reliable energy system. However, effective energy routing involves several interrelated challenges, most notably determining the producer subset and selecting loss-efficient paths. This chapter addressed these challenges by introducing a physically grounded routing framework that explicitly accounts for transmission losses within a realistic Smart Grid architecture.

To address the path selection problem, all feasible transmission paths between routing nodes were examined, and power losses were explicitly calculated for each path using electrical parameters. The optimal route was selected by minimizing total transmission loss, ensuring accurate, physically consistent energy delivery decisions. In parallel, the producer subset determination problem was formulated as a combinatorial optimization task and solved using a Simulated Annealing approach, enabling efficient exploration of the solution space under complex network constraints.

Simulation results demonstrate that the proposed SA-based energy routing framework consistently outperforms the IACO-ERP benchmark in terms of transmission loss reduction and solution quality, particularly in constrained and heterogeneous network scenarios. These findings confirm the effectiveness of incorporating detailed power loss modeling and metaheuristic optimization into energy routing strategies.

Future work will extend this framework by incorporating transmission scheduling mechanisms to address simultaneous energy transfers and congestion management. Additionally, further validation on different network topologies will be conducted to assess scalability and reinforce the applicability of the proposed approach in real-world Smart Grid deployments.

Chapter 5

GQA-RA: A Quantum Genetic-based Routing Protocol for Real-Time Peer-to-Peer Energy Transactions

Contents

5.1 Introduction . . . 57
5.2 Energy Internet: Paramount Component and Topology . . . 58
5.2.1 Network Model . . . 58
5.2.2 Energy router . . . 59
5.3 Energy routing protocol . . . 60
5.3.1 Minimum path loss algorithm . . . 60
5.3.2 Producer subset determination using quantum genetic algorithm . . . 64
5.3.3 Dynamic Scheduling for Smart Grid Networks . . . 68
5.4 Simulation and performance analysis . . . 69
5.4.1 Network topologies and simulation parameters . . . 69
5.4.2 Evaluation metrics . . . 70
5.4.3 6-Node network . . . 70
5.4.4 30-Node network . . . 74
5.4.5 Greedy search comparison analyses . . . 77
5.5 Complexity and scalability analysis . . . 78
5.6 Discussion . . . 80
5.7 Conclusion . . . 81

5.1 Introduction

As decentralized energy systems evolve toward large-scale and real-time operation, energy routing mechanisms must simultaneously satisfy physical feasibility, economic efficiency, and computational scalability. This chapter focuses on advancing energy routing toward practical deployment by addressing the challenges that arise when multiple energy transactions occur concurrently over constrained Smart Grid infrastructures.

The routing frameworks developed in the previous chapters progressively improved the realism and efficiency of energy routing in SG and EI environments. Despite these advances, several critical challenges remain unresolved, particularly in congestion management, real-time operation, and scalability amid increasing network complexity.

In practical Smart Grid deployments, energy routing decisions must account not only for transmission losses but also for router capacities, shared line congestion, and simultaneous energy transactions.

Metaheuristic approaches such as Simulated Annealing improve solution quality for producer selection but may exhibit increased computation time as network size grows, limiting their suitability for real-time peer-to-peer energy trading. Furthermore, existing evaluations often rely on limited network sizes or simplified traffic conditions, providing insufficient insight into scalability and robustness.

To address these limitations, this chapter introduces a Quantum Genetic Algorithm (QGA)–based energy routing framework that explicitly incorporates real network constraints into the routing process. The proposed approach jointly optimizes producer–consumer matching, loss-efficient path selection, and congestion-aware transmission scheduling. By leveraging quantum-inspired population encoding and probabilistic state evolution, QGA achieves faster convergence and improved exploration of large and complex solution spaces compared to classical metaheuristics.

In addition to algorithmic enhancements, this chapter presents a comprehensive simulation framework to evaluate the proposed approach across diverse network topologies and traffic conditions. Scalability analysis is conducted across increasing network sizes, and performance is compared against multiple benchmark routing algorithms, including greedy, bio-inspired, and heuristic-based methods. The results demonstrate that the QGA-based framework achieves superior performance across transmission loss, cost efficiency, congestion mitigation, and computational scalability, making it suitable for real-time operation in decentralized energy markets.

5.2 Energy Internet: Paramount Component and Topology

5.2.1 Network Model

The EI network can be represented as an undirected graph $G = \{V, E, W\}$, as depicted in Figure 5.1. The nodes (V) of the graph represent energy routers, and the edges (E) represent unidirectional power lines. The node's weight w_i represents the conversion loss of ER_i, while the edge's weight $w_{(i,j)}$ represents the transmission loss in line (i, j). Each power line has multiple characteristics, such as resistance, capacity, and voltage. Each node in the network represents a microgrid, which in turn functions as a prosumer. These prosumers are equipped with smart meters that monitor real-time energy production and consumption, and communicate this data to their associated energy routers to facilitate accurate energy transfer

The control center is another key component of the EI system. Deployed as a cloud-based server, it receives real-time energy demand data for sale or consumption from energy routers, executes the routing protocol, and informs participants of the results. The control center supervises energy transmission scheduling and ensures there are no collisions. It is initially equipped with the network topology and uses data routing to continuously track every change in the network.

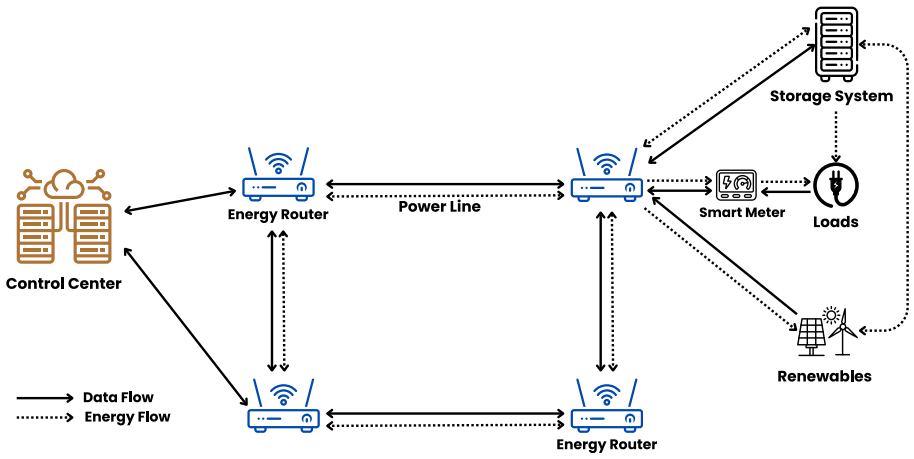

Figure 5.1: Energy internet architecture.

Security Concerns

The presence of a control center enhances security by providing oversight, managing data privacy, and enforcing consistent security protocols throughout the network. This reduces the risks associated with fully decentralized systems, such as data breaches and lack of coordination [143].

As stated in [144], a centralized system offers higher security and is more efficient in the short term; however, less is known about the long-term effects of both centralized and decentralized energy systems. Especially in designs that lack storage systems. A fully decentralized system offers maximum autonomy and flexibility, but at the cost of increased security risks and potential inefficiencies. In contrast, a semi-decentralized system strikes a balance by maintaining a central authority that ensures security and coordination, while still leveraging the benefits of decentralization [145]. This makes semi-decentralized systems more secure and easier to manage, particularly in complex energy networks.

5.2.2 Energy router

An Energy Router (ER) is a device that connects various sources of energy , such as solar photovoltaics (PV) and wind turbines, to the energy grid through advanced interfaces [146]. It effectively manages the intermittency and variability associated with renewable energy resources, which are inherently dependent on unpredictable weather conditions [147].

While Chapter 1 introduced the ER conceptually, this chapter focuses on its operational role within the proposed QGA-based routing framework.

An energy router consists of two main layers: the **physical layer** and the **data layer**, as shown in Figure 5.2.

The physical layer primarily manages the flow of electricity. Its core component is the converter, composed of a series of interconnected solid-state transformers. These transformers can convert AC to DC and adjust voltage levels to meet the specific requirements of different loads.

The data layer is where intelligent routing energy management occurs. This layer includes an intelligent module and a plug-and-play interface that work together to optimize the energy router's operation. The plug-and-play interface bridges the physical and data layers, enabling seamless integration of new devices into the system without manual configuration. On the other hand, the intelligent module is composed of the following key units:

- **Communication Unit**: Responsible for collecting and forwarding data within the system.
- **Control Unit**: This unit includes a **Security Management Unit** that ensures data integrity and security through encryption and authentication protocols. The **Quality Control Unit** ensures that the energy supplied meets high standards. Additionally, the **Energy Management Unit** performs complex mathematical operations to optimize energy routing, including energy forecasting and resource allocation.

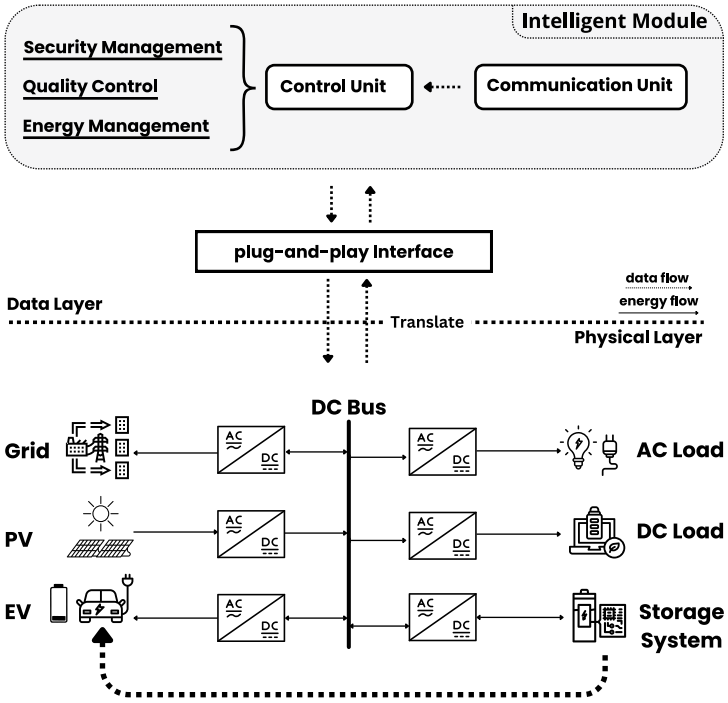

Figure 5.2: Energy router Architecture.

In addition to all the previously mentioned functionalities, the router's integration with real-time weather forecasting and predictive algorithms enables it to optimize the operation of PV solar panels and wind turbines, ensuring they are powered and utilized efficiently based on current and anticipated weather conditions.

5.3 Energy routing protocol

An efficient and reliable power system requires a highly functional, secure, and robust routing protocol to address its most prominent challenges: identifying the most energy-efficient path, selecting the appropriate subset of producers, and scheduling transmissions effectively. In this section, we present a real-time energy routing protocol that uses quantum genetics and a greedy algorithm with dynamic scheduling to address all of the above problems.

The modified greedy algorithm, coupled with the quantum genetic algorithm, is specifically tailored to solve the producer subset problem, ensuring that each consumer is paired with the most efficient producer and path available at any given moment. Our protocol has semi-decentralized control and robust congestion management, all of which contribute to its effectiveness and scalability in dynamic network environments.

5.3.1 Minimum path loss algorithm

Determining the Minimum Path Loss (MPL) is a critical task in energy transmission; it involves selecting an optimal path that minimizes power loss. However, it is a difficult procedure. The difficulty in determining the MPL stems from the complex nature of energy transmission networks. The optimal path for power transmission depends on two primary factors: the energy loss during transmission and the energy loss during conversion, as shown in Equation 5.1.

$$P_{\text{loss}} = \sum_{i \in R} P_{\text{c}_{(i)}} + \sum_{(i,j) \in R} P_{\text{t}_{(i,j)}} \tag{5.1}$$

Where P_{loss} is the total active power loss, which equals the sum of power lost in conversion at all routers along the path $P_{\text{c}_{(i)}}$ and power lost in transmission among all power lines along the path $P_{\text{t}_{(i,j)}}$.

Active transmission power loss is calculated using Equation 5.2. For simplicity, we neglect the reactive power:

$$P_{t_{(i,j)}} = \frac{R_{(i,j)}}{V_{(i,j)}^2} \times \left[(Re + Ee)^2 - Ee^2\right] \tag{5.2}$$

Where R is the resistance of the transmission line, V is the voltage of the transmission line, Re is the remaining energy to be transmitted through the line, and Ee is the existing energy in the power cable.

The conversion loss is calculated using Equation 5.3:

$$P_{c_{(i)}} = (1 - \eta) \times E \tag{5.3}$$

Where $P_{c_{(i)}}$ is the power loss due to conversion, η is the efficiency of the conversion process (a value between 0 and 1), and E is the energy being transmitted.

Capacity constraint

The transmitted power should not exceed the capacity of the power line and the capacity of the router, as described in the following equations.

- Power line capacity constraint:
$$C_c \geq E_t$$
- Router capacity constraint:
$$C_r \geq E_t$$
- Transmitted power constraint:
$$E_t \leq \min(C_c, C_r)$$

Where C_c represents the capacity of the canal, C_r represents the router capacity, and E_t represents the energy transmitted.

To solve the MPL problem, we proposed a modified greedy search algorithm. It prioritizes paths based on their estimated total cost and progressively explores nodes until it finds the optimal path, as shown in Algorithm 4 and Figure 5.3.

Algorithm 4 Optimal Path Calculation in an Energy Network.

Input: Graph G, Source node s, Destination node d, Initial energy E.
Output: Optimal path from s to d, Total power loss along the path.
Initialize a priority queue Q with elements (Cost, Node, Path, Energy)
Set $Q \leftarrow (\text{NodeLoss}(s, E), s, [s], E)$
Set opt_path $\leftarrow$ None and opt_cost $\leftarrow \infty$
Initialize visited set VS as empty
Sort the priority queue from smallest to largest
while Q is not empty **do**
    Dequeue (Cost, Node, Path, Energy) with minimum cost from Q
    if Node $= d$ and Cost $<$ opt_cost **then**
        Update opt_path $\leftarrow$ Path and opt_cost $\leftarrow$ Cost
    end if
    if Node has been visited **then**
        continue
    end if
    for each neighbor N of Node **do**
        Retrieve edge e_{nodeN} connecting Node and N
        if adding E to the energy on e_{nodeN} exceeds its capacity **then**
            continue
        end if
        Calculate power loss using Eq. 5.1
        Update Energy $\leftarrow$ Energy $-$ Power Loss
        Push $(\text{Cost}', \text{N}, \text{Path} \cup \{\text{N}\}, \text{Energy})$ into Q
    end for
end while
if opt_path = None **then**
    return None ▷ No feasible path found
else
    return opt_path and opt_power_loss
end if

The Modified Greedy Search Algorithm (Algorithm 4) addresses the Minimum Power Loss (MPL) problem by selecting paths based on cumulative power loss, while considering both energy availability and link capacity constraints. Unlike traditional greedy search, which selects the next node based on immediate cost, this modified version accounts for cumulative power loss along the path and filters out infeasible links.

At each step, the algorithm evaluates power loss between the current node and its neighbors, considering only those links that can support the remaining energy. The neighbor with the lowest power loss is added to the priority queue, and visited nodes are skipped. If a better path to the destination is found, then the optimal cost and path are updated. This process continues until the destination is reached or no feasible path exists. If no valid path is found—typically due to insufficient capacity—the algorithm returns `None`. In such cases, a fallback mechanism based on the Quantum Genetic Algorithm (QGA-RA) is triggered (Algorithm 5), which splits the energy demand across multiple partial paths starting from the producer's neighbors, prioritizing high-capacity links.

The detailed steps of Algorithm 4 are presented as follows:

- The algorithm takes as input: a graph G, source node s, a destination node d, an initial energy demand E
- A priority queue Q is initialized with a tuple of the form (Cost, Node, Path, Energy), where:
  - Cost is the power loss at the source node s

  - Node is the current node (initially s)
  - Path is the list of visited nodes (initially $[s]$)
  - Energy is the remaining energy (initially E)
- A visited set VS is initialized to keep track of explored nodes.
- While the priority queue Q is not empty:
  - Dequeue the tuple with the minimum cost.
  - If the current node equals d and the cost is better than opt_cost, update opt_path and opt_cost.
  - If the current node has been visited before, skip to the next iteration.
  - Otherwise, For each neighbor N of the current node:
    * Retrieve the edge $e_{\text{node},N}$.
    * If the edge capacity is insufficient for the remaining energy, skip it.
    * Compute the power loss using Eq. 5.1, and update the remaining energy.
    * Compute the new total cost and updated path.
    * Push the tuple $(\text{Cost}', N, \text{Path} \cup \{N\}, E')$ into the priority queue Q.
- If no valid path is found, return `None`; otherwise, return the optimal path and its associated total power loss.

Figure 5.3 presents a step-by-step example illustrating the operation of the Modified Greedy Search Algorithm. In this example, the algorithm incrementally constructs an energy transmission path from the source to the destination by selecting at each step the neighboring node that results in the minimal incremental power loss, while accounting for edge capacities and remaining energy.

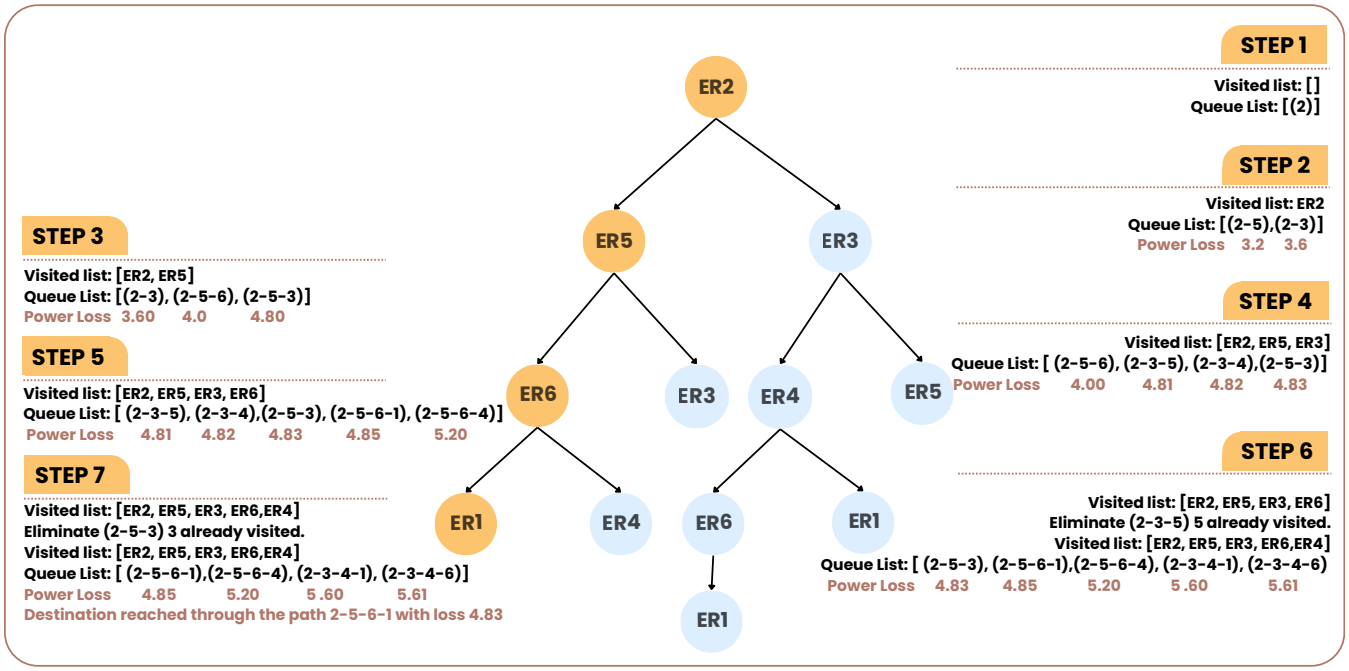

Figure 5.3: Steps of the Modified Greedy Search Algorithm.

When Algorithm 4 fails to return a valid energy transmission path, typically due to capacity constraints or excessive power loss, Algorithm 5 is triggered as a fallback mechanism. This algorithm

begins by retrieving the set of neighboring nodes N of the consumer c from the graph G and initializing a capacity map C to store the capacities of the power lines connecting each neighbor to the consumer. For each neighbor $n \in N$, it retrieves the capacity of the connecting edge (power line) (n, c) and stores it in C. The capacities in C are then sorted in descending order to prioritize allocation from the highest-capacity links. The algorithm iterates through each edge-capacity pair $(e, \text{cap}) \in C$, and as long as the remaining demand is larger than 0 ($d > 0$), it attempts to fulfill the demand:

- If the current capacity cap is less than the remaining demand d, it invokes the QGA-RA Algorithm with cap as the new demand and updates $d \leftarrow d - \text{cap}$.
- Otherwise, it executes the QGA-RA with the remaining demand d and sets $d \leftarrow 0$.

After each allocation, the algorithm updates the power line's transmitted energy, the producer's remaining energy, and the consumer's remaining demand. If the entire demand is satisfied or no more viable edges remain, the process terminates. This mechanism ensures that energy is allocated through the most capacitated links first, as mentioned in Algorithm 5.

Algorithm 5 Capacity-Aware Allocation.

```
Input: Graph G, consumer c, demand d, producers P.
if opt_path = None then
    Retrieve neighbors of c: N ← Neighbors(G, c)
    Initialize capacities: C ← {}
    for each n ∈ N do
        Retrieve capacity between n and c
        Store in C[(n, c)]
    end for
    Sort C in descending order based on capacity
    for each (e, cap) in C do
        if d > 0 then
            if cap < d then
                Execute c using QGA-RA with cap
                Update d: d ← d − cap
            else
                Execute c using QGA-RA with d
                d ← 0
            end if
            Update power line energy, producer energy, and consumer demand
        else
            break
        end if
    end for
end if
```

5.3.2 Producer subset determination using quantum genetic algorithm

To solve the Producer Subset Determination problem, we propose an optimization strategy based on the Quantum Genetic Algorithm (QGA). QGA is an optimization algorithm that combines principles of quantum computing with those of classical genetic algorithms (GAs). It represents the solution as quantum bits (qubits). Each qubit can be in a superposition of states, allowing the algorithm to explore a larger solution space simultaneously.

The proposed algorithm iterates over five main QGA steps, as shown in Figure 5.4.

1. Parameter initialization: The optimization process's parameter initialization involves defining producers and consumers, along with their respective attributes. Producers are specified with

unique identifiers, available energy, and unit prices. Consumers are characterized by their unique identifiers and energy demand. Additionally, the number of chromosomes, representing the potential solutions in the initial population of the genetic algorithm, is defined. The rotation angle θ (used by the rotation function) is initially set to a small value to guide the population towards better solutions during the optimization process. This careful parameter initialization ensures the algorithm has a strong foundation for effectively exploring and optimizing the solution space.

2. Quantum Encoding: In our proposed Quantum Genetic Algorithm (QGA), a solution $Q(t)$ represents a set of chromosomes depicted as quantum bits (qubits) as shown in Equation 5.4.

$$Q(t) = \left[q_1^t, q_2^t, \ldots, q_j^t, \ldots, q_n^t\right] \tag{5.4}$$

$Q(t)$ represents a population at generation t, while n and q_j^t represent the size of the population and a chromosome j at generation t, respectively.

A qubit is the most basic unit of information in quantum computing, capable of existing in a superposition of both $|0\rangle$ and $|1\rangle$ states simultaneously as depicted in Equation 5.5.

$$|\Psi\rangle = \alpha|0\rangle + \beta|1\rangle \tag{5.5}$$

Where α and β are complex numbers, representing probability amplitudes [148] and can satisfy Equation 5.6.

$$|\alpha|^2 + |\beta|^2 = 1 \tag{5.6}$$

Based on α and β, the qubit is shaped in this format $\begin{bmatrix}\alpha \\ \beta\end{bmatrix}$.

To represent our solution in a readable format, we transform the qubits into a binary string using the proposed MeasureQbits function. This encoding method is similar to the binary representation used in solving the knapsack problem. Each potential solution is encoded as a binary string (chromosome), where each bit (gene) indicates whether a specific producer is included ('1') or excluded ('0'). However, because of the nature of our problem, the state '1' can indicate that we have either taken all of the producer's energy or a fraction of it, depending on our needs.

3. Population Initialization: The algorithm starts by initializing the first solution as a set of ($\frac{1}{\sqrt{2}}$, $\frac{1}{\sqrt{2}}$). This state represents an equal probability of being 0 and 1 at time t=0 [149].

4. Processing Producers: To extract a real solution from a quantum chromosome, we need to measure the qubits. Measuring qubits collapses the superposition state of each qubit into a classical binary state (0 or 1). To accomplish this, we propose a function called MeasureQbits following Algorithm 6.

The MeasureQbits Algorithm is a probabilistic decoding procedure that interprets a quantum chromosome (a list of gene amplitudes representing a quantum individual's state) into a classical binary solution. It determines which producers will supply energy and how much energy they should provide to satisfy a given consumer's demand. Bc and Ec represent the binary and decimal solutions, respectively. D is the consumer's total energy demand, while Q_d is the temporary variable that represents the remaining demand that still needs to be fulfilled. The algorithm starts by initializing Q_d to the initial consumer's demand. Bc and Ec are initialized as empty lists for binary and real-valued solutions, and the `valid_solution` flag is set to `False`. For each gene in the chromosome, it generates a random number r between 0 and 1. If r is greater than the square of the gene value, and if there is still unmet demand and the producer has available energy to provide the consumer with:

- The producer is selected
- The algorithm checks if the producer's available energy is less than or equal to the remaining demand:

Algorithm 6 Process Producers (MeasureQbits)

```
1: procedure MeasureQbits(individual, producers, D)
2:     valid_solution ← False
3:     while ¬valid_solution do
4:         Initialize Q_d to D
5:         Initialize Bc and Ec as empty lists
6:         for each gene_value in chromosome do
7:             Generate Random Number r between 0 and 1
8:             Fetch the energy available from the producer (gene)
9:             if r > gene_value^2 and Q_d > 0 and energy > 0 then
10:                if energy ≤ Q_d then
11:                    Allocate energy to Q_d
12:                else
13:                    Partially allocate Q_d to energy
14:                end if
15:                Set corresponding binary gene to 1
16:            else
17:                Set corresponding binary gene to 0
18:            end if
19:            if ∑(Ec) = D then
20:                valid_solution ← True
21:            end if
22:            Update Bc and Ec accordingly
23:        end for
24:    end while
25:    return Bc, Q_d, Ec
26: end procedure
```

  - If so, all of the producer's energy is used.
  - If not, only the needed portion of energy (Q_d) is allocated.
- The allocated energy is appended to Ec, and (Q_d) is reduced accordingly.

  If the condition is not satisfied, the producer is not selected, and zero energy is allocated.

The resulting binary string represents the inclusion or exclusion of each producer, and the solution E_c represents the energy amount the consumer will buy from each producer.

Solving the producer subset problem aims to allocate the exact amount of energy requested by consumers to producers. To verify if the obtained solution is feasible, we sum the allocated energies and check if the total matches the consumer's demand. Any deviation from the requested amount, whether surplus or deficit, renders the solution unacceptable.

5. Fitness Function: The best chromosome in a population is the one with the least fitness value. In our problem, fitness represents the power lost in transmission and conversion, and the cost of energy, as defined in Equation 5.7. To calculate the power loss, we use the algorithm described in Section 5.3.1, which is based on a modified greedy search.

$$\text{solution\_fitness} = (0.5 \times \text{total\_cost}) + (0.5 \times \text{total\_loss}) \tag{5.7}$$

6. Rotation Function: Passing from one generation to another in a Quantum Genetic Algorithm (QGA) requires the use of the rotation function. This function updates the quantum chromosomes by adjusting the probabilities of the quantum bits based on the fitness of the solutions. This process involves calculating the rotation angles and applying these rotations to guide the qubits toward better solutions following Equation 5.8:

$$\begin{bmatrix} \alpha_i^{t+1} \\ \beta_i^{t+1} \end{bmatrix} = \begin{bmatrix} \cos(\theta_i) & -\sin(\theta_i) \\ \sin(\theta_i) & \cos(\theta_i) \end{bmatrix} \cdot \begin{bmatrix} \alpha_i^{t} \\ \beta_i^{t} \end{bmatrix} \tag{5.8}$$

where the new value of the angle of rotation θ_i for the quantum qubit gate is calculated using Equation 5.9:

$$\theta_i = S(\alpha_i, \beta_i) \cdot \Delta\theta_i \tag{5.9}$$

Where $S(\alpha_i, \beta_i)$ determines the direction of the angle, and the value of $\Delta\theta_i$ is determined from the lookup table depicted in Table 5.1, which is inspired by the work in [149].

Table 5.1: Lookup Table of Rotation Angle

x_i	b_i	$f(x) \geq f(b)$	$\Delta\theta_i$	$S(\alpha_i\beta_i)$			
				$\alpha_i\beta_i > 0$	$\alpha_i\beta_i < 0$	$\alpha_i = 0$	$\beta_i = 0$
0	0	False	0	0	0	0	0
0	0	True	0	0	0	0	0
0	1	False	δ	+1	-1	0	$\pm$1
0	1	True	δ	-1	+1	$\pm$1	0
1	0	False	δ	-1	+1	$\pm$1	0
1	0	True	δ	+1	-1	0	$\pm$1
1	1	False	0	0	0	0	0
1	1	True	0	0	0	0	0

In Table 5.1, x_i represent the i-th bit of binary solution x, b_i is the i-th bit of the best solution b, $f(.)$ is the fitness function, and $S(\alpha_i\beta_i)$ is the sign of the rotation angle θ_i.

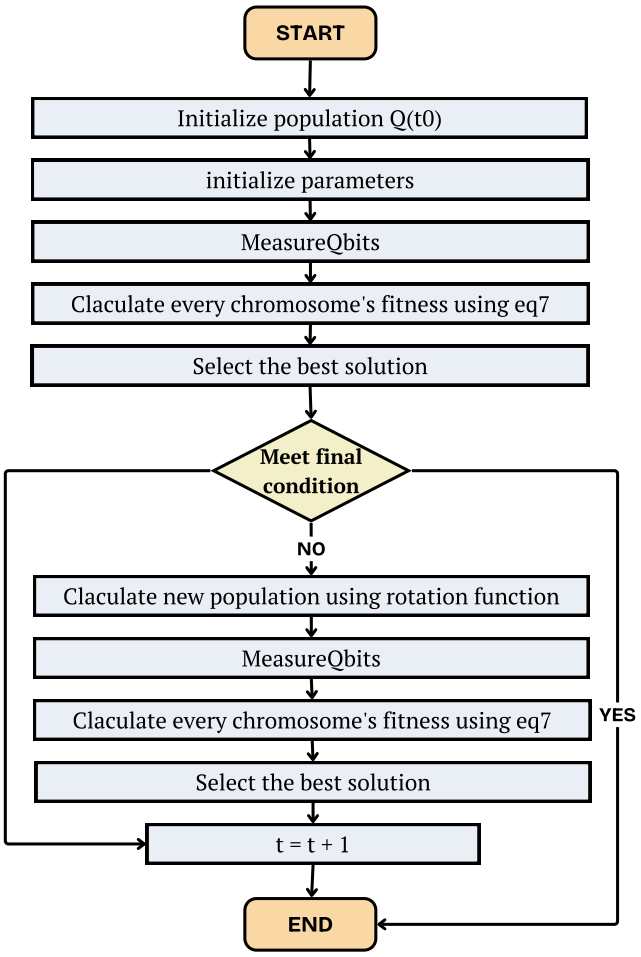

Figure 5.4: GRA-RA Flowchart.

5.3.3 Dynamic Scheduling for Smart Grid Networks

To efficiently manage energy transmission and prevent collisions in Smart Grid Networks, we propose a two-step scheduling mechanism that operates as follows:

- Inter-Consumer Path Management: Within the same consumer, the QGA-RA algorithm ensures that no paths overlap when allocating multiple energy sources. This process uses the Minimum Path Loss algorithm (MPL) proposed in Section 5.2. During this process, producers are sorted in ascending order based on their IDs. After generating each path, the MPL algorithm updates the existing energy on power lines and verifies their capacity before finalizing the path selection. This ensures that energy distribution across different paths is collision-free and does not exceed the capacity of the power lines.
- Outer-Consumer Path Management: This is divided into two cases: Consumer Transmission Overlap and Simultaneous Consumer Arrival.
  - Consumer Transmission Overlap: In this case, consumers arrive at different times, but their transmission times overlap during a certain period. This scenario is also handled by the MPL algorithm, which selects an alternative path that satisfies capacity constraints and considers the existing energy in the power links.
  - Simultaneous Consumer Arrival: In this case, we propose a clustering mechanism to ensure that consumers are all executed at the same time. The algorithm forms non-collision clusters and calculates each cluster's priority based on two factors: the size of the cluster (i.e., the number of paths within the cluster) and the number of unique destinations (i.e., the count of

unique consumer endpoints within the cluster), following Equation 5.10. The highest-priority cluster is chosen first and allocated resources, while the remaining clusters are executed based on the remaining resources.

$$priority \leftarrow size\_of\_cluster + num\_destinations\_cluster \tag{5.10}$$

Figure 5.5 represents the QGA-RA protocol running flowchart.

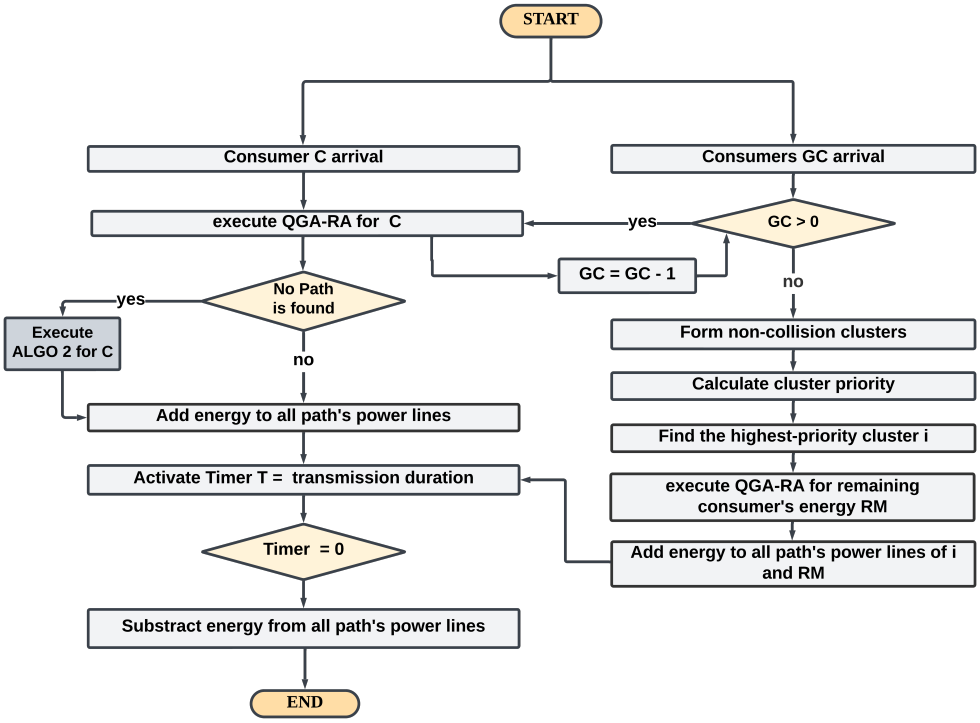

Figure 5.5: QGA-RA running Workflow for one consumer

5.4 Simulation and performance analysis

The RA protocol is evaluated by comparing it with the MLR protocol presented in [114], as both approaches address the efficient path problem, producer subset determination, and scheduling mechanisms. Furthermore, the minimum path loss algorithm is evaluated against several existing methods: the Dijkstra algorithm used in MLR, the genetic algorithm proposed in [128], the SA-based approach described in [130], and the brute-force method used in [55].

A multi-hour simulation was conducted using Python in PyCharm on a computer equipped with a 6th-generation Intel i7 CPU and 8 GB of RAM. To evaluate the performance of our proposed energy routing algorithm. Our algorithm was tested in networks of varying sizes, and the results were compared with those reported in [114].

5.4.1 Network topologies and simulation parameters

Our network consists of microgrids interconnected through power lines with the help of ERs, as shown in Figure 5.6 and 5.7. We apply QGA-RA to two network topologies with 6 to 30 nodes to test its scalability compared to the MLR proposed in [114]. Each network is then tested for four case studies, the parameters of the Quantum Genetic Algorithm are:

- Number of iterations: 5

- Rotation angle θ: 0.01
- Population size: 3
- Chromosome length (genes per chromosome): number of producers

5.4.2 Evaluation metrics

The proposed algorithm was evaluated based on total power cost, post-transaction power loss, routing decision accuracy, execution time, computational complexity, and scalability.

5.4.3 6-Node network

For the 6-node network analysis, we employed the topology based on the Ward-Hale 6-bus system, as modified in [114]. We applied our algorithm to this network and compared the results with the findings from [114] to assess its performance and efficiency.

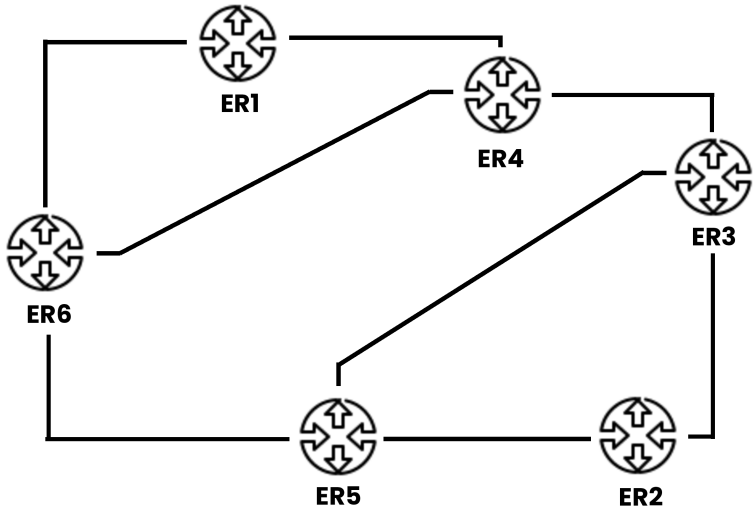

Figure 5.6: 6-Node Network Topology.

Tables 5.2 and 5.3 detail the parameters of energy routers and power lines, respectively.

Table 5.2: Parameters of Energy Routers (6 MGs)

Parameter	ER1	ER2	ER3	ER4	ER5	ER6
Interface capacity/kW	80	160	160	120	160	80
Conversion efficiency	0.98	0.95	0.96	0.97	0.97	0.98

The algorithm's performance was compared with MLR across four scenarios, each representing a distinct state of the system. These scenarios were used to test the algorithm's reliability, flexibility, efficiency, scalability, and cost reduction.

Table 5.4 details the energy trading data for the 6-node network. The table highlights the energy consumption and production of all prosumers. Negative energy values represent the energy demand of consumers, while positive values indicate the surplus energy producers are willing to sell at time t.

Table 5.3: Power lines parameters (6 MGs)

Power Lines	**Resistance(Ω)**	**Capacity(kW)**	**Voltage (V)**
(1,4)	0.675	70	800
(1,6)	0.780	65	800
(2,3)	0.341	145	800
(2,5)	0.365	145	800
(3,5)	0.585	105	800
(4,6)	0.683	70	800
(5,6)	1.268	50	800
(3,4)	0.594	105	800

Table 5.4: Energy profile for 6-MGs Network

Energy profile		**MG1**	**MG2**	**MG3**	**MG4**	**MG5**	**MG6**
Price ($/kW.h)		-	0.065	0.041	-	0.043	-
Energy (kW)	Case 1&2	-40	80	50	-30	35	-45
	Case 3	-65	40	50	-20	45	-50
	Case 4	-15	40	50	-5	45	-100
Time (h)	Case 1	09:00-10:00	09:00-11:00	14:00-15:00	10:00-11:00	15:20-16:20	14:00-16:00
	Case 2	09:00-10:00	09:00-11:00	09:20-10:20	09:10-10:10	09:30-10:30	09:10-11:00
	Case 3	10:00-12:00	09:00-12:00	09:20-12:20	10:00-11:00	09:00-13:00	10:00-12:00
	Case 4	09:00-10:00	09:00-10:30	10:00-12:00	09:10-11:00	10:20-13:20	10:30-12:30

Table 5.5: Transmission times, consumer demand, and energy values for different cases

Case	**Transmission Time**	**Consumer**	**Consumer Demand**	**MLR Producers**	**MLR Energy**	**QGA-RA Producers**	**QGA-RA Energy**
Case 1	9:00-10:00	MG1	40	MG2	40	MG2	40
	10:00-11:00	MG4	30	MG2	30	MG2	30
	14:00-16:00	MG6	45	MG3	45	MG3	45
Case 2	9:00-10:00	MG1	40	MG2	40	MG2	40
	9:10-10:10	MG4	30	MG2	30	MG2	30
	9:10-11:00	MG6	45	MG3	20	MG2	10
					25	MG3	35
Case 3	10:00-12:00	MG1	65	MG3	50	MG5	45
	10:00-11:00	MG4	20	MG5	15	MG3	20
				MG5	20	MG3	20
	10:00-12:00	MG6	50	MG5	10	MG2	40
				MG2	40	MG3	10
Case 4	9:00-10:00	MG1	15	MG2	15	MG2	15
	9:10-11:00	MG4	5	MG2	5	MG2	5
	10:30-12:30	MG6	100	MG2	40	MG2	20
				MG3	50	MG3	50
				MG5	10	MG5	30

Table 5.6: Transmission paths and power loss for different cases

Case	Transit time	Consumer	MLR Generated Path	QGA-RA Generated Path	MLR Power Loss	QGA-RA Power Loss
Case 1	9:00-10:00	MG1	2→3→4→1	2→5→6→1	5.603	4.805
	10:00-11:00	MG4	2→3→4	2→3→4	3.601	3.601
	14:00-16:00	MG6	3→4→6	3→4→6	4.05	4.05
Case 2	9:00-10:00	MG1	2→3→4→1	2→5→6→1	5.603	4.805
	9:10-10:10	MG4	2→3→4	2→3→4	3.601	3.601
	9:10-11:00	MG6	3→5→6 (20)	2→5→6 (10)	1.8	1.0
			25 3→4→1→6 (25)	3→4→6 (35)	2.75	3.1
Case 3	10:00-12:00	MG1	3→4→1 (50)	3→4→1 (20)	4.504	1.40
			5→6→1 (15)	5→6→1 (45)	1.05	3.15
	10:00-11:00	MG4	5→6→4 (20)	3→4 (20)	1.602	1.75
	10:00-12:00	MG6	5→6 (10)	3→4→6 (10)	0.501	0.9
			2→3→4→6 (40)	2→3→4→6 (40)	5.608	5.608
Case 4	9:00-10:00	MG1	2→3→4→1	2→5→6→1	2.1	1.8008
	9:10-11:00	MG4	2→3→4	2→3→4	0.6	0.6
			2→3→4→6 (40)	2→5→6 (20)	5.604	2.0
	10:30-12:30	MG6	3→4→1→6 (40)	3→4→6 (50)	5.513	4.505
			5→6 (10)	5→6 (30)	0.5	1.501

Table 5.5 outlines the transmission windows, consumer demands, and the energy allocations from producers selected by QGA-RA and MLR. It compares the producer subset selection results of both methods across different demand scenarios and time intervals, specifying the producers each consumer buys energy from and the corresponding amounts. In parallel, Table 5.6 presents the transmission paths established for each selected producer-consumer pair, highlighting the routing decisions made by the Djikstra algorithm proposed in paper [114] and the MLP proposed in this paper.

1. **Case 1:** Non-Overlapping Transmission Periods: As shown in Table 5.5, consumers arrive at different times and have different transmission periods, eliminating the possibility of collisions. In this scenario, transmissions run smoothly with no interference. Each consumer is allocated the best prices available at the time of their demand. The algorithm executes consumer transmissions directly without any time delays, unlike when no path is available. Consequently, the system operates with high efficiency and effectiveness.

   We can also observe that both algorithms' producer allocation choices are the same. However, comparing the results in Table 5.6, we can see that QGA-RA outperforms MLR in selecting the path with the least power loss, thus reducing energy costs for consumer MG1. The remaining results are consistent across both algorithms.

2. **Case 2:** Overlapping Transmission Periods with capacity issues:

   In this scenario, and as shown in Table 5.5, consumers MG1, MG4, and MG6 share overlapping transmission periods, particularly around 9:10. This overlap introduces the risk of a potential collision in energy transmission, which could lead to inefficiencies and increased power losses.

   To address this challenge, both the MLR and QGA-RA algorithms select different transmission paths to avoid these collisions as depicted in Table 5.6:

   For MG1 (First Arriving Consumer), the algorithms allocate optimal resources, as in Case 1. Since MG1 is the first to request energy at this overlapping time, it is granted the best available path (2→3→4→1) for MLR and (2→5→6→1) for QGA-RA.

   Since MG4 requested energy shortly after MG1, both algorithms allocate the best available path to MG4, taking into account the remaining energy in the network. This adjustment ensures that MG4's demand is met while minimizing power losses and avoiding collisions.

It is also observed that the MLR algorithm processes MG4 before MG6, even though they have the same arrival time. By contrast, the QGA-RA algorithm executes both MG4 and MG6 simultaneously, ensuring optimal resource allocation for both consumers. The generated paths are then managed using a dynamic scheduling algorithm that ensures all paths with no overlapping power links are selected. Any remaining paths are then allocated based on the best available energy in the system.

In this scenario, the best cluster consists only of paths 2→3→4, as the system at 9:10 does not have enough energy to fully satisfy MG6's demand. To ensure that MG6 is not left without energy, the QGA-RA algorithm allocates the remaining 10 kW of energy in the system to MG6 until producer MG3 arrives at 9:20 (since MG2 does not have 45kW after supplying MG1 with 40), which will then satisfy the remaining demand.

On the other hand, MLR faces additional limitations due to capacity constraints. The generated path for MG6 cannot transmit the full 45 kW demand because the link 3•4 power line capacity is 105 kW, with 70 kW already in use, leaving only 35 kW available. The MLR algorithm therefore waits until producer MG3 arrives at 9:20 and splits MG6's demand into two parts: 25 kW and 20 kW, to be transmitted sequentially, resulting in a 10-minute delay.

3. **Case 3:** Overlapping Transmission Periods with Simultaneous Consumer Arrivals: In this case, MG1, MG4, and MG6 arrive at the same time as shown in the energy profile Table 5.4. The MLR algorithm treats consumers according to their bidding prices in descending order, while producers are treated in ascending order. On the other hand, the QGA-RA algorithm allocates resources to all consumers simultaneously, ensuring each receives the best possible resources. The dynamic scheduling mechanism guarantees that all consumers meet their demands within their desired transmission time. As shown in Table 5.5 and Table 5.6, the QGA-RA algorithm selected producers MG5 and MG3 to satisfy MG1's demand, MG3 to satisfy MG4's demand, and MG2 and MG3 to satisfy MG6's demand. The generated path cluster has five different paths: [5, 6, 1], [3, 4, 1], [3, 4], [2, 5, 6], [3, 4, 6]. The highest-priority clusters with no overlap are [5, 6, 1], [3, 4, 1], [3, 4], and [3, 4, 6], with transmitted powers of 45, 20, 20, and 10, respectively. since power line (3, 4) has a capacity of 105kW, [3, 4, 1], [3, 4], and [3, 4, 6] can be used simultaneously. The last path [3, 4, 6] is executed after updating the power lines and all participants' energy levels, taking into account the remaining energy in the network. The new path is [2, 3, 4, 6]. After calculating the total power loss of both algorithms, we found that the MLR algorithm resulted in a total loss of 13.266 kW, while the QGA-RA algorithm had a loss of 12.808 kW. Although the difference may seem small, any loss is significant in systems with limited production capacity.

4. **Case 4:** Overlapping Transmission Periods with Heavy Load Demand This case illustrates the results of both algorithms under a heavy load scenario. In this scenario, consumers MG1 and MG4 both have relatively small energy demands, while MG6 has a substantial demand of 100 kW, as shown in Table 5.5 and the energy profile Table 5.4. The chosen paths are also depicted in Table 5.6. For MG1 and MG4, the results are consistent with Cases 1 and 2, in which both consumers required only one producer to meet their energy needs. For MG6, however, the situation is different. Due to its high energy demand, it is impossible to meet its requirements solely with a single producer. Consequently, MG6 needs to source energy from all available producers: MG2, MG3, and MG5. The QGA-RA algorithm is designed to handle such multi-source requirements effectively. It ensures that MG6 receives the optimal combination of energy sources to meet its demand while minimizing power losses and costs, accounting for capacity constraints and potential collisions. On the other hand, the MLR algorithm is not well-suited for multi-source scenarios. As a result, MLR power loss is substantially higher than that of QGA-RA.

5.4.4 30-Node network

For the 30-Node network analysis, we employed the topology used in [114] to check the performance of both algorithms as shown in Figure 5.7.

Table 5.7 details the energy trading data for the 30-node network.

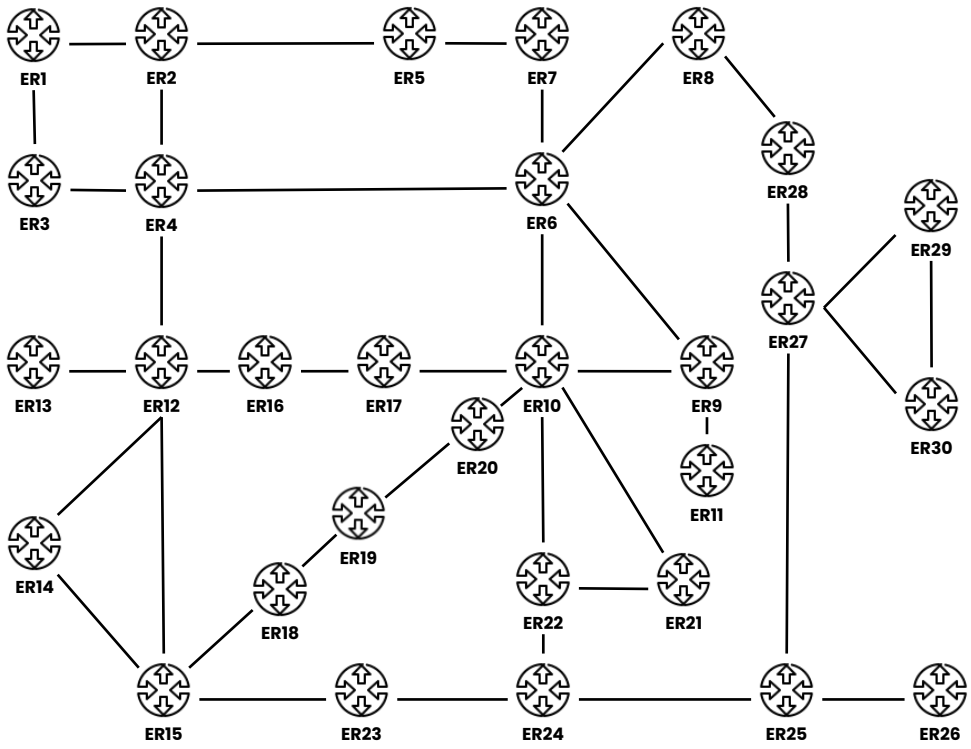

Figure 5.7: 30 Nodes Network Topology.

Table 5.7: Energy profile for 30-MGs Network

Energy profile		**MG2**	**MG8**	**MG16**	**MG17**	**MG22**
Price ($/kW.h)		0.065	-	-	-	0.041
Energy (kW)	Case 1, 2, 3	40	-15	-5	-20	10
	Case 4	30	-5	-40	-10	28
Time (h)	Case 1	09:00-11:30	09:00-10:00	14:00-16:00	10:00-11:00	14:00-15:00
	Case 2	09:00-11:00	09:00-10:00	09:10-11:00	09:10-10:10	09:20-10:20
	Case 3	09:00-11:30	09:10-11:00	09:10-11:00	09:10-11:00	09:00-11:00
	Case 4	09:00-12:00	09:10-11:00	09:15-11:40	09:30-12:00	09:00-12:00

1. **Case 1:** Non-Overlapping Transmission Periods: As shown in Tables 5.8 and 5.9, and similar to the 6-node network, the results of both the MLR and QGA-RA algorithms are identical because there is no power transmission conflict. Both algorithms generate the same paths and achieve identical power loss values across all consumers, indicating that neither method has an advantage in scenarios without overlap.

2. **Case 2:** Overlapping Transmission Periods: An overlap occurs at 9:10 as shown in Table 5.8 when consumers MG16 and MG17 require energy simultaneously. Paths generated by both methods are

Table 5.8: Transmission times, consumer demand, and energy values for different cases

Case	Transit Time	Consumer	Consumer Demand	MLR Producers	MLR Energy	QGA-RA Producers	QGA-RA Energy
Case 1	9:00-10:00	MG8	15	MG2	15	MG2	15
	10:00-11:00	MG17	20	MG2	20	MG2	5
	14:00-16:00	MG16	5	MG22	5	MG22	20
Case 2	9:00-10:00	MG8	15	MG2	15	MG2	15
	9:10-11:00	MG17	20	MG2	10	MG22	20
					10		
	9:10-10:10	MG16	5	MG2	5	MG2	5
Case 3	9:00-10:00	MG8	15	MG22	10	MG2	15
				MG2	5		
	9:10-11:00	MG17	20	MG2	20	MG2	10
						MG22	10
	9:10-10:10	MG16	5	MG2	5	MG2	5
Case 4	9:10-11:00	MG8	5	MG2	5	MG2	5
	9:15-11:40	MG17	10	MG2	10	MG2	10
	9:30-12:00	MG16	40	MG2	30	MG2	24
				MG22	10	MG22	16

Table 5.9: Transmission paths and power loss for different cases

Case	Transit Time	MG	MLR Generated Path	MLR Loss	QGA-RA Generated Path	QGA-RA Loss
Case 1	9:00–10:00	MG8	2→6→8	0.6008	2→6→8	0.6008
	10:00–11:00	MG17	2→6→10→17	1.813	2→6→10→17	1.813
	14:00–16:00	MG16	22→10→17→16	0.554	22→10→17→16	0.554
Case 2	9:10–11:00	MG17	2→6→8 (15)	0.600	2→6→8 (15)	0.600
	9:10–11:00	MG17	2→6→10→17 (10)	0.904	2→4→6→10→17 (20)	2.412
			2→4→12→16→17 (10)	1.114		
	9:10–11:00	MG16	22→24→23→15→12→16 (5)	0.570	2→4→12→16	0.402
Case 3	9:00–10:00	MG8	22→10→6→8 (10)	0.906	2→6→8 (15)	0.6008
			2→6→8 (5)	0.200		
	9:10–10:10	MG17	2→6→10→17 (20)	1.824	2→6→10→17 (10)	0.904
					22→10→17 (10)	0.910
	9:10–11:00	MG16	2→4→12→16 (5)	0.402	2→4→12→16 (5)	0.402
Case 4	9:10–11:00	MG8	2→6→8	0.200	2→6→8	0.200
	9:15–11:40	MG17	2→6→10→17	0.903	2→6→10→17	0.903
	9:30–12:00	MG16	2→1→3→4→12→16	3.680	2→4→12→16	1.970
			22→10→17→16	1.119	22→10→17→16	1.803

listed in Table 5.9. Before this overlap, both algorithms produced the same result for consumer MG8, using the same producer and energy values. To resolve the overlapping problem: The MLR algorithm prioritizes MG17, followed by MG16, while accounting for the existing energy in the system. It splits MG17's energy demand into two halves and selects two different transmission paths to meet it. This approach reduces power loss but increases the likelihood of exhausting transmission paths during periods of high demand. Conversely, QGA-RA focuses on minimizing the number of paths used, resulting in a single path with slightly higher power loss for MG17. For MG16, the QGA-RA approach outperforms MLR by generating a shorter transmission path with lower power loss.

Additionally, QGA-RA simultaneously meets the requests of both consumers, providing them equal access to resources. The algorithm generates all paths and forms non-overlapping clusters. In this case, the cluster includes all generated paths, allowing consumers to benefit from arriving early.

3. **Case 3:** In this scenario, all consumers arrive at the same time with conflicting transmission times as depicted in Table 5.8. To address this issue, the QGA-RA (Quantum Genetic Algorithm with Resource Allocation) executes all consumers simultaneously, ensuring that no consumer is given priority over another and that no consumer is left behind. The algorithm then generates non-collision clusters and executes the highest-priority cluster.

   On the other hand, the Minimum Loss Routing (MLR) algorithm starts with the consumer offering the highest price, MG8, and selects the producer with the lowest price, MG22. However, since MG22 does not have enough energy to meet MG8's demand, MG8 must purchase additional energy from the next lowest-priced producer, MG2. The total loss for QGA-RA is 2.816, while the total loss for MLR is 3.332, as shown in Table 5.9, which highlights the superiority of QGA-RA compared to MLR in reducing lower loss.

4. **Case 4:** Overlapping Transmission Periods with Heavy Load Demand: In this case, we focus more on the result of MG16, which is introduced as a heavy load with 40kW in demand, which explains the identical results of Consumers MG8 and MG17 for both algorithms. To satisfy this demand, both algorithms need to source energy from multiple producers. As shown in Table 5.8, the MLR algorithm chooses to purchase 30 kW from MG2 and 10 kW from MG22, while the QGA-RA algorithm opts to purchase 24 kW from MG2 and 16 kW from MG22. From the results shown in Table 5.9, the total power loss for the MLR algorithm is higher than that of the QGA-RA algorithm. This difference in performance is due to the large search space of the quantum algorithm introduced in QGA-RA. Specifically, for MG16, the QGA-RA algorithm's path selection (2→4→12→16) results in a power loss of 1.970, which is substantially lower than the MLR's path (2→1→3→4→12→16) with a power loss of 3.680 despite the small difference in transmitted energy (30kW for MLR and 24kW for QGA-RA). These results highlight the superiority of QGA-RA in achieving better, more efficient results.

Figure 5.8 demonstrates the differences in energy loss between MLR and QGA-RA in the 6-node network. Based on the results shown in Figure 5.8, we observe that both QGA-RA and MLR exhibit the same energy loss in Case 1 due to their similar results. However, in Case 2, MLR has a lower energy loss because it delayed supplying consumer MG6 for 10 minutes, waiting for a better resource. By contrast, QGA-RA chose to supply the consumer with the energy available in the system at that time. In this case, QGA-RA prioritized minimizing waiting time over reducing energy loss. For Cases 3 and 4, the results indicate that QGA-RA achieves lower energy loss compared to MLR.

Figure 5.9 demonstrates the differences in energy loss between MLR and QGA-RA in the 30-node network. The figure shows that QGA-RA consistently results in lower power loss across all scenarios, highlighting its effectiveness in reducing energy loss in larger networks compared to MLR.

Figure 5.10 presents the differences in energy cost between QGA-RA and MLR in the 6-node network. In cases 1 and 3, both MLR and QGA-RA have the same energy cost. In Case 2, MLR has a slightly lower cost than QGA-RA due to the previously explained delay. However, the difference is not significant. In Case 4, QGA-RA demonstrates a significantly lower cost than MLR.

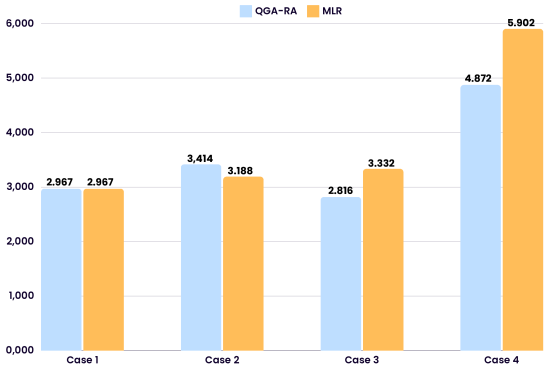

Figure 5.8: Power Loss Comparison in the 6-Node Network.

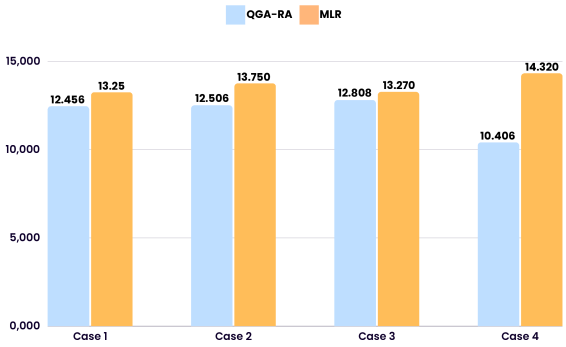

Figure 5.9: Power Loss Comparison in the 30-Node Network.

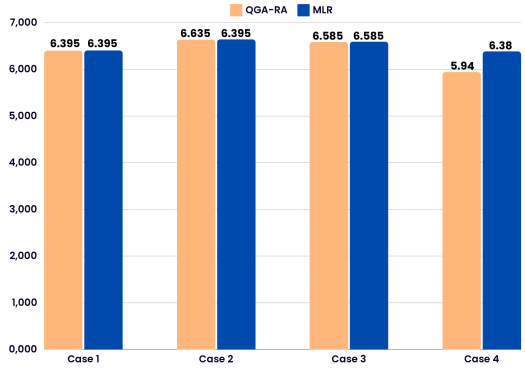

Figure 5.10: Cost Comparison in the 6-Node Network.

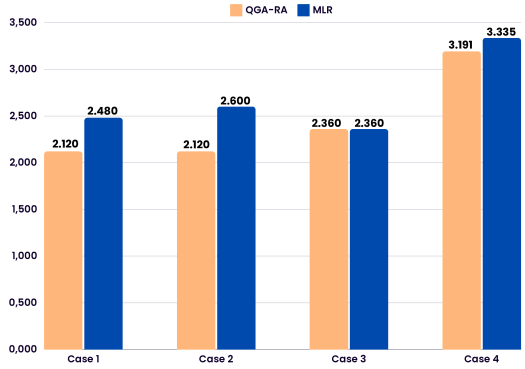

Figure 5.11: Cost Comparison in the 30-Node Network.

Figure 5.11 presents the differences in energy cost between QGA-RA and MLR in the 30-node network. Except for Case 3, where both algorithms yield similar results, QGA-RA consistently shows lower energy costs than MLR across the other cases.

5.4.5 Greedy search comparison analyses

We compared our modified greedy algorithm to the Dijkstra algorithm proposed in [114], the genetic algorithm proposed in [128], the simulated annealing algorithm proposed in [130], and the brute force method proposed in [55]. All of these algorithms were applied to both a 6-node topology and a 30-node topology. To test the performance of each algorithm, we selected two random producers and two random consumers with varying demands, as detailed in Table 5.10.

The performance of all algorithms was evaluated based on the generated path, power loss, and execution time.

The results are highlighted in Tables 5.11, 5.12, 5.13, and 5.14.

Table 5.11 presents the generated path from producer MG3 to consumer MG1 with a demand of 30kW. Table 5.12 shows the generated path from producer MG2 to consumer MG4 with a demand of 50kW. Table 5.13 displays the results for the generated path from producer MG2 to consumer MG8 with a demand of 30kW in the 30-node topology. Table 5.14 illustrates the generated path from producer MG22 to consumer MG16 with a demand of 10kW, also in the 30-node topology.

Table 5.10: Test Parameters for 6-Node and 30-Node Topologies

Topology	Producer	Consumer	Demand (kW)
6-Node	MG3	MG1	30
	MG2	MG4	50
30-Node	MG2	MG8	30
	MG22	MG16	10

Table 5.11: Test results for 6-Node Topology with a demand of 30kW

	MLR[114]	GA[128]	SA[130]	Greedy	Brute force[55]
Efficient Path	3→4→1	3→4→6→1	3→4→1	3→4→1	3→4→1
power loss (kW)	2.701	3.302	2.701	2.701	2.701
Execution Time (ms)	0.461	2.397	19.122	0.171	0.974

Table 5.14: Test results for 30-Node Topology with a demand of 10kW

	MLR[114]	GA[128]	SA[130]	Greedy	Brute force[55]
Efficient Path	22→10→17→16	22→10→17→16	22→10→17→16	22→10→17→16	22→10→17→16
Power loss (kW)	1.113	1.113	1.113	1.113	1.113
Execution Time (ms)	3.831	3.125	12.782	0.332	14.325

Based on the results shown in Tables 5.11 and 5.12, we observe that all algorithms, except GA, consistently generated the same path. The GA algorithm generated a slightly different path (3→4→6→1) and (2→5→6→4). The power loss was identical across all algorithms, except for GA, which showed a higher power loss. This suggests that GA may not have been as effective in minimizing losses for this scenario. The Greedy algorithm had the fastest execution time, followed alternatively by MLR and Brute Force. The SA algorithm was the slowest, indicating that it may require more computational resources in a smaller topology. The results are consistent with the changing nodes and demand.

Results in Tables 5.13 and 5.14 indicate that all algorithms generated the same path, consistently identifying the optimal route in this larger topology. Power loss was identical across all algorithms, indicating that each approach was equally effective at minimizing power loss in this scenario. The Greedy algorithm remained the fastest, while both MLR and GA had moderate execution times, while SA and Brute Force were significantly slower. In conclusion, the modified Greedy algorithm consistently generates optimal paths with the lowest execution times while maintaining power losses comparable to or lower than those of other algorithms. Although the SA and Brute Force methods also produce optimal solutions, their execution times grow exponentially with the number of nodes. This makes the Greedy algorithm a highly effective and efficient choice for energy routing in both small and large network topology.

5.5 Complexity and scalability analysis

To evaluate the effectiveness and scalability of the proposed QGA-RA protocol, a comparison with MLR was conducted based on the computational complexities of both algorithms. Initially, the Dijkstra algorithm used in MLR for power-loss calculation was compared with the Greedy search algorithm employed in the QGA-RA protocol. The results are highlighted in Table 5.15:

Table 5.12: Test results for 6-Node Topology with a demand of 50kW

	MLR[114]	**GA[128]**	**SA[130]**	**Greedy**	**Brute force[55]**
Efficient Path	2→3→4	2→5→6→4	2→3→4	2→3→4	2→3→4
power loss (kW)	6.003	6.508	6.003	6.003	6.003
Execution Time (ms)	0.570	2.635	28.702	0.151	3.603

Table 5.13: Test results for 30-Node Topology with a demand of 30kW

	MLR[114]	**GA[128]**	**SA[130]**	**Greedy**	**Brute force[55]**
Efficient Path	2→6→8	2→6→8	2→6→8	2→6→8	2→6→8
power loss (kW)	3.601	3.601	3.601	3.601	3.601
Execution Time (ms)	0.662	2.638	11.134	0.191	14.327

Table 5.15: Comparison of Routing Algorithms

Algorithm	**Complexity**	**Description**
Greedy	$\mathcal{O}(T \cdot (V \log V + E))$	Simple and fast, yields optimal solutions, handles dynamic weight adjustment.
Dijkstra	$\mathcal{O}(T \cdot (V \log V + E \log V))$	Reaches optimal results but slower for large networks, does not handle dynamic weight adjustment well.

Here, V represents the number of nodes, E the number of transmission lines, and T the number of consumers.

To further compare the protocols, the overall complexity of both QGA-RA and MLR was computed by accounting for power-loss calculation, producer subset determination, and the scheduling mechanisms involved. Table 5.16 summarizes the findings:

Table 5.16: Comparison of MLR Protocol and QGA-RA Protocol

Criteria	**MLR**	**QGA-RA**
Time Complexity	$\mathcal{O}(T \cdot P \cdot K \cdot \log V \cdot (V + E))$	$\mathcal{O}\left(I \cdot T \cdot P \cdot (E + V \log V)\right)$
Scalability	Less scalable for large graphs	Efficient for real-time or large-scale systems
Memory Usage	High due to priority queues and full graph tracking	Lower; uses fewer data structures
Suitability	Suitable for critical systems needing accuracy	Better suited for fast, adaptive routing

Where P is the number of chromosomes in the population (producers), I is the number of iterations in the QGA loop, and K is the maximum number of retries or path splits due to capacity.

Based on the complexity analysis presented in Table 5.16, it can be concluded that the QGA-RA protocol demonstrates slightly better scalability compared to MLR, making MLR less suitable for larger networks. Although the time complexity difference is not substantial, the spatial complexity of MLR is significantly higher than that of QGA-RA, as MLR introduces considerable computational overhead due to its scheduling mechanism and buffer-based packet handling. In contrast, the proposed QGA-RA protocol scales more efficiently, particularly in real-time contexts where speed and responsiveness are critical.

5.6 Discussion

The protocol was tested on 6-node and 30-node networks to evaluate its scalability, accuracy, power loss reduction, and total cost optimization. Each network was analyzed through multiple case studies. In the first case (Non-Overlapping Transmission), both algorithms produced similar results, with QGA-RA achieving better power loss reduction for MG1. In the second case (Overlapping Transmission Periods with capacity issues)two key challenges were encountered: the system did not have enough energy to satisfy MG6's demand, and the power lines connected to MG6 lacked enough existing capacity to transmit 45kW. Each algorithm handled these issues differently. MLR opted to wait for a producer (MG3) with enough energy to meet the demand, resulting in a 10-minute delay. In contrast, QGA-RA provided MG6 with the remaining 10 kW of energy available in the system until another producer arrived.

Both approaches have their pros and cons: MLR's decision to wait for MG3 caused a delay, but it benefited from MG3's lower energy price (0.041 $/kW.h). On the other hand, QGA-RA minimized waiting time but incurred higher costs by purchasing from both MG3 and MG2, as MG2's energy price (0.065 $/kW.h) was significantly higher than that of MG3. Our approach focuses more on system reliability at the expense of energy cost; it also simultaneously processes consumers with the same arrival time, reducing waiting time and ensuring no consumer is left behind, as shown in case 3. This outcome is achieved through the dynamic cluster scheduling used by the QGA-RA to handle transmission overlap.

In the heavy-load scenario (case 4), QGA-RA returns better results than MLR for power loss and energy cost, as it is better equipped to handle such scenarios.

The 30-node network further tested the scalability of both algorithms under more complex conditions. As shown in Tables 5.8 and 5.9, QGA-RA consistently outperformed MLR, particularly in scenarios with overlapping transmission periods and high load demands. In Case 1, both algorithms generated identical paths and power-loss results for consumers MG8, MG17, and MG16, as no transmission overlap occurred. However, in Case 2, when MG16 and MG17 required energy simultaneously at 9:10, QGA-RA efficiently handled the overlap via dynamic cluster scheduling, resulting in lower power loss than MLR. Additionally, QGA-RA minimized the generated paths, unlike the MLR approach, which split MG17's demand across two paths, increasing the likelihood of network congestion. In Case 3, where all consumers arrived at the same time, QGA-RA dynamically allocated resources to meet the demands of all consumers while minimizing energy loss. The total power loss for QGA-RA was 12.808 kW, compared to 13.270 kW for MLR, indicating a significant improvement in efficiency. The QGA-RA approach also demonstrated better performance in reducing total energy costs, consistently outperforming MLR across all cases except Case 3, where both algorithms yielded similar results.

In Case 4, which involved heavy load demand for MG16, QGA-RA once again outperformed MLR by efficiently distributing the load across multiple producers, resulting in a power loss of 10.406 kW compared to MLR's 14.320 kW. This highlights the advantage of QGA-RA in handling complex, high-demand scenarios and further underscores the scalability of the quantum genetic algorithm for larger networks.

The modified greedy search algorithm was compared to several other approaches, including Dijkstra, genetic algorithms (GA), simulated annealing (SA), and brute force, across both the 6-node and 30-node topologies. In both topologies, the greedy algorithm consistently generated optimal paths with the lowest execution times, while maintaining power losses comparable to or better than the other algorithms. As shown in Tables 5.11, 5.12, 5.13, and 5.14, the greedy algorithm performed well in all test cases. For the 6-node topology, it achieved the same power loss as the MLR and brute force methods but with faster execution times, particularly in Case 2, where it completed the computation in 0.151 ms compared to MLR's 0.570 ms and brute force's 3.603 ms. In the 30-node topology, the greedy algorithm continued to demonstrate superior performance, achieving the lowest execution times while maintaining optimal power loss levels (e.g., 1.113 kW in Case 4).

5.7 Conclusion

Energy routing is a critical function in modern SG and EI systems, particularly with high RER penetration, where intermittent and uncertain generation patterns require intelligent, adaptive management. This chapter proposed a novel Quantum Genetic Algorithm–based energy routing protocol (QGA-RA) that jointly addresses three core challenges in decentralized energy systems: producer subset determination, loss-efficient path selection, and energy transmission scheduling.

The proposed framework employs a modified Greedy Search Algorithm for efficient path discovery, while producer subset determination is handled through a Quantum Genetic Algorithm integrated with the greedy routing mechanism. Energy transmission scheduling is addressed in two complementary stages: first, by embedding capacity constraints directly into the routing process, and second, through a dynamic clustering mechanism that coordinates concurrent energy transmissions and mitigates congestion.

Extensive simulation-based evaluation demonstrates that the proposed QGA-RA framework consistently outperforms existing routing approaches across transmission loss, economic cost, and congestion management. These results highlight the suitability of the proposed protocol for scalable and dynamic EI environments where multiple energy transactions must be coordinated in real time.

Despite these promising results, several limitations remain. The proposed framework has not yet been evaluated on very large-scale networks, and its performance under extreme network densities remains to be investigated. In addition, while renewable generation uncertainty is considered, the current evaluation relies on simulated environments and does not fully capture abrupt real-world fluctuations in energy availability. Furthermore, the reliance on real-time communication between routing nodes and control entities may introduce delays or bottlenecks that could affect routing decisions under constrained communication conditions.

Future work will focus on extending the proposed framework through more extensive simulation-based evaluation, including experiments on larger and more heterogeneous network topologies. In particular, real-world–inspired simulation scenarios will be considered to better capture practical operating conditions, such as varying supply–demand regimes, network congestion levels, and renewable generation uncertainty. Additional scenarios and stress conditions will be explored to further assess scalability, robustness, and performance consistency under diverse operating environments.s

Chapter 6

Adaptive MCF: Adaptive Multi-Objective Optimization for P2P Energy Trading: A Multi-Commodity Flow Approach with Mirror Descent Learning

Contents

6.1 Introduction . . . 82
6.2 Network model and system architecture . . . 83
6.2.1 Dataset and preprocessing . . . 83
6.2.2 Household aggregation into energy routers . . . 84
6.2.3 Router-level power aggregation . . . 85
6.2.4 Physical network topology . . . 85
6.2.5 Electrical parameters and line modeling . . . 86
6.2.6 Economic framework . . . 87
6.2.7 Utility grid modeling . . . 89
6.3 Methodology . . . 89
6.3.1 MCF formulation . . . 89
6.3.2 Mirror descent for adaptive weight learning . . . 90
6.3.3 Mirror Descent for Weight Adaptation . . . 91
6.4 Results and performance analysis . . . 92
6.4.1 Energy flow analysis . . . 95
6.4.2 Economic performance analysis . . . 97
6.4.3 Fairness analysis . . . 99
6.4.4 Adaptive weight learning dynamics . . . 102
6.4.5 Computational complexity and runtime analysis . . . 103
6.5 Discussion . . . 105
6.6 Conclusion . . . 105

6.1 Introduction

As established in the previous chapters, EI routing is fundamentally governed by three interdependent challenges: efficient path finding, producer subset selection, and time-dependent scheduling. While these problems have been extensively studied, existing approaches often address them in isolation or

through loosely coupled frameworks, limiting their ability to achieve globally optimal and adaptive solutions in dynamic environments.

This chapter builds upon this foundation by proposing a unified optimisation framework that simultaneously addresses these three challenges within a single model. The approach is based on a MCF formulation that captures physical routing, economic costs, and network constraints in a graph-based structure. Within this framework, efficient paths, optimal producer subsets, and per-interval scheduling decisions emerge jointly from the optimisation process rather than being treated as separate subproblems.

To enhance adaptability, the framework integrates a Mirror Descent mechanism that dynamically adjusts routing priorities in response to congestion, transmission losses, and fairness signals. This enables the system to continuously adapt to changing network conditions without manual parameter tuning, while preserving computational efficiency and real-time feasibility.

The proposed method is evaluated over 2,648 trading hours using real consumption and generation data for 300 households under multiple network configurations. The results demonstrate significant cost reductions, robust adaptive behaviour, and provide new insights into the interaction between infrastructure constraints, optimisation, and fairness in P2P energy trading systems.

The remainder of this chapter is organised as follows: Section 6.2 presents the system model and problem formulation, Section 6.3 describes the adaptive MCF framework, Section 6.4 reports the experimental results, and Section 6.5 discusses the implications of the findings.

6.2 Network model and system architecture

This section develops a comprehensive framework for adaptive P2P energy routing. The methodology proceeds in four stages: real-world data acquisition and preprocessing, construction of a physically realistic network topology, formulation of the multi-commodity flow optimization problem with adaptive cost functions, and integration of online learning for automatic weight adaptation.

6.2.1 Dataset and preprocessing

This work utilizes the *Ausgrid Solar Home Electricity Dataset (2012–2013)* [150], which provides half-hourly residential electricity consumption and photovoltaic (PV) generation measurements for 300 households in New South Wales, Australia. The dataset spans one full year (July 2012 to June 2013) and contains 2,626,056 half-hourly records. Each household is associated with a postcode, enabling approximate spatial localization through publicly available postcode centroid coordinates.

Temporal aggregation

Since P2P energy markets typically operate on hourly decision intervals, all half-hourly measurements are aggregated to hourly resolution. For each household i and hour t, we compute:

$$\begin{aligned} \text{Load}_i(t) &= \sum_{k=1}^{2} \text{Load}_i(t,k), \\ \text{PV}_i(t) &= \sum_{k=1}^{2} \text{PV}_i(t,k), \\ \text{Net}_i(t) &= \text{PV}_i(t) - \text{Load}_i(t). \end{aligned} \tag{6.1}$$

Positive net values indicate surplus generation (prosumer), while negative values indicate energy deficit (consumer). This aggregation yields 8,760 hourly records per household over the annual period.

Valid trading hours

A trading hour is classified as valid if the system simultaneously contains both surplus and deficit households, enabling P2P energy exchange. Formally, hour t is valid if:

$$\exists i, j : \text{Net}_i(t) > 0 \wedge \text{Net}_j(t) < 0 \tag{6.2}$$

This criterion yields 2,648 valid trading hours (30.2% of the year), consistent with typical residential solar generation patterns, in which all households simultaneously consume (nighttime) or generate (midday) during certain periods.

6.2.2 Household aggregation into energy routers

The network could be modeled with households directly trading with each other; however, this approach is neither scalable nor physically accurate. To address this issue, households are partitioned into k groups, each connected via an energy router that serves as an aggregation point.

Each household is characterized by a feature vector comprising:

- Mean hourly net power: $\bar{P}_i = \mathbb{E}[\text{Net}_i(t)]$
- Geographic coordinates: latitude ϕ_i, longitude λ_i (postcode centroid)

K-Means clustering

Households are partitioned into K routers using the K-means algorithm [151]:

$$\mathcal{R} = \{R_1, R_2, \ldots, R_K\}, \quad \bigcup_{k=1}^{K} R_k = \{1, 2, \ldots, N\}, \quad R_i \cap R_j = \emptyset \; \forall i \neq j \tag{6.3}$$

where $N = 300$ is the total number of households. We select $K = 12$ routers based on computational tractability and network resolution trade-offs. The resulting router assignments exhibit household counts ranging from 4 to 53 per router (mean: 25 households/router), reflecting realistic substation service areas.

Router centroid calculation

For each router $r \in \mathcal{R}$, the geographic centroid is computed as:

$$(\phi_r, \lambda_r) = \left(\frac{1}{|R_r|} \sum_{i \in R_r} \phi_i, \; \frac{1}{|R_r|} \sum_{i \in R_r} \lambda_i \right) \tag{6.4}$$

where $|R_r|$ denotes the number of households assigned to router r. These centroids define router locations for subsequent topology construction.

Algorithm 7 K-Means Clustering for Energy Router Construction

Input: Household feature matrix $X \in \mathbb{R}^{N \times 3}$ (mean net power, latitude, longitude)
Output: Router assignment vector $L = \{l_1, \ldots, l_N\}$
Normalize features: $X \leftarrow (X - \mu)/\sigma$
Initialize centroids $\{c_1, \ldots, c_K\}$ randomly from X
repeat
    for $i = 1$ to N **do**
        Assign $l_i \leftarrow \arg\min_k \|X_i - c_k\|_2$
    end for
    for $k = 1$ to K **do**
        Update centroid $c_k \leftarrow \frac{1}{|\{i : l_i = k\}|} \sum_{i : l_i = k} X_i$
    end for
until centroids converge
return L

6.2.3 Router-level power aggregation

Now that households are grouped into 12 clusters, their individual production, consumption, and net balance are summed up for each router r and hour t following these equations:

$$\begin{aligned} \text{Load}_r(t) &= \sum_{i \in R_r} \text{Load}_i(t), \\ \text{PV}_r(t) &= \sum_{i \in R_r} \text{PV}_i(t), \\ \text{Net}_r(t) &= \text{PV}_r(t) - \text{Load}_r(t). \end{aligned} \tag{6.5}$$

6.2.4 Physical network topology

Real distribution network topologies are proprietary and unavailable. Therefore, we constructed the topology using available data, specifically a postcode file containing geographic coordinates and regional information. This approach allowed us to generate a realistic network structure while respecting data confidentiality constraints. For the simulation, we use two network topologies: the first uses MST (Minimum Spanning Tree) for optimal connectivity, and the second, used later for comparison, enhances the MST with k-NN edges to add alternative routing paths.

Minimum spanning tree network construction

We construct a synthetic yet physically plausible network using the router centroids. First, a complete graph $G_{complete} = (\mathcal{R}, E_{complete})$ is formed where edge weights represent geographic distances computed via the Haversine formula [152]:

$$d(r_u, r_v) = 2R \arcsin\left(\sqrt{\sin^2\left(\frac{\phi_v - \phi_u}{2}\right) + \cos(\phi_u)\cos(\phi_v)\sin^2\left(\frac{\lambda_v - \lambda_u}{2}\right)}\right) \tag{6.6}$$

where $R = 6371$ km is Earth's radius. A minimum spanning tree (MST) is then extracted using Kruskal's algorithm:

$$G_{MST} = \arg\min_{T \in \mathcal{T}} \sum_{(u,v) \in E(T)} d(r_u, r_v) \tag{6.7}$$

where $\mathcal{T}$ is the set of all spanning trees of $G_{complete}$. The resulting MST comprises 11 edges spanning 180.49 km total length (mean edge length: 16.4 km) and guarantees network connectivity.

Dense network construction

To model redundant pathways typical of real distribution networks, we augment the MST with k-nearest neighbor edges. For each router r, we add edges to its $k = 3$ geographically closest neighbors not already connected in the MST:

$$E_{final} = E_{MST} \cup \bigcup_{r \in \mathcal{R}} \{\text{KNN}_k(r, \mathcal{R} \setminus N_{MST}(r))\} \tag{6.8}$$

where $N_{MST}(r)$ denotes neighbors of r in the MST and $\text{KNN}_k(\cdot)$ returns the k nearest nodes by distance. This increases edge count from 11 (MST) to 22 (MST + KNN), providing routing diversity while avoiding excessive mesh connectivity. $\text{KNN}_k(r, S)$ returns the k nearest nodes to router r within set S, measured by Haversine distance.

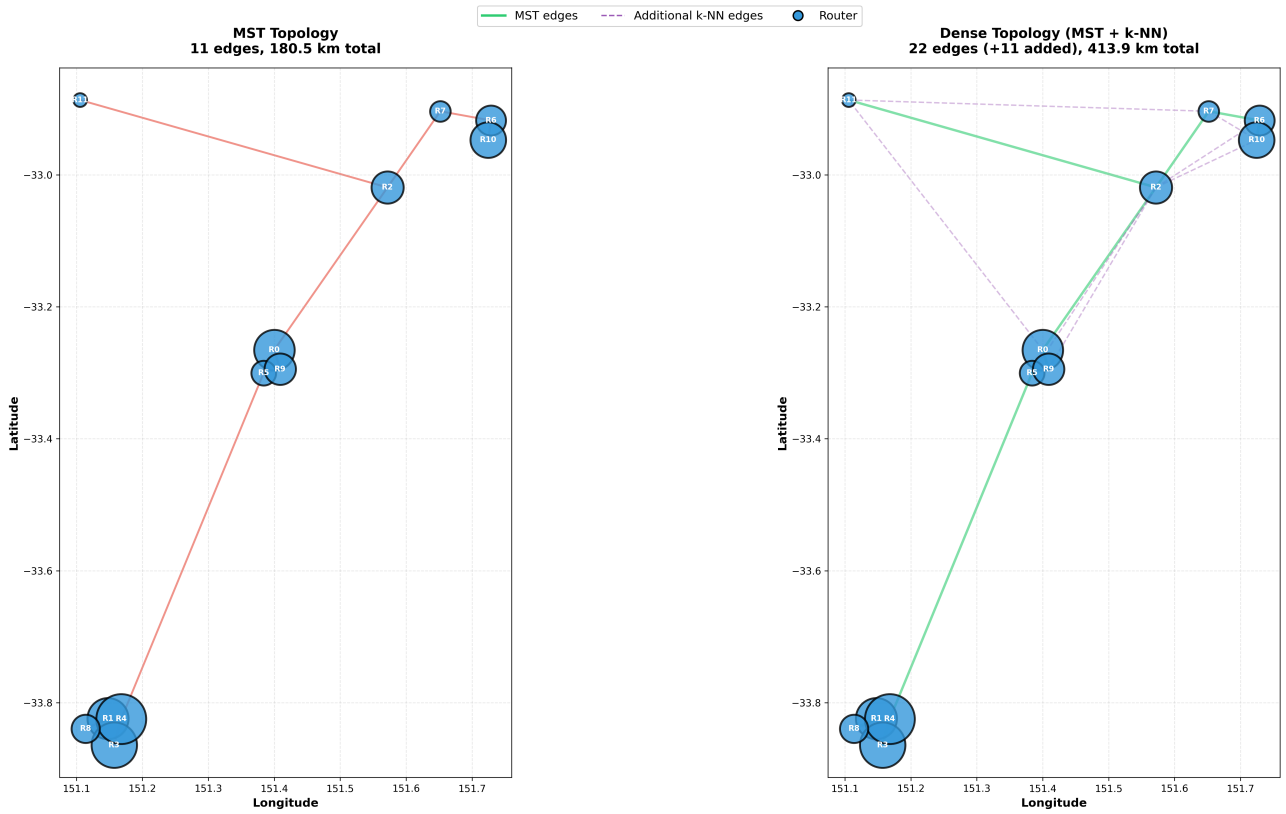

Figure 6.1: Geographic network topologies. **Left:** MST (11 edges, 180.5 km). **Right:** Dense topology (22 edges, 413.9 km) with MST backbone (green) and k-NN shortcuts (gray).

Algorithm 8 Dense Network Construction (MST + k-NN)

Input: MST graph $G_{MST} = (\mathcal{R}, E_{MST})$, router centroids, $k = 3$
Output: Dense physical graph G_{dense}
Initialize $G_{dense} \leftarrow G_{MST}$
Compute all pairwise router distances using Eq. 6.6
for each router $r \in \mathcal{R}$ **do**
    Identify routers not connected to r in G_{dense}
    Select the k nearest such routers
    Add edges between r and the selected neighbors
end for
return G_{dense}

6.2.5 Electrical parameters and line modeling

Since the Ausgrid dataset does not provide physical network specifications, we adopt representative Australian distribution network standards (Table 6.1). Each router represents an aggregation of households connected via low-voltage (LV) infrastructure, with inter-router links modeled using a hybrid voltage hierarchy.

Hybrid LV-MV transmission model

To accurately model transmission losses, we employ a distance-dependent voltage model. Short links ($d \leq 1$ km) use pure LV transmission at 415 V, representing local connections. Long links ($d > 1$ km) employ a hybrid LV-MV-LV architecture: 0.5 km LV segments at each end with MV transmission for

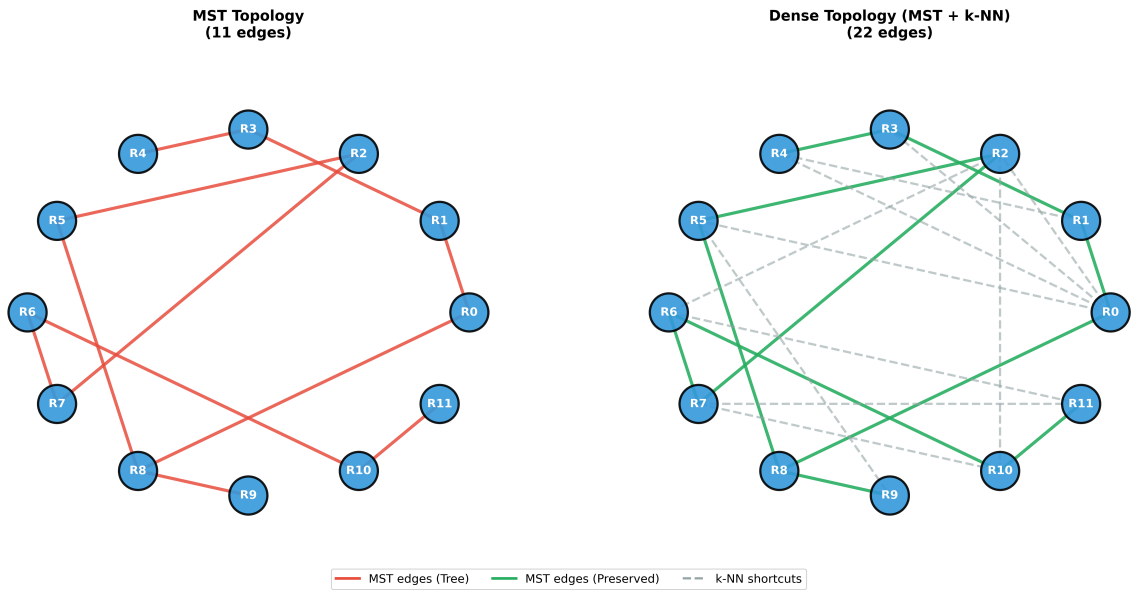

Figure 6.2: Schematic comparison of network topologies showing logical connectivity structure. *Notes:***Left:** MST topology (11 edges) forms a tree with no cycles, requiring single-path routing between any node pair. **Right:** Dense topology (22 edges) preserves MST structure (green solid edges) while adding k-NN shortcuts (gray dashed edges) to create routing alternatives

Table 6.1: Electrical Network Parameters

Parameter	**Value**	**Description**
V_{LV}	415 V	Low voltage (line-to-line, 3-phase)
V_{MV}	11 kV	Medium voltage (distribution)
$\cos\phi$	0.95	Power factor
Cable	240 mm^2 Al	XLPE cable [153]
I_{max}	406 A	Rated current
P_{line}^{max}	222 kW	Line capacity (80% derating)
R_{LV}	0.32 Ω/km	LV resistance
R_{MV}	0.10 Ω/km	MV resistance

the middle section. This reflects real distribution practice where voltage is stepped up for long-distance transmission and stepped down for final delivery, significantly reducing resistive losses.

Loss calculation

Transmission losses are computed using I^2R losses with voltage-dependent current. For power flow P (kW) over distance d (km):

$$L_{loss}(P,d) = \begin{cases} \frac{I_{LV}^2 R_{LV} d}{1000}, & d \leq 1 \text{ km} \\ \frac{I_{LV}^2 R_{LV}}{1000} + \frac{I_{MV}^2 R_{MV}(d-1)}{1000}, & d > 1 \text{ km} \end{cases} \tag{6.9}$$

where $I_{LV} = \frac{1000P}{\sqrt{3}V_{LV}\cos\phi}$ and $I_{MV} = \frac{1000P}{\sqrt{3}V_{MV}\cos\phi}$. This model produces realistic loss rates of 1.1–1.4% of transmitted energy, compared to 5–10% for pure LV models over long distances.

6.2.6 Economic framework

Grid tariff structure

We adopt standard Australian residential electricity tariffs representative of the dataset period:

- **Grid purchase price:** $\lambda_b = \$0.30$/kWh (retail electricity price)
- **Feed-in tariff:** $\lambda_s = \$0.06$/kWh (solar export compensation)

This 5:1 price differential creates substantial economic incentive for local P2P trading as an alternative to grid-mediated transactions.

Dynamic P2P pricing mechanism

P2P transaction prices are determined hourly using the Supply-Demand Ratio (SDR) mechanism proposed by Long et al. [154] and validated by Samende et al. [155]. The SDR quantifies system-wide energy balance:

$$\mathrm{SDR}(t) = \frac{\sum_{r:\mathrm{Net}_r(t)>0} \mathrm{Net}_r(t)}{\sum_{r:\mathrm{Net}_r(t)<0} |\mathrm{Net}_r(t)|} \tag{6.10}$$

This ratio provides a single global scarcity signal: SDR < 1 indicates a supply shortage (demand-side market), and SDR > 1 indicates a supply abundance (supply-side market).

Pricing rules:

For $\mathrm{SDR}(t) \leq 1$ (shortage):

$$\begin{aligned} p_{sell}(t) &= \frac{(\lambda_s + \lambda_c)\lambda_b}{(\lambda_b - \lambda_s - \lambda_c) \cdot \mathrm{SDR}(t) + (\lambda_s + \lambda_c)} \\ p_{buy}(t) &= \mathrm{SDR}(t) \cdot p_{sell}(t) + (1 - \mathrm{SDR}(t)) \cdot \lambda_b \end{aligned} \tag{6.11}$$

For $\mathrm{SDR}(t) > 1$ (surplus):

$$\begin{aligned} p_{sell}(t) &= \lambda_s + \frac{\lambda_c}{\mathrm{SDR}(t)} \\ p_{buy}(t) &= \lambda_s + \lambda_c \end{aligned} \tag{6.12}$$

where $\lambda_c = 0.2(\lambda_b - \lambda_s) = \$0.048$/kWh is the compensation parameter ensuring seller profitability while preventing arbitrage. Prices are bounded within $[\lambda_s, \lambda_b]$ and satisfy $p_{sell} \leq p_{buy}$ to maintain economic consistency.

Key properties:

- Shortage (SDR < 1): p_{buy} increases toward λ_b, penalizing buyers
- Surplus (SDR > 1): Prices converge ($p_{buy} \approx p_{sell}$), reducing trading incentive
- Balanced (SDR ≈ 1): Mid-range prices maximize P2P profitability

Congestion pricing

To reflect transmission capacity scarcity and incentivize congestion-aware routing, we introduce an economic congestion penalty. Let $f_{uv}(t)$ denote the power flow on edge (u, v) at hour t, and define the congestion threshold $\theta \in [0, 1]$ as the fraction of line capacity beyond which penalties apply. The congestion cost is:

$$C_{cong}(t) = \sum_{(u,v)\in E} \max\left(0, f_{uv}(t) - \theta \cdot P_{line}^{max}\right) \cdot \lambda_{cong} \tag{6.13}$$

where $\lambda_{cong} = \$0.15$/kWh is the congestion price. In our experiments:

- **Baseline scenario:** $\theta = 0.8$, $P_{line}^{max} = 222$ kW (ample capacity)
- **Stress test scenario:** $\theta = 0.5$, $P_{line}^{max} = 10$ kW (severe constraint)
- **Dense topology scenario:** $\theta = 0.5$, $P_{line}^{max} = 10$ kW (routing alternatives under stress)

This mechanism penalizes line utilization beyond safe operating limits, creating economic incentive for algorithms to route flows through underutilized pathways. Under baseline conditions, congestion penalties remain negligible ($C_{cong} \approx 0$), whereas under stress they account for $\sim$5% of total system cost, demonstrating the economic significance of intelligent congestion management as infrastructure approaches saturation.

6.2.7 Utility grid modeling

To ensure system-wide energy balance under all conditions, a utility grid node G is introduced as a global slack bus. This node serves two complementary roles:

1. **Energy import:** Supplies deficit when local P2P generation is insufficient
2. **Energy export:** Absorbs surplus when local demand is saturated

Grid transactions are assigned significantly higher routing costs ($10^7\times$ P2P edge costs) to prioritize local renewable trading whenever physically feasible, while guaranteeing feasibility under extreme supply-demand imbalances. The grid node has unlimited capacity, emulating the role of a bulk power system that can balance local microgrids.

6.3 Methodology

6.3.1 MCF formulation

At each trading hour t, energy routing is formulated as a MCF problem on a directed graph $G = (\mathcal{V}, \mathcal{E})$ constructed as follows:

Node-splitting for router capacity constraints

To enforce router-level capacity limits (preventing infinite power throughput), each physical router r is split into two nodes:

- **Input node** r_{in}: Receives incoming flows, demand $d_{r_{in}} = -\text{Net}_r(t) \times S$
- **Output node** r_{out}: Sends outgoing flows, demand $d_{r_{out}} = 0$
- **Internal edge** $r_{in} \to r_{out}$: Capacity $C_{router} = P_{line}^{max} \times S$, zero cost

where $S = 10$ is an integer scaling factor for numerical stability in the network simplex solver. Demand sign convention: negative demand indicates supply (source), positive demand indicates consumption (sink).

Physical edges with adaptive costs

For each physical link $(u, v) \in E_{phys}$ with distance d_{uv}, we create bidirectional directed edges:

$$\begin{aligned} \text{Edge: } & u_{out} \to v_{in}, \quad v_{out} \to u_{in} \\ \text{Capacity: } & C_{line} = P_{line}^{max} \times S \\ \text{Cost: } & c_{uv} = \lfloor 1000 \times (w_\alpha R_{uv} + w_\beta \Phi_{uv} + w_\gamma \Psi_{uv}) \rfloor \end{aligned} \tag{6.14}$$

where the cost components are:
1. Loss component (R_{uv}): Resistance-based distance factor

$$R_{uv} = \begin{cases} R_{LV} \cdot d_{uv} & \text{if } d_{uv} \leq 1 \text{ km} \\ 2 \times R_{LV} \times 0.5 + R_{MV} \times (d_{uv} - 1) & \text{otherwise} \end{cases} \tag{6.15}$$

2. Congestion component (Φ_{uv}): Penalizes overutilized lines

$$\Phi_{uv}(t) = \max\left(0, \frac{f_{uv}(t-1)}{P_{line}^{max}} - \theta\right) \tag{6.16}$$

where $f_{uv}(t-1)$ is the realized flow from the previous hour. This creates a feedback mechanism discouraging repeated use of congested links.

3. Fairness component (Ψ_{uv}): Penalizes overused routers

$$\Psi_{uv}(t) = \frac{1}{2}\left(\frac{\max(0, H_u(t) - \bar{H}(t))}{\bar{H}(t) + \epsilon} + \frac{\max(0, H_v(t) - \bar{H}(t))}{\bar{H}(t) + \epsilon}\right) \tag{6.17}$$

where $H_r(t) = \sum_{\tau=t-T_w}^{t-1} E_{r,P2P}(\tau)$ is the cumulative P2P energy participation of router r over a sliding window of $T_w = 168$ hours (one week), and $\bar{H}(t) = \frac{1}{K}\sum_r H_r(t)$ is the mean participation. This penalizes routing through routers that have dominated recent trading, encouraging equitable opportunity distribution across geographic communities (router service areas).

Grid connections

The utility grid node G connects to all routers with high-cost, high-capacity edges:

$$\begin{aligned} \text{Edges: } & G \to r_{in}, \quad r_{out} \to G \quad \forall r \in \mathcal{R} \\ \text{Capacity: } & C_{grid} = 10^6 \times S \quad \text{(effectively unlimited)} \\ \text{Cost: } & c_{grid} = 10^7 \quad \text{(penalty to prioritize P2P)} \end{aligned} \tag{6.18}$$

MCF objective

The MCF problem minimizes total weighted routing cost while satisfying flow conservation and capacity constraints:

$$\begin{aligned} \min \quad & \sum_{(u,v)\in\mathcal{E}} c_{uv} f_{uv} \\ \text{s.t.} \quad & \sum_{v:(u,v)\in\mathcal{E}} f_{uv} - \sum_{v:(v,u)\in\mathcal{E}} f_{vu} = d_u \quad \forall u \in \mathcal{V} \\ & 0 \le f_{uv} \le C_{uv} \quad \forall (u,v) \in \mathcal{E} \end{aligned} \tag{6.19}$$

This is solved efficiently in $O(|V|^3)$ time using the network simplex algorithm [**network_simplex_orlin**], implemented via NetworkX [**networkx**].

6.3.2 Mirror descent for adaptive weight learning

The core innovation of this work is the application of Mirror Descent online learning to automatically discover optimal objective weights without manual tuning.

The multi-objective optimization challenge

The MCF formulation in Equation 6.19 combines three competing objectives through weighted linear scalarization:

$$\min_f \quad w_\alpha \underbrace{\sum_{(u,v)} R_{uv} f_{uv}}_{\text{minimize losses}} + w_\beta \underbrace{\sum_{(u,v)} \Phi_{uv} f_{uv}}_{\text{avoid congestion}} + w_\gamma \underbrace{\sum_{(u,v)} \Psi_{uv} f_{uv}}_{\text{promote fairness}} \tag{6.20}$$

subject to flow conservation and capacity constraints. The critical question is: How should we choose weights $\mathbf{w} = [w_\alpha, w_\beta, w_\gamma]$?

Traditional fixed-weight approaches face three fundamental challenges:

- Manual weight tuning through exhaustive grid search
- Weights optimized for one scenario fail when conditions change

These limitations are particularly problematic because P2P energy systems operate in non-stationary environments: network conditions change continuously due to weather variations (affecting solar generation), seasonal demand patterns, infrastructure upgrades, and evolving participation levels.

This adaptive approach addresses these challenges through online learning, which is a class of algorithms designed for non-stationary environments. Rather than fixing weights in advance, the algorithm learns optimal weights through continuous interaction with the system, automatically adapting as conditions evolve.

6.3.3 Mirror Descent for Weight Adaptation

Mirror Descent [156, 157] is an online learning algorithm designed for constrained optimization problems. It maintains valid weight distributions ($\mathbf{w} \geq 0$, $\sum_i w_i = 1$) through exponential gradient updates, also known as the multiplicative weights method [158]. With normalized performance signals $g_i(t) \in [0, 1]$ and learning rate $\eta = 0.12$, the algorithm achieves $O(\sqrt{T})$ regret, meaning cumulative performance converges to that of the best fixed weight strategy in hindsight [159].

Performance signal construction

After each trading hour t, realized flows $\{f_{uv}(t)\}$ are observed and three normalized performance signals are computed:

1. Loss signal (transmission efficiency):

$$g_\alpha(t) = \begin{cases} \frac{L_{total}(t)/E_{P2P}(t)}{\ell_{ref}} & \text{if } E_{P2P}(t) > 0 \\ 0 & \text{otherwise} \end{cases} \tag{6.21}$$

where $L_{total}(t)$ is total I^2R loss and $\ell_{ref} = 0.02$ normalizes to $[0, 1]$. High g_α indicates inefficient routing; the algorithm responds by prioritizing shorter paths.

2. Congestion signal (network utilization):

$$g_\beta(t) = \frac{1}{|E| \cdot c_{ref}} \sum_{(u,v)\in E} \max\left(0, \frac{f_{uv}(t-1)}{P_{line}^{max}} - \theta\right) \tag{6.22}$$

where $c_{ref} = 0.05$ and $f_{uv}(t-1)$ is the previous hour's flow serving as a predictive signal for congestion risk. A high g_β indicates widespread line utilization beyond the threshold θ; the algorithm responds by routing via alternative paths.

3. Fairness signal (participation equity):

$$g_\gamma(t) = \frac{1 - J(t)}{f_{ref}}, \quad J(t) = \frac{\left(\sum_{r=1}^{K} H_r(t)\right)^2}{K \sum_{r=1}^{K} H_r(t)^2} \tag{6.23}$$

where $J(t)$ is Jain's fairness index over cumulative router participation $H_r(t) = \sum_{\tau=t-168}^{t-1} E_{r,P2P}(\tau)$ in the past 168 hours, and $f_{ref} = 0.5$. High g_γ indicates unequal participation; the algorithm responds by penalizing overused routers.

Gradient smoothing

Raw performance signals exhibit hour-to-hour variability. Exponential moving average smoothing stabilizes learning:

$$\bar{\mathbf{g}}(t) = \rho \bar{\mathbf{g}}(t-1) + (1-\rho)\mathbf{g}(t), \quad \bar{\mathbf{g}}(0) = \mathbf{0} \tag{6.24}$$

where $\rho = 0.9$ provides a weighted average over approximately 10 recent hours.

Weight update rule

The smoothed gradient drives the Mirror Descent exponential update:

$$w_i(t+1) = \frac{w_i(t) \cdot \exp\left(\eta \cdot \bar{g}_i(t)\right)}{\sum_{j=1}^{3} w_j(t) \cdot \exp\left(\eta \cdot \bar{g}_j(t)\right)}, \quad i \in \{1,2,3\} \tag{6.25}$$

with weights clipped to $[0.05, 0.90]$ to prevent single-objective dominance, learning rate $\eta = 0.12$, and automatic normalization ensuring $\sum_i w_i = 1$. This multiplicative update is provably optimal for simplex-constrained problems [160].

Complete adaptive MCF algorithm

Algorithm 9 presents the complete adaptive MCF trading procedure integrating Mirror Descent weight learning.

Algorithm 9 Adaptive Multi-Commodity Flow with Mirror Descent

Input: Physical network $G_{phys} = (\mathcal{R}, E_{phys})$, hourly net injections $\{\text{Net}_r(t)\}_{t=1}^{T}$
Output: Flow solutions $\{f_{uv}(t)\}$ and learned weights $\{\mathbf{w}(t)\}$
Initialize weights $\mathbf{w}(1) = [0.4, 0.3, 0.3]$
Initialize smoothed gradients $\bar{\mathbf{g}}(0) = \mathbf{0}$
Initialize participation history $H_r(0) = 0$ for all routers r
Initialize previous flows $f_{uv}(0) = 0$
for $t = 1$ to T **do**
    Construct directed MCF graph $G(t) = (\mathcal{V}, \mathcal{E})$
    Create split nodes (r_{in}, r_{out}) for each router r
    Add grid node with high-capacity, high-cost edges
    Assign edge costs:

$$c_{uv}(t) = \lfloor 1000 \cdot (w_\alpha R_{uv} + w_\beta \Phi_{uv}(t) + w_\gamma \Psi_{uv}(t)) \rfloor$$

    Solve the MCF problem (Eq. 6.19)
    Obtain optimal flows $\{f_{uv}(t)\}$
    Update router participation:

$$H_r(t) = \sum_{\tau=\max(1,t-T_w)}^{t} E_{r,P2P}(\tau)$$

    Compute performance signals $g_\alpha(t)$, $g_\beta(t)$, $g_\gamma(t)$
    Smooth gradients:

$$\bar{\mathbf{g}}(t) = \rho \bar{\mathbf{g}}(t-1) + (1-\rho)\mathbf{g}(t)$$

    Update weights using Mirror Descent (Eq. 6.25)
    Clip weights to $[0.05, 0.90]$ and normalize
end for
return $\{f_{uv}(t)\}$, $\{\mathbf{w}(t)\}$

6.4 Results and performance analysis

To validate the efficacy of the Adaptive MCF framework, this section provides a multi-dimensional performance analysis. The system's behavior is evaluated across four scenarios (S1–S4) designed to isolate the impacts of network topology and capacity constraints on P2P trading dynamics. These dynamics are analyzed across three distinct algorithmic configurations, structured as follows:

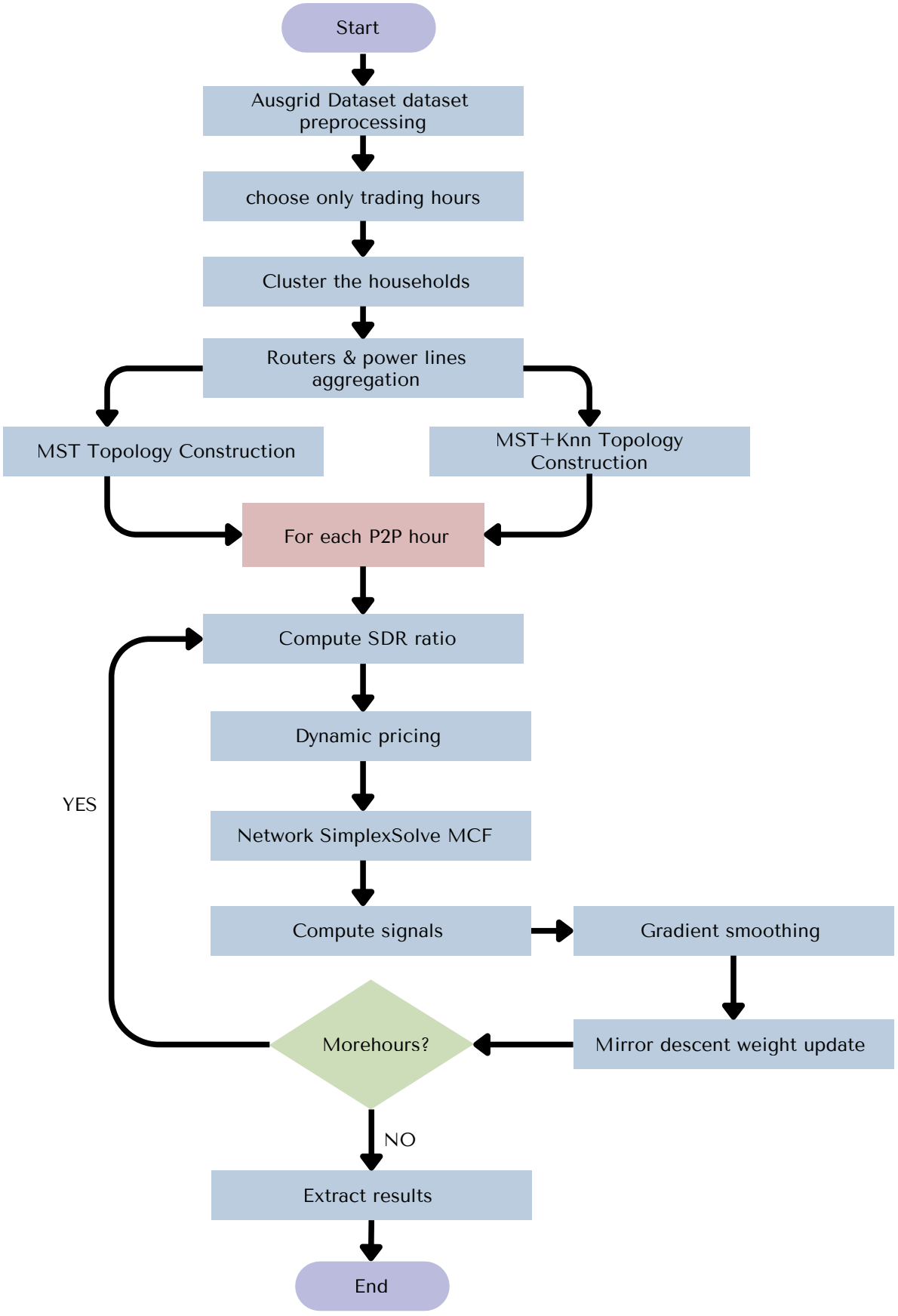

Figure 6.3: Flowchart of adaptive MCF-based P2P energy trading system.

1. **Grid-Only Baseline:** No P2P trading; all transactions via the utility grid at fixed tariffs $\lambda_b = \$0.30/\text{kWh}$ and $\lambda_s = \$0.06/\text{kWh}$.
2. **MCF Static:** Multi-commodity flow with fixed weights $\mathbf{w} = [\alpha, \beta, \gamma] = [0.4, 0.3, 0.3]$, held constant throughout the simulation.
3. **MCF Adaptive:** The proposed method, in which all three objective weights are updated online at every trading hour via mirror descent learning.

The three configurations are evaluated across four experimental scenarios designed to isolate the effects of line capacity and network topology:

Table 6.2: Experimental scenario specifications

Scenario	**Topology**	**Capacity**
S1 Normal/MST	MST (11 edges)	221.79 kW
S2 Stress/MST	MST (11 edges)	10.0 kW
S3 Stress/Dense	Dense (22 edges)	10.0 kW
S4 Normal/Dense	Dense (22 edges)	221.79 kW

The **S1 baseline** represents a well-provisioned distribution network operating under normal capacity conditions using an MST topology of 11 edges.

The **S2 stress scenario** reduces line capacity to 10 kW (22× reduction), simulating aging infrastructure or demand growth without corresponding grid upgrades, while retaining the MST topology to isolate the capacity effect.

The **S3 scenario** combines the same 10 kW stress capacity with the augmented dense topology, isolating whether additional routing pathways can mitigate the bottlenecks introduced by capacity constraints.

S4 scenario retains the dense topology under normal capacity, isolating the pure topological effect without infrastructure stress. Together, S1 and S4 quantify the effect of topology at normal capacity, while S2 and S3 quantify the interaction between capacity constraints and routing flexibility.

The simulation framework is implemented in Python 3.11 and executed on a Kaggle notebook environment.

Algorithm performance is assessed across five criteria:

- **Energy flow:** P2P trading volume (kWh), grid import and export (kWh), transmission losses (kWh), and loss rate defined as total line losses divided by total P2P energy traded (%).
- **Economic efficiency:** Total system cost ($), average hourly cost ($/h), cost reduction relative to the grid-only baseline (%), total system revenue ($), average hourly revenue ($/h), and congestion penalty ($).
- **Trading fairness:** Jain's fairness index

$$J = \frac{\left(\sum_{i=1}^{n} x_i\right)^2}{n \sum_{i=1}^{n} x_i^2} \tag{6.26}$$

  computed over a rolling 168-hour window of cumulative P2P participation per router, where x_i denotes the total energy traded by router i within the window. A value of $J = 1$ indicates perfectly equal participation across all routers.
- **Adaptive weight evolution:** Per-hour trajectory of the three objective weights $[\alpha, \beta, \gamma]$ learned by mirror descent, including the dominant weight at convergence, the number of hours required to reach 90%, 95%, and 99% of the final value, and the 168-hour stable window. This analysis reveals how the algorithm automatically identifies which objective is binding under each network condition.
- **Complexity and runtime:** Average computational time per trading hour (ms), confirming real-time feasibility across all scenarios.

6.4.1 Energy flow analysis

The primary objective of P2P trading is to maximize local consumption of renewable energy. This subsection quantifies the total P2P exchange and the resulting reduction in utility grid dependence.

Table 7.1 summarises the energy flow breakdown for each algorithm across all four scenarios over the 2,648 trading hours. Energy losses are not reported for the Grid-Only baseline, as the utility grid is assumed to absorb transmission losses internally. Figure 6.4(a) reports the transmission loss rate defined as total line losses divided by total P2P energy traded enabling routing efficiency to be compared across scenarios independently of trading volume. Figure 6.4(b) shows the absolute energy decomposition for each scenario: the light segment represents grid import and the dark segment represents P2P energy traded, with percentages indicating each algorithm's P2P share of total community demand (125,464 kWh).

Table 6.3: Energy Flow Summary Across All Scenarios (2,648 Trading Hours).

Algorithm	**Scenario**	**P2P Energy (kWh)**	**Grid import (kWh)**	**Grid export (kWh)**	**Energy Loss (kWh)**
Grid-Only	Baseline	0.00	125,464.39	176,199.37	0.00
MCF Static	S1 Normal/MST	44,369.06	81,095.33	131,830.31	506.99
	S2 Stress/MST	32,193.58	93,270.81	144,005.79	169.03
	S3 Stress/Dense	40,825.34	84,639.04	135,374.02	190.76
	S4 Normal/Dense	44,369.06	81,095.33	131,830.31	306.54
MCF Adaptive	S1 Normal/MST	44,369.06	81,095.33	131,830.31	501.02
	S2 Stress/MST	32,193.58	93,270.81	144,005.79	166.18
	S3 Stress/Dense	40,825.34	84,639.04	135,374.02	202.79
	S4 Normal/Dense	44,369.06	81,095.33	131,830.31	297.65

Topology effect: Under normal line capacity (221,kW), topology does not affect trading volume; As seen in Figure 6.4(b) S1 and S4 achieve identical P2P exchange (44, 369,kWh each) and the same 35.4% reduction in grid imports relative to the baseline. However, topology does affect transmission loss, which is 39.5% lower in the dense topology (306.54 kWh vs. 506.99 kWh). Figure 6.4(a) makes this contrast explicit: the loss rate drops from 1.143% in S1 to 0.691% in S4. This confirms that the additional edges in the dense topology provide shorter alternative paths that the solver naturally prioritizes to minimize resistance costs. Under stressed line capacity (10,kW), S2 and S3 report significantly lower traded volumes than their normal-capacity counterparts (S1 and S4) due to the restrictive 10 kW capacity, which prevents a large portion of the available energy from being transmitted. Between the two stressed cases, S3 achieves higher P2P traded energy because its dense topology offers additional routing paths that are not available in the MST-based S2. Consequently, S2 and S3 also report lower absolute losses than S1 and S4. However, this reduction does not represent an efficiency improvement; rather, the 10 kW line capacity constraint limits the total volume of energy that can be traded, and lower flow volumes naturally result in lower cumulative losses. This also explains why S3 exhibits slightly higher absolute losses than S2: the increased trading volume facilitated by the dense topology leads to a proportional increase in energy dissipation. This demonstrates that capacity affects both trading volume and power loss, as does the topology in stressed scenarios.

MCF Adaptive vs. MCF Static: Both algorithms produce identical P2P and grid-flow volumes across all four scenarios, confirming that the adaptive weighting mechanism does not change the amount of energy traded but only affects how flows are routed within the network. In three of the four scenarios (S1, S2, and S4), MCF Adaptive achieves slightly lower transmission losses than MCF Static. The

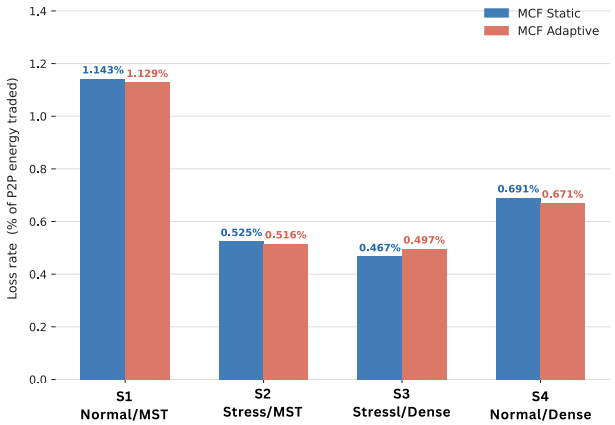

(a) Transmission loss rate (% of P2P energy traded) for MCF Static and MCF Adaptive across the four experimental scenarios.

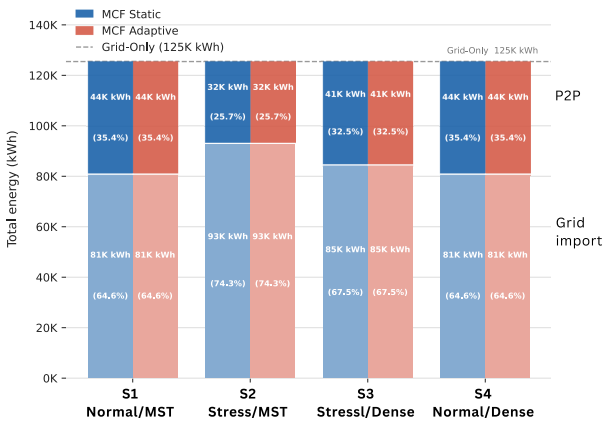

(b) Energy flow decomposition showing grid import (light segment) and P2P energy traded (dark segment) per scenario. Percentages indicate share of total community demand (125,464 kWh).

Figure 6.4: Energy performance of MCF Static and MCF Adaptive across scenarios S1–S4 over 2,648 trading hours.

loss rate decreases from 1.143% to 1.129% in S1, from 0.525% to 0.516% in S2, and from 0.691% to 0.671% in S4, indicating that the adaptive weights tend to steer flows toward shorter or less resistive routes when routing flexibility exists. The sole exception is S3 (Stress/Dense), where the loss rate increases from 0.467% to 0.497% (+12.03 kWh, +6.3%) and congestion charges rise by $457. In this scenario, the stress capacity and dense topology create structurally conflicting objectives: reducing congestion requires concentrating flow on fewer paths, while improving fairness requires spreading flow across more routers, which in a dense stressed network means routing through already loaded links. The online mirror-descent learner responds correctly to both objective penalties every hour, but no routing policy can simultaneously satisfy all three objectives in this network configuration. The result is higher transmission losses and increased congestion, with only a modest fairness gain, reflecting the fundamental tension of the network.

Table 6.4: Average Energy Flow by SDR Regime

Algorithm	**Scenario**	**Low SDR (1,125 h)**			**Normal SDR (62 h)**			**High SDR (1,461 h)**		
		P2P (kWh/h)	**Grid Import**	**Grid Export**	**P2P (kWh/h)**	**Grid Import**	**Grid Export**	**P2P (kWh/h)**	**Grid Import**	**Grid Export**
Grid-Only	All	0.00	86.91	14.88	0.00	43.38	43.35	0.00	17.11	107.31
MCF Static	S1 Normal/MST	14.88	72.03	0.00	42.45	0.93	0.90	17.11	0.00	90.20
	S2 Stress/MST	11.86	75.05	3.02	22.82	20.57	20.54	11.94	5.17	95.37
	S3 Stress/Dense	13.93	72.98	0.95	33.20	10.18	10.15	15.81	1.30	91.50
	S4 Normal/Dense	14.88	72.03	0.00	42.45	0.93	0.90	17.11	0.00	90.20
MCF Adaptive	S1 Normal/MST	14.88	72.03	0.00	42.45	0.93	0.90	17.11	0.00	90.20
	S2 Stress/MST	11.86	75.05	3.02	22.82	20.57	20.54	11.94	5.17	95.37
	S3 Stress/Dense	13.93	72.98	0.95	33.20	10.18	10.15	15.81	1.30	91.50
	S4 Normal/Dense	14.88	72.03	0.00	42.45	0.93	0.90	17.11	0.00	90.20

Impact of Supply-Demand Ratio (SDR) on Energy Flow

The Supply-Demand Ratio (SDR) acts as the primary determinant of the community's role within the broader electrical ecosystem, dictating the transition between net consumption, self-sufficiency, and net exportation. As shown in Table 6.4, the energy flow dynamics across the three identified regimes reveal critical insights into P2P efficiency:

- **Low SDR (Scarcity):** In this regime, local generation is the limiting factor. Under normal capacity (S1/S4), the P2P volume (14.88 kWh/h) exactly matches the total available surplus recorded in the Grid-Only baseline. This indicates that the MCF framework successfully achieves 100% local absorption of renewable energy. However, due to the supply deficit, the community remains dependent on the utility grid, requiring an average import of 72.03 kWh/h.
- **Normal SDR (Equilibrium):** This regime represents the peak of P2P activity. In unconstrained scenarios (S1/S4), P2P exchange reaches its maximum at 42.45 kWh/h, facilitating near-total energy autonomy with grid imports dropping to a negligible 0.93 kWh/h. While this regime maximizes community benefit, it also places the highest stress on local infrastructure, resulting in the highest absolute power losses due to the increased current flow across distribution lines.
- **High SDR (Surplus):** When local generation exceeds demand, the P2P volume is capped by the community's total consumption (17.11 kWh/h). Once local needs are met, the remaining surplus (90.20 kWh/h in S1/S4) is exported to the utility grid. In this state, grid imports are eliminated entirely (0.00 kWh/h).

Intersection of SDR and topology constraints: The results further highlight a critical "bottleneck effect" in stressed scenarios (S2/S3). The impact of the 10 kW capacity constraint is most pronounced during the *Normal SDR* regime; whereas S1 facilitates 42.45 kWh/h of P2P trade, the constrained S2 is restricted to 22.82 kWh/h. This physical limitation necessitates a "re-dependency" on the grid, with imports increasing from 0.93 kWh/h to 20.57 kWh/h because the local network cannot physically distribute the available local energy.

Interestingly, the dense topology (S3) demonstrates a "buffering" effect during *High SDR* and *Normal SDR* regimes. By providing alternative routing paths, S3 sustains higher P2P volumes (e.g., 15.81 kWh/h vs. 11.94 kWh/h in S2 during High SDR), proving that topological redundancy can partially mitigate the economic losses induced by capacity scarcity.

6.4.2 Economic performance analysis

The economic viability of P2P energy trading is the primary driver for consumer adoption and grid-edge investment. Table 7.3 summarizes the cost and revenue outcomes for each algorithm and scenario over the 2,648-hour simulation period.

Table 6.5: Cost and Revenue Summary Across All Scenarios (2,648 Trading Hours).

Algorithm	**Scenario**	**Net Cost ($)**	**Cong. ($)**	**Total +Cong. ($)**	**Avg Cost /hr ($)**	**Sell Rev. ($)**	**Avg Rev. /hr ($)**	**Cost Red. (%)**	**Sell Rev. Δ (%)**
Grid-Only	Baseline	27,067.35	0.00	27,067.35	10.22	10,571.96	3.99	0.00	0.00
MCF Static	S1 Normal/MST	16,418.78	0.00	16,418.78	6.20	12,752.41	4.82	39.34	+20.62
	S2 Stress/MST	19,340.89	2,043.33	21,384.23	8.08	12,189.95	4.60	21.00	+15.30
	S3 Stress/Dense	17,269.27	1,786.14	19,055.41	7.20	12,583.48	4.75	29.60	+19.03
	S4 Normal/Dense	16,418.78	0.00	16,418.78	6.20	12,752.41	4.82	39.34	+20.62
MCF Adaptive	S1 Normal/MST	16,418.78	0.00	16,418.78	6.20	12,752.41	4.82	39.34	+20.62
	S2 Stress/MST	19,340.89	2,038.54	21,379.43	8.07	12,189.95	4.60	21.01	+15.30
	S3 Stress/Dense	17,269.27	2,243.36	19,512.63	7.37	12,583.48	4.75	27.91	+19.03
	S4 Normal/Dense	16,418.78	0.00	16,418.78	6.20	12,752.41	4.82	39.34	+20.62

The Grid-Only baseline, representing a traditional consumer-utility relationship, incurs a net cost of \$27,067.35 (\$10.22/h) while generating \$10,571.96 in revenue from feed-in exports. Both MCF Static and MCF Adaptive configurations substantially reduce this net expenditure by substituting high-tariff grid imports with lower-cost peer-to-peer exchanges. **Effect of topology (S1 vs. S4 and S2 vs. S3):** Under normal capacity, topology has no effect on cost outcomes. S1 and S4 produce identical results across every column. This confirms that when line capacity is unconstrained, the MCF solver reaches the same optimal matching regardless of whether the network contains 11 or 22 edges.

Under stress, topology makes a substantial difference. Scenario S3 (Dense) reduces total cost by \$2,328.81 relative to S2 (MST), improving cost reduction by 8.60 percentage points (29.60% vs. 21.00%) and sell-revenue change by 3.73 percentage points (−19.03% vs. −15.30%) for MCF Static. Similar results are observed for MCF Adaptive.

The dense topology achieves this improvement by enabling substantially more P2P trading (40,825 kWh vs. 32,194 kWh), which reduces grid imports and their associated cost. At the same time, more locally traded energy reduces the amount of surplus exported to the grid, redirecting energy toward higher-value peer transactions instead of the lower feed-in tariff. Additionally, congestion charges are \$257.19 lower in S3, as the additional routing paths distribute flows more evenly across network links.

Effect of capacity (S1 vs. S2 and S4 vs. S3): Reducing line capacity from 221 kW to 10 kW has a severe impact. On the MST, stress erodes cost reduction from 39.34% to 21.00%, a loss of 18.34 percentage points, and introduces \$2,043.33 in congestion charges. On the dense topology the damage is more contained: cost reduction falls from 39.34% to 29.60%, losing only 9.74 percentage points, and congestion is limited to \$1,786.14. The dense topology therefore roughly halves the cost penalty of the capacity constraint. Sell revenue also drops under stress because less energy is traded locally, leaving more surplus exported to the grid at only \$0.06/kWh, a poor substitute for P2P trading.

MCF Static vs. MCF Adaptive: In S1 and S4, both algorithms produce identical cost and revenue outcomes across every column. In these scenarios, line capacity is sufficiently large (221 kW) that congestion never binds, so both solvers converge to the same routing solution. Differences between the two algorithms emerge only under network stress. In Scenario S2 (Stress/MST), MCF Adaptive performs marginally better than the Static baseline, reducing congestion charges by \$4.79 (\$2,038.54 vs. \$2,043.33). This near-identical performance is expected, as the lack of alternative routing paths in the MST topology severely restricts the adaptive mechanism's ability to redistribute flow. While the resulting saving is minor, it is sufficient to produce a 0.01 percentage point improvement in total cost reduction (21.01% vs. 21.00%) and a slight reduction in average hourly cost from \$8.08 to \$8.07. These results confirm that while the adaptive learner can identify minor efficiency gains even in restrictive topologies, its primary impact is reserved for networks with higher degrees of routing freedom.

In contrast, Scenario S3 (Stress/Dense) exhibits a substantial divergence that illustrates a functional trade-off between efficiency and equity. MCF Adaptive incurs \$2,243.36 in congestion charges compared with \$1,786.14 for MCF Static—an increase of \$457.22. This raises the final total cost and reduces the community cost reduction from 29.60% to 27.91%.

This difference arises because the adaptive Mirror Descent updates prioritize fairness among routers, intentionally redirecting flows toward participants with lower trading history even when this requires utilizing longer or more congested paths. As a result, the adaptive solver accepts a modest increase in congestion cost to achieve a more balanced distribution of trading activity across the network. This outcome confirms that in a capacity-constrained dense network, the framework is capable of prioritizing distributional equity over absolute cost minimization, identifying the measurable "price of fairness" required for market balance.

Despite these routing differences, the net grid cost before congestion remains identical for both algorithms in all scenarios, confirming that the observed variation reflects a routing-efficiency trade-off rather than a change in trading volume or market matches.

Impact of SDR on economic performance:

While the aggregate results provide a high-level view of system performance, the economic efficiency of P2P trading is fundamentally driven by the real-time balance between local generation and consumer load. Table 6.6 presents the average hourly cost for each regime across all scenarios. Negative values in the High SDR regime indicate net revenue.

Table 6.6: Average Hourly Cost ($/h) by SDR Regime.

Algorithm	**Scenario**	**Low SDR (1,125 h)**	**Normal SDR (62 h)**	**High SDR (1,461 h)**
Grid-Only	All Scenarios	25.18	10.41	−1.30
MCF Static	S1 Normal/MST	21.61	0.22	−5.41
	S2 Stress/MST	22.34	4.94	−4.17
	S3 Stress/Dense	21.84	2.45	−5.10
	S4 Normal/Dense	21.61	0.22	−5.41
MCF Adaptive	S1 Normal/MST	21.61	0.22	−5.41
	S2 Stress/MST	22.34	4.94	−4.17
	S3 Stress/Dense	21.84	2.45	−5.10
	S4 Normal/Dense	21.61	0.22	−5.41

Figure 6.5 illustrates the average hourly cost across the three SDR regimes for all algorithmic configurations. Table 6.6 and Figure 6.5 reveal the following observations across the three regimes:

- **Low SDR Regime (Net Import):** Under low SDR,SDR < 0.98), community demand exceeds local generation, forcing participants to import electricity from the grid. As a result, all algorithms incur positive costs. The Grid-Only baseline records the highest average cost ($25.18/h), while P2P trading reduces this cost by enabling local energy exchanges. Among the P2P configurations, S1 and S4 achieve the lowest cost ($21.61/h), while the stressed scenarios incur slightly higher costs due to congestion penalties.
- **Normal SDR Regime (Balanced):** Under normal SDR,$0.98 \leq$ SDR ≤ 1.02), local generation roughly matches community demand. In this regime, the benefits of P2P trading become most pronounced: the Normal-capacity scenarios (S1 and S4) reduce the average cost to nearly zero ($0.22/h), indicating that local matching between producers and consumers almost completely eliminates grid purchases. In contrast, stressed scenarios exhibit higher costs because the 10 kW capacity limit introduces congestion charges that prevent the network from fully exploiting local generation.
- **High SDR Regime (Net Export):** Under high SDR (SDR > 1.02), generation exceeds demand, creating a community surplus. This results in negative costs (i.e., net revenue) because the excess electricity is exported to the grid at the sell tariff. P2P trading increases the amount of energy exchanged locally before export, leading to higher net revenue than the grid-only baseline. Again, S1 and S4 achieve the best outcomes (-5.41/h), while stressed scenarios earn slightly less due to congestion costs that limit optimal routing of surplus energy.

6.4.3 Fairness analysis

Beyond economic efficiency, the long-term sustainability of a P2P energy market depends on the equitable distribution of trading opportunities among participants. In a network-constrained environment, a purely cost-minimizing solver tends to favor "electrically cheap" paths, potentially marginalizing

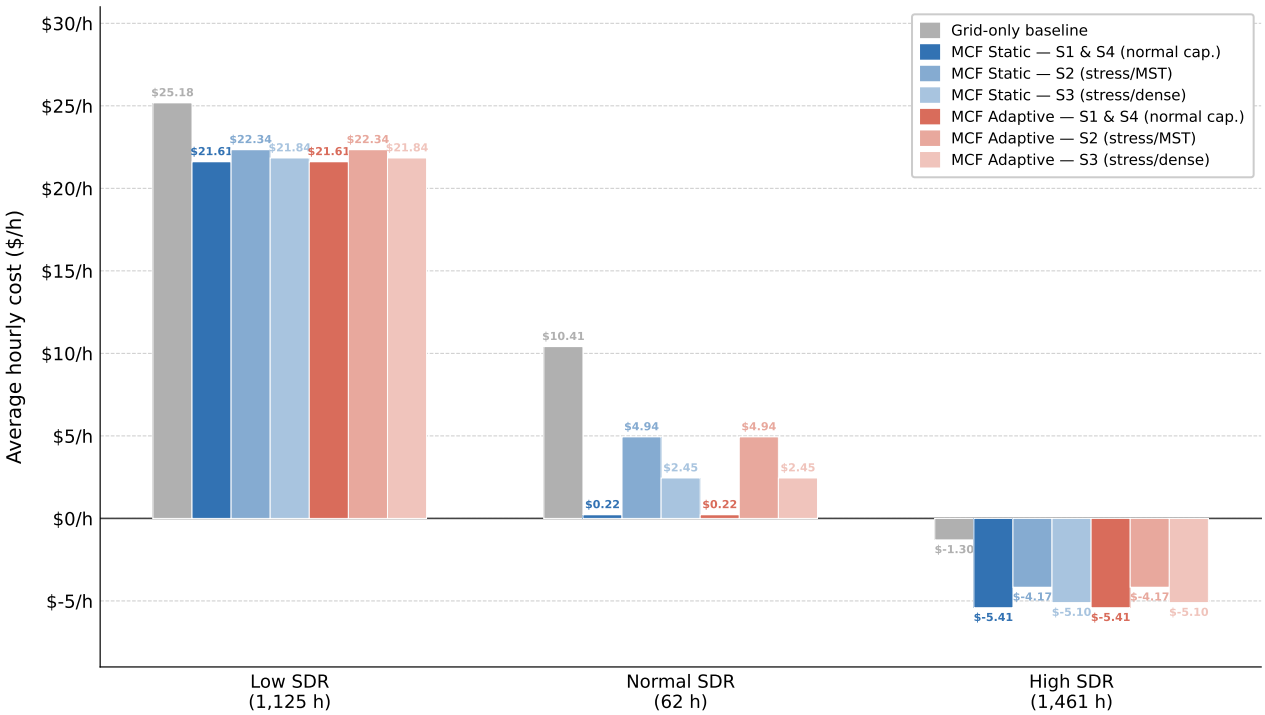

Figure 6.5: Average hourly cost ($/h) by SDR regime and network scenario across all algorithmic configurations over 2,648 trading hours.

routers located at the network periphery or behind congestion bottlenecks. This section evaluates the performance of the MCF Adaptive algorithm in mitigating these disparities. Fairness is quantified using the Jain Fairness Index, calculated over a rolling 168-hour (one-week) window to capture the temporal distribution of trading volumes. A value of 1.0 represents perfect equity, where all routers participate equally in the market volume.

Table 6.7: Trading Fairness Across All Scenarios (2,648 Trading Hours).

Algorithm	**Scenario**	**Avg Fairness (Jain Index)**	**N Hours**
Grid-Only	Baseline	—	2,648
MCF Static	S1 Normal/MST	0.7652	2,648
	S2 Stress/MST	0.7721	2,648
	S3 Stress/Dense	0.7396	2,648
	S4 Normal/Dense	0.7397	2,648
MCF Adaptive	S1 Normal/MST	0.7900	2,648
	S2 Stress/MST	0.7931	2,648
	S3 Stress/Dense	0.7700	2,648
	S4 Normal/Dense	0.7937	2,648

Table 7.5 and Figure 6.6 report the average Jain index for all algorithms and scenarios. Grid-Only has no P2P trading and therefore no fairness metric.

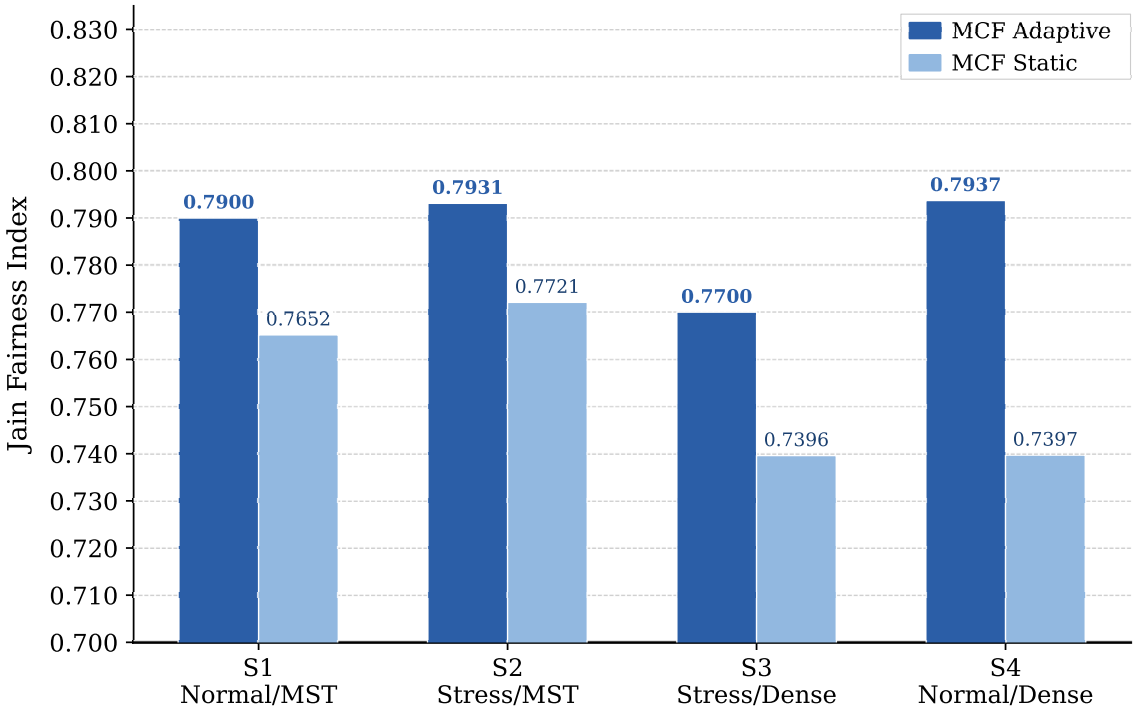

Figure 6.6: Average Jain fairness index per scenario for MCF Adaptive and MCF Static, computed over 2,648 trading hours.

Among the P2P algorithms, MCF Adaptive consistently improves fairness over MCF Static in all scenarios. The MST topology under stress (S2) achieves the highest fairness for both algorithms, as capacity limits force a more even distribution of energy flows. Dense topologies (S3, S4) slightly reduce fairness for Static, as energy is routed over multiple paths unevenly, but the adaptive weights compensate, resulting in the highest fairness overall (0.7937 in S4 for Adaptive).

The results demonstrate that the MCF Adaptive algorithm consistently outperforms the static version across all scenarios. Interestingly, under MCF Static, the MST topology under stress (S2) achieves higher fairness (0.7721) than the unconstrained scenarios. This suggests that capacity limits can act as a structural equalizer, preventing "dominant" routers from monopolizing flow. However, in dense topologies (S3, S4), Static fairness drops to approximately 0.7397 as the solver exploits the most efficient paths at the expense of others. The MCF Adaptive mechanism successfully reverses this trend; by dynamically adjusting routing weights, it achieves its highest overall fairness in S4 (0.7937), proving that the algorithm effectively utilizes topological flexibility to promote equity.

These results confirm that the adaptive routing algorithm effectively balances energy distribution, achieving a more equitable trading outcome, particularly in topologies with multiple routing options.

Impact of SDR on fairness

Table 7.6 reports the average Jain fairness index broken down by SDR regime, from which the following observations are drawn:

- **Regime stability:** Fairness remains remarkably stable across all SDR regimes within each scenario (maximum variation < 0.006). This confirms that the equity behavior of the routing mechanism is governed primarily by network topology and capacity constraints rather than the prevailing supply-demand balance.
- **Consistent algorithmic gain:** MCF Adaptive consistently outperforms MCF Static by approximately 0.025 across all scenarios and SDR regimes. This demonstrates that the adaptive weight mechanism delivers a stable fairness benefit that is functionally independent of energy availability.

Table 6.8: Average Fairness by SDR Regime

Algorithm	**Scenario**	**Low SDR (1,125 h)**	**Normal SDR (62 h)**	**High SDR (1,461 h)**
Grid-Only	All Scenarios	—	—	—
MCF Static	S1 Normal/MST	0.7669	0.7644	0.7639
	S2 Stress/MST	0.7715	0.7661	0.7728
	S3 Stress/Dense	0.7402	0.7368	0.7393
	S4 Normal/Dense	0.7407	0.7389	0.7389
MCF Adaptive	S1 Normal/MST	0.7923	0.7911	0.7881
	S2 Stress/MST	0.7938	0.7884	0.7928
	S3 Stress/Dense	0.7719	0.7675	0.7687
	S4 Normal/Dense	0.7956	0.7930	0.7923

- **Structural Constraints vs. Active Adaptation:** A central finding is that under the *MCF Static* model, fairness is dictated by physical constraints rather than optimization. We observe a "topological dominance" where simple MST structures (S1, S2) outperform complex Dense networks (S3, S4) because the latter allow the solver to concentrate flow on a small subset of efficient paths. Furthermore, we identify a paradox of *forced equity* in Scenario S2, where tight capacity limits (10 kW) physically prevent any single router from monopolizing the market. In contrast, the *MCF Adaptive* algorithm successfully breaks these structural dependencies; it achieves its peak performance (0.7937) by utilizing the flexibility of a Dense/Normal network (S4), proving that algorithmic intelligence can convert topological complexity into an equity advantage rather than a disadvantage.

6.4.4 Adaptive weight learning dynamics

Figure 6.7 illustrates the mirror descent weight trajectories for MCF Adaptive across all four experimental scenarios over the 2,648 trading hours. Each panel shows the per-hour evolution of the three objective weights: α (power loss), β (congestion avoidance), and γ (trading fairness) along with their convergence milestones. The left column of each panel shows the full 2,648-hour run; the right column zooms into the convergence window to make the transition visible.

All four scenarios converge to a stable weight vector, but the dominant objective and the speed of convergence differ substantially depending on network conditions. Table 6.9 summarizes the final converged weights and the four convergence milestones for each scenario.

Table 6.9: MCF Adaptive weight convergence summary across experimental scenarios.

Scenario	**Final weights**			**Dominant**	**Convergence (hours)**		
	α	β	γ		**90%**	**99%**	**168-h stable**
S1 Normal/MST	0.856	0.047	0.097	α	91	130	297
S2 Stress/MST	0.048	0.857	0.095	β	49	61	233
S3 Stress/Dense	0.047	0.851	0.102	β	66	88	256
S4 Normal/Dense	0.090	0.048	0.862	γ	191	308	378

S1 Normal/MST, α-dominant: With 221 kW capacity, lines never saturate, so the congestion signal is almost zero after conversion and β decays from 0.3 as α absorbs the weight budget. Long MST

paths (mean 16.4 km) produce high losses, keeping the loss signal consistently high. γ remains at a low residual value as the fairness signal weakens once the algorithm begins redistributing flows. The algorithm converges to $\alpha = 0.856$, $\beta = 0.047$, $\gamma = 0.097$ by hour 130, stabilising at hour 297.

S2 Stress/MST, β-dominant: The 10 kW cap saturates lines frequently, making the congestion signal large and persistent. Congestion limits traded volume so flows per path are small, keeping I^2R losses low and the loss signal weak. γ remains low as the reduced trading volume naturally limits participation imbalance. With β rising strongly and α, γ both decaying, this is the fastest convergence of all scenarios: $\alpha = 0.048$, $\beta = 0.857$, $\gamma = 0.095$ by hour 61, stabilising by hour 233.

S3 Stress/Dense, β-dominant: Congestion dominates as in S2, but the dense topology activates the fairness signal as the solver repeatedly favors the same efficient paths. The loss signal remains weak for the same reason as S2. The competing fairness pressure slows convergence relative to S2 (99% at hour 88 vs. hour 61) and leaves γ at a higher residual value than S2 (0.102 vs. 0.095), converging to $\alpha = 0.047$, $\beta = 0.851$, $\gamma = 0.102$.

S4 Normal/Dense, γ-dominant: With ample capacity, the congestion signal is near zero and β decays as in S1. The dense topology's short paths reduce loss pressure, weakening the loss signal relative to S1. However, the solver repeatedly concentrates flows on the same efficient routes, generating a persistent participation imbalance that sustains the fairness signal. With both α and β decaying, γ gradually prevails, converging to $\alpha = 0.090$, $\beta = 0.048$, $\gamma = 0.862$ by hour 308 and stabilising at hour 378 — the slowest convergence of all scenarios, and the largest fairness gain over MCF Static (+0.054).

Mirror descent successfully discovers the binding constraint in each scenario without any prior knowledge of network conditions. The algorithm learns that congestion is the dominant pressure under capacity stress (S2, S3), that loss efficiency matters most under normal MST operation (S1), and that fairness is the primary opportunity in a well-provisioned dense network (S4). No manual tuning or scenario-specific configuration is required.

Convergence speed is determined by signal strength and unambiguity. S2 converges fastest because the congestion signal is large, consistent, and unchallenged by competing objectives. S4 converges slowest because two objectives, loss and fairness, are simultaneously active and of comparable magnitude, requiring more observations before the algorithm can distinguish which pressure is dominant.

The weight trajectories explain the performance differences reported in the earlier sections. The α-dominant solution in S1 steers flows toward shorter resistive paths, producing the loss rate reduction from 1.143% (Static) to 1.129% (Adaptive). The γ-dominant solution in S4 redistributes flows toward underserved routers, producing the largest fairness gain (+0.054). The conflicted dynamics of S3 explain why MCF Adaptive incurs higher congestion charges than MCF Static in that scenario: the competing γ signal forces the algorithm to accept suboptimal routing from a congestion perspective in order to partially satisfy the fairness objective.

6.4.5 Computational complexity and runtime analysis

Real-time feasibility is a necessary requirement for any P2P energy market mechanism. This subsection evaluates the computational cost of the proposed framework from two perspectives: (i) the **theoretical time complexity** of each component, and (ii) the **empirical runtime per trading hour**, measured over 2,648 hours across all scenarios.

Theoretical time complexity

At each trading hour, both MCF Static and MCF Adaptive construct a directed graph and solve an MCF problem using the Network Simplex algorithm. The graph contains $|\mathcal{V}| = 3K + 1$ nodes, where K is the number of routers ($K = 12$, hence $|\mathcal{V}| = 37$). The number of directed edges is:

$$|\mathcal{E}| = 3K + 2\,|\mathcal{E}_{\text{phys}}| + 2K \tag{6.27}$$

where $|\mathcal{E}_{\text{phys}}|$ denotes the number of physical links (11 for MST, 22 for dense), yielding $|\mathcal{E}| \in \{58, 82\}$.

The Network Simplex algorithm solves the MCF problem in:

$$\mathcal{O}(|\mathcal{V}| \cdot |\mathcal{E}| \cdot \log|\mathcal{V}| \cdot \log(|\mathcal{V}|C)) \tag{6.28}$$

time in the worst case [161], where C is the maximum arc capacity. Since $|\mathcal{V}|$ and $|\mathcal{E}|$ depend only on the router topology and not on the number of households ($N = 300$), the per-hour complexity is effectively constant with respect to N.

MCF Adaptive introduces three additional operations: (i) congestion computation in $\mathcal{O}(|\mathcal{E}_{\text{phys}}|)$, (ii) Mirror Descent update in $\mathcal{O}(1)$, and (iii) fairness update in $\mathcal{O}(K)$. The total overhead, $\mathcal{O}(|\mathcal{E}_{\text{phys}}| + K)$, is negligible relative to the MCF solve step. Hence, the adaptive mechanism introduces **no asymptotic complexity increase**.

Table 6.10 summarises the complexity of all components. The Network Simplex solver dominates in all configurations.

Table 6.10: Theoretical time complexity of each algorithmic component.

Component	**Time Complexity**	**Dominant Factor**
Graph construction	$\mathcal{O}(K^2)$	All-pair router distances
MCF solve (Static/Adaptive)	$\mathcal{O}(\lvert\mathcal{V}\rvert \cdot \lvert\mathcal{E}\rvert \cdot \log \lvert\mathcal{V}\rvert \cdot \log(\lvert\mathcal{V}\rvert C))$	Network Simplex
Mirror Descent update	$\mathcal{O}(\lvert\mathcal{E}_{\text{phys}}\rvert + K)$	Congestion + normalisation
Fairness (Jain index)	$\mathcal{O}(K)$	Rolling update
Flow parsing	$\mathcal{O}(K^2 \cdot P)$	Path reconstruction
Per-hour total	$\mathcal{O}(\lvert\mathcal{V}\rvert \cdot \lvert\mathcal{E}\rvert \cdot \log \lvert\mathcal{V}\rvert \cdot \log(\lvert\mathcal{V}\rvert C))$	Solver dominates

With $|\mathcal{V}| = 37$ and $|\mathcal{E}| \leq 82$, the theoretical bound lies in the sub-millisecond regime, consistent with empirical results.

Empirical runtime analysis

Table 7.7 reports the average per-hour runtime (ms) for MCF Static and MCF Adaptive across all scenarios (2,648 trading hours).

Table 6.11: Average per-hour runtime (ms) across all scenarios.

Scenario	$\lvert\mathcal{V}\rvert$	$\lvert\mathcal{E}\rvert$	**Static** (ms/h)	**Adaptive** (ms/h)	**Δ** (ms)	**Overhead** (%)
S1 Normal/MST	37	58	2.16	2.27	+0.11	5.3
S2 Stress/MST	37	58	2.03	2.25	+0.22	11.0
S3 Stress/Dense	37	82	2.41	2.71	+0.29	12.1
S4 Normal/Dense	37	82	2.29	2.70	+0.42	18.2
Mean	—	—	**2.22**	**2.48**	**+0.26**	**11.7**

All configurations remain below 3 ms per trading hour, confirming real-time feasibility. MCF Static averages 2.22 ms/h and MCF Adaptive 2.48 ms/h, implying a total optimisation time below 7 seconds for the full simulation and compatibility with short market intervals.

Runtime is primarily driven by topology: dense graphs ($|\mathcal{E}| = 82$) consistently incur higher costs than MST configurations ($|\mathcal{E}| = 58$), while capacity constraints have a secondary effect. The adaptive overhead remains modest (5.3%–18.2%) and increases with routing flexibility, as persistent weight updates remain active in less constrained settings.

6.5 Discussion

This study demonstrates that system performance in P2P energy trading is governed by a hierarchy of constraints in which **infrastructure capacity is the dominant factor**, followed by network topology, while algorithmic adaptation primarily refines allocation within these limits. Across all scenarios, unconstrained capacity (221 kW) enables substantial cost reductions (39.34% in both S1 and S4), whereas capacity stress reduces these gains to 21.00%–29.60%, depending on topology, with limited sensitivity to the choice of algorithm. Under unconstrained conditions, efficient energy exchange is achieved irrespective of network structure; in contrast, capacity saturation enforces more uniform allocation patterns and diminishes the influence of both topology and adaptive optimization. These results indicate that, under the considered model assumptions, infrastructure availability fundamentally bounds achievable system efficiency.

The integration of adaptive routing through Mirror Descent demonstrates that algorithmic learning enhances performance primarily in unconstrained or moderately constrained environments. In such cases, adaptive weights successfully exploit network structure to reduce costs and improve energy distribution. However, as constraints become binding, the feasible solution space contracts, and adaptive behaviour converges toward uniform allocation patterns. This indicates that learning-based optimisation is most effective when sufficient flexibility exists in the system, but its influence diminishes under strict physical limitations.

A central outcome of the analysis is the identification of a systematic trade-off between efficiency and fairness. In capacity-constrained scenarios, limited transmission resources enforce a more equitable distribution of energy among consumers, leading to higher fairness indices. However, this equity is achieved at the expense of increased system costs, as energy must be routed through suboptimal or longer paths. Quantitative results confirm this directly: in Scenario S3, a 0.0304 improvement in the Jain fairness index is achieved at a cost premium of $457.22 in congestion charges relative to the static baseline, highlighting the economic implications of constrained infrastructure.

This leads to the distinction between *forced equity* and *active equity*. Forced equity arises when physical constraints impose uniform distribution, independent of algorithmic design, whereas active equity results from deliberate optimisation strategies in flexible systems. The results show that high fairness levels do not necessarily indicate optimal system performance, but may instead reflect underlying infrastructure limitations. Consequently, fairness metrics must be interpreted in conjunction with system constraints to avoid misleading conclusions.

From a system design perspective, these findings support an infrastructure-first principle, whereby investments in transmission capacity yield greater performance improvements than increasing algorithmic sophistication alone. While adaptive optimisation enhances efficiency, it cannot compensate for insufficient infrastructure. This insight has direct implications for smart grid planning, suggesting that physical network upgrades should precede or accompany the deployment of advanced optimisation mechanisms.

6.6 Conclusion

This chapter proposed an adaptive MCF framework for P2P energy trading that integrates physical routing, economic pricing, and learning-based adaptation within a unified optimisation model. By combining a graph-based MCF formulation with a Mirror Descent update mechanism, the approach enables dynamic adjustment of routing priorities in response to congestion, transmission losses, and fairness signals, while preserving computational efficiency and avoiding manual parameter tuning.

From an Energy Internet (EI) perspective, the proposed framework addresses the three fundamental routing challenges in a unified manner. First, **efficient path finding** is achieved through the MCF formulation, which guarantees globally optimal routing under network constraints. Second, **producer subset selection** emerges implicitly from the flow optimisation process, as the solver selects the optimal set of producers and routing paths that minimise system cost while respecting capacity limits. Third, **scheduling** is handled through repeated per-interval optimisation, enabling dynamic adaptation to time-varying demand, generation, and network conditions. Unlike traditional approaches that treat

these problems separately, the proposed framework solves them jointly within a single optimisation structure.

The experimental evaluation over 2,648 trading hours and 300 households demonstrates that the framework achieves cost reductions of up to 39.34% under normal infrastructure conditions and maintains reductions of 21.00%–29.60% under capacity stress, while sustaining real-time performance (2.22 ms/h for MCF Static and 2.48 ms/h for MCF Adaptive). The results reveal a clear hierarchy of constraints: infrastructure capacity is the dominant factor governing system performance, followed by network topology, while adaptive optimisation refines allocation within these physical limits.

The adaptive mechanism further demonstrates a robust ability to identify the binding system constraint without prior configuration, adjusting routing priorities according to the dominant factor in each scenario. This property highlights the practical relevance of learning-based adaptation in dynamic energy trading environments.

A key contribution of this work is the identification and quantification of the trade-off between efficiency and fairness. Under constrained conditions, limited transmission capacity enforces more equitable energy distribution at the expense of increased system cost. In Scenario S3, a 0.0304 improvement in the Jain fairness index is achieved at an additional congestion cost of $457.22, providing a concrete basis for evaluating fairness–efficiency trade-offs. This leads to the distinction between *forced equity*, driven by physical constraints, and *active equity*, resulting from optimisation, emphasising that fairness metrics must be interpreted in the context of system limitations.

From a practical perspective, the findings support an *infrastructure-first* design principle: investments in transmission capacity yield greater performance improvements than increasing algorithmic sophistication alone. While adaptive routing enhances efficiency in flexible systems, it cannot compensate for insufficient physical resources. At the same time, the framework remains scalable, as its computational complexity depends on the router-level graph (K) rather than the number of prosumers (N), enabling deployment in larger communities.

This study has several limitations, including the use of deterministic demand and generation profiles, a fixed network size, and non-strategic agents. Future work will extend the framework to stochastic environments, incorporate strategic market behaviour, and explore reinforcement learning approaches for joint pricing and routing optimisation. Scaling to larger and dynamically evolving network topologies also remains an important direction.

To conclude, this work demonstrates that efficient and adaptive P2P energy trading can be achieved through the integration of network flow optimisation and online learning, while simultaneously addressing the core challenges of energy routing and P2PET within EI framework.

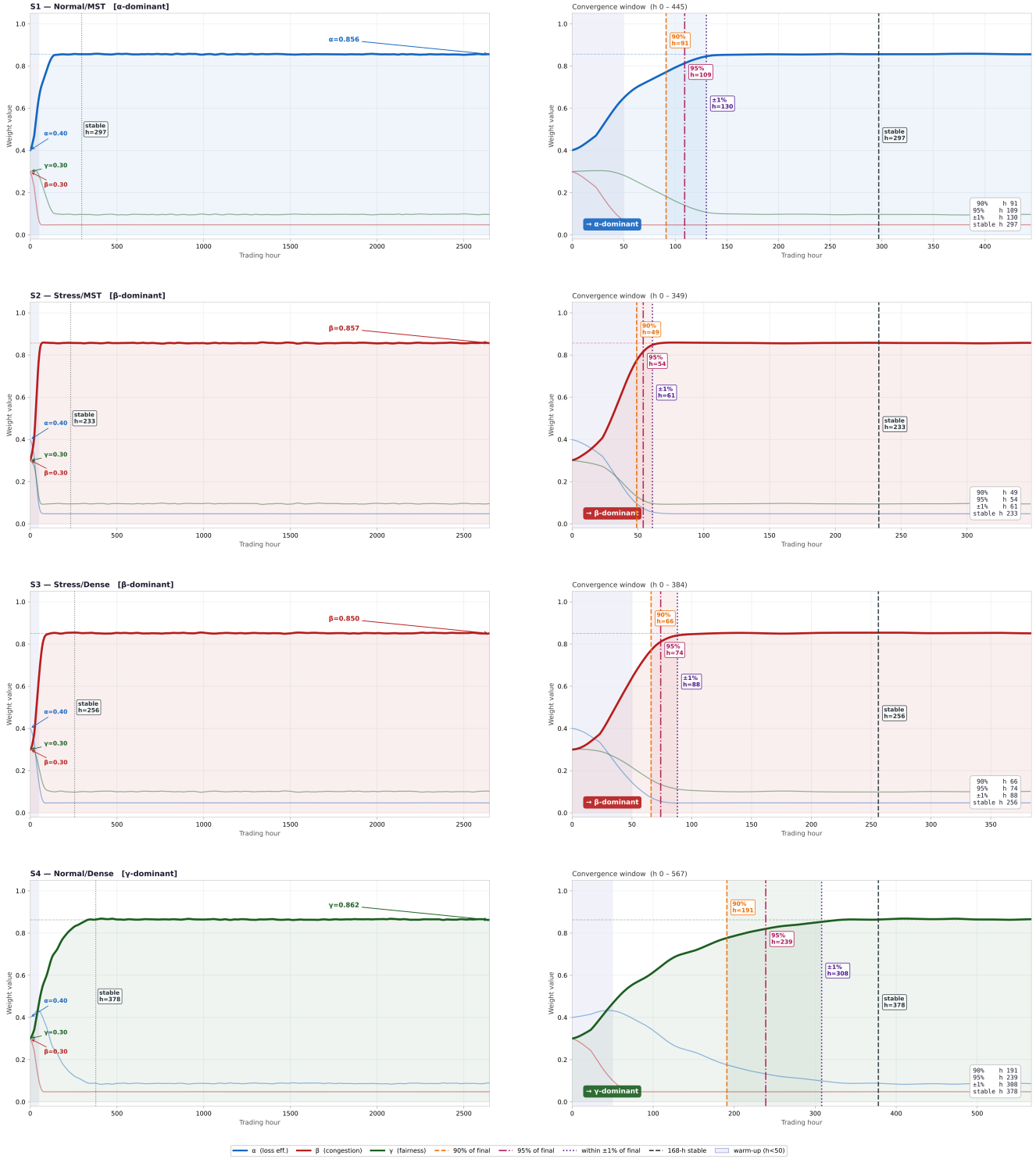

Figure 6.7: MCF Adaptive weight evolution across scenarios.

Chapter 7

Comparative Analysis and Discussion

This chapter presents a unified comparative evaluation of the four energy routing protocols developed across Chapters 3–6: FKD-RA (Chapter 3), SA-RA (Chapter 4), QGA-RA (Chapter 5), and MCF Adaptive (Chapter 6). All algorithms were evaluated on the same real-world dataset of 300 Australian households (Ausgrid Solar Home Electricity Dataset, 2012–2013) [**ausgrid2013**], using an identical 12-router cluster network, the same four experimental scenarios detailed in Section 6.2 of Chapter 6, and the same SDR-based dynamic pricing mechanism. This ensures that all performance differences are attributable solely to algorithmic design choices rather than experimental conditions.

The analysis covers four dimensions. Sections 7.1–7.3 compare energy flow, cost, and fairness outcomes across scenarios and SDR regimes. Section 7.4 compares computational tractability through theoretical complexity analysis and measured execution times, statistically validated by pairwise Wilcoxon signed-rank tests. Section 7.5 synthesises the cross-cutting findings.

7.1 Energy flow analysis

Table 7.1 presents the energy flow breakdown for each algorithm across all four scenarios over 2,648 trading hours, and Figure 7.1(a) visualises the resulting P2P trading volumes and cost reductions side by side.

Under normal capacity (S1, S4). All four algorithms achieve near-identical P2P volumes (43,296–44,419 kWh), confirming that algorithmic differences are negligible when physical constraints are inactive. The key differentiator is transmission loss: MCF Adaptive achieves the lowest losses (501 kWh in S1), while FKD-RA records the highest (883 kWh), a direct consequence of its distance-based routing ignoring electrical resistance.

Under capacity stress (S2). Stress reveals the fundamental divide between the algorithms. FKD-RA maintains its full trading volume by ignoring the capacity constraint entirely, accumulating congestion penalties instead. In contrast, SA-RA, QGA-RA, and MCF Adaptive all reduce P2P volume to respect capacity limits (−36.8%, −38.9%, and −27.4% respectively), with MCF Adaptive sacrificing the least volume while still enforcing feasibility. Transmission losses drop across all capacity-aware algorithms, not from improved efficiency but from reduced flow volumes.

Effect of topology densification (S2 → S3). Additional routing paths benefit all capacity-aware algorithms by offering alternative routes around congested links. SA-RA gains the most (27,793 → 38,597 kWh), followed by MCF Adaptive (32,194 → 40,825 kWh) and QGA-RA (26,441 → 35,008 kWh). FKD-RA is unaffected, as it neither detects nor responds to congestion.

SDR regime breakdown (Table 7.2). Under Low and High SDR, all algorithms behave similarly regardless of scenario, as trading is bounded by supply scarcity or demand scarcity respectively rather than by algorithmic choice. The differences emerge in the Normal SDR regime, where both supply and

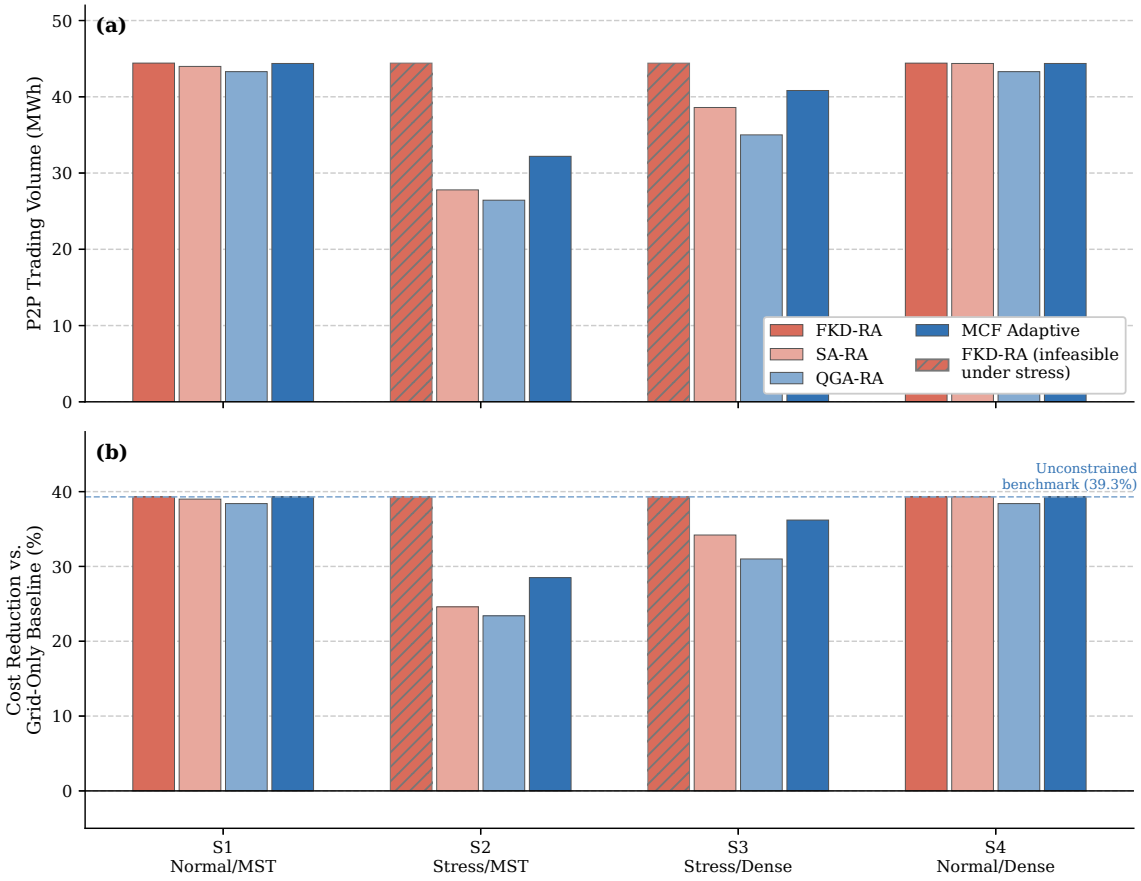

Figure 7.1: P2P trading volume (a) and cost reduction relative to the grid-only baseline (b) for all four algorithms across the four experimental scenarios.

Table 7.1: Energy Flow Summary Across All Scenarios (2,648 Trading Hours).

Scenario	Algorithm	P2P (kWh)	Grid Import (kWh)	Grid Export (kWh)	Loss (kWh)
Baseline	Grid-Only	0.00	125,464.39	176,199.37	0.00
S1 Normal/MST	FKD-RA	**44,418.87**	81,095.59	131,780.50	882.87
	SA-RA	43,982.64	81,481.75	132,216.73	672.05
	QGA-RA	43,295.82	82,168.57	132,903.55	759.94
	MCF Adaptive	44,369.06	**81,095.33**	**131,830.31**	**501.02**
S2 Stress/MST	FKD-RA	44,418.87†	81,095.59	131,780.50	882.87
	SA-RA	27,792.90	97,671.49	148,406.47	252.32
	QGA-RA	26,440.82	99,023.57	149,758.55	255.92
	MCF Adaptive	**32,193.58**	**93,270.81**	**144,005.79**	**166.18**
S3 Stress/Dense	FKD-RA	44,413.70†	81,095.66	131,785.67	480.17
	SA-RA	38,596.98	86,867.40	137,602.38	244.69
	QGA-RA	35,007.62	90,456.76	141,191.75	214.17
	MCF Adaptive	**40,825.34**	**84,639.04**	**135,374.02**	**202.79**
S4 Normal/Dense	FKD-RA	**44,413.70**	81,095.66	131,785.67	480.17
	SA-RA	44,369.06	**81,095.32**	**131,830.31**	398.44
	QGA-RA	43,295.82	82,168.57	132,903.55	417.68
	MCF Adaptive	44,369.06	**81,095.33**	**131,830.31**	**297.65**

† FKD-RA maintains full volume under stress by violating capacity constraints; see Section 7.2.

demand are simultaneously large: FKD-RA sustains peak volumes (42.59 kWh/h) across all scenarios, while SA-RA, QGA-RA, and MCF Adaptive drop sharply under stress (18.18, 17.30, and 22.82 kWh/h respectively in S2), reflecting the sensitivity of capacity-aware algorithms to line congestion precisely when trading potential is highest. MCF Adaptive recovers more volume than SA-RA and QGA-RA in S2, consistent with its lower overall volume loss under stress.

Table 7.2: Average Energy Flow (kWh/h) by SDR Regime.

		Low SDR (1,125 h)			**Normal SDR (62 h)**			**High SDR (1,461 h)**		
Algorithm	**Scenario**	P2P	Buy	Sell	P2P	Buy	Sell	P2P	Buy	Sell
Grid-Only	All	0.00	86.91	14.88	0.00	43.38	43.35	0.00	17.11	107.31
FKD-RA	S1 Normal/MST	14.88	72.03	0.00	42.59	0.93	0.76	17.14	0.00	90.17
	S2 Stress/MST	14.88	72.03	0.00	42.59	0.93	0.76	17.14	0.00	90.17
	S3 Stress/Dense	14.88	72.03	0.00	42.58	0.93	0.77	17.14	0.00	90.17
	S4 Normal/Dense	14.88	72.03	0.00	42.58	0.93	0.77	17.14	0.00	90.17
SA-RA	S1 Normal/MST	14.82	72.09	0.06	39.60	3.78	3.75	17.01	0.10	90.29
	S2 Stress/MST	10.30	76.61	4.57	18.18	25.20	25.17	10.32	6.79	96.99
	S3 Stress/Dense	13.00	73.91	1.87	29.97	13.41	13.38	15.13	1.98	92.17
	S4 Normal/Dense	14.88	72.03	0.00	42.45	0.93	0.90	17.11	0.00	90.19
QGA-RA	S1 Normal/MST	13.96	72.95	0.92	41.79	1.60	1.56	17.11	0.00	90.19
	S2 Stress/MST	9.51	77.40	5.37	17.30	26.09	26.05	10.04	7.07	97.27
	S3 Stress/Dense	11.68	75.23	3.19	26.08	17.30	17.27	13.86	3.25	93.45
	S4 Normal/Dense	13.96	72.95	0.92	41.79	1.60	1.56	17.11	0.00	90.19
MCF Adaptive	S1 Normal/MST	14.88	72.03	0.00	42.45	0.93	0.89	17.11	0.00	90.19
	S2 Stress/MST	11.86	75.05	3.02	22.82	20.57	20.53	11.94	5.17	95.37
	S3 Stress/Dense	13.93	72.98	0.95	33.20	10.18	10.15	15.81	1.30	91.50
	S4 Normal/Dense	14.88	72.03	0.00	42.45	0.93	0.90	17.11	0.00	90.19

7.2 Cost analysis

Table 7.3 compares cost and revenue outcomes for each algorithm and scenario over the 2,648 trading hours, and Figure 7.1(b) visualises the corresponding cost reductions relative to the grid-only baseline of $27,067.35 ($10.22/h).

Under normal capacity (S1, S4). All four algorithms achieve comparable cost reductions (38.3–39.3%), confirming that algorithmic differences have negligible economic impact when capacity is unconstrained. MCF Adaptive and SA-RA lead at 39.3%, while QGA-RA trails slightly due to its lower P2P volume. The aggregate differences amount to less than $258 over 2,648 hours.

Under capacity stress (S2): The algorithms diverge sharply. FKD-RA accumulates the largest congestion penalty ($13,273), pushing its total cost above the grid-only baseline ($29,695 vs. $27,067), making it the only algorithm that worsens under stress. SA-RA and QGA-RA contain their penalties through capacity-aware volume reduction ($2,852 and $2,858 respectively), achieving 24.6% and 23.4% cost reduction. MCF Adaptive shows the most robust response, with the smallest congestion penalty ($2,039) and the best cost reduction among capacity-aware algorithms (28.6%).

Effect of topology densification (S2 → S3): Additional routing paths improve cost outcomes for all capacity-aware algorithms by allowing energy to bypass congested links. SA-RA improves from 24.6% to 34.2%, MCF Adaptive from 28.6% to 36.2%, and QGA-RA from 23.4% to 31.0%. FKD-RA's reported net cost reduction remains 39.3% in both stress scenarios, but its total cost including congestion ($22,214 in S3) remains well above the unconstrained case.

Table 7.3: Cost and Revenue Summary Across All Scenarios (2,648 Trading Hours).

Algo.	Scenario	Net Cost ($)	Cong. ($)	Total ($)	Avg/hr ($)	Sell Rev. ($)	Red. (%)
Grid-Only	Baseline	27,067.35	0.00	27,067.35	10.22	10,571.96	0.00
FKD-RA	S1 Normal/MST	16,421.85	0.00	16,421.85	6.20	12,754.53	39.33
	S2 Stress/MST	16,421.85	13,272.69	29,694.54	11.21	12,754.53	39.33
	S3 Stress/Dense	16,421.56	5,792.00	22,213.56	8.39	12,754.32	39.33
	S4 Normal/Dense	16,421.56	0.00	16,421.56	6.20	12,754.32	39.33
SA-RA	S1 Normal/MST	16,511.52	0.00	16,511.52	6.24	12,733.91	39.00
	S2 Stress/MST	20,397.05	2,851.74	23,248.80	8.78	11,978.27	24.64
	S3 Stress/Dense	17,804.08	2,277.49	20,081.57	7.58	12,470.78	34.22
	S4 Normal/Dense	16,418.78	0.00	16,418.78	6.20	12,752.41	39.34
QGA-RA	S1 Normal/MST	16,676.36	0.00	16,676.36	6.30	12,665.54	38.39
	S2 Stress/MST	20,721.55	2,858.03	23,579.58	8.90	11,884.64	23.44
	S3 Stress/Dense	18,665.53	1,868.24	20,533.77	7.75	12,278.27	31.04
	S4 Normal/Dense	16,676.36	0.00	16,676.36	6.30	12,665.54	38.39
MCF Adaptive	S1 Normal/MST	16,418.78	0.00	16,418.78	6.20	12,752.41	39.34
	S2 Stress/MST	19,340.89	2,038.54	21,379.43	8.07	12,189.95	28.55
	S3 Stress/Dense	17,269.27	2,243.36	19,512.63	7.37	12,583.48	36.20
	S4 Normal/Dense	16,418.78	0.00	16,418.78	6.20	12,752.41	39.34

Total = Net Cost + Congestion penalty.

SDR regime breakdown (Table 7.4). The Normal SDR regime is where algorithmic differences are most pronounced. Under unconstrained scenarios, MCF Adaptive and FKD-RA reduce the average cost to \$0.22–\$0.23/h, nearly eliminating grid purchases. Under stress, QGA-RA and SA-RA incur the highest Normal SDR costs (\$6.26/h and \$6.05/h in S2), as this regime is most sensitive to capacity-driven volume reductions. MCF Adaptive contains this effect better (\$4.94/h in S2), consistent with its lower overall volume loss under stress. Under Low and High SDR, differences across algorithms are small, as trading is bounded by supply or demand scarcity rather than by congestion.

7.3 Fairness analysis

Table 7.5 reports the average Jain fairness index for all algorithms and scenarios over 2,648 trading hours. Figure 7.2 reveals the fairness hierarchy across algorithms and scenarios.

Overall ranking. MCF Adaptive consistently achieves the highest fairness in S1, S3, and S4 (0.770–0.794), a direct consequence of its explicit fairness penalty term. The single exception is S2, where QGA-RA marginally exceeds MCF Adaptive (0.7938 vs. 0.7931), as its scheduling mechanism enforces broad capacity redistribution across routers when congestion is tight. FKD-RA records the lowest fairness in all scenarios (0.602–0.629), as its greedy cost-ordered selection systematically concentrates trading on the same low-cost routers.

Effect of capacity stress. Stress improves fairness for SA-RA and QGA-RA (+12.9% and +14.0% respectively), as tight capacity limits prevent any single path from monopolising available flow. MCF Adaptive is nearly unaffected (+0.4%), since its adaptive weights already enforce equity under normal conditions. FKD-RA shows no change, as it neither detects nor responds to congestion.

Effect of topology densification. Moving to the dense topology slightly reduces fairness for all algorithms (−2.7% to −4.4%), as multiple alternative paths allow some routers to dominate trading in certain hours without being physically blocked. This effect is most pronounced for FKD-RA and QGA-RA (−4.4% and −4.1%).

Table 7.4: Average Hourly Cost ($/h) by SDR Regime.

Algorithm	**Scenario**	**Low SDR (1,125 h)**	**Normal SDR (62 h)**	**High SDR (1,461 h)**
Grid-Only	All	25.18	10.41	−1.30
FKD-RA	S1 Normal/MST	21.61	0.23	−5.41
	S2 Stress/MST	21.61	0.23	−5.41
	S3 Stress/Dense	21.61	0.23	−5.41
	S4 Normal/Dense	21.61	0.23	−5.41
SA-RA	S1 Normal/MST	21.62	0.91	−5.39
	S2 Stress/MST	22.71	6.05	−3.78
	S3 Stress/Dense	22.06	3.22	−4.94
	S4 Normal/Dense	21.61	0.22	−5.41
QGA-RA	S1 Normal/MST	21.83	0.39	−5.41
	S2 Stress/MST	22.90	6.26	−3.71
	S3 Stress/Dense	22.38	4.16	−4.63
	S4 Normal/Dense	21.83	0.39	−5.41
MCF Adaptive	S1 Normal/MST	21.61	0.22	−5.41
	S2 Stress/MST	22.34	4.94	−4.17
	S3 Stress/Dense	21.84	2.45	−5.10
	S4 Normal/Dense	21.61	0.22	−5.41

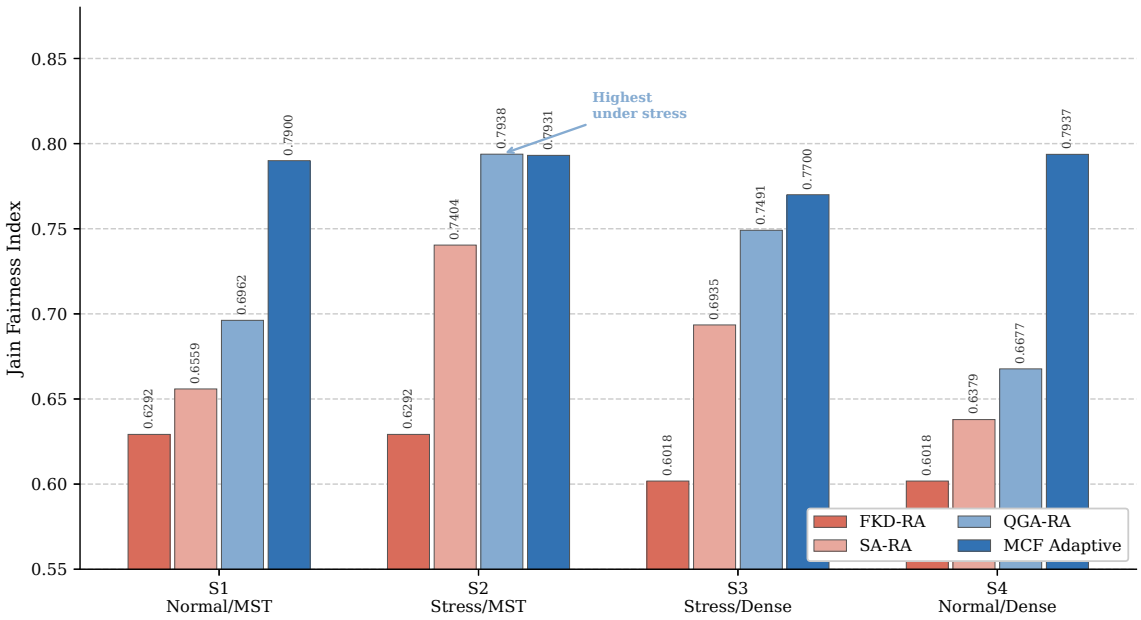

Figure 7.2: Average Jain fairness index for all four algorithms across the four experimental scenarios, computed over a rolling 168-hour window.

SDR regime breakdown (Table 7.6). Fairness is remarkably stable across SDR regimes within each algorithm-scenario combination (variation <0.005), confirming that trading equity is determined by algorithmic design and network topology rather than supply-demand balance.

Table 7.5: Trading Fairness Across All Scenarios (2,648 Trading Hours). Bold values indicate the highest fairness per scenario.

Algorithm	Scenario	Avg Fairness (Jain Index)	N Hours
Grid-Only	Baseline	—	2,648
FKD-RA	S1 Normal/MST	0.6292	2,648
	S2 Stress/MST	0.6292	2,648
	S3 Stress/Dense	0.6018	2,648
	S4 Normal/Dense	0.6018	2,648
SA-RA	S1 Normal/MST	0.6559	2,648
	S2 Stress/MST	0.7404	2,648
	S3 Stress/Dense	0.6935	2,648
	S4 Normal/Dense	0.6379	2,648
QGA-RA	S1 Normal/MST	0.6962	2,648
	S2 Stress/MST	**0.7938**	2,648
	S3 Stress/Dense	0.7491	2,648
	S4 Normal/Dense	0.6677	2,648
MCF Adaptive	S1 Normal/MST	**0.7900**	2,648
	S2 Stress/MST	0.7931	2,648
	S3 Stress/Dense	**0.7700**	2,648
	S4 Normal/Dense	**0.7937**	2,648

7.4 Computational analysis

A critical dimension of the algorithmic comparison is computational tractability, as it directly determines whether an algorithm is deployable in real-time P2P markets. Table 7.7 reports measured execution times per trading hour, averaged over all 2,648 hours on identical hardware. All pairwise runtime differences are statistically significant ($p \ll 10^{-10}$, two-sided Wilcoxon signed-rank test), so the analysis focuses on the magnitude and practical significance of the differences.

7.4.1 Theoretical complexity

The four algorithms represent a clear progression in how they trade computational cost for algorithmic capability.

FKD-RA operates in $\mathcal{O}(n \log n + |E| \log |V|)$ per hour, where n is the number of prosumers, $|E|$ the number of edges, and $|V|$ the number of routers. The greedy fractional knapsack matching runs in $\mathcal{O}(n \log n)$ and the Dijkstra path selection in $\mathcal{O}(|E| \log |V|)$; the two stages are independent and sequential, so neither topology nor congestion level affects the complexity class.

SA-RA adds a metaheuristic outer loop, giving $\mathcal{O}(I \cdot n \cdot P(|V|, |E|))$ per consumer, where I is the number of SA iterations and $P(|V|, |E|)$ is the cost of enumerating candidate paths via DFS. On a sparse MST ($|E| = |V| - 1$), path enumeration is manageable. On the dense k-NN graph the number of simple paths grows combinatorially with $|E|$, causing the DFS to explore an exponentially larger search space. This is not a worst-case anomaly but a structural consequence of the algorithm's design.

QGA-RA replaces the DFS path enumeration with a priority-queue shortest-path search ($\mathcal{O}(|E| \log |V|)$ per evaluation), iterated over a population of P_s chromosomes for G generations: $\mathcal{O}(G \cdot P_s \cdot |E| \log |V|)$

Table 7.6: Average Jain Fairness Index by SDR Regime.

Algorithm	**Scenario**	**Low SDR (1,125 h)**	**Normal SDR (62 h)**	**High SDR (1,461 h)**
Grid-Only	All	—	—	—
FKD-RA	S1 Normal/MST	0.6291	0.6310	0.6292
	S2 Stress/MST	0.6291	0.6310	0.6292
	S3 Stress/Dense	0.6028	0.6050	0.6008
	S4 Normal/Dense	0.6028	0.6050	0.6008
SA-RA	S1 Normal/MST	0.6569	0.6570	0.6551
	S2 Stress/MST	0.7429	0.7432	0.7384
	S3 Stress/Dense	0.6974	0.6960	0.6903
	S4 Normal/Dense	0.6381	0.6406	0.6376
QGA-RA	S1 Normal/MST	0.6988	0.6978	0.6942
	S2 Stress/MST	**0.7981**	**0.8008**	**0.7903**
	S3 Stress/Dense	0.7546	0.7514	0.7448
	S4 Normal/Dense	0.6701	0.6681	0.6658
MCF Adaptive	S1 Normal/MST	**0.7923**	**0.7911**	**0.7881**
	S2 Stress/MST	0.7938	0.7884	0.7928
	S3 Stress/Dense	**0.7719**	**0.7675**	**0.7687**
	S4 Normal/Dense	**0.7956**	**0.7930**	**0.7923**

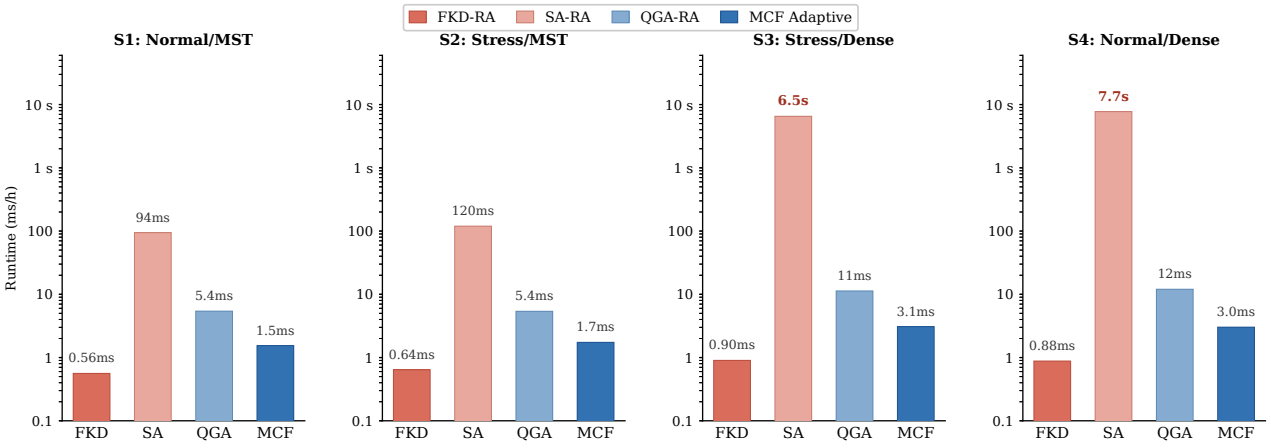

Figure 7.3: Mean execution time per trading hour (ms, log scale) for all four algorithms across the four experimental scenarios.

per hour. This eliminates the combinatorial explosion of SA-RA while retaining heuristic search over the prosumer matching space.

MCF Adaptive reformulates the entire problem as a minimum-cost flow network solved by the network simplex method. The network simplex algorithm runs in $\mathcal{O}(|V| \cdot |E| \cdot \log |V| \cdot \log(|V| \cdot C_{\max}))$, where $C_{\max}$ is the maximum edge capacity [**orlin1997**]. Critically, the network simplex solver operates on a spanning tree basis that grows only linearly with $|V|$, so adding edges to the dense topology does not trigger combinatorial path enumeration. Space requirements are $\mathcal{O}(|V| + |E|)$ for the flow network plus $\mathcal{O}(|E|)$ for the adaptive weight vector, remaining lightweight despite the unified formulation.

7.4.2 Measured execution times

Under MST topology (S1, S2). FKD-RA is the fastest algorithm at 0.56–0.64 ms/h, consistent with its $\mathcal{O}(n \log n + |E| \log |V|)$ complexity and absence of iterative search. MCF Adaptive follows at 1.54–1.74 ms/h despite solving a full network flow problem each hour. QGA-RA averages 5.38–5.42 ms/h due to its population-based evolution. SA-RA is the slowest by a wide margin, averaging 94–120 ms/h, as its DFS path enumeration is already costly on the 11-edge MST.

Effect of topology densification (S3, S4). Moving to the dense k-NN topology reveals a critical scalability failure in SA-RA: its average runtime increases by over 8,000% to 6,518 ms/h in S3 and 7,747 ms/h in S4, with individual peak hours exceeding 90 minutes (95th percentile: 12,847 ms in S3). This collapse confirms the combinatorial DFS analysis above and makes SA-RA entirely impractical for real-time operation in dense networks, despite its competitive cost reduction in S3. QGA-RA roughly doubles to 11–12 ms/h, a moderate increase consistent with the larger graph traversal in the priority-queue path search. FKD-RA increases by only 57% to 0.88–0.90 ms/h. MCF Adaptive increases by 95% to 3.01–3.08 ms/h, remaining stable at sub-5 ms/h across all topologies due to the topology-invariant spanning-tree basis of the network simplex solver.

Table 7.7: Execution Time per Trading Hour (ms) Across All Scenarios (2,648 Hours). Bold values indicate the fastest algorithm per scenario. SA-RA 95th-percentile values are reported in place of the maximum due to extreme outliers caused by DFS path explosion on dense topologies.

Scenario	Algorithm	Mean (ms)	Median (ms)	Std (ms)	95th pct (ms)
S1 Normal/MST	FKD-RA	**0.56**	0.51	0.37	1.10
	SA-RA	94.43	77.80	86.50	197.21
	QGA-RA	5.42	5.19	3.94	10.72
	MCF Adaptive	1.54	1.21	3.08	2.59
S2 Stress/MST	FKD-RA	**0.64**	0.55	0.52	1.43
	SA-RA	119.54	92.24	105.15	301.47
	QGA-RA	5.38	4.50	4.01	12.54
	MCF Adaptive	1.74	1.21	5.11	3.42
S3 Stress/Dense	FKD-RA	**0.90**	0.72	0.67	2.23
	SA-RA	6,517.72	3,868.54	95,195.90	11,731.28
	QGA-RA	11.26	9.73	9.06	24.94
	MCF Adaptive	3.08	2.11	18.25	4.89
S4 Normal/Dense	FKD-RA	**0.88**	0.74	0.58	2.05
	SA-RA	7,746.51	3,732.52	134,041.55	10,245.70
	QGA-RA	11.99	11.27	6.38	23.88
	MCF Adaptive	3.01	2.10	21.65	4.14

All pairwise runtime differences are statistically significant ($p \ll 10^{-10}$, two-sided Wilcoxon signed-rank test, $n = 2{,}648$ paired hours).

Figure 7.3 quantifies the computational cost of each algorithm and exposes the most critical practical limitation of SA-RA. Under MST topology (S1, S2), the four algorithms span roughly two orders of magnitude, from FKD-RA at under 1 ms/h to SA-RA at 94–120 ms/h. Moving to the dense topology (S3, S4) leaves FKD-RA, QGA-RA, and MCF Adaptive largely unchanged, but triggers a catastrophic collapse in SA-RA whose mean runtime jumps to over 6,500 ms/h with a 95th percentile above 11 seconds — making real-time operation impossible. MCF Adaptive remains the most stable algorithm across all scenarios, staying below 5 ms/h regardless of topology, which combined with its leading

performance across energy flow, cost, and fairness makes it the only algorithm simultaneously suitable for all four evaluation dimensions.

Summary. The runtime results confirm and quantify the algorithmic progression narrative of this thesis. FKD-RA is fastest but fails under congestion. SA-RA introduces capacity awareness at the cost of a scalability collapse on dense topologies. QGA-RA resolves this collapse through a quantum-inspired population search while remaining an order of magnitude slower than MCF Adaptive. MCF Adaptive achieves the best performance across energy flow, cost, and fairness while delivering sub-5 ms/h runtime regardless of topology — making it the only algorithm among the four that is simultaneously physically sound, economically efficient, fair, and deployable in real-time operation.

7.5 Discussion

The results across Sections 7.1–7.4 collectively reveal how each successive algorithm in the thesis addresses a specific limitation of its predecessor, and what trade-offs remain.

FKD-RA establishes the baseline: it achieves strong cost reduction under normal conditions (39.3%) but has no mechanism to detect or respond to capacity constraints, causing its total cost to exceed the grid-only baseline under stress ($29,695 vs. $27,067). SA-RA introduces capacity-aware path selection via simulated annealing, successfully containing congestion penalties ($2,852 in S2) — but its DFS-based path enumeration collapses on dense topologies, producing runtimes three to four orders of magnitude above FKD-RA. QGA-RA resolves the scalability issue through quantum-inspired population search, maintaining 11–12 ms/h even on the dense graph, while also introducing an explicit scheduling mechanism that produces the highest fairness under stressed MST conditions (0.7938). MCF Adaptive synthesises all of these capabilities within a single minimum-cost flow formulation: it enforces capacity constraints optimally, minimises transmission losses across all scenarios (167–501 kWh), leads on fairness in three of four scenarios, and does so at 1.5–3.1 ms/h regardless of topology.

Trade-offs and complementary strengths. No algorithm dominates across all dimensions simultaneously. FKD-RA remains the practical choice for resource-constrained embedded hardware where congestion is infrequent: it is the simplest, fastest (<1 ms/h), and achieves equivalent cost reduction to MCF Adaptive under normal conditions. QGA-RA produces the highest fairness specifically under stressed MST topology, through capacity-enforcement-driven redistribution rather than an explicit fairness objective — indicating that tight capacity constraints can act as an implicit fairness mechanism in networks where congestion is the norm. SA-RA achieves statistically equivalent cost reduction to MCF Adaptive under the dense stressed topology (S3), but its runtime renders it impractical for any real-time deployment in dense networks. MCF Adaptive is the only algorithm that performs competitively across all four evaluation dimensions simultaneously.

The findings suggest that the choice of algorithm should be governed by the deployment context. In resource-constrained environments with infrequent congestion, FKD-RA provides 39% cost reduction at sub-millisecond latency. In networks where congestion is frequent but topology is sparse (MST-like), QGA-RA offers a good balance of fairness, capacity awareness, and moderate runtime. For dense, real-world distribution networks operating in real-time, MCF Adaptive is the only viable option among the four, combining physical feasibility, economic efficiency, fairness, and computational tractability in a single unified formulation.

7.6 Conclusion

This chapter presented a unified comparative evaluation of four P2P energy routing algorithms across 2,648 real-world trading hours and four network scenarios, covering energy flow, cost, fairness, and computational tractability. The key findings are as follows.

1. Under normal capacity, all four algorithms achieve 38–39% cost reduction over the grid-only baseline, confirming the economic value of local P2P energy exchange regardless of algorithmic design.

2. MCF Adaptive is the most robust algorithm: it achieves the lowest transmission losses in all scenarios (167–501 kWh), the best cost reduction under stress (28.6% in S2, vs. a cost increase for FKD-RA), the highest fairness in three of four scenarios, and sub-5 ms/h runtime across all topologies.

3. FKD-RA is the only algorithm that fails under congestion, incurring costs above the grid-only baseline in S2 ($29,695 vs. $27,067) by ignoring capacity constraints entirely. It remains the best choice for uncongested, resource-constrained deployments.

4. SA-RA and QGA-RA both enforce capacity-aware volume reduction under stress (SA-RA: −36.8%; QGA-RA: −38.9%), containing congestion penalties substantially below FKD-RA. SA-RA is eliminated as a real-time option in dense networks by its runtime collapse (>6,500 ms/h in S3–S4).

5. QGA-RA achieves the highest fairness under the stressed MST scenario (0.7938 vs. 0.7931 for MCF Adaptive), through scheduling-enforced capacity redistribution rather than an explicit fairness objective.

6. Topology densification has negligible effect on total cost (<0.6% for all algorithms) but reduces absolute transmission losses by 40–46%, confirming that routing path availability primarily affects transmission efficiency rather than market economics under unconstrained capacity.

7. Fairness is stable across SDR regimes within each algorithm-scenario combination (variation <0.005), confirming that trading equity is determined by algorithmic design and network topology rather than the prevailing supply-demand balance.

General Conclusion

This thesis addresses the critical gap between energy routing and peer-to-peer energy trading by developing unified optimization frameworks that simultaneously consider both physical transmission constraints and economic efficiency objectives. Rather than building a comprehensive energy management system, this work focuses on solving the integrated routing-trading problem, which optimizes matching prosumers, selecting transmission paths, and managing congestion while accounting for topology capacity constraints.

We begin by establishing a comprehensive theoretical foundation through an extensive literature review that identifies critical gaps in existing approaches that treat energy routing and P2P trading as independent problems.

In Chapter 3, we present FKD-RA, which formulates the initial solution by modeling prosumer-consumer matching as a fractional knapsack problem solved using greedy algorithms, with path selection based on Dijkstra's algorithm. Trading pairs are determined by jointly considering transmission distance and energy prices, thereby establishing a fundamental sequential optimization framework.

Recognizing the limitations of distance-based routing, Chapter 4 introduces SA-RA, which incorporates power-loss calculations into optimal path determination and solves the producer subset selection problem via SA optimization, demonstrating superior performance under network constraints compared to purely greedy approaches.

To improve solution quality and scalability, and to introduce capacity constraints, Chapter 5 proposes QGA-RA, which employs a modified greedy search algorithm to solve the complex path-selection problem while accounting for network parameters and power loss. A quantum genetic algorithm is employed for prosumer pairing to minimize simultaneous power loss and total cost, significantly reducing search time while maximizing profits for both consumers and producers. A dynamic scheduling method is implemented to reduce congestion, prevent collisions, and introduce fairness and reliability into the system.

To address the high complexity of heuristic algorithms and to enhance scalability, Chapter 6 presents our final contribution: Adaptive MCF, which fundamentally departs from the staged approaches of Chapters 3–5. This unified framework employs MCF with Mirror Descent online learning to simultaneously optimize prosumer-consumer matching, loss-minimal path selection, congestion avoidance, and fairness without requiring manual parameter tuning. We summarized our contributions in Figure 7.4.

Limitations

Despite the comprehensive approach, this research acknowledges certain limitations that present opportunities for future work:

- The Ausgrid dataset (2012–2013) may not fully reflect current solar technology efficiency and pricing structures. Validation on contemporary datasets from diverse geographic regions would strengthen generalizability.
- The synthetic MST and k-NN topologies, while physically plausible, do not capture proprietary real distribution network constraints such as voltage limits, transformer capacities, and protection coordination requirements.

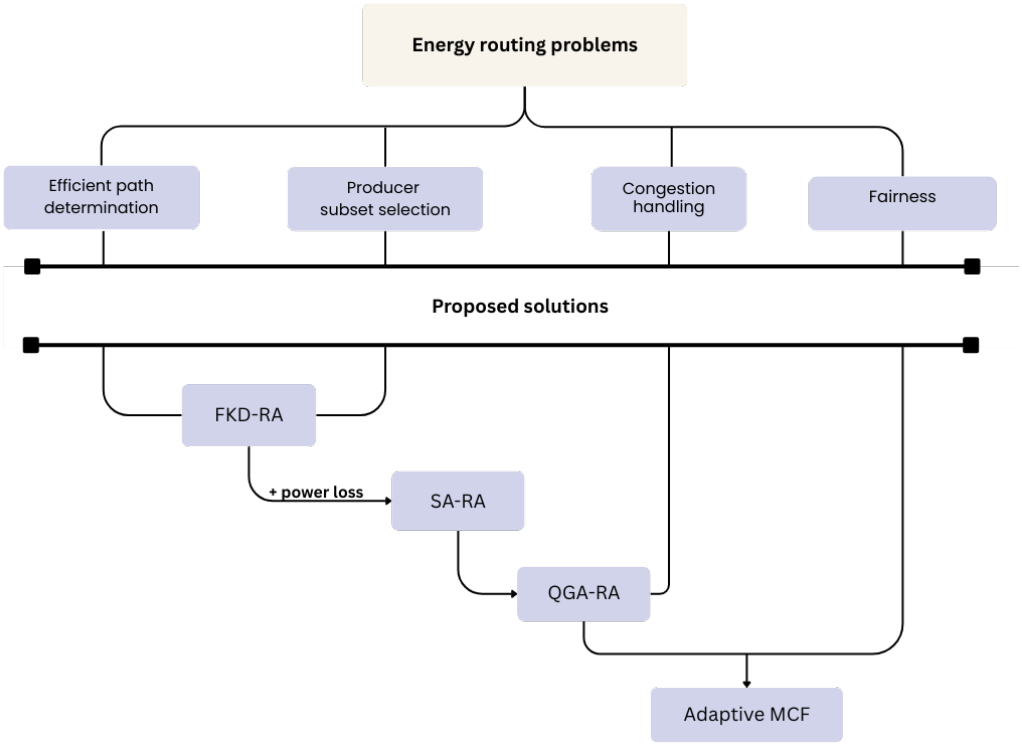

Figure 7.4: Overview of energy routing problems and proposed solutions.

- The research focuses on technical and economic aspects, while practical implementation requires addressing regulatory barriers, privacy concerns, liability frameworks, and market design policies not covered in this work.

Future Research Directions

Despite the substantial advances achieved in this thesis, several promising directions remain for future investigation:

- Extending our framework to incorporate battery storage systems and electric vehicle fleets as flexible resources that can shift energy temporally, not just spatially.
- Developing chance-constrained or robust algorithm formulations that explicitly account for renewable generation and demand forecast uncertainty.
- Integrating differential privacy, secure multi-party computation, or blockchain-based smart contracts to protect sensitive household energy data while enabling market operation.
- Conducting controlled field trials in operational microgrids to validate theoretical findings under real hardware constraints, communication latency, and regulatory environments.

List of Publications

Journal Articles

- Published, 30 September 2025 Nacef, A., Mechta, D., Benchikh, L., Louail, L., Harous, S., Belmahdi, A. "A Quantum Genetic-based Routing Protocol for Real-Time Peer-to-Peer Energy Transactions", Journal of Cluster Computing.
- Published, 10 October 2024 Nacef, A., Mechta, D., Louail, L., & Harous, S. "Advancements in Optimization Strategies for Energy Routing, Demand Response, and Load Forecasting in Energy Internet and Smart Grid: An Overview."
- Submitted Nacef, A., Benchikh, L., Mechta, D., Louail, L., & Harous, S. "Adaptive Multi-Commodity Flow Optimization for Peer-to-Peer Energy Trading in the Energy Internet".

Conference Articles

- Nacef, A., Mechta, D., Louail, L., & Benchikh, L. (2023, September). Efficient energy routing in smart grid networks using fractional knapsack and dijkstra algorithm. In 2023 International Conference on Decision Aid Sciences and Applications (DASA) (pp. 565–569). IEEE.
- Nacef, A., Mechta, D., Louail, L., & Harous, S. (2023, December). Genetic algorithm-based path selection for power-efficient energy routing in smart grids and energy internet. In 2023 2nd International Engineering Conference on Electrical, Energy, and Artificial Intelligence (EICEEAI) (pp. 1–6). IEEE.
- Nacef, A., Louail, L., Mechta, D., Benchikh, L., & Harous, S. (2023, November). Simulated annealing for optimal path selection and scheduling in energy routing for smart grids. In 2023 International Conference on Computer and Applications (ICCA) (pp. 1–5). IEEE.
- Nacef, A., Mechta, D., Benchikh, L., Louail, L., & Berchi, R. (2025, May). Optimized Producer Subset Determination for Energy Routing in Smart Grids. In 2025 3rd International Conference on Electronics, Energy and Measurement (IC2EM) (pp. 1–6). IEEE.

Bibliography

[1] Ruhi Dharmendra Dalal. "AI And Energy Demand: Trends, Impacts, And Solutions". In: *Journal of Software Engineering and Simulation* (2025). DOI: 10.35629/3795-11070108.

[2] Satyam Chauhan. "The Growing Energy Demand of Data Centers: Impacts of AI and Cloud Computing". In: *International Journal For Multidisciplinary Research* (2024). DOI: 10.36948/ijfmr.2024.v06i04.26591.

[3] Yayu Yang et al. "Toward 100% Renewable Power Grids: A Review". In: *IEEE Access* 13 (2025), pp. 69690–69704. DOI: 10.1109/access.2025.3558772.

[4] M. Khalid. "Smart grids and renewable energy systems: Perspectives and grid integration challenges". In: *Energy Strategy Reviews* (2024). DOI: 10.1016/j.esr.2024.101299.

[5] Xuesong Zhou, Fuzhi Wang, and Youjie Ma. "An overview on energy internet". In: *2015 IEEE International Conference on Mechatronics and Automation (ICMA)*. IEEE. 2015, pp. 126–131.

[6] F. Abrahamsen, Y. Ai, and M. Cheffena. "Communication Technologies for Smart Grid: A Comprehensive Survey". In: *Sensors (Basel, Switzerland)* 21 (2021). DOI: 10.3390/s21238087.

[7] Huaguang Zhang et al. "Distributed optimal energy management for energy internet". In: *IEEE Transactions on Industrial Informatics* 13.6 (2017), pp. 3081–3097.

[8] Kirsi Kotilainen et al. "Prosumer centric digital energy ecosystem framework". In: *Proceedings of the 8th international conference on Management of Digital EcoSystems*. 2016, pp. 47–51.

[9] Amani Fawaz et al. "Energy routing protocols for Energy Internet: A review on multi-agent systems, metaheuristics, and Artificial Intelligence approaches". In: *IEEE Access* (2025).

[10] S. Talari et al. "Mechanism design for decentralized peer-to-peer energy trading considering heterogeneous preferences". In: *Sustainable Cities and Society* (2022). DOI: 10.1016/j.scs.2022.104182.

[11] Assala Nacef et al. "Advancements in optimization strategies for energy routing, demand response, and load forecasting in energy internet and smart grid: an overview". In: *Energy efficiency* 18.7 (2025), pp. 1–42.

[12] T. Chirwa and N. Odhiambo. "Electricity consumption and economic growth". In: *International Journal of Energy Sector Management* (2019). DOI: 10.1108/IJESM-11-2018-0014.

[13] Ying Wu et al. "Digitalization and decentralization driving transactive energy Internet: Key technologies and infrastructures". In: *International Journal of Electrical Power & Energy Systems* 126 (2021), p. 106593. ISSN: 0142-0615. DOI: https://doi.org/10.1016/j.ijepes.2020.106593. URL: https://www.sciencedirect.com/science/article/pii/S0142061520328210.

[14] Massoud Amin and John Stringer. "The Electric Power Grid: Today and Tomorrow". In: *MRS Bulletin* 33.4 (2008), 399–407. DOI: 10.1557/mrs2008.80.

[15] Assala Nacef et al. "Efficient Energy Routing in Smart Grid Networks Using Fractional Knapsack and Dijkstra Algorithm". In: *2023 International Conference on Decision Aid Sciences and Applications (DASA)*. 2023, pp. 565–569. DOI: 10.1109/DASA59624.2023.10286736.

[16] Bilal Naji Alhasnawi et al. "A Novel Internet of Energy Based Optimal Multi-Agent Control Scheme for Microgrid including Renewable Energy Resources". In: *International Journal of Environmental Research and Public Health* 18.15 (2021). ISSN: 1660-4601. DOI: 10.3390/ijerph18158146. URL: https://www.mdpi.com/1660-4601/18/15/8146.

[17] Lina Benchikh, Lemia Louail, and Djamila Mechta. "A survey on energy routing approaches in energy internet". In: *Energy Systems* (2024), pp. 1–38.

[18] The Economist. *Building the energy internet*. Accessed on March 13, 2004. 2004. URL: https://www.economist.com/technology-quarterly/2004/03/13/building-the-energy-internet.

[19] LH Tsoukalas and R Gao. "From smart grids to an energy internet: Assumptions, architectures and requirements". In: *2008 Third international conference on electric utility deregulation and restructuring and power technologies*. IEEE. 2008, pp. 94–98.

[20] Alex Q. Huang et al. "The Future Renewable Electric Energy Delivery and Management (FREEDM) System: The Energy Internet". In: *Proceedings of the IEEE* 99.1 (2011), pp. 133–148. DOI: 10.1109/JPROC.2010.2081330.

[21] Sean Davies. "Internet of energy". In: *Engineering & Technology* 5.16 (2010), pp. 42–45. DOI: 10.1049/et.2010.1608.

[22] Tongdan Jin and Mahmoud Mechehoul. "Ordering Electricity via Internet and its Potentials for Smart Grid Systems". In: *IEEE Transactions on Smart Grid* 1.3 (2010), pp. 302–310. DOI: 10.1109/TSG.2010.2072995.

[23] Yi Xu et al. "Energy router: Architectures and functionalities toward Energy Internet". In: *2011 IEEE International Conference on Smart Grid Communications (SmartGridComm)*. 2011, pp. 31–36. DOI: 10.1109/SmartGridComm.2011.6102340.

[24] Wencong Su and Alex Q. Huang. "Proposing a electricity market framework for the Energy Internet". In: *2013 IEEE Power & Energy Society General Meeting*. 2013, pp. 1–5. DOI: 10.1109/PESMG.2013.6672224.

[25] Miltiadis Alamaniotis and Lefteri H. Tsoukalas. "Layered-based approach to virtual storage for smart power systems". In: *IISA 2013*. 2013, pp. 1–6. DOI: 10.1109/IISA.2013.6623732.

[26] Felix F. Wu, Pravin P. Varaiya, and Ron S.Y. Hui. "Smart Grids with Intelligent Periphery: An Architecture for the Energy Internet". In: *Engineering* 1.4 (2015), pp. 436–446. ISSN: 2095-8099. DOI: https://doi.org/10.15302/J-ENG-2015111. URL: https://www.sciencedirect.com/science/article/pii/S2095809916300248.

[27] Kaile Zhou, Shanlin Yang, and Zhen Shao. "Energy Internet: The business perspective". In: *Applied Energy* 178 (2016), pp. 212–222. ISSN: 0306-2619. DOI: https://doi.org/10.1016/j.apenergy.2016.06.052. URL: https://www.sciencedirect.com/science/article/pii/S0306261916308273.

[28] Y. R. Kafle et al. "Towards an internet of energy". In: *2016 IEEE International Conference on Power System Technology (POWERCON)*. 2016, pp. 1–6. DOI: 10.1109/POWERCON.2016.7754036.

[29] Dan Wang et al. "Review of key problems related to integrated energy distribution systems". In: *CSEE Journal of Power and Energy Systems* 4.2 (2018), pp. 130–145. DOI: 10.17775/CSEEJPES.2018.00570.

[30] Kun Wang et al. "A Survey on Energy Internet: Architecture, Approach, and Emerging Technologies". In: *IEEE Systems Journal* 12.3 (2018), pp. 2403–2416. DOI: 10.1109/JSYST.2016.2639820.

[31] Bernd Reifenhaeuser and Andreas Sumper. "13 - Quantum Grid: A packet-based power approach". In: *The Energy Internet*. Ed. by Wencong Su and Alex Q. Huang. Woodhead Publishing, 2019, pp. 283–314. ISBN: 978-0-08-102207-8. DOI: 10.1016/B978-0-08-102207-8.00013-8. URL: https://www.sciencedirect.com/science/article/pii/B9780081022078000138.

[32] DKE German Commission for Electrical, Electronic & Information Technologies. *E-Energy/Smart Grids 2.0 Standardization Roadmap*. https://www.dke.de/en/areas-of-work/energy/german-standardization-roadmap-e-energy-smart-grids-2-0. Accessed: 2024-05-18. 2024.

[33] Rikiya Abe, Hisao Taoka, and David McQuilkin. "Digital Grid: Communicative Electrical Grids of the Future". In: *IEEE Transactions on Smart Grid* 2.2 (2011), pp. 399–410. DOI: 10.1109/TSG.2011.2132744.

[34] Celestine Iwendi and Gai-Ge Wang. "Combined power generation and electricity storage device using deep learning and internet of things technologies". In: *Energy Reports* 8 (2022), pp. 5016–5025. ISSN: 2352-4847. DOI: https://doi.org/10.1016/j.egyr.2022.02.304. URL: https://www.sciencedirect.com/science/article/pii/S2352484722005510.

[35] Xiaotong Ji et al. "A novel graph theory based two-stage minimum cost routing mechanism in energy internet". In: *International Journal of Electrical Power & Energy Systems* 142 (2022), p. 108346. ISSN: 0142-0615. DOI: https://doi.org/10.1016/j.ijepes.2022.108346. URL: https://www.sciencedirect.com/science/article/pii/S0142061522003659.

[36] Martin Geidl and Goran Andersson. "A modeling and optimization approach for multiple energy carrier power flow". In: *2005 IEEE Russia Power Tech*. 2005, pp. 1–7. DOI: 10.1109/PTC.2005.4524640.

[37] Hafiz Majid Hussain et al. "What is Energy Internet? Concepts, Technologies, and Future Directions". In: *IEEE Access* 8 (2020), pp. 183127–183145. DOI: 10.1109/ACCESS.2020.3029251.

[38] L. C. Xin et al. "Design and application of energy router to realise Energy Internet". In: *10th International Conference on Advances in Power System Control, Operation & Management (APSCOM 2015)*. 2015, pp. 1–6. DOI: 10.1049/ic.2015.0225.

[39] A. Cagnano, E. D. Tuglie, and P. Mancarella. "Microgrids: Overview and guidelines for practical implementations and operation". In: *Applied Energy* (2020). DOI: 10.1016/j.apenergy.2019.114039.

[40] Assala Nacef, Khadidja Medani, and Zibouda Aliouat. "Energy Efficient Bio-Inspired Clustering in Flying Ad-Hoc Network". In: *2023 International Conference on Networking and Advanced Systems (ICNAS)*. IEEE. 2023, pp. 1–6.

[41] M. Rahman et al. "Formal Synthesis of Trajectories for Unmanned Aerial Vehicles to Perform Resilient Surveillance of Critical Power Transmission Lines". In: *2020 25th International Conference on Engineering of Complex Computer Systems (ICECCS)* (2020), pp. 103–112. DOI: 10.1109/ICECCS51672.2020.00019.

[42] Zhenyu Zhou et al. "Energy-Efficient Industrial Internet of UAVs for Power Line Inspection in Smart Grid". In: *IEEE Transactions on Industrial Informatics* 14 (2018), pp. 2705–2714. DOI: 10.1109/TII.2018.2794320.

[43] G. Gaggero et al. "A Possible Smart Metering System Evolution for Rural and Remote Areas Employing Unmanned Aerial Vehicles and Internet of Things in Smart Grids". In: *Sensors (Basel, Switzerland)* 21 (2021). DOI: 10.3390/s21051627.

[44] Khaled Osmani and D. Schulz. "Comprehensive Investigation of Unmanned Aerial Vehicles (UAVs): An In-Depth Analysis of Avionics Systems". In: *Sensors (Basel, Switzerland)* 24 (2024). DOI: 10.3390/s24103064.

[45] Jianwei Wei et al. "A User Association and Resource Allocation Algorithm for UAV-Assisted Smart Grid". In: *Sensors (Basel, Switzerland)* 24 (2024). DOI: 10.3390/s24248195.

[46] Amartya Mukherjee et al. "iGridEdgeDrone: Hybrid mobility aware intelligent load forecasting by edge enabled Internet of Drone Things for smart grid networks". In: *International Journal of Parallel Programming* 49.3 (2021), pp. 285–325.

[47] Chengang Tanlei. "Blockchain 2.0[M]". In: *Beijing Industrial Press* (2015).

[48] Xin Sun et al. “Research on the Application of Blockchain Technology in Energy Internet”. In: *2018 2nd IEEE Conference on Energy Internet and Energy System Integration (EI2)*. 2018, pp. 1–6. DOI: 10.1109/EI2.2018.8582599.

[49] Bilal Naji Alhasnawi et al. “A new communication platform for smart EMS using a mixed-integer-linear-programming”. In: *Energy Systems* (2023), pp. 1–18.

[50] Michael Grieves. “Digital twin: manufacturing excellence through virtual factory replication”. In: *White paper* 1.2014 (2014), pp. 1–7.

[51] Mohd Javaid, Abid Haleem, and Rajiv Suman. “Digital Twin applications toward Industry 4.0: A Review”. In: *Cognitive Robotics* 3 (2023), pp. 71–92. ISSN: 2667-2413. DOI: https://doi.org/10.1016/j.cogr.2023.04.003. URL: https://www.sciencedirect.com/science/article/pii/S2667241323000137.

[52] Wei Yu et al. “Energy digital twin technology for industrial energy management: Classification, challenges and future”. In: *Renewable and Sustainable Energy Reviews* 161 (2022), p. 112407.

[53] Mou Mahmood et al. “Impacts of digitalization on smart grids, renewable energy, and demand response: An updated review of current applications”. In: *Energy Conversion and Management: X* 24 (2024), p. 100790. ISSN: 2590-1745. DOI: https://doi.org/10.1016/j.ecmx.2024.100790. URL: https://www.sciencedirect.com/science/article/pii/S259017452400268X.

[54] Hani Muhsen et al. “Business Model of Peer-to-Peer Energy Trading: A Review of Literature”. In: *Sustainability* 14.3 (2022). ISSN: 2071-1050. DOI: 10.3390/su14031616. URL: https://www.mdpi.com/2071-1050/14/3/1616.

[55] Dijo P. Koottappillil et al. “Distribution of renewable energy through the energy internet: A routing algorithm for energy routers”. In: *Energy Reports* 8 (2022). Selected papers from 2022 7th International Conference on Advances on Clean Energy Research, pp. 355–363. ISSN: 2352-4847. DOI: https://doi.org/10.1016/j.egyr.2022.10.201. URL: https://www.sciencedirect.com/science/article/pii/S2352484722021370.

[56] Bilal Naji Alhasnawi et al. “A new methodology for reducing carbon emissions using multi-renewable energy systems and artificial intelligence”. In: *Sustainable Cities and Society* 114 (2024), p. 105721.

[57] Jiayu Bai et al. “Two-timescale coordinated operation of wind-advanced adiabatic compressed air energy storage system: A bilevel stochastic dynamic programming method”. In: *Journal of Energy Storage* 67 (2023), p. 107502. ISSN: 2352-152X. DOI: https://doi.org/10.1016/j.est.2023.107502. URL: https://www.sciencedirect.com/science/article/pii/S2352152X2300899X.

[58] Yaxi Pan and Jian Dong. “Design and Optimization of an Ultrathin and Broadband Polarization-Insensitive Fractal FSS Using the Improved Bacteria Foraging Optimization Algorithm and Curve Fitting”. In: *Nanomaterials* 13.1 (2023). ISSN: 2079-4991. DOI: 10.3390/nano13010191. URL: https://www.mdpi.com/2079-4991/13/1/191.

[59] Guillermo Alonso et al. “Enhanced Artificial Immune Systems and Fuzzy Logic for Active Distribution Systems Reconfiguration”. In: *Energies* 15.24 (2022). ISSN: 1996-1073. DOI: 10.3390/en15249419. URL: https://www.mdpi.com/1996-1073/15/24/9419.

[60] Bilal Naji Alhasnawi, Marek Zanker, and Vladimír Bureš. “A smart electricity markets for a decarbonized microgrid system”. In: *Electrical Engineering* (2024), pp. 1–21.

[61] Mohammad Safayet Hossain and Hisham Mahmood. “Intelligent Energy Management of a Microgrid Using Reinforcement Learning”. In: *2024 IEEE Power & Energy Society General Meeting (PESGM)*. 2024, pp. 1–5. DOI: 10.1109/PESGM51994.2024.10689163.

[62] Sara Hebal et al. “Hybrid energy routing approach for energy internet”. In: *Energies* 14.9 (2021), p. 2579.

[63] Lina Benchikh, Lemia Louail, and Djamila Mechta. “Subscriber matching in energy internet using the firefly algorithm”. In: *Proceedings of the Second International Conference on Innovations in Computing Research (ICR’23)*. Springer. 2023, pp. 418–432.

[64] Amani Fawaz, Imad Mougharbel, and Hadi Y. Kanaan. "New Routing Application Using Bees Colony for Energy Internet". In: *2022 3rd International Conference on Smart Grid and Renewable Energy (SGRE)*. 2022, pp. 1–8. DOI: 10.1109/SGRE53517.2022.9774114.

[65] Ruichi Wang et al. "A Graph Theory Based Energy Routing Algorithm in Energy Local Area Network". In: *IEEE Transactions on Industrial Informatics* 13.6 (2017), pp. 3275–3285. DOI: 10.1109/TII.2017.2713040.

[66] Xiaoying Shi, Yinliang Xu, and Hongbin Sun. "A biased min-consensus-based approach for optimal power transaction in multi-energy-router systems". In: *IEEE Transactions on Sustainable Energy* 11.1 (2018), pp. 217–228.

[67] Juhar Abdella, Khaled Shuaib, and Saad Harous. "Energy Routing Algorithms for the Energy Internet". In: *2018 International Conference on Intelligent Systems (IS)*. 2018, pp. 80–86. DOI: 10.1109/IS.2018.8710585.

[68] Luxin Zhang, Eric C. Kerrigan, and Bikash C. Pal. "Optimal Communication Scheduling in the Smart Grid". In: *IEEE Transactions on Industrial Informatics* 15.9 (2019), pp. 5257–5265. DOI: 10.1109/TII.2019.2915051.

[69] Naqash Ahmad et al. "Load Forecasting Techniques for Power System: Research Challenges and Survey". In: *IEEE Access* 10 (2022), pp. 71054–71090. DOI: 10.1109/ACCESS.2022.3187839.

[70] Xudong Pang et al. "Construction of smart grid load forecast model by edge computing". In: *Energies* 15.9 (2022), p. 3028.

[71] Ai-Xia Wang and Jing-Jiao Li. "A novel cloud-edge collaboration based short-term load forecasting method for smart grid". In: *Frontiers in Energy Research* 10 (2022), p. 977026.

[72] Qi Liu et al. "A spatio-temporal graph convolutional approach to real-time load forecasting in an edge-enabled distributed Internet of Smart Grids energy system". In: *Concurrency and Computation: Practice and Experience* 36.13 (2024), e8060.

[73] Yixing Liu et al. "FedForecast: A federated learning framework for short-term probabilistic individual load forecasting in smart grid". In: *International Journal of Electrical Power & Energy Systems* 152 (2023), p. 109172.

[74] Mohamad Moussa et al. "Towards a Scalable Compute Continuum Platform Applied to Electrical Energy Forecasting". In: *European Conference on Parallel Processing*. Springer. 2023, pp. 68–80.

[75] Amartya Mukherjee et al. "Lightweight sustainable intelligent load forecasting platform for smart grid applications". In: *Sustainable Computing: Informatics and Systems* 25 (2020), p. 100356.

[76] Vasileios Pentsos et al. "A Hybrid LSTM-Transformer Model for Power Load Forecasting". In: *IEEE Transactions on Smart Grid* 16.3 (2025), pp. 2624–2634. DOI: 10.1109/TSG.2025.3535407.

[77] Kaleem Ullah et al. "Hybrid BiGRU-CNN Model for Load Forecasting in Smart Grids with High Renewable Energy Integration". In: *IET Generation, Transmission & Distribution* 19.1 (2025), e70060.

[78] Xinyu Wen et al. "Deep learning-driven hybrid model for short-term load forecasting and smart grid information management". In: *Scientific reports* 14.1 (2024), p. 13720.

[79] Mashael M Asiri et al. "Short-term load forecasting in smart grids using hybrid deep learning". In: *IEEE Access* 12 (2024), pp. 23504–23513.

[80] Heng-Yi Su and Chia-Ching Lai. "Toward Improved Load Forecasting in Smart Grids: A Robust Deep Ensemble Learning Framework". In: *IEEE Transactions on Smart Grid* 15.4 (2024), pp. 4292–4296. DOI: 10.1109/TSG.2024.3402011.

[81] Abdul Azeem et al. "Mitigating concept drift challenges in evolving smart grids: An adaptive ensemble LSTM for enhanced load forecasting". In: *Energy Reports* 13 (2025), pp. 1369–1383.

[82] N. Giamarelos et al. "A Machine Learning Model Ensemble for Mixed Power Load Forecasting across Multiple Time Horizons". In: *Sensors (Basel, Switzerland)* 23 (2023). DOI: 10.3390/s23125436.

[83] Jiang Yanmei et al. "Enhanced neighborhood node graph neural networks for load forecasting in smart grid". In: *International journal of machine learning and cybernetics* 15.1 (2024), pp. 129–148.

[84] Ratun Rahman, Neeraj Kumar, and Dinh C. Nguyen. "Electrical Load Forecasting in Smart Grid: A Personalized Federated Learning Approach". In: *2025 IEEE 22nd Consumer Communications & Networking Conference (CCNC)*. 2025, pp. 1–2. DOI: 10.1109/CCNC54725.2025.10976072.

[85] Mohamed I. Ibrahem et al. "Privacy-preserving, Lightweight, and Decentralized Load Forecasting in Smart Grid AMI Networks". In: *ICC 2024 - IEEE International Conference on Communications*. 2024, pp. 2222–2227. DOI: 10.1109/ICC51166.2024.10622466.

[86] Muhammad Yasir Masood et al. "Demand-side load forecasting in smart grids using machine learning techniques". In: *PeerJ Computer Science* 10 (2024), e1987.

[87] Georgios Tsoumplekas et al. "Few-Shot Load Forecasting Under Data Scarcity in Smart Grids: A Meta-Learning Approach". In: *Energies* 18.3 (2025). ISSN: 1996-1073. DOI: 10.3390/en18030742. URL: https://www.mdpi.com/1996-1073/18/3/742.

[88] S. Aslam et al. "Towards Electric Price and Load Forecasting Using CNN-Based Ensembler in Smart Grid". In: *Sustainability* (2021). DOI: 10.3390/su132212653.

[89] Tanveer Ahmad and Huanxin Chen. "Potential of three variant machine-learning models for forecasting district level medium-term and long-term energy demand in smart grid environment". In: *Energy* 160 (2018), pp. 1008–1020. ISSN: 0360-5442. DOI: https://doi.org/10.1016/j.energy.2018.07.084. URL: https://www.sciencedirect.com/science/article/pii/S0360544218313811.

[90] Peng Liu et al. "A New Multi-Scale Model for Medium-Term Load Forecasting". In: *2023 35th Chinese Control and Decision Conference (CCDC)* (2023), pp. 1014–1019. DOI: 10.1109/CCDC58219.2023.10326981.

[91] Zeyu Wang et al. "Hierarchical parameter optimization based support vector regression for power load forecasting". In: *Sustainable Cities and Society* (2021), p. 102937. DOI: 10.1016/J.SCS.2021.102937.

[92] N. Shirzadi et al. "Medium-Term Regional Electricity Load Forecasting through Machine Learning and Deep Learning". In: *Designs* 5 (2021), p. 27. DOI: 10.3390/DESIGNS5020027.

[93] Saikat Gochhait, Deepak K. Sharma, and Mrinal Bachute. "Comparative Long-Term Electricity Forecasting Analysis: A Case Study of Load Dispatch Centres in India". In: *Iraqi Journal for Electrical and Electronic Engineering* (2024). DOI: 10.37917/ijeee.20.2.17.

[94] Xianghao Zhan et al. "Reliable Long-Term Energy Load Trend Prediction Model for Smart Grid Using Hierarchical Decomposition Self-Attention Network". In: *IEEE Transactions on Reliability* 72 (2023), pp. 609–621. DOI: 10.1109/TR.2022.3174093.

[95] J. Jasmine, M. Germin Nisha, and Rajesh Prasad. "Enhancing smart grid reliability with advanced load forecasting using deep learning". In: *Electrical Engineering* (2025). DOI: 10.1007/s00202-024-02946-z.

[96] Vikash Kumar and R. Mandal. "Long-term load forecasting for Smart Grid". In: *Engineering Research Express* (2024). DOI: 10.1088/2631-8695/ad8f92.

[97] Renzhi Lu and Seung Ho Hong. "Incentive-based demand response for smart grid with reinforcement learning and deep neural network". In: *Applied Energy* 236 (2019), pp. 937–949. ISSN: 0306-2619. DOI: https://doi.org/10.1016/j.apenergy.2018.12.061. URL: https://www.sciencedirect.com/science/article/pii/S0306261918318798.

[98] A. Rezaee Jordehi. "Optimisation of demand response in electric power systems, a review". In: *Renewable and Sustainable Energy Reviews* 103 (2019), pp. 308–319. ISSN: 1364-0321. DOI: https://doi.org/10.1016/j.rser.2018.12.054. URL: https://www.sciencedirect.com/science/article/pii/S1364032118308566.

[99] Cunbin Li et al. "A microgrids energy management model based on multi-agent system using adaptive weight and chaotic search particle swarm optimization considering demand response". In: *Journal of Cleaner Production* 262 (2020), p. 121247. ISSN: 0959-6526. DOI: https://doi.org/10.1016/j.jclepro.2020.121247. URL: https://www.sciencedirect.com/science/article/pii/S0959652620312944.

[100] Bergrivier Municipality. *What is the Smart Grid?* https://bvm.gov.za/wp-content/uploads/2020/08/Focus-on-Finance-Inclining-Block-Tariff-Explanation-Final-Version.pdf. 2020.

[101] Bilal Naji Alhasnawi et al. "A novel efficient energy optimization in smart urban buildings based on optimal demand side management". In: *Energy Strategy Reviews* 54 (2024), p. 101461.

[102] Fei Wang et al. "Household profile identification for behavioral demand response: A semi-supervised learning approach using smart meter data". In: *Energy* 238 (2022), p. 121728. ISSN: 0360-5442. DOI: https://doi.org/10.1016/j.energy.2021.121728. URL: https://www.sciencedirect.com/science/article/pii/S0360544221019769.

[103] Reza Razi et al. "A Novel Graph-based Routing Algorithm in Residential Multi-Microgrid Systems". In: *IEEE Transactions on Industrial Informatics* PP (May 2020), pp. 1–1. DOI: 10.1109/TII.2020.2997516.

[104] Hui Guo et al. "An energy routing algorithm based on power transaction in energy internet". In: *2018 IEEE Energy Conversion Congress and Exposition (ECCE)*. IEEE. 2018, pp. 54–59.

[105] Hui Guo et al. "Graph Theory Based Topology Design and Energy Routing Control of the Energy Internet". In: *IET Generation, Transmission & Distribution* 12 (Sept. 2018). DOI: 10.1049/iet-gtd.2018.6238.

[106] SM Suhail Hussain et al. "Optimal energy routing in microgrids with IEC 61850 based energy routers". In: *IEEE Transactions on Industrial Electronics* 67.6 (2019), pp. 5161–5169.

[107] Jie Lin et al. "On distributed energy routing protocols in the smart grid". In: *Software engineering, artificial intelligence, networking and parallel/distributed computing*. Springer. 2013, pp. 143–159.

[108] Yuanhui Wang and Yan Zhang. "Energy routing strategy based on minimum loss and transaction price". In: *2022 41st Chinese Control Conference (CCC)*. IEEE. 2022, pp. 6073–6078.

[109] Xingyue Jiang et al. "Semi-decentralized energy routing algorithm for minimum-loss transmission in community energy internet". In: *International Journal of Electrical Power & Energy Systems* 135 (2022), p. 107547.

[110] Neethu Maya, Narasimman Sundararajan, and Suresh Sundaram. "An Optimal Multi-Path Power Routing and Transmission Scheduling Approach for Peer-to-Peer Power Trading in Energy Internet". In: *2024 IEEE International Conference on Systems, Man, and Cybernetics (SMC)*. 2024, pp. 2447–2452. DOI: 10.1109/SMC54092.2024.10831946.

[111] Haochen Hua et al. "Carbon Emission Flow Based Energy Routing Strategy in Energy Internet". In: *IEEE Transactions on Industrial Informatics* 20.3 (2024), pp. 3974–3985. DOI: 10.1109/TII.2023.3316183.

[112] Yunfei Du et al. "Energy router based minimum loss cost routing strategy in energy internet". In: *2020 IEEE 1st China International Youth Conference on Electrical Engineering (CIYCEE)*. 2020, pp. 1–6. DOI: 10.1109/CIYCEE49808.2020.9332577.

[113] Tarek AlSkaif et al. "Blockchain-Based Fully Peer-to-Peer Energy Trading Strategies for Residential Energy Systems". In: *IEEE Transactions on Industrial Informatics* 18.1 (2022), pp. 231–241. DOI: 10.1109/TII.2021.3077008.

[114] Hui Guo et al. "A minimum loss routing algorithm based on real-time transaction in energy internet". In: *IEEE Transactions on Industrial Informatics* 15.12 (2019), pp. 6446–6456.

[115] Xingyue Jiang et al. "Peer-to-peer energy trading in energy local area network considering decentralized energy routing". In: *Sustainable Energy, Grids and Networks* 34 (2023), p. 100994. ISSN: 2352-4677. DOI: https://doi.org/10.1016/j.segan.2023.100994. URL: https://www.sciencedirect.com/science/article/pii/S2352467723000024.

[116] Neethu Maya, Narasimman Sundararajan, and Suresh Sundaram. "A Genetic Algorithm based Deterministic Multi-step Peer-to-Peer Power Routing for Energy Internet in Sparsely Connected Microgrid Communities". In: *2025 IEEE Symposia on Computational Intelligence for Energy, Transport and Environmental Sustainability (CIETES)*. 2025, pp. 1–6. DOI: 10.1109/CIETES63869.2025.10995137.

[117] Hamza El Hafdaoui and Ahmed Khallaayoun. "Internet of energy (IoE) adoption for a secure semi-decentralized renewable energy distribution". In: *Sustainable Energy Technologies and Assessments* 57 (2023), p. 103307. ISSN: 2213-1388. DOI: https://doi.org/10.1016/j.seta.2023.103307. URL: https://www.sciencedirect.com/science/article/pii/S2213138823003004.

[118] Artiom Blinovas et al. "A Game Theoretic Approach for Cost-Effective Management of Energy Harvesting Smart Grids". In: *2022 International Wireless Communications and Mobile Computing (IWCMC)*. 2022, pp. 18–23. DOI: 10.1109/IWCMC55113.2022.9825181.

[119] June Hong and Mihui Kim. "Game-Theory-Based Approach for Energy Routing in a Smart Grid Network". In: *Journal of Computer Networks and Communications* 2016 (Jan. 2016), pp. 1–8. DOI: 10.1155/2016/4761720.

[120] Xingyue Jiang et al. "Decentralized local energy trading with cooperative energy routing in energy local area network". In: *International Journal of Electrical Power & Energy Systems* 152 (2023), p. 109209. ISSN: 0142-0615. DOI: https://doi.org/10.1016/j.ijepes.2023.109209. URL: https://www.sciencedirect.com/science/article/pii/S0142061523002661.

[121] Sara Hebal, Djamila Mechta, and Saad Harous. "Aco-based distributed energy routing protocol in smart grid". In: *2019 IEEE 10th Annual Ubiquitous Computing, Electronics & Mobile Communication Conference (UEMCON)*. IEEE. 2019, pp. 0568–0571.

[122] Sara Hebal, Saad Harous, and Djamila Mechta. "Latency and energy transmission cost optimization using bco-aware energy routing for smart grid". In: *2020 International Wireless Communications and Mobile Computing (IWCMC)*. IEEE. 2020, pp. 1170–1175.

[123] Sara Hebal, Saad Harous, and Djamila Mechta. "Solving energy routing problem in energy internet using a discrete artificial bee colony algorithm". In: *2022 International Wireless Communications and Mobile Computing (IWCMC)*. IEEE. 2022, pp. 641–646.

[124] Djamila Mechta, Saad Harous, and Sara Hebal. "Energy-efficient path-aware routing Protocol based on PSO for Smart Grids". In: *2020 IEEE International Conference on Electro Information Technology (EIT)*. IEEE. 2020, pp. 093–097.

[125] Huili Ye et al. "Virtual Energy Routing Strategy for Energy Internet with Renewable Energy". In: *2021 IEEE 12th Energy Conversion Congress & Exposition-Asia (ECCE-Asia)*. IEEE. 2021, pp. 1459–1463.

[126] Lina Benchikh et al. "Optimal Path Selection and Producer Allocation for Energy Distribution in Energy Internet". In: *2023 International Conference on Networking and Advanced Systems (ICNAS)*. 2023, pp. 1–6. DOI: 10.1109/ICNAS59892.2023.10330529.

[127] John H Holland. "Genetic algorithms and adaptation". In: *Adaptive control of ill-defined systems* (1984), pp. 317–333.

[128] Assala Nacef et al. "Genetic Algorithm-Based Path Selection for Power-Efficient Energy Routing in Smart Grids and Energy Internet". In: *2023 2nd International Engineering Conference on Electrical, Energy, and Artificial Intelligence (EICEEAI)*. 2023, pp. 1–6. DOI: 10.1109/EICEEAI60672.2023.10590502.

[129] Lina Benchikh, Lemia Louail, and Assala Nacef. "Solving Energy Routing problems in Energy Internet using Genetic Algorithm". In: *2023 International Conference on Computer and Applications (ICCA)*. 2023, pp. 1–6. DOI: 10.1109/ICCA59364.2023.10401656.

[130] Assala Nacef et al. "Simulated Annealing for Optimal Path Selection and Scheduling in Energy Routing for Smart Grids". In: *2023 International Conference on Computer and Applications (ICCA)*. 2023, pp. 1–5. DOI: 10.1109/ICCA59364.2023.10401668.

[131] Ashutosh Timilsina and Simone Silvestri. "P2p energy trading through prospect theory, differential evolution, and reinforcement learning". In: *ACM Transactions on Evolutionary Learning* 3.3 (2023), pp. 1–22.

[132] Olamide Jogunola, Weizhuo Wang, and Bamidele Adebisi. "Prosumers matching and least-cost energy path optimisation for peer-to-peer energy trading". In: *IEEE Access* 8 (2020), pp. 95266–95277.

[133] Xu Chen and Yan Zhang. "Energy Router Optimization Strategy Based on LSTM algorithm for Real-Time Congestion Prediction". In: *2022 IEEE 11th Data Driven Control and Learning Systems Conference (DDCLS)*. IEEE. 2022, pp. 380–384.

[134] Xinyang Han et al. "An open energy routing network for low-voltage distribution power grid". In: *2017 IEEE International Conference on Energy Internet (ICEI)*. IEEE. 2017, pp. 320–325.

[135] Nan Zhou et al. "Coordinated planning of multi-area multi-energy systems by a novel routing algorithm based on random scenarios". In: *International Journal of Electrical Power & Energy Systems* 131 (2021), p. 107028. ISSN: 0142-0615. DOI: https://doi.org/10.1016/j.ijepes.2021.107028. URL: https://www.sciencedirect.com/science/article/pii/S0142061521002684.

[136] Dina Emad et al. "A Real-Time Zbus-based Method for Peer-to-Peer Energy Transactions in The Energy Internet". In: *International Journal of Electrical Power & Energy Systems* 159 (2024), p. 110028.

[137] Amani Fawaz, Imad Mougharbel, and Hadi Y Kanaan. "New routing application using bees colony for energy internet". In: *2022 3rd International Conference on Smart Grid and Renewable Energy (SGRE)*. IEEE. 2022, pp. 1–8.

[138] Lina Benchikh, Lemia Louail, and Djamila Mechta. "Subscriber Matching in Energy Internet Using the Firefly Algorithm". In: *International Conference on Interactive Collaborative Robotics*. Springer. 2023, pp. 418–432.

[139] Assala Nacef et al. "Genetic Algorithm-Based Path Selection for Power-Efficient Energy Routing in Smart Grids and Energy Internet". In: *2023 2nd International Engineering Conference on Electrical, Energy, and Artificial Intelligence (EICEEAI)*. IEEE. 2023, pp. 1–6.

[140] Zhikang Shuai et al. "Microgrid stability: Classification and a review". In: *Renewable and Sustainable Energy Reviews* 58 (2016), pp. 167–179. ISSN: 1364-0321. DOI: https://doi.org/10.1016/j.rser.2015.12.201. URL: https://www.sciencedirect.com/science/article/pii/S1364032115015841.

[141] Jacek Malczewski. "1.15 - Multicriteria Analysis". In: *Comprehensive Geographic Information Systems*. Ed. by Bo Huang. Oxford: Elsevier, 2018, pp. 197–217. ISBN: 978-0-12-804793-4. DOI: https://doi.org/10.1016/B978-0-12-409548-9.09698-6. URL: https://www.sciencedirect.com/science/article/pii/B9780124095489096986.

[142] Sara Hebal et al. "Hybrid energy routing approach for energy internet". In: *Energies* 14.9 (2021), p. 2579.

[143] Primavera De Filippi. "The interplay between decentralization and privacy: the case of blockchain technologies". In: *Journal of Peer Production, Issue* 7 (2016).

[144] Victor Ahlqvist, Pär Holmberg, and Thomas Tangerås. "A survey comparing centralized and decentralized electricity markets". In: *Energy Strategy Reviews* 40 (2022), p. 100812.

[145] Arzoo Miglani et al. "Blockchain for Internet of Energy management: Review, solutions, and challenges". In: *Computer Communications* 151 (2020), pp. 395–418.

[146] Lei Chen et al. "Design of a novel energy router and its application in energy internet". In: *2015 Chinese Automation Congress (CAC)*. IEEE. 2015, pp. 1462–1467.

[147] Muhammad Khalid. "Smart grids and renewable energy systems: Perspectives and grid integration challenges". In: *Energy Strategy Reviews* 51 (2024), p. 101299. ISSN: 2211-467X. DOI: https://doi.org/10.1016/j.esr.2024.101299. URL: https://www.sciencedirect.com/science/article/pii/S2211467X24000063.

[148] Raouf Belmahdi et al. "SQGA: Quantum Genetic Algorithm-based Workflow Scheduling in Fog-Cloud Computing". In: *2022 International Wireless Communications and Mobile Computing (IWCMC)*. IEEE. 2022, pp. 131–136.

[149] Huaixiao Wang et al. "The improvement of quantum genetic algorithm and its application on function optimization". In: *Mathematical problems in engineering* 2013.1 (2013), p. 730749.

[150] Ausgrid. *Solar Home Electricity Data*. Dataset from July 2012 to June 2013. 2014. URL: https://github.com/pierre-haessig/ausgrid-solar-data (visited on 01/15/2024).

[151] J. MacQueen. "Some methods for classification and analysis of multivariate observations". In: 1 (1967), pp. 281–297.

[152] R. W. Sinnott. "Virtues of the Haversine". In: *Sky and Telescope* 68.2 (1984), p. 159.

[153] *IEC 60287: Electric Cables – Calculation of the Current Rating*. International Electrotechnical Commission, 2014.

[154] Chao Long, Yue Zhou, and Jianzhong Wu. "Evaluation of peer-to-peer energy sharing mechanisms based on a multiagent simulation framework". In: *Applied Energy* 222 (2018), pp. 993–1022.

[155] Cephas Samende, Jun Cao, and Zhong Fan. "Multi-agent deep deterministic policy gradient algorithm for peer-to-peer energy trading considering distribution network constraints". In: *arXiv preprint arXiv:2108.09053* (2021).

[156] A. Beck and M. Teboulle. "Mirror descent and nonlinear projected subgradient methods for convex optimization". In: *Oper. Res. Lett.* 31 (2003), pp. 167–175. DOI: 10.1016/s0167-6377(02)00231-6.

[157] A. Nemirovski et al. "Robust Stochastic Approximation Approach to Stochastic Programming". In: *SIAM J. Optim.* 19 (2008), pp. 1574–1609. DOI: 10.1137/070704277.

[158] Sanjeev Arora, Elad Hazan, and Satyen Kale. "The Multiplicative Weights Update Method: a Meta-Algorithm and Applications". In: *Theory Comput.* 8 (2012), pp. 121–164. DOI: 10.4086/toc.2012.v008a006.

[159] Shai Shalev-Shwartz. "Online Learning and Online Convex Optimization". In: *Found. Trends Mach. Learn.* 4 (2012), pp. 107–194. DOI: 10.1561/2200000018.

[160] Jyrki Kivinen and Manfred K. Warmuth. "Exponentiated Gradient Versus Gradient Descent for Linear Predictors". In: *Inf. Comput.* 132 (1997), pp. 1–63. DOI: 10.1006/inco.1996.2612.

[161] James B. Orlin. "A polynomial time primal network simplex algorithm for minimum cost flows". In: *Mathematical Programming* 78.2 (1997), pp. 109–129.